

ANTIBIOTIC DISCOVERY AND INFECTION TREATMENT AND PREVENTION

USING BIOFILMS TO IDENTIFY NOVEL ANTIBIOTICS AND ASSESS INFECTION
PREVENTION METHODS

By VICTORIA ELIZABETH COLES, B.Sc.

A Thesis Submitted to the School of Graduate Studies in Partial Fulfillment of the
Requirements of the Degree Doctor of Philosophy

McMaster University © Copyright by Victoria Elizabeth Coles, August 2024

McMaster University DOCTOR OF PHILOSOPHY (2024) Hamilton, Ontario (Health Sciences)

TITLE: Using Biofilms to Identify Novel Antibiotics and Assess Infection Prevention Methods

AUTHOR: Victoria E. Coles, B.Sc. (McMaster University)

SUPERVISOR: Lori L. Burrows

NUMBER OF PAGES: xvi, 180

Foreword

Lay Abstract

Antibiotics are pivotal to the success of modern medicine, but are becoming increasingly less effective because of antibiotic resistance. Resistance occurs when bacteria evolve ways of surviving exposure to antibiotics, and the overuse and misuse of antibiotics contributes to the spread of resistance through bacterial populations. This makes antibiotics currently used in the clinic less effective. Resistant strains of *Staphylococcus aureus* represent a major public health concern and are one of the most common causes of infections following joint replacement and medical device implantation. There are multiple approaches to prevent the rise of resistant *S. aureus* infections. In this thesis I: (1) identify a new antibiotic with activity against resistant species; (2) explore this antibiotic's ability to re-sensitize resistant species to existing antibiotics; and (3) validate the activity of antiseptics used to prevent biofilm infections during surgery. Used together, these approaches help limit the spread of resistant infections.

Abstract

As antimicrobial resistance proliferates, standard treatments for bacterial infections are rendered ineffective. There is therefore a need to both prevent infections and develop new treatment options. This need is especially urgent for priority pathogens like methicillin-resistant strains of *Staphylococcus aureus* (MRSA). Developing new antibiotics is difficult for a variety of reasons, including virulence traits like the formation of biofilms, surface-associated bacterial communities that are less susceptible to antibiotics. Here we used biofilms to our advantage, since their formation is stimulated when bacteria are exposed to sub-lethal concentrations of antibiotics, allowing us to screen for compounds with antimicrobial activity that would be missed with traditional methods. Using this approach, we identified the anti-inflammatory compound BAY 11-7082 as an antibiotic. We showed that it inhibits growth of priority pathogens including MRSA and provide evidence to suggest it has a novel (and potentially multifaceted) mechanism. We also found it re-sensitizes MRSA to inexpensive and readily available β -lactam antibiotics like penicillin G. This finding was of particular interest since using antibiotic adjuvants in combination with existing antibiotics provides a promising and complementary strategy to antibiotic discovery. We showed that wall teichoic acids, polymer chains anchored to the *S. aureus* cell wall, were required for sensitization to occur; however, unlike existing adjuvants, BAY 11-7082 did not appear to impact cell morphology or division, suggesting it instead targets a factor of β -lactam resistance that may be less well understood. Lastly, we examined the impact of common surgical antiseptics on bacterial growth and biofilm formation, with a goal of preventing infections following joint replacement. We found these solutions to be effective; however, it is important to define the concentrations at which they inhibit microbial growth *in*

vivo, since sub-lethal concentrations stimulate biofilm formation. Taken together, the findings in this thesis bolster our understanding of how to reduce and treat resistant infections.

Acknowledgements

There are a lot of people I would like to thank for helping me get here. First and foremost, thank you to my supervisor, Dr. Lori Burrows, for putting your trust in me to work on such a cool (but often confusing) project. I have loved every minute of it and am so proud to say I did my PhD in the Burrows lab. To my committee members, Dr. Elliot and Dr. Magolan: I could not have asked for a kinder, more helpful committee. Marie, thank you not only for all the advice you have given me over the last five years, but also for teaching the first microbiology course I ever took and for inspiring a love in the subject I will carry with me always. Jake, thank you for taking me into your lab when I was a third-year undergrad who knew nothing about research and even less about organic chemistry; you have been a trusted collaborator and mentor ever since, and I never could have imagined all the places this project would go.

Thank you to my amazing lab mates. Hanjeong, you have helped and guided me in so many ways. Ikram, Nathan, and Veronica, these past few years would not have been the same without you. Thank you also to Derek, Katie, and Luke for helping me navigate the crazy world of starting grad school. Thank you to the undergraduate students who helped me throughout these projects: Jake McNairn, Angela Yang, and Andrew Alexandrescu. I am also grateful for my wonderful office mates, fellow grad students, and friends - our lunchtime chats, coffee houses, and Phoenix nights kept me sane. And a special thank you to Sommer, for being there for me for every step of our academic journeys together.

To my family, thank you for believing in me, loving me, and never doubting that I could do this. Mom and dad, your support has meant the world to me. And to Adam, for absolutely everything.

Table of Contents

Foreword	iii
Lay Abstract	iii
Abstract	iv
Acknowledgements.....	vi
Table of Contents	vii
List of Figures.....	xi
List of Tables.....	xiii
List of all Abbreviations and Symbols.....	xiv
Declaration of Academic Achievement	xvi
Chapter One: The importance and challenges of identifying new treatments for bacterial infections	1
Antibiotics and Antibiotic Resistance.....	2
The Cell Wall as a Historic and Valuable Antibiotic Target.....	4
Bacterial cell wall synthesis.....	4
β -lactams and β -lactam resistance	8
Moenomycins.....	10
Glycopeptides and vancomycin resistance	10
Biofilms Decrease Antibiotic Susceptibility and Complicate Treatment	11
Bacterial biofilm formation.....	12
Biofilms in the clinic.....	13
Approaches to Identifying New Antibiotics with Novel Targets	15
Antibiotic adjuvants	17
Purpose and Goals of This Thesis	18
References.....	20
Chapter Two: Exploration of BAY 11-7082 as a potential antibiotic	31
Preface.....	32
Abstract	33
Keywords	33
Results.....	36
BAY 11-7082 stimulates <i>P. aeruginosa</i> biofilm formation and has potent anti-MRSA activity.....	36

Synthesis and antibacterial activity of analogues	38
Evolving mutants resistant to BAY 11-7082 and PSPC.....	42
Exploring inhibition of TAT secretion as a potential mechanism	43
Insight into BAY 11-7082's uptake and effect on the proton motive force	45
BAY 11-7082 synergizes with multiple classes of antibiotics	46
Anti-inflammatory properties of BAY 11-7082 and its analogues	48
Discussion	49
Conclusion	53
Methods.....	54
Bacterial strains, culture conditions, and chemicals	54
Compound screening	54
Inhibitory concentration assays.....	55
Biofilm modulation assays.....	55
Liquid serial passage assays.....	56
Genome assembly and identification of SNPs.....	56
Growth curves.....	57
DiSC ₃ (5) assays	57
Checkerboard assays.....	58
NLRP3 inflammasome assays	59
Acknowledgments.....	60
Abbreviations Used.....	60
References.....	61
Supporting Information.....	66
References for supporting information	112
Chapter Three: BAY 11-7082 synergizes with PBP2-targeting β-lactams to inhibit the growth of methicillin-resistant <i>Staphylococcus aureus</i>	113
Preface.....	114
Abstract.....	115
Introduction.....	116
Results.....	119
BAY 11-7082 synergizes with β -lactams that primarily target the bifunctional penicillin binding protein PBP2.....	119
Wall teichoic acid synthesis may play a role in BAY 11-7082- β -lactam synergy	121

WTA glycosylation is not required for BAY 11-7082- β -lactam synergy.....	124
BAY 11-7082 does not impact cell division	125
Discussion.....	126
Conclusions.....	129
Methods.....	130
Bacterial strains, culture conditions, and chemicals	130
Inhibitory concentration assays.....	131
Checkerboard assays.....	131
Transmission electron microscopy.....	131
References.....	132
Supporting Information.....	137
Chapter Four: The effects of chlorhexidine, povidone-iodine, and vancomycin on growth and biofilms of pathogens that cause prosthetic joint infections: an <i>in vitro</i> model.....	141
Preface.....	142
Summary	143
Introduction.....	144
Materials and Methods.....	146
Microbial strains, culture conditions, and chemicals.....	146
Inhibitory concentration and biofilm formation assays	147
Biofilm disruption assays.....	148
Checkerboard assays.....	148
Results.....	149
CHG and PI have broad spectrum antimicrobial and anti-biofilm activity at dilutions below those used in surgery.....	149
CHG and PI can disperse established biofilms	152
PI and CHG lack synergistic or antagonistic activity when used in combination	152
The effects of combining wound irrigation with intrawound vancomycin administration.	153
Discussion.....	155
Conclusions.....	159
Acknowledgments.....	160
Conflict of interest statement	160
Funding sources	160
References.....	161

Supplementary Information	164
Chapter Five: Discussion and Future Directions	165
Overview of Findings	166
The importance and limitations of infection prevention.....	167
The importance of measuring biofilm formation.....	167
<i>S. aureus</i> biofilm inhibitors for infection treatment and prevention.....	169
Identification of a novel antibiotic scaffold	173
Antibiotic adjuvants as an alternative strategy to antibiotic discovery.....	174
Significance and Concluding Remarks	177
References.....	177

List of Figures

Chapter One

Figure 1. Major antibacterial classes	3
Figure 2. Peptidoglycan biosynthesis	7
Figure 3. Core structures of key subgroups of β -lactams.	8
Figure 4. The biofilm lifecycle	13

Chapter Two

Figure 1. BAY 11-7082 1 stimulates <i>P. aeruginosa</i> biofilm formation and has modest antibacterial activity against Gram-negative species and potent antibacterial activity against Gram-positive species	38
Figure 2. Synthesis and antibacterial activity of BAY 11-7082 1 and its analogues 5-19	40
Figure 3. Synthesis and antibacterial activity of PSPC 20 and its analogues 24-34	41
Figure 4. Mutants resistant to BAY 11-7082 and PSPC	43
Figure 5. Planktonic growth of the parent strain <i>P. aeruginosa</i> PA14 and a <i>tatC</i> transposon.....	44
Figure 6. Planktonic growth of <i>S. aureus</i> 15981 grown in pH adjusted MHB with increasing concentrations of BAY 11-7082, PSPC, or tetracycline	46
Figure 7. Checkerboards of <i>S. aureus</i> USA300	47
Figure 8. Production of IL-1 β by bone marrow-derived macrophages stimulated with 200 ng/mL LPS and 10 μ M nigericin in the presence or absence of BAY 11-7082, or the analogue 5 , 12 , 17 , or 19 at 1 or 2.5 μ M	49
Figure S1. Planktonic growth of seven bacterial species grown in LB or MHB with increasing concentrations of BAY 11-7082.....	66
Figure S2. BAY 11-7082 inhibits the growth of a collection of clinically relevant pathogens and strains from the Antibiotic Resistance Platform	67
Figure S3. PSPC, like BAY 11-7082, stimulates biofilm formation and has potent anti-Staphylococcal activity	68
Figure S4. BAY 11-7082 and PSPC-resistant mutants and the parent strain <i>S. aureus</i> 15981 are equally susceptible to tetracycline and piperacillin	69

Chapter Three

Figure 1. Wall teichoic acid biosynthetic pathway in <i>S. aureus</i>	118
Figure 2. BAY 11-7082 synergizes with PBP2-targeting β -lactams against MRSA	120
Figure 3. The absence of WTA does not impact BAY 11-7082 activity	122
Figure 4. BAY 11-7082 does not impact WTA levels.....	123
Figure 5. WTA glycosyltransferase TarS is not required for BAY 11-7082- β -lactam synergy...	124
Figure 6. BAY 11-7082 treatment does not result in morphological changes or septal abnormalities.....	125

Figure S1. Structures of β -lactams and non- β -lactam peptidoglycan-targeting antibiotics tested for activity against <i>S. aureus</i> USA300 (MRSA) and ATCC 29213 (MSSA) in combination with BAY 11-7082	137
Figure S2. Checkerboards of <i>S. aureus</i> USA300 (MRSA).....	138
Figure S3. Checkerboards of <i>S. aureus</i> ATCC 29213 (MSSA)	139
Figure S4. Planktonic growth of <i>S. aureus</i> 15981 (MRSA), the BAY 11-7082-resistant mutant B13, and the PSPC-resistant mutant P11	140
Figure S5. Additional fields of view of electron micrographs.....	140

Chapter Four

Figure 1. The antiseptic solutions CHG and PI inhibit growth and biofilm formation of model PJI-associated pathogens	150
Figure 2. CHG and PI inhibit growth and biofilm formation of <i>S. aureus</i> and <i>P. aeruginosa</i> clinical isolates.....	151
Figure 3. CHG and PI disperse established biofilms	152
Figure 4. CHG and PI do not synergize nor antagonize one another's activity.....	153
Figure 5. Vancomycin does not synergize with nor antagonize the activity of clinical antiseptics.	154

Chapter Five

Figure 1. Workflow diagram of a proposed screen to identify antibiofilm compounds to be used in joint replacement to prevent or treat prosthetic joint infections	171
Figure 2. Structures that inhibit <i>P. aeruginosa</i> biofilm formation from our pilot biofilm screen or those reported in literature and validated in our lab	173

List of Tables

Chapter Four

Supplementary Table I. Strain name and antibiotic susceptibility of <i>S. aureus</i> clinical strains isolated from patient samples as indicated.....	164
---	-----

List of all Abbreviations and Symbols

AMR	Antimicrobial resistance
ARP	Antibiotic resistance platform
BMDM	Bone marrow-derived macrophages
BSA	Bovine serum albumin
CCCP	Carbonyl cyanide m-chlorophenyl hydrazine
c-di-GMP	3',5'-cyclic diguanylic acid
CHG	Chlorhexidine gluconate
DiSC ₃ (5)	3,3'-dipropylthiadicarbocyanine iodide
DMEM	Dulbecco's Modified Eagle Medium
DMSO	Dimethyl sulfoxide
DNA	Deoxyribonucleic acid
ELISA	Enzyme linked immunosorbent assay
EPS	Exopolysaccharides
ESKAPE	<i>Enterococcus faecium</i> , <i>Staphylococcus aureus</i> , <i>Klebsiella pneumoniae</i> , <i>Acinetobacter baumannii</i> , <i>Pseudomonas aeruginosa</i> , and <i>Enterobacter</i> species
FDA	Food and Drug Administration
FICI	Fractional inhibitory concentration index
GlcNAc	<i>N</i> -acetylglucosamine
GTP	Guanosine triphosphate
HRMS	High resolution mass spectrometry
LB	Lysogeny broth
LPS	Lipopolysaccharide
LTA	Lipoteichoic acid
ManNAc	<i>N</i> -acetylmannosamine
MHA	Mueller-Hinton agar
MHB	Mueller-Hinton broth
MIC	Minimum inhibitory concentration
MRSA	Methicillin-resistant <i>Staphylococcus aureus</i>
MSSA	Methicillin-sensitive <i>Staphylococcus aureus</i>
MurNAc	<i>N</i> -acetylmuramic acid
NMR	Nuclear magnetic resonance
OD	Optical density
PAMP	Pathogen-associated molecular patterns
PBP	Penicillin binding protein
PBS	Phosphate buffered saline
PI	Povidone-iodine
PJI	Prosthetic joint infection
PMF	Proton motive force
PSPC	3-(phenylsulfonyl)-2-pyrazinecarbonitrile
PTP	Protein tyrosine phosphatase
RNA	Ribonucleic acid
RPM	Revolutions per minute
SAR	Structure-activity relationship
SCC _{mec}	Staphylococcal cassette chromosome <i>mec</i>

SEDS	Shape, elongation, division, and sporulation
SNP	Single nucleotide polymorphism
TAT	Twin arginine translocase
TEM	Transmission electron microscopy
TJR	Total joint replacement
UDP	Uridine diphosphate
VISA	Vancomycin-intermediate <i>Staphylococcus aureus</i>
WT	Wild type
WTA	Wall teichoic acid

Declaration of Academic Achievement

I performed all research in this body of work except where indicated in the preface of each chapter.

Chapter One: The importance and challenges of identifying new treatments for bacterial infections

Antibiotics and Antibiotic Resistance

Although they can usually be treated with inexpensive drugs, bacterial infections were still responsible for the loss of 704 million disability-adjusted life-years globally in 2019.¹ These infections are most frequently caused by difficult-to-treat pathogens including the ESKAPE group (*Enterococcus faecium*, *Staphylococcus aureus*, *Klebsiella pneumoniae*, *Acinetobacter baumannii*, *Pseudomonas aeruginosa*, and *Enterobacter* species), which often develop resistance to antibiotics.² Antimicrobial resistance (AMR) was the direct cause of 1.27 million deaths in 2019, and has steadily increased over past decades.^{3,4} AMR occurs when bacteria express or acquire factors that cause antibacterials to lose their activity, limiting treatment options for infections.

There are multiple classes of antibacterials (Figure 1) that target different cellular processes.^{5,6} One of the oldest and most widely used classes, β -lactams, inhibit the activity of penicillin-binding proteins (PBPs), essential enzymes involved in the biosynthesis of the bacterial cell wall. Other classes of antibiotics, like glycopeptides, also inhibit key steps in peptidoglycan biosynthesis, while newer antibiotics like the lipopeptide daptomycin target the cell membrane. Ansamycins target RNA synthesis. Several classes of antibiotics inhibit protein synthesis, by targeting the 30S (aminoglycosides, tetracyclines) or 50S (chloramphenicol, macrolides, streptogramins) ribosomal subunits. These classes all include natural products, compounds produced by microorganisms during microbial competition. Many classes also include semi-synthetics, synthetic compounds based on natural product scaffolds. Entirely synthetic antibacterials like sulfonamides, quinolones, and oxazolidinones target folate synthesis, DNA replication, and protein synthesis, respectively.

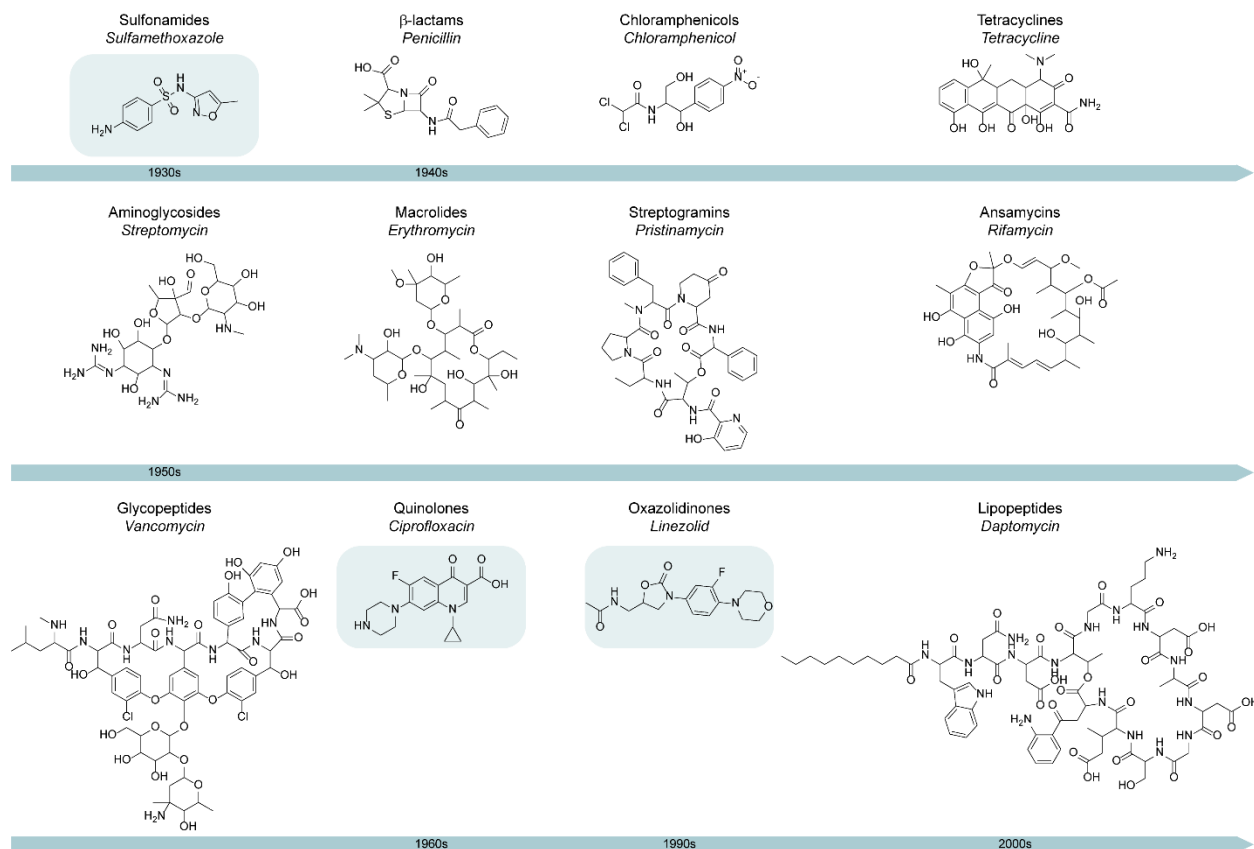


Figure 1. Major antibacterial classes. Twelve major classes of antibacterials, ordered by year of discovery (left to right, top to bottom). Structures are shown for one member of each class; antibacterial names are italicized. Classes that originated with a synthetic compound as opposed to a natural product are highlighted in boxes. Information adapted from Walsh and Wenciewicz and Brown and Wright.^{5,6}

Despite these diverse mechanisms of action, resistance has been observed for all major classes of antibiotics. Resistance mechanisms vary; some are general, such as the induction of genes that encode for efflux pumps to remove antibiotics from the cell, while others are more specific to an antibiotic's mechanism of action.⁷ Some species mutate the antibiotic's target, reducing affinity, or increase its copy number, effectively diluting the drug. Others use alternative enzymes or pathways to accomplish biological functions, thus bypassing the target entirely. Alternatively, bacteria may acquire genes that encode for enzymes that modify or degrade the antibiotic. Since most clinically used antibiotics are natural products, producing microbes have developed

mechanisms to avoid self-intoxication and competing species have developed resistance mechanisms over a period of millions of years.^{8,9} AMR is therefore an ancient phenomenon that predates modern antibiotic use.¹⁰ While some bacteria are naturally resistant to certain antibiotics through intrinsic factors, others acquire resistance genes through horizontal gene transfer.⁶ Bacteria may also spontaneously develop resistance to an antibiotic. These resistant isolates can come to make up the entirety of a bacterial population when antibiotic use selectively inhibits the growth of susceptible individuals. While often associated with a fitness defect, resistance can become stable when compensatory mutations make the resistance phenotype sustainable.¹¹ Resistance genes often cluster together on mobile genetic elements, enabling pathogens to develop multi-drug resistance, further decreasing treatment options for infections.¹² The over- and misuse of antibiotics therefore contributes to the proliferation of AMR, threatening the continued use of this valuable class of medicine. Reducing the spread of AMR requires appropriate stewardship to ensure existing antibiotics retain their activity, as well as the development of new treatment options to which resistance is not already widespread.

The Cell Wall as a Historic and Valuable Antibiotic Target

Bacterial cell wall synthesis

The bacterial cell wall is an essential component for viability and not present in eukaryotic cells, making it an ideal target for antibiotics. While the exact chemical structure and thickness of the cell wall, composed of cross-linked strands of peptidoglycan, differs between bacterial species, its biosynthesis is broadly conserved.^{13,14} Peptidoglycan biosynthesis (Figure 2A) begins when fructose-6-phosphate is converted to uridine diphosphate-*N*-acetylglucosamine (UDP-GlcNAc), which is then converted to UDP-*N*-acetylmuramic acid (UDP-MurNAc).¹⁴ A pentapeptide stem

is synthesized on UDP-MurNAc, after which the MurNAc-pentapeptide is transferred to an undecaprenyl phosphate molecule, forming the precursor lipid I. The composition of the pentapeptide stem differs between species but is typically terminated by two *D*-alanine residues. GlcNAc from UDP-GlcNAc is then added to lipid I, forming lipid II. Lipid II is the peptidoglycan building block; it is flipped to the outer leaflet of the membrane, where lipid II monomers are polymerized into a growing glycan strand by PBPs and SEDS (shape, elongation, division, and sporulation) proteins.¹⁵ PBPs come in two flavours: aPBPs, which have a glycosyltransferase domain to polymerize lipid II molecules and a transpeptidase domain to crosslink glycan strands, and bPBPs, which only have transpeptidase function and rely on the glycosyltransferase activity of their cognate SEDS protein.^{16–18} SEDS-bPBP pairs are involved in cell division or elongation, while aPBPs are involved in maintaining and repairing the cell wall.¹⁹ In *S. aureus*, lipid II is modified prior to its transport to the outer leaflet of the membrane. The enzymes FemX, FemA, and FemB sequentially add five glycine residues to the *L*-lysine residue of the pentapeptide (Figure 2B).²⁰ This pentaglycine bridge facilitates cross-linking and is required for *S. aureus* viability.²¹

Many Gram-positive organisms also produce wall teichoic acids (WTAs), which are anchored to the peptidoglycan (Figure 2C). These strands of poly(ribitol phosphate) or poly(glycerol phosphate) are synthesized by the *tar* or *tag* genes, respectively, using some of the same substrates that are used in peptidoglycan biosynthesis.²² The enzyme TarO or TagO facilitates the transfer of GlcNAc from UDP-GlcNAc to an undecaprenyl phosphate molecule, to which an *N*-acetylmannosamine (ManNAc) molecule is then added.²² Approximately 40-60 glycerol or ribitol phosphates are added to complete the polymer, which is flipped to the outer leaflet of the

membrane and anchored to a MurNAc residue in the cell wall.²³ WTAs are nonessential but play important roles in growth, division, and virulence.²³ They are involved in shape determination, with rod-shaped species like *Bacillus subtilis* becoming spherical in their absence; localization of enzymes involved in peptidoglycan synthesis, such as PBP4 and FmtA in *S. aureus*; and they provide protection from host immune factors like lysozymes.^{24–28} The role of WTAs in β -lactam resistance is further explored in Chapter Three. Despite their structural similarities, lipoteichoic acids, which are anchored to the membrane and are comprised of glycerol phosphate units, are synthesized via a separate pathway.²⁹

Many antibiotics target different aspects of bacterial cell wall synthesis (Figure 2A).³⁰ For example, fosfomycin inhibits MurA, the first enzyme involved in generating UDP-MurNAc from UDP-GlcNAc.³¹ D-cycloserine targets the *D*-alanyl-*D*-alanine ligase and the isomerase alanine racemase, which are required to synthesize the pentapeptide stem.³² Tunicamycin inhibits MraY, which catalyzes the synthesis of lipid I from UDP-MurNAc-pentapeptide and undecaprenyl phosphate.³³ Interestingly, it also binds TarO, blocking WTA biosynthesis.³⁴ β -lactams, moenomycins, and glycopeptides represent key antibiotic classes that target peptidoglycan biosynthesis; the following sections describe their mechanisms.

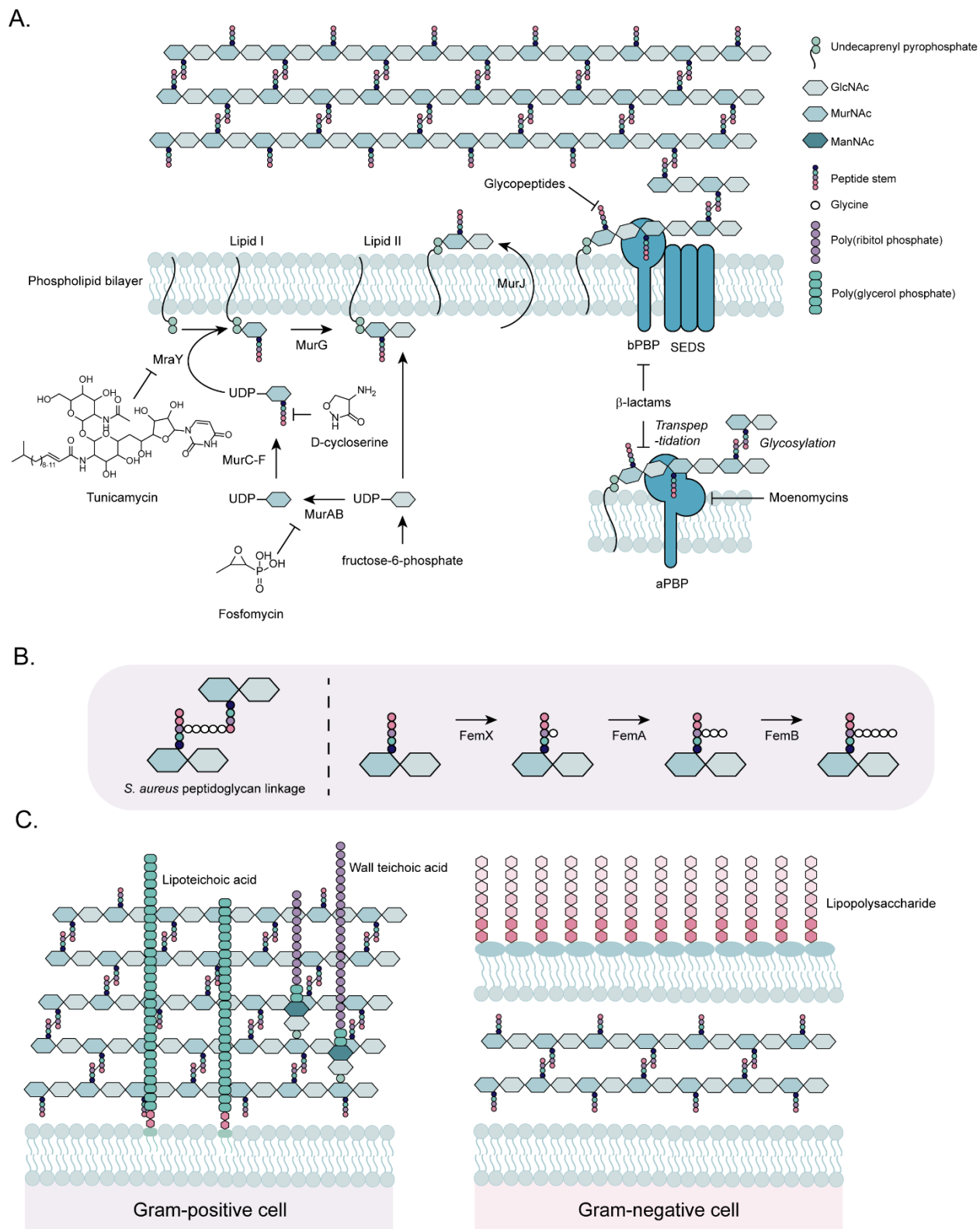


Figure 2. Peptidoglycan biosynthesis. (A) Fructose-6-phosphate is converted to UDP-GlcNAc and UDP-MurNAc, which are attached to an undecaprenyl pyrophosphate carrier to form lipid II.¹⁴ Lipid II molecules are polymerized and cross-linked by a SEDS-bBP pair (top) or an aBP

(bottom) to form mature peptidoglycan.¹⁵ Names and structures of specific antibiotics or names of antibiotic classes that inhibit peptidoglycan biosynthesis are identified. (B) *S. aureus* lipid II is modified with a pentaglycine bridge (white circles) that plays a role in cross-linking that is synthesized by enzymes FemX, FemA, and FemB. (C) Comparison between the cell envelopes of Gram-positive (left) and Gram-negative (right) species. Gram-positive species produce wall teichoic acids, which are anchored to the peptidoglycan, and lipoteichoic acids, which are anchored to the membrane.

β -lactams and β -lactam resistance

Penicillin, a β -lactam, was among the first antibiotics discovered (Figure 1) and has had a massive impact on human health in the decades since. Following its discovery, many derivatives were isolated or synthesized, including the cephalosporins, monobactams, and carbapenems (Figure 3). While carbapenems resemble penicillins, they bear a dihydropyrrole instead of a thiazolidine ring. Cephalosporins have a characteristic dihydrothiazine ring, while in monobactams like aztreonam the β -lactam is not fused to another ring. Today β -lactams make up over half of all antibiotics prescribed in Canada and broad-spectrum β -lactams are central to empiric therapy.³⁵ They covalently bind and inactivate the transpeptidase domain of PBPs, preventing peptidoglycan crosslinking and inducing a constant cycle of peptidoglycan synthesis and degradation, exhausting cellular resources.³⁶

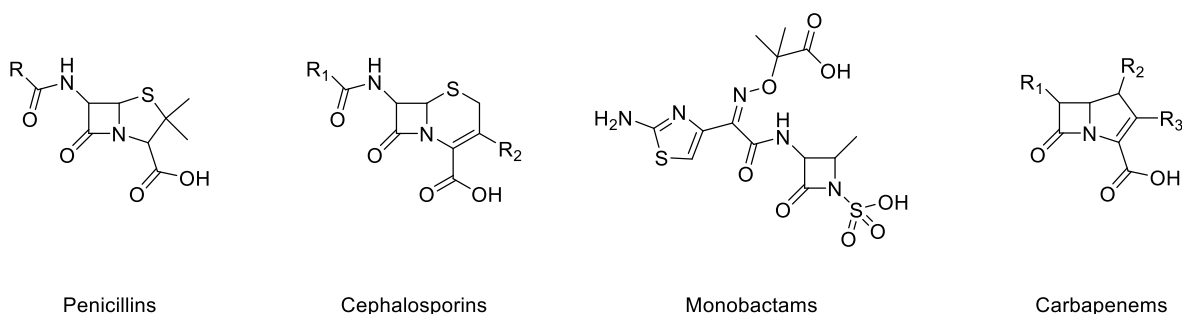


Figure 3. Core structures of key subgroups of β -lactams.

Some species are resistant to certain β -lactams due to the presence of intrinsic or acquired β -lactamases, enzymes that hydrolyze the β -lactam ring. *P. aeruginosa*, for example,

chromosomally encodes the β -lactamase AmpC, and certain strains of *S. aureus* have acquired a plasmid encoding BlaZ, both of which hydrolyze penicillins, necessitating the development of less susceptible β -lactams like piperacillin and methicillin.^{37,38} While carbapenems and cephalosporins retain activity in these strains, the dissemination of carbapenemases, cephalosporinases, and extended-spectrum β -lactamases make β -lactams a less viable treatment option.³⁹ In response, β -lactamase-inhibitors like clavulanic acid have been developed. When given in combination, clavulanic acid irreversibly binds certain β -lactamases, restoring the activity of β -lactams like amoxicillin.⁴⁰

Several other mechanisms of resistance against β -lactams have been characterized. Some strains of *S. aureus* have acquired mutations that result in overexpression of endogenous PBPs or reduce their affinity for β -lactams.⁴¹ An increasing number of strains have acquired SCC*mec* (staphylococcal cassette chromosome *mec*), a mobile genetic element that contains *mecA*, which encodes an exogenous bPBP, PBP2A (sometimes called PBP2'), with low affinity for β -lactams.⁴² While initially identified to be methicillin-resistant, leading to the popularization of the term methicillin-resistant *S. aureus* (MRSA), PBP2A-containing strains are broadly β -lactam resistant. These strains also express other proteins that play a role in PBP2A-mediated resistance, often termed fem (factors essential for methicillin-resistance) or aux (auxiliary) factors.⁴³ The dissemination of *mecA*-harbouring strains is a severe global health problem; in 2019, MRSA was responsible for 100,000 deaths globally.³

Moenomycins

Moenomycins, natural products first isolated in the 1960s, target glycosyltransferase enzymes involved in peptidoglycan synthesis, including the glycosyltransferase domain of aPBPs. They also have activity against monofunctional glycosyltransferase enzymes, such as SgtA and SgtB (also called Mgt) in *S. aureus*, but lack activity against SEDS proteins.^{16,44,45} By inhibiting the essential glycosyltransferase domain of the only aPBP in *S. aureus*, moenomycins are acutely toxic alone. They also restore β -lactam activity against MRSA, making them a valuable class of antibiotics; however, they are not used clinically due to poor pharmacokinetic properties.^{46,47}

Glycopeptides and vancomycin resistance

The current standard of care antibiotic for treating MRSA is vancomycin, a naturally occurring glycopeptide that non-covalently binds the terminal *D*-alanyl-*D*-alanine residues of the pentapeptide stem of lipid II, preventing transglycosylation and transpeptidation. This mechanism of action is conserved among other glycopeptides including the semi-synthetic derivatives, teicoplanin and telavancin. To avoid self-intoxication, vancomycin-producers have altered pentapeptide stems of either *D*-alanyl-*D*-lactate or *D*-alanyl-*D*-serine, impeding vancomycin-binding.⁴⁸ Plasmid-borne vancomycin resistance first entered the clinic in the 1980s.⁴⁹ Like producers, these strains of vancomycin-resistant Enterococci expressed the ligase VanA, along with regulatory system VanSR and biosynthesis proteins VanHX, to hydrolyze *D*-alanyl-*D*-alanine and produce *D*-alanyl-*D*-lactate.⁵⁰ Vancomycin resistance is of particular concern in strains that are already extensively β -lactam resistant. In the late 1990s, MRSA with decreased susceptibility to vancomycin was first reported.⁵¹ Termed vancomycin-intermediate *S. aureus* (VISA), these strains develop mutations in a variety of genes that increase fitness in the

presence of vancomycin.⁵² More recently, MRSA strains that have acquired the *vanA* gene cluster were isolated, representing a significant threat to public health.⁵³ Despite concerns surrounding rising resistance rates, vancomycin use has only increased in recent decades. While previously considered an antibiotic of last resort, used only in the case of drug-resistant Gram-positive infections, vancomycin has been used more liberally, including use in empiric therapy and prophylactic use during surgery to prevent Gram-positive infections.⁵⁴⁻⁵⁶

While glycopeptide antibiotics are currently effective against Gram-positive species, treatment options are more limited for Gram-negative pathogens, which have a thinner layer of peptidoglycan that is shielded by an outer membrane of phospholipids and lipopolysaccharides that blocks the entry of large or hydrophobic molecules (Figure 2C). Antibiotics designed to target Gram-negative species must therefore adhere to a different set of physiochemical properties to ensure their uptake into the cell.^{57,58}

Biofilms Decrease Antibiotic Susceptibility and Complicate Treatment

Virulence factors enhance bacterial fitness *in vivo*, further complicating treatment. In certain species these can include surface appendages required for motility, like flagella and type IV pili, secretion systems like the type III secretion system that inject toxins into host cells, and the ability to form protective biofilms.⁵⁹ Biofilms are communities of surface-associated bacteria enveloped in a self-produced extracellular matrix of proteins, DNA, lipids, and exopolysaccharides (EPS). They provide increased antibiotic protection compared to planktonic growth states, making biofilm-based infections even more difficult to eradicate.⁶⁰ This increased tolerance is due to decreased penetrance of antimicrobials and immune factors into the biofilm,

heterogeneous growth rates, and increased production of persister cells, resulting in tolerant biofilm infections even with antibiotic treatment.⁶¹ The protective environment of a biofilm can also provide more opportunity for the development of spontaneous mutations that further increase resistance.

Bacterial biofilm formation

In addition to being an ESKAPE pathogen, *P. aeruginosa* is a model biofilm-forming organism. It transitions from a planktonic to biofilm lifecycle when polar flagella reversibly adhere to a surface (Figure 4). Though flagellar-dependent (swimming and swarming) and type IV pili-dependent (twitching) motility are required for the initial stages of attachment,⁶² the transition from reversible polar attachment to irreversible attachment requires repression of motility and increased production of EPS, which contributes to the biofilm matrix.⁶³ These processes are in part regulated by changes in the levels of 3',5'-cyclic diguanylic acid (c-di-GMP), an intracellular secondary messenger synthesized from two molecules of GTP by diguanylate cyclase enzymes.⁶⁴ Microcolony formation is marked by increased EPS production, which, in *P. aeruginosa*, includes the production of alginate, Pel, and Psl, though the exact composition varies by strain and environment.^{65,66} Over time, microcolonies develop into mature biofilms that eventually disperse with the release of planktonic cells and aggregates when there is an increase in nutrient availability, such as succinate, glutamate, and glucose, and when increased environmental nitric oxide stimulates the activity of phosphodiesterases, which break down c-di-GMP.^{67,68} Iron regulation also plays a role in biofilm formation, with low-iron environments, such as those induced by the addition of chelators, contributing to increased twitching motility and decreased biofilm formation, possibly mediated by quorum sensing.^{69,70} Many other priority

pathogens including *S. aureus* also form biofilms. Since it lacks surface appendages like flagellum and type IV pili found in *P. aeruginosa*, *S. aureus* senses and adheres to surfaces using adhesins, cell surface-associated proteins that bind to organic or inorganic surfaces.^{71,72}

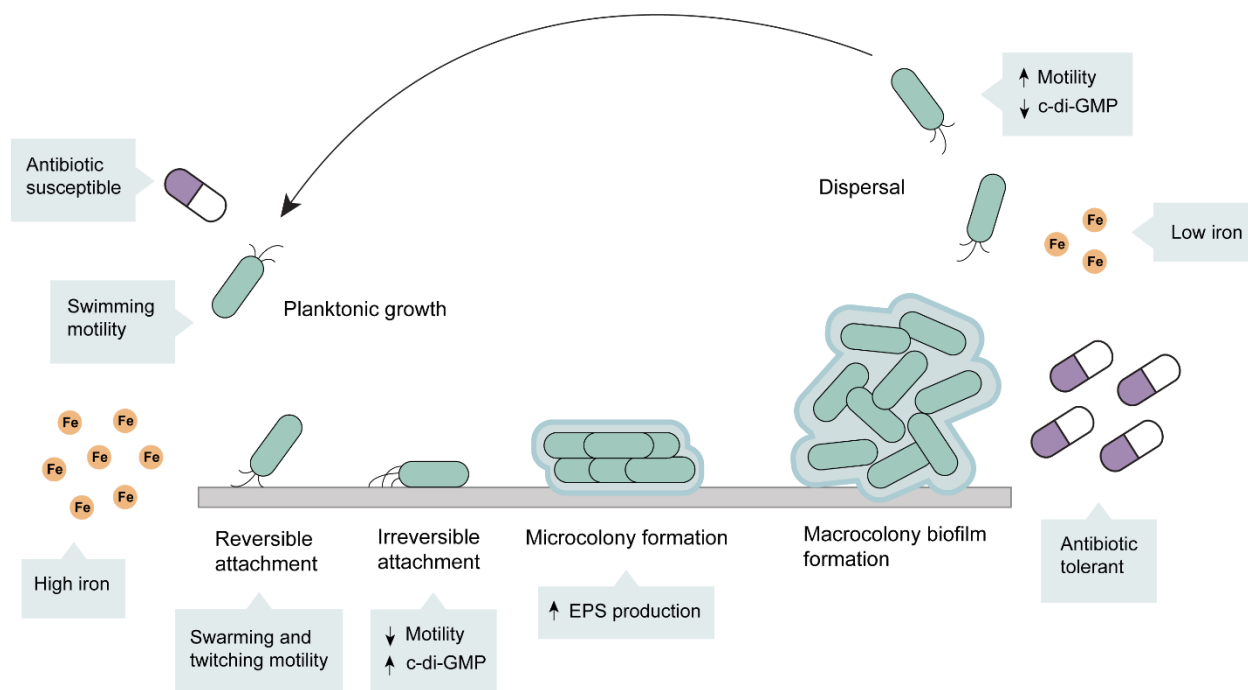


Figure 4. The biofilm lifecycle. Biofilm formation begins when planktonic cells attach to a surface and form antibiotic tolerant, matrix-encased colonies. Cells from these colonies can disperse in response to environmental cues and grow planktonically.

Biofilms in the clinic

Bacteria or fungi growing as biofilms cause infections in a wide range of body sites including the lungs of cystic fibrosis patients, the urinary tract, chronic wounds, and on implanted medical devices and prosthetic joints.⁷³ These biofilms are often polymicrobial, worsening patient outcomes.⁷⁴ One exception is prosthetic joint infections (PJIs), which are typically caused by only one species, most commonly *S. aureus* or *Staphylococcus epidermidis*.⁷⁵ One method to treat biofilm-based infections is physical removal of the biofilm, such as through irrigation.⁷⁶

Antibiotics are often prescribed but while they can reduce microbial load and lessen symptoms, they may not clear the infection.⁷⁷ This is typically the case for catheter-associated *S. aureus* infections, for which device removal is usually recommended.⁷⁷ In the case of PJIs, surgical revision of the infected joint is typically required.^{78,79} Because of limited treatment options and the high morbidity resulting from surgery, preventing biofilm-based infections is crucial. Surgical antiseptics and prophylactic antibiotics play a major role in preventing infection in cases of indwelling medical devices and prosthetics; however, increased antibiotic exposure raises concerns about resistance.^{56,80} Developing specific anti-biofilm small molecules to inhibit biofilm formation and resensitize bacteria to traditional antibiotics represents a promising strategy for infection control. Many *in vitro* studies have identified anti-biofilm compounds, including those that target transcriptional regulators of quorum sensing, regulators of iron uptake, and diguanylate cyclase enzymes.^{76,81–83} Antibody therapies that target biofilm components to induce dispersion are also in development, including one therapeutic designed for use in PJIs, however, no biofilm-based treatments have made it to the clinic.⁸⁴

Despite their importance in establishing reservoirs for infection and impacting antimicrobial susceptibility, biofilms are rarely considered in antibiotic prescribing and dosing. The antibiotic concentrations required to eradicate biofilms can be up to 1000 times higher than the concentration required for planktonic cells.⁶⁰ Biofilm formation is especially important to consider in contexts where antibiotics may not be delivered at an appropriate concentration, as multiple species experience increased biofilm production in response to subinhibitory concentrations of antibiotics.⁸⁵ Biofilm production is stimulated upon exposure to multiple different classes of antibiotics. It does not occur in response to exogenous DNA or cell lysate, but

does occur in response to antibiotics that have been modified to attenuate their activity, suggesting the presence of an antibiotic itself, and not the presence of nearby lysed cells, may activate a stress response that promotes biofilm formation; however, this pathway is not yet fully understood.^{86,87} There are multiple well-described methods for measuring biofilm formation, such as the Calgary biofilm device; however, they are not a part of standard laboratory guidelines for determining antibiotic susceptibility, meaning biofilm production is typically not captured in a clinical context.^{60,77,88}

Approaches to Identifying New Antibiotics with Novel Targets

One approach to treating resistant infections is developing new antibiotics to which bacteria have not yet become resistant; however, regulatory approvals of new antibiotics have decreased in recent decades for a variety of reasons, including large pharmaceutical companies largely abandoning the field.⁸⁹ Despite several reports and calls to action published over the last 20 years, few new treatment options are available for drug-resistant priority pathogens.^{3,4,89-95} Extensive research is still being done to identify new classes of antibiotics, primarily in small companies and academic labs, however; limited progress has been made. Traditional methods for identifying antibiotics include screening soil extracts for secondary metabolite natural products but, although incredibly effective initially, common scaffolds were repeatedly re-identified, limiting the utility of this approach.⁶ While methods to reduce replication have been implemented, only one novel natural product class, the lipopeptides, has reached the clinic this century.^{96,97} Medicinal chemistry has allowed for the diversification of molecules in existing classes, resulting in the development of second- and third-generation antibiotics, but many of these have become ineffective in the face of increasing resistance.⁶ Modern screening approaches

include high-throughput *in vitro* target screening with a focus on synthetic small molecules, genomic approaches, and rational target-based drug design, which often fail to identify compounds with good *in vivo* efficacy.^{98,99}

While natural products represent the majority of currently used antibiotics, they can be difficult to synthesize or modify due to their structural complexity, and resistance may already be widespread in microbial communities as a response to interbacterial competition.^{100,101} Synthetic small molecules are easier to produce and derivatize, but are not without their drawbacks.

Homing in on a useful scaffold from an arbitrary list of small molecules can be difficult, and the hit rate for promising antibacterial leads in a library of small molecules is often quite low. Many chemical libraries were designed to conform to common drug-like features such as Lipinski's rules, which are not necessarily reflective of the properties of effective antibiotics.^{102,103} Very few currently used antibiotics are from synthetic classes, and no new synthetic classes have been approved since the discovery of the oxazolidinones in the 1990s (Figure 1). Machine learning offers an exciting new method to identify synthetic scaffolds of interest without the need to manually screen large numbers of compounds; however, this technology is still in its early stages.¹⁰⁴⁻¹⁰⁶ One way to increase the hit rate in a group of synthetic small molecules is to use compounds previously demonstrated to have biological, but not necessarily microbiological, activity since compounds active for one indication are more likely to be active in another.^{107,108}

Another way to increase hit rates is to screen compounds for activity in nutrient-limited media, which better mimic physiological conditions. In nutrient-limited media, a larger subset of the bacterial genome becomes essential for growth.¹⁰⁹ These conditionally essential gene products represent possible antibiotic targets that are masked in nutrient-rich screening protocols.

For example, recent work from our lab has shown the antibiotics thioestrepton and vancomycin, previously thought to only have activity against Gram-positive species, are able to penetrate certain Gram-negative species under physiologically-relevant iron concentrations.^{110,111}

Conversely, traditional bacterial growth media may be too low in certain nutrients; bicarbonate, which is naturally present at high levels in the human body, potentiates the activity of certain antibiotics and buffers the effects of macrolide resistance.^{112,113}

Even when new antibiotics are discovered, companies struggle to get them to market, due in no small part to unfavourable economics.¹¹⁴ While expensive to develop, new antibiotics designed to treat relatively uncommon resistant infections rarely make it through clinical trials and, once approved, are infrequently prescribed. Creative economic strategies like the United Kingdom's subscription-based model aim to protect the investment of companies developing new drugs, but programs like these remain far from widespread.¹¹⁵

Antibiotic adjuvants

As the supply of new antibiotics with novel mechanisms dwindles, another approach is to extend the usability of existing antibiotics with antibiotic adjuvants. In clinical settings, multiple antibiotics are often used in combination to treat infections, but combinations of antibiotics and non-antibiotic drugs also have the potential to increase antibacterial efficacy.¹¹⁶ Adjuvants can act through a variety of different mechanisms, including blocking antibiotic modification by proteins in the cell, inhibiting antibiotic efflux, or increasing antibiotic uptake.^{117,118} Adjuvants can also enhance antibacterial activity by bolstering host immune responses, or by inhibiting bacterial virulence factors that contribute to the pathogen's *in vivo* fitness.^{117,118}

A classic and clinically proven example of antibiotic adjuvants is β -lactamase inhibitors.

Following the successful introduction of amoxicillin-clavulanic acid, ten β -lactam- β -lactamase-inhibitor pairs have come to the market in the last 40 years. Their record of safety and efficacy means that β -lactam- β -lactamase inhibitor combinations make more money than any other new antibiotic.¹¹⁴ As one of the few areas in antibiotic development with minimal financial risk, new β -lactam- β -lactamase inhibitor combinations dominate the list of new antibiotics in the pipeline.¹¹⁹ Despite this notable success, antibiotic adjuvants for other targets are few and far between. While compounds to combat *mecA*-mediated β -lactam resistance are plentiful in the literature, many target the same pathways and none have progressed to commercialization.^{34,120–}

126

Purpose and Goals of This Thesis

The main objectives of this thesis were to identify and characterize novel antibiotics and antibiotic adjuvants with activity against priority pathogens, as well as explore the role of biofilms, both as a screening tool and as a potential complication associated with infections. Based on findings that *P. aeruginosa* biofilm formation is stimulated in response to sub-inhibitory concentrations of antibiotics, previous work aimed to identify compounds that stimulate biofilm formation and thus have potential antibacterial activity.¹¹⁰ We reasoned that screening for compounds that stimulate biofilm formation, in addition to those that inhibit bacterial growth, would allow us to capture more hits. We aimed to further increase our hit rate by using a library of compounds with known bioactivity. While not necessarily potent antibiotics, these hits could be optimized through medicinal chemistry. Chapter Two focuses on one such hit, the anti-inflammatory BAY 11-7082. In this chapter, we conclude that BAY 11-7082 and its

synthetic analogues likely have a novel mechanism of action and show its activity extends to drug-resistant isolates. These findings both confirm the utility of biofilm-based screening and add a new scaffold to our arsenal of known compounds with antibacterial activity against priority pathogens. Our finding that BAY 11-7082 is a potent inhibitor of MRSA and that it potentiates β -lactams extended our interest in the molecule as a possible adjuvant, especially since few non- β -lactamase inhibitor adjuvants have been identified. In Chapter Three we explore the potential mechanism of synergy. Many known potentiators of β -lactams against MRSA act on WTA biosynthesis. We show that, like these other potentiators, WTA biosynthesis is required for synergy, but, unlike many other previously reported potentiators, it is not required for the compound's activity. This compound may represent a first-in-class potentiator that restores the activity of an inexpensive and effective class of antibiotics.

In Chapter Four, we examine biofilms not only as a screening tool, but as an important factor in infection treatment and prevention. We look specifically at PJIs, finding the common clinical antiseptics chlorhexidine (CHG) and povidone-iodine (PI) inhibit both growth and biofilm formation of priority pathogens, justifying their prophylactic use in joint replacement. We also examine the antibiotic vancomycin, which is increasingly used preventatively at surgical sites, confirming its activity against susceptible species. We showed that subinhibitory concentrations of both the antibiotic and the antiseptics stimulate *P. aeruginosa* biofilm production, making it imperative to determine effective concentration ranges for in-wound use, especially in cases where *P. aeruginosa* may be present.

Chapter Five discusses the importance of measuring biofilm formation. It is key to ensuring antibiotics and antiseptics are used at the correct concentration, since sub-inhibitory concentrations can have the unintended consequence of increasing the proportion of cells in this hard-to-treat growth state. Biofilm-based screening should continue to be used to increase hit rates; our efforts thus far have focused on small molecules, but this method could also be useful in screening natural product extracts, especially since solutions of mixed extracts are typically less active than fractionated samples, meaning their activity is more likely to be missed in a traditional screen. Optimizing this screening approach to look for small molecules or natural products that inhibit *S. aureus* biofilm formation could identify much-needed biofilm inhibitors for use during orthopedic surgeries, decreasing reliance on vancomycin. Lastly, many questions remain about the mechanism(s) of antibacterial activity and β -lactam potentiation of BAY 11-7082 and its related analogues. This chapter discusses the importance of identifying antibiotic adjuvants to extend the lifespan of safe, available, and reliable antibiotics, as opposed to continually developing new antibiotics, and identifies potential next steps to determine where this scaffold fits into the existing body of antibiotic potentiators.

References

- (1) Naghavi, M.; Mestrovic, T.; Gray, A.; Hayoon, A. G.; Swetschinski, L. R.; Aguilar, G. R.; Weaver, N. D.; Ikuta, K. S.; Chung, E.; Wool, E. E.; Han, C.; Araki, D. T.; Albertson, S. B.; Bender, R.; Bertolacci, G.; Browne, A. J.; Cooper, B. S.; Cunningham, M. W.; Dolecek, C.; Doxey, M.; Dunachie, S. J.; Ghoba, S.; Haines-Woodhouse, G.; Hay, S. I.; Hsu, R. L.; Iregbu, K. C.; Kyu, H. H.; Ledesma, J. R.; Ma, J.; Moore, C. E.; Mosser, J. F.; Mouglin, V.; Naghavi, P.; Novotney, A.; Rosenthal, V. D.; Sartorius, B.; Stergachis, A.; Troeger, C.; Vongpradith, A.; Walters, M. K.; Wunrow, H. Y.; Murray, C. J. Global Burden Associated with 85 Pathogens in 2019: A Systematic Analysis for the Global Burden of Disease Study 2019. *Lancet Infect. Dis.* **2024**, 0 (0). [https://doi.org/10.1016/S1473-3099\(24\)00158-0](https://doi.org/10.1016/S1473-3099(24)00158-0).
- (2) De Oliveira, D. M. P.; Forde, B. M.; Kidd, T. J.; Harris, P. N. A.; Schembri, M. A.; Beatson, S. A.; Paterson, D. L.; Walker, M. J. Antimicrobial Resistance in ESKAPE

- Pathogens. *Clin. Microbiol. Rev.* **2020**, *33* (3), 10.1128/cmr.00181-19.
<https://doi.org/10.1128/cmr.00181-19>.
- (3) Murray, C. J.; Ikuta, K. S.; Sharara, F.; Swetschinski, L.; Robles Aguilar, G.; Gray, A.; Han, C.; Bisignano, C.; Rao, P.; Wool, E.; Johnson, S. C.; Browne, A. J.; Chipeta, M. G.; Fell, F.; Hackett, S.; Haines-Woodhouse, G.; Kashef Hamadani, B. H.; Kumaran, E. A. P.; McManigal, B.; Agarwal, R.; Akech, S.; Albertson, S.; Amuasi, J.; Andrews, J.; Aravkin, A.; Ashley, E.; Bailey, F.; Baker, S.; Basnyat, B.; Bekker, A.; Bender, R.; Bethou, A.; Bielicki, J.; Boonkasidecha, S.; Bukosia, J.; Carvalheiro, C.; Castañeda-Orjuela, C.; Chansamouth, V.; Chaurasia, S.; Chiurchiù, S.; Chowdhury, F.; Cook, A. J.; Cooper, B.; Cressey, T. R.; Criollo-Mora, E.; Cunningham, M.; Darboe, S.; Day, N. P. J.; De Luca, M.; Dokova, K.; Dramowski, A.; Dunachie, S. J.; Eckmanns, T.; Eibach, D.; Emami, A.; Feasey, N.; Fisher-Pearson, N.; Forrest, K.; Garrett, D.; Gastmeier, P.; Giref, A. Z.; Greer, R. C.; Gupta, V.; Haller, S.; Haselbeck, A.; Hay, S. I.; Holm, M.; Hopkins, S.; Iregbu, K. C.; Jacobs, J.; Jarovsky, D.; Javanmardi, F.; Khorana, M.; Kisson, N.; Kobeissi, E.; Kostyanev, T.; Krapp, F.; Krumkamp, R.; Kumar, A.; Kyu, H. H.; Lim, C.; Limmathurotsakul, D.; Loftus, M. J.; Lunn, M.; Ma, J.; Mturi, N.; Munera-Huertas, T.; Musicha, P.; Mussi-Pinhata, M. M.; Nakamura, T.; Nanavati, R.; Nangia, S.; Newton, P.; Ngoun, C.; Novotney, A.; Nwakanma, D.; Obiero, C. W.; Olivás-Martínez, A.; Olliaro, P.; Ooko, E.; Ortiz-Brizuela, E.; Peleg, A. Y.; Perrone, C.; Plakkal, N.; Ponce-de-Leon, A.; Raad, M.; Ramdin, T.; Riddell, A.; Roberts, T.; Robotham, J. V.; Roca, A.; Rudd, K. E.; Russell, N.; Schnall, J.; Scott, J. A. G.; Shivamallappa, M.; Sifuentes-Osornio, J.; Steenkeste, N.; Stewardson, A. J.; Stoeva, T.; Tasak, N.; Thaiprakong, A.; Thwaites, G.; Turner, C.; Turner, P.; van Doorn, H. R.; Velaphi, S.; Vongpradith, A.; Vu, H.; Walsh, T.; Waner, S.; Wangrangsimakul, T.; Wozniak, T.; Zheng, P.; Sartorius, B.; Lopez, A. D.; Stergachis, A.; Moore, C.; Dolecek, C.; Naghavi, M. Global Burden of Bacterial Antimicrobial Resistance in 2019: A Systematic Analysis. *The Lancet* **2022**.
[https://doi.org/10.1016/S0140-6736\(21\)02724-0](https://doi.org/10.1016/S0140-6736(21)02724-0).
- (4) The Council of Canadian Academies. *When Antibiotics Fail: The Expert Panel on the Potential Socio-Economic Impacts of Antimicrobial Resistance in Canada*; 2019.
<https://cca-reports.ca/wp-content/uploads/2018/10/When-Antibiotics-Fail.pdf> (accessed 2019-11-18).
- (5) Walsh, C.; Wencewicz, T. *Antibiotics: Challenges, Mechanisms, Opportunities*; John Wiley & Sons, 2020.
- (6) Brown, E. D.; Wright, G. D. Antibacterial Drug Discovery in the Resistance Era. *Nature* **2016**, *529* (7586), 336–343. <https://doi.org/10.1038/nature17042>.
- (7) Wright, G. D. Molecular Mechanisms of Antibiotic Resistance. *Chem. Commun.* **2011**, *47* (14), 4055–4061. <https://doi.org/10.1039/C0CC05111J>.
- (8) Waglechner, N.; McArthur, A. G.; Wright, G. D. Phylogenetic Reconciliation Reveals the Natural History of Glycopeptide Antibiotic Biosynthesis and Resistance. *Nat. Microbiol.* **2019**, *4* (11), 1862–1871. <https://doi.org/10.1038/s41564-019-0531-5>.
- (9) Barlow, M.; Hall, B. G. Phylogenetic Analysis Shows That the OXA B-Lactamase Genes Have Been on Plasmids for Millions of Years. *J. Mol. Evol.* **2002**, *55* (3), 314–321.
<https://doi.org/10.1007/s00239-002-2328-y>.
- (10) D'Costa, V. M.; King, C. E.; Kalan, L.; Morar, M.; Sung, W. W. L.; Schwarz, C.; Froese, D.; Zazula, G.; Calmels, F.; Debruyne, R.; Golding, G. B.; Poinar, H. N.; Wright, G. D.

- Antibiotic Resistance Is Ancient. *Nature* **2011**, 477 (7365), 457–461.
<https://doi.org/10.1038/nature10388>.
- (11) Andersson, D. I.; Hughes, D. Persistence of Antibiotic Resistance in Bacterial Populations. *FEMS Microbiol. Rev.* **2011**, 35 (5), 901–911. <https://doi.org/10.1111/j.1574-6976.2011.00289.x>.
- (12) Zhanel, G. G.; DeCorby, M.; Laing, N.; Weshnoweski, B.; Vashisht, R.; Tailor, F.; Nichol, K. A.; Wierzbowski, A.; Baudry, P. J.; Karlowsky, J. A.; Lagacé-Wiens, P.; Walkty, A.; McCracken, M.; Mulvey, M. R.; Johnson, J.; The Canadian Antimicrobial Resistance Alliance (CARA); Hoban, D. J. Antimicrobial-Resistant Pathogens in Intensive Care Units in Canada: Results of the Canadian National Intensive Care Unit (CAN-ICU) Study, 2005-2006. *Antimicrob. Agents Chemother.* **2008**, 52 (4), 1430–1437.
<https://doi.org/10.1128/aac.01538-07>.
- (13) Vollmer, W.; Blanot, D.; De Pedro, M. A. Peptidoglycan Structure and Architecture. *FEMS Microbiol. Rev.* **2008**, 32 (2), 149–167. <https://doi.org/10.1111/j.1574-6976.2007.00094.x>.
- (14) van Heijenoort, J. Recent Advances in the Formation of the Bacterial Peptidoglycan Monomer Unit. *Nat. Prod. Rep.* **2001**, 18 (5), 503–519.
<https://doi.org/10.1039/A804532A>.
- (15) Rohs, P. D. A.; Bernhardt, T. G. Growth and Division of the Peptidoglycan Matrix. *Annu. Rev. Microbiol.* **2021**, 75 (Volume 75, 2021), 315–336. <https://doi.org/10.1146/annurev-micro-020518-120056>.
- (16) Meeske, A. J.; Riley, E. P.; Robins, W. P.; Uehara, T.; Mekalanos, J. J.; Kahne, D.; Walker, S.; Kruse, A. C.; Bernhardt, T. G.; Rudner, D. Z. SEDS Proteins Are a Widespread Family of Bacterial Cell Wall Polymerases. *Nature* **2016**, 537 (7622), 634–638. <https://doi.org/10.1038/nature19331>.
- (17) Reichmann, N. T.; Tavares, A. C.; Saraiva, B. M.; Jouselin, A.; Reed, P.; Pereira, A. R.; Monteiro, J. M.; Sobral, R. G.; VanNieuwenhze, M. S.; Fernandes, F.; Pinho, M. G. SEDS–bPBP Pairs Direct Lateral and Septal Peptidoglycan Synthesis in *Staphylococcus aureus*. *Nat. Microbiol.* **2019**, 4 (8), 1368–1377. <https://doi.org/10.1038/s41564-019-0437-2>.
- (18) Taguchi, A.; Welsh, M. A.; Marmont, L. S.; Lee, W.; Sjodt, M.; Kruse, A. C.; Kahne, D.; Bernhardt, T. G.; Walker, S. FtsW Is a Peptidoglycan Polymerase That Is Functional Only in Complex with Its Cognate Penicillin-Binding Protein. *Nat. Microbiol.* **2019**, 4 (4), 587–594. <https://doi.org/10.1038/s41564-018-0345-x>.
- (19) Cho, H.; Wivagg, C. N.; Kapoor, M.; Barry, Z.; Rohs, P. D. A.; Suh, H.; Marto, J. A.; Garner, E. C.; Bernhardt, T. G. Bacterial Cell Wall Biogenesis Is Mediated by SEDS and PBP Polymerase Families Functioning Semi-Autonomously. *Nat. Microbiol.* **2016**, 1 (10), 1–8. <https://doi.org/10.1038/nmicrobiol.2016.172>.
- (20) Schneider, T.; Senn, M. M.; Berger-Bächi, B.; Tossi, A.; Sahl, H.-G.; Wiedemann, I. In Vitro Assembly of a Complete, Pentaglycine Interpeptide Bridge Containing Cell Wall Precursor (Lipid II-Gly5) of *Staphylococcus aureus*. *Mol. Microbiol.* **2004**, 53 (2), 675–685. <https://doi.org/10.1111/j.1365-2958.2004.04149.x>.
- (21) Rohrer, S.; Berger-Bächi, B. FemABX Peptidyl Transferases: A Link between Branched-Chain Cell Wall Peptide Formation and β -Lactam Resistance in Gram-Positive Cocci. *Antimicrob. Agents Chemother.* **2003**, 47 (3), 837–846.
<https://doi.org/10.1128/aac.47.3.837-846.2003>.

- (22) Swoboda, J. G.; Campbell, J.; Meredith, T. C.; Walker, S. Wall Teichoic Acid Function, Biosynthesis, and Inhibition. *ChemBioChem* **2010**, *11* (1), 35–45. <https://doi.org/10.1002/cbic.200900557>.
- (23) Brown, S.; Santa Maria, J. P.; Walker, S. Wall Teichoic Acids of Gram-Positive Bacteria. *Annu. Rev. Microbiol.* **2013**, *67*, 10.1146/annurev-micro-092412–155620. <https://doi.org/10.1146/annurev-micro-092412-155620>.
- (24) Atilano, M. L.; Pereira, P. M.; Yates, J.; Reed, P.; Veiga, H.; Pinho, M. G.; Filipe, S. R. Teichoic Acids Are Temporal and Spatial Regulators of Peptidoglycan Cross-Linking in *Staphylococcus aureus*. *Proc. Natl. Acad. Sci.* **2010**, *107* (44), 18991–18996. <https://doi.org/10.1073/pnas.1004304107>.
- (25) Qamar, A.; Golemi-Kotra, D. Dual Roles of FmtA in *Staphylococcus Aureus* Cell Wall Biosynthesis and Autolysis. *Antimicrob. Agents Chemother.* **2012**, *56* (7), 3797–3805. <https://doi.org/10.1128/aac.00187-12>.
- (26) D'Elia, M. A.; Millar, K. E.; Beveridge, T. J.; Brown, E. D. Wall Teichoic Acid Polymers Are Dispensable for Cell Viability in *Bacillus subtilis*. *J. Bacteriol.* **2006**, *188* (23), 8313–8316. <https://doi.org/10.1128/jb.01336-06>.
- (27) Bhavsar, A. P.; Beveridge, T. J.; Brown, E. D. Precise Deletion of tagD and Controlled Depletion of Its Product, Glycerol 3-Phosphate Cytidylyltransferase, Leads to Irregular Morphology and Lysis of *Bacillus subtilis* Grown at Physiological Temperature. *J. Bacteriol.* **2001**, *183* (22), 6688–6693. <https://doi.org/10.1128/jb.183.22.6688-6693.2001>.
- (28) Bera, A.; Biswas, R.; Herbert, S.; Kulauzovic, E.; Weidenmaier, C.; Peschel, A.; Götz, F. Influence of Wall Teichoic Acid on Lysozyme Resistance in *Staphylococcus aureus*. *J. Bacteriol.* **2007**, *189* (1), 280–283. <https://doi.org/10.1128/jb.01221-06>.
- (29) Xia, G.; Kohler, T.; Peschel, A. The Wall Teichoic Acid and Lipoteichoic Acid Polymers of *Staphylococcus aureus*. *Int. J. Med. Microbiol.* **2010**, *300* (2), 148–154. <https://doi.org/10.1016/j.ijmm.2009.10.001>.
- (30) Sarkar, P.; Yarlagadda, V.; Ghosh, C.; Haldar, J. A Review on Cell Wall Synthesis Inhibitors with an Emphasis on Glycopeptide Antibiotics. *MedChemComm* **2017**, *8* (3), 516–533. <https://doi.org/10.1039/c6md00585c>.
- (31) Silver, L. L. Fosfomycin: Mechanism and Resistance. *Cold Spring Harb. Perspect. Med.* **2017**, *7* (2), a025262. <https://doi.org/10.1101/cshperspect.a025262>.
- (32) Lambert, M. P.; Neuhaus, F. C. Mechanism of D-Cycloserine Action: Alanine Racemase from *Escherichia coli*. *J. Bacteriol.* **1972**, *110* (3), 978–987. <https://doi.org/10.1128/jb.110.3.978-987.1972>.
- (33) Hakulinen, J. K.; Hering, J.; Brändén, G.; Chen, H.; Snijder, A.; Ek, M.; Johansson, P. MraY–Antibiotic Complex Reveals Details of Tunicamycin Mode of Action. *Nat. Chem. Biol.* **2017**, *13* (3), 265–267. <https://doi.org/10.1038/nchembio.2270>.
- (34) Campbell, J.; Singh, A. K.; Santa Maria, J. P.; Kim, Y.; Brown, S.; Swoboda, J. G.; Mylonakis, E.; Wilkinson, B. J.; Walker, S. Synthetic Lethal Compound Combinations Reveal a Fundamental Connection between Wall Teichoic Acid and Peptidoglycan Biosyntheses in *Staphylococcus aureus*. *ACS Chem. Biol.* **2011**, *6* (1), 106–116. <https://doi.org/10.1021/cb100269f>.
- (35) Crosby, M.; von den Baumen, T. R.; Chu, C.; Gomes, T.; Schwartz, K. L.; Tadrous, M. Interprovincial Variation in Antibiotic Use in Canada, 2019: A Retrospective Cross-Sectional Study. *CMAJ Open* **2022**, *10* (1), E262–E268. <https://doi.org/10.9778/cmajo.20210095>.

- (36) Cho, H.; Uehara, T.; Bernhardt, T. G. Beta-Lactam Antibiotics Induce a Lethal Malfunctioning of the Bacterial Cell Wall Synthesis Machinery. *Cell* **2014**, *159* (6), 1300–1311. <https://doi.org/10.1016/j.cell.2014.11.017>.
- (37) Lister, P. D.; Wolter, D. J.; Hanson, N. D. Antibacterial-Resistant *Pseudomonas aeruginosa*: Clinical Impact and Complex Regulation of Chromosomally Encoded Resistance Mechanisms. *Clin. Microbiol. Rev.* **2009**, *22* (4), 582–610. <https://doi.org/10.1128/cmr.00040-09>.
- (38) Olsen, J. E.; Christensen, H.; Aarestrup, F. M. Diversity and Evolution of bla_Z from *Staphylococcus aureus* and Coagulase-Negative Staphylococci. *J. Antimicrob. Chemother.* **2006**, *57* (3), 450–460. <https://doi.org/10.1093/jac/dki492>.
- (39) Drawz, S. M.; Bonomo, R. A. Three Decades of β -Lactamase Inhibitors. *Clin. Microbiol. Rev.* **2010**, *23* (1), 160–201. <https://doi.org/10.1128/cmr.00037-09>.
- (40) Neu, H. C.; Fu, K. P. Clavulanic Acid, a Novel Inhibitor of β -Lactamases. *Antimicrob. Agents Chemother.* **1978**, *14* (5), 650–655. <https://doi.org/10.1128/aac.14.5.650>.
- (41) Tomasz, A.; Drugeon, H. B.; de Lencastre, H. M.; Jabes, D.; McDougall, L.; Bille, J. New Mechanism for Methicillin Resistance in *Staphylococcus aureus*: Clinical Isolates That Lack the PBP 2a Gene and Contain Normal Penicillin-Binding Proteins with Modified Penicillin-Binding Capacity. *Antimicrob. Agents Chemother.* **1989**, *33* (11), 1869–1874. <https://doi.org/10.1128/aac.33.11.1869>.
- (42) Hiramatsu, K.; Cui, L.; Kuroda, M.; Ito, T. The Emergence and Evolution of Methicillin-Resistant *Staphylococcus aureus*. *Trends Microbiol.* **2001**, *9* (10), 486–493. [https://doi.org/10.1016/S0966-842X\(01\)02175-8](https://doi.org/10.1016/S0966-842X(01)02175-8).
- (43) Roemer, T.; Schneider, T.; Pinho, M. G. Auxiliary Factors: A Chink in the Armor of MRSA Resistance to β -Lactam Antibiotics. *Curr. Opin. Microbiol.* **2013**, *16* (5), 538–548. <https://doi.org/10.1016/j.mib.2013.06.012>.
- (44) Wang, Q. M.; Peery, R. B.; Johnson, R. B.; Alborn, W. E.; Yeh, W.-K.; Skatrud, P. L. Identification and Characterization of a Monofunctional Glycosyltransferase from *Staphylococcus aureus*. *J. Bacteriol.* **2001**, *183* (16), 4779–4785. <https://doi.org/10.1128/JB.183.16.4779-4785.2001>.
- (45) Rebets, Y.; Lupoli, T.; Qiao, Y.; Schirner, K.; Villet, R.; Hooper, D.; Kahne, D.; Walker, S. Moenomycin Resistance Mutations in *Staphylococcus aureus* Reduce Peptidoglycan Chain Length and Cause Aberrant Cell Division. *ACS Chem. Biol.* **2014**, *9* (2), 459–467. <https://doi.org/10.1021/cb4006744>.
- (46) Pinho, M. G.; Lencastre, H. de; Tomasz, A. An Acquired and a Native Penicillin-Binding Protein Cooperate in Building the Cell Wall of Drug-Resistant Staphylococci. *Proc. Natl. Acad. Sci.* **2001**, *98* (19), 10886–10891. <https://doi.org/10.1073/pnas.191260798>.
- (47) Ostash, B.; Walker, S. Moenomycin Family Antibiotics : Chemical Synthesis, Biosynthesis , and Biological Activity. *Nat. Prod. Rep.* **2010**, *27* (11), 1594–1617. <https://doi.org/10.1039/C001461N>.
- (48) Courvalin, P. Vancomycin Resistance in Gram-Positive Cocci. *Clin. Infect. Dis.* **2006**, *42* (Supplement_1), S25–S34. <https://doi.org/10.1086/491711>.
- (49) Leclercq, R.; Derlot, E.; Duval, J.; Courvalin, P. Plasmid-Mediated Resistance to Vancomycin and Teicoplanin in *Enterococcus faecium*. *N. Engl. J. Med.* **1988**, *319* (3), 157–161. <https://doi.org/10.1056/NEJM198807213190307>.

- (50) Marshall, C. G.; Lessard, I. A. D.; Park, I.-S.; Wright, G. D. Glycopeptide Antibiotic Resistance Genes in Glycopeptide-Producing Organisms. *Antimicrob. Agents Chemother.* **1998**, *42* (9), 2215–2220. <https://doi.org/10.1128/aac.42.9.2215>.
- (51) Hiramatsu, K.; Aritaka, N.; Hanaki, H.; Kawasaki, S.; Hosoda, Y.; Hori, S.; Fukuchi, Y.; Kobayashi, I. Dissemination in Japanese Hospitals of Strains of *Staphylococcus aureus* Heterogeneously Resistant to Vancomycin. *The Lancet* **1997**, *350* (9092), 1670–1673. [https://doi.org/10.1016/S0140-6736\(97\)07324-8](https://doi.org/10.1016/S0140-6736(97)07324-8).
- (52) Gardete, S.; Tomasz, A. Mechanisms of Vancomycin Resistance in *Staphylococcus aureus*. *J. Clin. Invest.* **2014**, *124* (7), 2836–2840. <https://doi.org/10.1172/JCI68834>.
- (53) Sievert, D. M.; Rudrik, J. T.; Patel, J. B.; McDonald, L. C.; Wilkins, M. J.; Hageman, J. C. Vancomycin-Resistant *Staphylococcus aureus* in the United States, 2002–2006. *Clin. Infect. Dis.* **2008**, *46* (5), 668–674. <https://doi.org/10.1086/527392>.
- (54) Pogue, J. M.; Kaye, K. S.; Cohen, D. A.; Marchaim, D. Appropriate Antimicrobial Therapy in the Era of Multidrug-Resistant Human Pathogens. *Clin. Microbiol. Infect.* **2015**, *21* (4), 302–312. <https://doi.org/10.1016/j.cmi.2014.12.025>.
- (55) Bakhsheshian, J.; Dahdaleh, N. S.; Lam, S. K.; Savage, J. W.; Smith, Z. A. The Use of Vancomycin Powder in Modern Spine Surgery: Systematic Review and Meta-Analysis of the Clinical Evidence. *World Neurosurg.* **2015**, *83* (5), 816–823. <https://doi.org/10.1016/j.wneu.2014.12.033>.
- (56) Iorio, R.; Yu, S.; Anoushiravani, A. A.; Riesgo, A. M.; Park, B.; Vigdorichik, J.; Slover, J.; Long, W. J.; Schwarzkopf, R. Vancomycin Powder and Dilute Povidone-Iodine Lavage for Infection Prophylaxis in High-Risk Total Joint Arthroplasty. *J. Arthroplasty* **2020**, *35* (7), 1933–1936. <https://doi.org/10.1016/j.arth.2020.02.060>.
- (57) Muñoz, K. A.; Hergenrother, P. J. Facilitating Compound Entry as a Means to Discover Antibiotics for Gram-Negative Bacteria. *Acc. Chem. Res.* **2021**, *54* (6), 1322–1333. <https://doi.org/10.1021/acs.accounts.0c00895>.
- (58) Richter, M. F.; Drown, B. S.; Riley, A. P.; Garcia, A.; Shirai, T.; Svec, R. L.; Hergenrother, P. J. Predictive Compound Accumulation Rules Yield a Broad-Spectrum Antibiotic. *Nature* **2017**, *545* (7654), 299–304. <https://doi.org/10.1038/nature22308>.
- (59) Yaeger, L. N.; Coles, V. E.; Chan, D. C. K.; Burrows, L. L. How to Kill *Pseudomonas* — Emerging Therapies for a Challenging Pathogen. *Ann. N. Y. Acad. Sci.* **2021**, *1496* (1), 59–81. <https://doi.org/10.1111/nyas.14596>.
- (60) Ceri, H.; Olson, M. E.; Stremick, C.; Read, R. R.; Morck, D.; Buret, A. The Calgary Biofilm Device: New Technology for Rapid Determination of Antibiotic Susceptibilities of Bacterial Biofilms. *J. Clin. Microbiol.* **1999**, *37* (6), 1771–1776. <https://doi.org/10.1128/JCM.37.6.1771-1776.1999>.
- (61) Lewis, K. Riddle of Biofilm Resistance. *Antimicrob. Agents Chemother.* **2001**, *45* (4), 999–1007. <https://doi.org/10.1128/AAC.45.4.999-1007.2001>.
- (62) O’Toole, G. A.; Kolter, R. Flagellar and Twitching Motility Are Necessary for *Pseudomonas aeruginosa* Biofilm Development. *Mol. Microbiol.* **1998**, *30* (2), 295–304. <https://doi.org/10.1046/j.1365-2958.1998.01062.x>.
- (63) Ha, D.-G.; O’Toole, G. A. C-Di-GMP and Its Effects on Biofilm Formation and Dispersion: A *Pseudomonas aeruginosa* Review. *Microbiol. Spectr.* **2015**. <https://doi.org/10.1128/microbiolspec.MB-0003-2014>.

- (64) Chan, C.; Paul, R.; Samoray, D.; Amiot, N. C.; Giese, B.; Jenal, U.; Schirmer, T. Structural Basis of Activity and Allosteric Control of Diguanylate Cyclase. *Proc. Natl. Acad. Sci.* **2004**, *101* (49), 17084–17089. <https://doi.org/10.1073/pnas.0406134101>.
- (65) Friedman, L.; Kolter, R. Two Genetic Loci Produce Distinct Carbohydrate-Rich Structural Components of the *Pseudomonas aeruginosa* Biofilm Matrix. *J. Bacteriol.* **2004**. <https://doi.org/10.1128/JB.186.14.4457-4465.2004>.
- (66) Wozniak, D. J.; Wyckoff, T. J. O.; Starkey, M.; Keyser, R.; Azadi, P.; O’Toole, G. A.; Parsek, M. R. Alginate Is Not a Significant Component of the Extracellular Polysaccharide Matrix of PA14 and PAO1 *Pseudomonas aeruginosa* Biofilms. *Proc. Natl. Acad. Sci.* **2003**, *100* (13), 7907–7912. <https://doi.org/10.1073/pnas.1231792100>.
- (67) Sauer, K.; Cullen, M. C.; Rickard, A. H.; Zeef, L. A. H.; Davies, D. G.; Gilbert, P. Characterization of Nutrient-Induced Dispersion in *Pseudomonas aeruginosa* PAO1 Biofilm. *J. Bacteriol.* **2004**. <https://doi.org/10.1128/JB.186.21.7312-7326.2004>.
- (68) Barraud, N.; Schleheck, D.; Klebensberger, J.; Webb, J. S.; Hassett, D. J.; Rice, S. A.; Kjelleberg, S. Nitric Oxide Signaling in *Pseudomonas aeruginosa* Biofilms Mediates Phosphodiesterase Activity, Decreased Cyclic Di-GMP Levels, and Enhanced Dispersal. *J. Bacteriol.* **2009**. <https://doi.org/10.1128/JB.00975-09>.
- (69) Singh, P. K.; Parsek, M. R.; Greenberg, E. P.; Welsh, M. J. A Component of Innate Immunity Prevents Bacterial Biofilm Development. *Nature* **2002**, *417* (6888), 552–555. <https://doi.org/10.1038/417552a>.
- (70) Patriquin, G. M.; Banin, E.; Gilmour, C.; Tuchman, R.; Greenberg, E. P.; Poole, K. Influence of Quorum Sensing and Iron on Twitching Motility and Biofilm Formation in *Pseudomonas aeruginosa*. *J. Bacteriol.* **2008**. <https://doi.org/10.1128/JB.01473-07>.
- (71) Otto, M. Staphylococcal Biofilms. In *Bacterial Biofilms*; Romeo, T., Ed.; Springer: Berlin, Heidelberg, 2008; pp 207–228. https://doi.org/10.1007/978-3-540-75418-3_10.
- (72) Berry, K. A.; Verhoef, M. T. A.; Leonard, A. C.; Cox, G. *Staphylococcus aureus* Adhesion to the Host. *Ann. N. Y. Acad. Sci.* **2022**, *1515* (1), 75–96. <https://doi.org/10.1111/nyas.14807>.
- (73) Hall-Stoodley, L.; Stoodley, P. Evolving Concepts in Biofilm Infections. *Cell. Microbiol.* **2009**, *11* (7), 1034–1043. <https://doi.org/10.1111/j.1462-5822.2009.01323.x>.
- (74) Orazi, G.; O’Toole, G. A. “It Takes a Village”: Mechanisms Underlying Antimicrobial Recalcitrance of Polymicrobial Biofilms. *J. Bacteriol.* **2019**, *202* (1), 10.1128/jb.00530-19. <https://doi.org/10.1128/jb.00530-19>.
- (75) Flurin, L.; Greenwood-Quaintance, K. E.; Patel, R. Microbiology of Polymicrobial Prosthetic Joint Infection. *Diagn. Microbiol. Infect. Dis.* **2019**, *94* (3), 255–259. <https://doi.org/10.1016/j.diagmicrobio.2019.01.006>.
- (76) Koo, H.; Allan, R. N.; Howlin, R. P.; Stoodley, P.; Hall-Stoodley, L. Targeting Microbial Biofilms: Current and Prospective Therapeutic Strategies. *Nat. Rev. Microbiol.* **2017**, *15* (12), 740–755. <https://doi.org/10.1038/nrmicro.2017.99>.
- (77) Høiby, N.; Bjarnsholt, T.; Moser, C.; Bassi, G. L.; Coenye, T.; Donelli, G.; Hall-Stoodley, L.; Holá, V.; Imbert, C.; Kirketerp-Møller, K.; Lebeaux, D.; Oliver, A.; Ullmann, A. J.; Williams, C. ESCMID Guideline for the Diagnosis and Treatment of Biofilm Infections 2014. *Clin. Microbiol. Infect.* **2015**, *21*, S1–S25. <https://doi.org/10.1016/j.cmi.2014.10.024>.

- (78) Tande, A. J.; Gomez-Urena, E. O.; Barbari, E. F.; Osmon, D. R. Management of Prosthetic Joint Infection. *Infect. Dis. Clin. North Am.* **2017**, *31* (2), 237–252. <https://doi.org/10.1016/j.idc.2017.01.009>.
- (79) Gehrke, T.; Alijanipour, P.; Parvizi, J. The Management of an Infected Total Knee Arthroplasty. *Bone Jt. J.* **2015**, *97-B* (10_Supple_A), 20–29. <https://doi.org/10.1302/0301-620x.97b10.36475>.
- (80) Darouiche, R.; Mosier, M.; Voigt, J. Antibiotics and Antiseptics to Prevent Infection in Cardiac Rhythm Management Device Implantation Surgery. *Pacing Clin. Electrophysiol.* **2012**, *35* (11), 1348–1360. <https://doi.org/10.1111/j.1540-8159.2012.03506.x>.
- (81) Starkey, M.; Lepine, F.; Maura, D.; Bandyopadhyaya, A.; Lesic, B.; He, J.; Kitao, T.; Righi, V.; Milot, S.; Tzika, A.; Rahme, L. Identification of Anti-Virulence Compounds That Disrupt Quorum-Sensing Regulated Acute and Persistent Pathogenicity. *PLoS Pathog.* **2014**, *10* (8), e1004321. <https://doi.org/10.1371/journal.ppat.1004321>.
- (82) Kaneko, Y.; Thoendel, M.; Olakanmi, O.; Britigan, B. E.; Singh, P. K. The Transition Metal Gallium Disrupts *Pseudomonas aeruginosa* Iron Metabolism and Has Antimicrobial and Antibiofilm Activity. *J. Clin. Invest.* **2007**, *117* (4), 877–888. <https://doi.org/10.1172/JCI30783>.
- (83) Sambanthamoorthy, K.; Sloup, R. E.; Parashar, V.; Smith, J. M.; Kim, E. E.; Semmelhack, M. F.; Neiditch, M. B.; Waters, C. M. Identification of Small Molecules That Antagonize Diguanylate Cyclase Enzymes to Inhibit Biofilm Formation. *Antimicrob. Agents Chemother.* **2012**, *56* (10), 5202–5211. <https://doi.org/10.1128/AAC.01396-12>.
- (84) Duffy, E. M.; Buurman, E. T.; Chiang, S. L.; Cohen, N. R.; Uria-Nickelsen, M.; Alm, R. A. The CARB-X Portfolio of Nontraditional Antibacterial Products. *ACS Infect. Dis.* **2021**, *7* (8), 2043–2049. <https://doi.org/10.1021/acsinfecdis.1c00331>.
- (85) Ranieri, M. R.; Whitchurch, C. B.; Burrows, L. L. Mechanisms of Biofilm Stimulation by Subinhibitory Concentrations of Antimicrobials. *Curr. Opin. Microbiol.* **2018**, *45*, 164–169. <https://doi.org/10.1016/j.mib.2018.07.006>.
- (86) Yaeger, L. N.; Ranieri, M. R. M.; Chee, J.; Karabelas-Pittman, S.; Rudolph, M.; Giovannoni, A. M.; Harvey, H.; Burrows, L. L. A Genetic Screen Identifies a Role for oprF in *Pseudomonas aeruginosa* Biofilm Stimulation by Subinhibitory Antibiotics. *Npj Biofilms Microbiomes* **2024**, *10* (1), 1–12. <https://doi.org/10.1038/s41522-024-00496-7>.
- (87) Bleich, R.; Watrous, J. D.; Dorrestein, P. C.; Bowers, A. A.; Shank, E. A. Thiopeptide Antibiotics Stimulate Biofilm Formation in *Bacillus Subtilis*. *Proc. Natl. Acad. Sci.* **2015**, *112* (10), 3086–3091. <https://doi.org/10.1073/pnas.1414272112>.
- (88) Coenye, T. Biofilm Antimicrobial Susceptibility Testing: Where Are We and Where Could We Be Going? *Clin. Microbiol. Rev.* **2023**, *36* (4), e00024-23. <https://doi.org/10.1128/cmr.00024-23>.
- (89) *Bad Bugs, No Drugs: As Antibiotic Discovery Stagnates...a Public Health Crisis Brews*; Infectious Diseases Society of America, 2004.
- (90) Spellberg, B.; Powers, J. H.; Brass, E. P.; Miller, L. G.; Edwards, J. E. Trends in Antimicrobial Drug Development: Implications for the Future. *Clin. Infect. Dis.* **2004**, *38* (9), 1279–1286. <https://doi.org/10.1086/420937>.
- (91) Talbot, G. H.; Bradley, J.; Edwards, J. E., Jr.; Gilbert, D.; Scheld, M.; Bartlett, J. G. Bad Bugs Need Drugs: An Update on the Development Pipeline from the Antimicrobial Availability Task Force of the Infectious Diseases Society of America. *Clin. Infect. Dis.* **2006**, *42* (5), 657–668. <https://doi.org/10.1086/499819>.

- (92) Spellberg, B.; Guidos, R.; Gilbert, D.; Bradley, J.; Boucher, H. W.; Scheld, W. M.; Bartlett, J. G.; Edwards, J., Jr; the Infectious Diseases Society of America. The Epidemic of Antibiotic-Resistant Infections: A Call to Action for the Medical Community from the Infectious Diseases Society of America. *Clin. Infect. Dis.* **2008**, *46* (2), 155–164. <https://doi.org/10.1086/524891>.
- (93) Boucher, H. W.; Talbot, G. H.; Bradley, J. S.; Edwards, J. E.; Gilbert, D.; Rice, L. B.; Scheld, M.; Spellberg, B.; Bartlett, J. Bad Bugs, No Drugs: No ESKAPE! An Update from the Infectious Diseases Society of America. *Clin. Infect. Dis.* **2009**, *48* (1), 1–12. <https://doi.org/10.1086/595011>.
- (94) Bush, K.; Courvalin, P.; Dantas, G.; Davies, J.; Eisenstein, B.; Huovinen, P.; Jacoby, G. A.; Kishony, R.; Kreiswirth, B. N.; Kutter, E.; Lerner, S. A.; Levy, S.; Lewis, K.; Lomovskaya, O.; Miller, J. H.; Mobashery, S.; Piddock, L. J. V.; Projan, S.; Thomas, C. M.; Tomasz, A.; Tulkens, P. M.; Walsh, T. R.; Watson, J. D.; Witkowski, J.; Witte, W.; Wright, G.; Yeh, P.; Zgurskaya, H. I. Tackling Antibiotic Resistance. *Nat. Rev. Microbiol.* **2011**, *9* (12), 894–896. <https://doi.org/10.1038/nrmicro2693>.
- (95) Boucher, H. W. Bad Bugs, No Drugs 2002–2020: Progress, Challenges, and Call to Action. *Trans. Am. Clin. Climatol. Assoc.* **2020**, *131*, 65–71.
- (96) Cox, G.; Sieron, A.; King, A. M.; Pascale, G. D.; Pawlowski, A. C.; Koteva, K.; Wright, G. D. A Common Platform for Antibiotic Dereplication and Adjuvant Discovery. *Cell Chem. Biol.* **2017**, *24* (1), 98–109. <https://doi.org/10.1016/j.chembiol.2016.11.011>.
- (97) Allen, N. E.; Hobbs, J. N.; Alborn, W. E. Inhibition of Peptidoglycan Biosynthesis in Gram-Positive Bacteria by LY146032. *Antimicrob. Agents Chemother.* **1987**, *31* (7), 1093–1099. <https://doi.org/10.1128/aac.31.7.1093>.
- (98) Brown, E. D.; Wright, G. D. New Targets and Screening Approaches in Antimicrobial Drug Discovery. *Chem. Rev.* **2005**, *105* (2), 759–774. <https://doi.org/10.1021/cr030116o>.
- (99) Martens, E.; Demain, A. L. The Antibiotic Resistance Crisis, with a Focus on the United States. *J. Antibiot. (Tokyo)* **2017**, *70* (5), 520–526. <https://doi.org/10.1038/ja.2017.30>.
- (100) D’Costa, V. M.; McGrann, K. M.; Hughes, D. W.; Wright, G. D. Sampling the Antibiotic Resistome. *Science* **2006**. <https://doi.org/10.1126/science.1120800>.
- (101) Pawlowski, A. C.; Wang, W.; Koteva, K.; Barton, H. A.; McArthur, A. G.; Wright, G. D. A Diverse Intrinsic Antibiotic Resistome from a Cave Bacterium. *Nat. Commun.* **2016**, *7* (1), 13803. <https://doi.org/10.1038/ncomms13803>.
- (102) O’Shea, R.; Moser, H. E. Physicochemical Properties of Antibacterial Compounds: Implications for Drug Discovery. *J. Med. Chem.* **2008**, *51* (10), 2871–2878. <https://doi.org/10.1021/jm700967e>.
- (103) Ruggiu, F.; Yang, S.; Simmons, R. L.; Casarez, A.; Jones, A. K.; Li, C.; Jansen, J. M.; Moser, H. E.; Dean, C. R.; Reck, F.; Lindvall, M. Size Matters and How You Measure It: A Gram-Negative Antibacterial Example Exceeding Typical Molecular Weight Limits. *ACS Infect. Dis.* **2019**, *5* (10), 1688–1692. <https://doi.org/10.1021/acsinfecdis.9b00256>.
- (104) Stokes, J. M.; Yang, K.; Swanson, K.; Jin, W.; Cubillos-Ruiz, A.; Donghia, N. M.; MacNair, C. R.; French, S.; Carfrae, L. A.; Bloom-Ackermann, Z.; Tran, V. M.; Chiappino-Pepe, A.; Badran, A. H.; Andrews, I. W.; Chory, E. J.; Church, G. M.; Brown, E. D.; Jaakkola, T. S.; Barzilay, R.; Collins, J. J. A Deep Learning Approach to Antibiotic Discovery. *Cell* **2020**, *180* (4), 688–702.e13. <https://doi.org/10.1016/j.cell.2020.01.021>.
- (105) Liu, G.; Catacutan, D. B.; Rathod, K.; Swanson, K.; Jin, W.; Mohammed, J. C.; Chiappino-Pepe, A.; Syed, S. A.; Fragis, M.; Rachwalski, K.; Magolan, J.; Surette, M. G.;

- Coombes, B. K.; Jaakkola, T.; Barzilay, R.; Collins, J. J.; Stokes, J. M. Deep Learning-Guided Discovery of an Antibiotic Targeting *Acinetobacter baumannii*. *Nat. Chem. Biol.* **2023**, *19* (11), 1342–1350. <https://doi.org/10.1038/s41589-023-01349-8>.
- (106) Swanson, K.; Liu, G.; Catacutan, D. B.; Arnold, A.; Zou, J.; Stokes, J. M. Generative AI for Designing and Validating Easily Synthesizable and Structurally Novel Antibiotics. *Nat. Mach. Intell.* **2024**, *6* (3), 338–353. <https://doi.org/10.1038/s42256-024-00809-7>.
- (107) Noto Guillen, M.; Li, C.; Rosener, B.; Mitchell, A. Antibacterial Activity of Nonantibiotics Is Orthogonal to Standard Antibiotics. *Science* **2024**, *384* (6691), 93–100. <https://doi.org/10.1126/science.adk7368>.
- (108) Sateriale, A.; Bessoff, K.; Sarkar, I. N.; Huston, C. D. Drug Repurposing: Mining Protozoan Proteomes for Targets of Known Bioactive Compounds. *J. Am. Med. Inform. Assoc.* **2014**, *21* (2), 238–244. <https://doi.org/10.1136/amiajnl-2013-001700>.
- (109) D’Elia, M. A.; Pereira, M. P.; Brown, E. D. Are Essential Genes Really Essential? *Trends Microbiol.* **2009**, *17* (10), 433–438. <https://doi.org/10.1016/j.tim.2009.08.005>.
- (110) Ranieri, M. R. M.; Chan, D. C. K.; Yaeger, L. N.; Rudolph, M.; Karabelas-Pittman, S.; Abdo, H.; Chee, J.; Harvey, H.; Nguyen, U.; Burrows, L. L. Thiostrepton Hijacks Pyoverdine Receptors to Inhibit Growth of *Pseudomonas aeruginosa*. *Antimicrob. Agents Chemother.* **2019**, *63* (9). <https://doi.org/10.1128/AAC.00472-19>.
- (111) Chan, D. C. K.; Dykema, K.; Fatima, M.; Harvey, H.; Qaderi, I.; Burrows, L. L. Nutrient Limitation Sensitizes *Pseudomonas aeruginosa* to Vancomycin. *ACS Infect. Dis.* **2023**, *9* (7), 1408–1423. <https://doi.org/10.1021/acsinfecdis.3c00167>.
- (112) Farha, M. A.; French, S.; Stokes, J. M.; Brown, E. D. Bicarbonate Alters Bacterial Susceptibility to Antibiotics by Targeting the Proton Motive Force. *ACS Infect. Dis.* **2018**, *4* (3), 382–390. <https://doi.org/10.1021/acsinfecdis.7b00194>.
- (113) Farha, M. A.; MacNair, C. R.; Carfrae, L. A.; El Zahed, S. S.; Ellis, M. J.; Tran, H.-K. R.; McArthur, A. G.; Brown, E. D. Overcoming Acquired and Native Macrolide Resistance with Bicarbonate. *ACS Infect. Dis.* **2020**. <https://doi.org/10.1021/acsinfecdis.0c00340>.
- (114) Shlaes, D. M. The Economic Conundrum for Antibacterial Drugs. *Antimicrob. Agents Chemother.* **2019**, *64* (1), 10.1128/aac.02057-19. <https://doi.org/10.1128/aac.02057-19>.
- (115) Glover, R. E.; Singer, A. C.; Roberts, A. P.; Kirchhelle, C. The Antibiotic Subscription Model: Fostering Innovation or Repackaging Old Drugs? *Lancet Microbe* **2023**, *4* (1), e2–e3. [https://doi.org/10.1016/S2666-5247\(22\)00235-X](https://doi.org/10.1016/S2666-5247(22)00235-X).
- (116) Ejim, L.; Farha, M. A.; Falconer, S. B.; Wildenhain, J.; Coombes, B. K.; Tyers, M.; Brown, E. D.; Wright, G. D. Combinations of Antibiotics and Nonantibiotic Drugs Enhance Antimicrobial Efficacy. *Nat. Chem. Biol.* **2011**, *7* (6), 348–350. <https://doi.org/10.1038/nchembio.559>.
- (117) Melander, R. J.; Melander, C. The Challenge of Overcoming Antibiotic Resistance: An Adjuvant Approach? *ACS Infect. Dis.* **2017**, *3* (8), 559–563. <https://doi.org/10.1021/acsinfecdis.7b00071>.
- (118) Wright, G. D. Antibiotic Adjuvants: Rescuing Antibiotics from Resistance. *Trends Microbiol.* **2016**, *24* (11), 862–871. <https://doi.org/10.1016/j.tim.2016.06.009>.
- (119) *Antibiotics Currently in Global Clinical Development*. <http://pew.org/1YkUFkT> (accessed 2024-06-26).
- (120) Farha, M. A.; Leung, A.; Sewell, E. W.; D’Elia, M. A.; Allison, S. E.; Ejim, L.; Pereira, P. M.; Pinho, M. G.; Wright, G. D.; Brown, E. D. Inhibition of WTA Synthesis Blocks the

- Cooperative Action of PBPs and Sensitizes MRSA to β -Lactams. *ACS Chem. Biol.* **2013**, 8 (1), 226–233. <https://doi.org/10.1021/cb300413m>.
- (121) Lee, S. H.; Wang, H.; Labroli, M.; Koseoglu, S.; Zuck, P.; Mayhood, T.; Gill, C.; Mann, P.; Sher, X.; Ha, S.; Yang, S.-W.; Mandal, M.; Yang, C.; Liang, L.; Tan, Z.; Tawa, P.; Hou, Y.; Kuvelkar, R.; DeVito, K.; Wen, X.; Xiao, J.; Batchlett, M.; Balibar, C. J.; Liu, J.; Xiao, J.; Murgolo, N.; Garlisi, C. G.; Sheth, P. R.; Flattery, A.; Su, J.; Tan, C.; Roemer, T. TarO-Specific Inhibitors of Wall Teichoic Acid Biosynthesis Restore β -Lactam Efficacy against Methicillin-Resistant Staphylococci. *Sci. Transl. Med.* **2016**, 8 (329), 329ra32–329ra32. <https://doi.org/10.1126/scitranslmed.aad7364>.
- (122) El-Halfawy, O. M.; Czarny, T. L.; Flannagan, R. S.; Day, J.; Bozelli, J. C.; Kuiack, R. C.; Salim, A.; Eckert, P.; Epanand, R. M.; McGavin, M. J.; Organ, M. G.; Heinrichs, D. E.; Brown, E. D. Discovery of an Antivirulence Compound That Reverses β -Lactam Resistance in MRSA. *Nat. Chem. Biol.* **2020**, 16 (2), 143–149. <https://doi.org/10.1038/s41589-019-0401-8>.
- (123) Farha, M. A.; Czarny, T. L.; Myers, C. L.; Worrall, L. J.; French, S.; Conrady, D. G.; Wang, Y.; Oldfield, E.; Strynadka, N. C. J.; Brown, E. D. Antagonism Screen for Inhibitors of Bacterial Cell Wall Biogenesis Uncovers an Inhibitor of Undecaprenyl Diphosphate Synthase. *Proc. Natl. Acad. Sci.* **2015**, 112 (35), 11048–11053. <https://doi.org/10.1073/pnas.1511751112>.
- (124) Bernal, P.; Lemaire, S.; Pinho, M. G.; Mobashery, S.; Hinds, J.; Taylor, P. W. Insertion of Epicatechin Gallate into the Cytoplasmic Membrane of Methicillin-Resistant *Staphylococcus aureus* Disrupts Penicillin-Binding Protein (PBP) 2a-Mediated β -Lactam Resistance by Delocalizing PBP2. *J. Biol. Chem.* **2010**, 285 (31), 24055–24065. <https://doi.org/10.1074/jbc.M110.114793>.
- (125) Tan, C. M.; Therien, A. G.; Lu, J.; Lee, S. H.; Caron, A.; Gill, C. J.; Lebeau-Jacob, C.; Benton-Perdomo, L.; Monteiro, J. M.; Pereira, P. M.; Elsen, N. L.; Wu, J.; Deschamps, K.; Petcu, M.; Wong, S.; Daigneault, E.; Kramer, S.; Liang, L.; Maxwell, E.; Claveau, D.; Vaillancourt, J.; Skorey, K.; Tam, J.; Wang, H.; Meredith, T. C.; Sillaots, S.; Wang-Jarantow, L.; Ramtohul, Y.; Langlois, E.; Landry, F.; Reid, J. C.; Parthasarathy, G.; Sharma, S.; Baryshnikova, A.; Lumb, K. J.; Pinho, M. G.; Soisson, S. M.; Roemer, T. Restoring Methicillin-Resistant *Staphylococcus aureus* Susceptibility to β -Lactam Antibiotics. *Sci. Transl. Med.* **2012**, 4 (126). <https://doi.org/10.1126/scitranslmed.3003592>.
- (126) Ferrer-González, E.; Kaul, M.; Parhi, A. K.; LaVoie, E. J.; Pilch, D. S. β -Lactam Antibiotics with a High Affinity for PBP2 Act Synergistically with the FtsZ-Targeting Agent TXA707 against Methicillin-Resistant *Staphylococcus aureus*. *Antimicrob. Agents Chemother.* **2017**. <https://doi.org/10.1128/AAC.00863-17>.

Chapter Two: Exploration of BAY 11-7082 as a potential antibiotic

Preface

The work presented in this chapter has been published in:

Coles, V. E.; Darveau, P.; Zhang, X.; Harvey, H.; Henriksbo, B. D.; Yang, A.; Schertzer, J. D.; Magolan, J.; Burrows, L. L. Exploration of BAY 11-7082 as a Potential Antibiotic. *ACS Infect. Dis.* **2022**, 8 (1), 170-182. <https://doi.org/10.1021/acsinfectdis.1c00522>.

Copyright © 2021 American Chemical Society

Permission has been granted by the publisher to reproduce the material herein, in accordance with the ACS' Policy on Theses and Dissertations.

VEC and HH completed antibacterial susceptibility testing. PD, XZ, and VEC completed chemical synthesis, supervised by JM. VEC and BDH conducted the NLRP3 inflammasome assays, supervised by JDS. VEC and AY compiled genetic data related to the resistant mutants. All other experiments were performed by VEC. VEC and LLB wrote the paper, with input from JM and JDS.

Abstract

Exposure of the Gram-negative pathogen *Pseudomonas aeruginosa* to sub-inhibitory concentrations of antibiotics increases formation of biofilms. We exploited this phenotype to identify molecules with potential antimicrobial activity in a biofilm-based high-throughput screen. The anti-inflammatory compound BAY 11-7082 induced dose-dependent biofilm stimulation, indicative of antibacterial activity. We confirmed that BAY 11-7082 inhibits growth of *P. aeruginosa* and other priority pathogens, including methicillin-resistant *Staphylococcus aureus* (MRSA). We synthesized 27 structural analogues, including a series based on the related scaffold 3-(phenylsulfonyl)-2-pyrazinecarbonitrile (PSPC), 10 of which displayed increased anti-*Staphylococcal* activity. Because the parent molecule inhibits the NLR Family Pyrin Domain Containing 3 (NLRP3) inflammasome, we measured the ability of select analogues to reduce IL-1 β production in mammalian macrophages, identifying minor differences in the structure-activity relationship for the anti-inflammatory and antibacterial properties of this scaffold. Although we could evolve stably resistant MRSA mutants with cross resistance to BAY 11-7082 and PSPC, their lack of shared mutations suggested that the two molecules could have multiple targets. Finally, we showed that BAY 11-7082 and its analogues synergize with penicillin G against MRSA, suggesting that this scaffold may serve as an interesting starting point for the development of antibiotic adjuvants.

Keywords

Methicillin-resistant *Staphylococcus aureus*; biofilm; antibiotics; drug discovery

The overuse and misuse of antibiotics has selected for resistant bacteria, increasing the prevalence of drug-resistant infections. As resistance renders standard treatment options less effective, there is a need for the development of novel pharmaceuticals to treat those infections, particularly those caused by the ESKAPE (*Enterococcus faecium*, *Staphylococcus aureus*, *Klebsiella pneumoniae*, *Acinetobacter baumannii*, *Pseudomonas aeruginosa*, and *Enterobacter* species) pathogens.^{1,2} Despite this urgent need, approval of new antimicrobials by the Food and Drug Administration (FDA) has decreased in recent decades, with only nine new antibiotics (rifampin, quinupristin-dalfopristin, moxifloxacin, gatifloxacin, linezolid, ceftidoren pivoxil, ertapenem, gemifloxacin, and daptomycin) approved between 1998-2002.³ The rate of approval increased slightly within the last ten years, with eight new antibiotics or combinations (ceftaroline, fidaxomicin, bedaquiline, dalbavancin, tedizolid, oritavancin, ceftolozane-tazobactam, and ceftazidime-avibactam) being approved between 2010-2015; however, of these, only three (ceftaroline, ceftolozane-tazobactam, and ceftazidime-avibactam) are active against ESKAPE pathogens and only one (bedaquiline, an adenosine triphosphate synthase inhibitor) has a novel mechanism of action, with the rest belonging to established antibiotic classes for which resistance is well characterized.⁴

For the ESKAPE pathogens, development of novel antimicrobials with potent activity against methicillin-resistant *S. aureus* (MRSA) is crucial. Since strains of MRSA are extensively β -lactam resistant, treatment options are scarce. They include vancomycin, daptomycin, linezolid, tetracyclines, and rifampin, though rifampin is given only in combination therapies due to high rates of resistance development.⁵ MRSA isolates resistant to vancomycin, daptomycin, and linezolid have already been observed in the clinic,⁶⁻⁸ and high rates of adverse reactions to

linezolid further complicate treatment.⁹ There is therefore a need for safe, orally available anti-MRSA compounds with novel antimicrobial mechanisms for which resistance has not yet been observed.

Traditional methods for identifying new antibiotics typically involve screening libraries of compounds for growth inhibition, but frequently fail to produce promising hits.¹⁰ Heavily-exploited historic techniques including screening soil extracts for natural products rarely uncover novel molecules, while high-throughput screening using *in vitro* targets often fails to produce hits with significant activity in whole-cell assays.^{11,12} One way to increase the likelihood of uncovering hit compounds is by using bioactive molecules, including drugs approved for non-antibiotic indications, since hit rates are significantly higher.¹³ To increase our chances of identifying new antimicrobials, we developed a biofilm-based assay for high-throughput screening of previously-approved drugs and compounds with known bioactivity. Formation of *P. aeruginosa* biofilms – surface-associated communities of bacteria encased in a self-produced extracellular matrix – acts as a sensitive proxy for detecting antimicrobial activity, since it is stimulated in a dose-dependent manner by sub-inhibitory concentrations of antibiotics.¹⁴ This phenotype allows us to screen compounds for growth inhibition at a low concentration of 10 μ M, while alerting us to compounds that may have antibiotic activity above this concentration. Compounds with weaker antibiotic activity can then be improved through medicinal chemistry optimization, ensuring we miss fewer potential hits.

Using the biofilm stimulation screen, we identified the anti-inflammatory BAY 11-7082 as having antibacterial activity against multiple species, including MRSA. BAY 11-7082 is a

synthetic anti-inflammatory that inhibits the nuclear factor- κ B (NF- κ B) pathway and the NLR Family Pyrin Domain Containing 3 (NLRP3)/caspase-1 inflammasome.^{15,16} It is proposed to act by blocking I κ B- α phosphorylation but may have alternate cellular targets, and its exact mechanism remains unknown.^{15,17} BAY 11-7082 has also been proposed to act on mammalian protein tyrosine phosphatases (PTPs), which are involved in numerous cellular processes.¹⁸ We re-synthesized BAY 11-7082 and began a medicinal chemistry effort to optimize its anti-*Staphylococcal* activity and determine the compound's structure-activity relationship (SAR). We ultimately transitioned to a similar scaffold, 3-(phenylsulfonyl)-2-pyrazinecarbonitrile (PSPC) and identified 10 analogues with improved anti-MRSA activity, validating the utility of biofilm stimulation as a tool for novel antibiotic discovery.

Results

BAY 11-7082 stimulates *P. aeruginosa* biofilm formation and has potent anti-MRSA activity

Using a previously described biofilm assay,^{19,20} we screened a library of 3,921 FDA approved or biologically active compounds. Compounds were screened in duplicate at 10 μ M against *P. aeruginosa* PAO1 in a dilute media comprising 10% lysogeny broth (LB), 90% phosphate buffered saline (PBS) (hereafter 10% LB). The screen yielded 60 compounds that inhibited *P. aeruginosa* growth to less than 50% of the vehicle (DMSO) control, 8 that inhibited biofilm formation to less than 50% of the control, and 60 that stimulated biofilm formation above 200% of the control.²⁰ One of these biofilm stimulators was the anti-inflammatory BAY 11-7082 **1** (Figure 1A), which we explored further here due to its previously unreported antibacterial activity. Using a dose-response assay (Figure 1B), we confirmed that BAY 11-7082 stimulated

biofilm formation at low concentrations and inhibited *P. aeruginosa* growth at higher concentrations.

To explore its antibacterial potency and spectrum of activity more broadly, we determined the minimal inhibitory concentration (MIC) in 10% LB for *P. aeruginosa* plus six other model and priority pathogens: *A. baumannii*, *Bacillus subtilis*, *Escherichia coli*, *K. pneumoniae*, and two strains of MRSA (*S. aureus* 15981 and USA300) (Figure 1C). While BAY 11-7082 displayed modest activity against *P. aeruginosa* (MIC: 100 μ M, 20.73 μ g/mL) and other Gram-negatives, it was particularly potent against Gram-positives, including MRSA (MIC: 0.78 μ M, 0.16 μ g/mL), leading us to focus our efforts on developing BAY 11-7082 as an anti-*Staphylococcal* agent. We also determined the MIC in two standard nutrient-rich growth media, LB and Mueller-Hinton Broth (MHB) (Figure S1). Based on the MIC in MHB, we selected *S. aureus* 15981 over *S. aureus* USA300 as the strain of choice for comparing synthetic analogues, since the lower baseline MIC would allow us to see a greater range of activities.

To test whether BAY 11-7082 has activity against drug-resistant strains, we exploited its modest activity against *E. coli* to use the Antibiotic Resistance Platform (ARP),²¹ a collection of hyperpermeable efflux deficient *E. coli* BW25113 Δ *bamB* Δ *tolC* strains carrying genes that confer resistance to a wide variety of antibiotics. A subset of the ARP was pinned onto Mueller Hinton Agar (MHA) containing BAY 11-7082 at 25, 50, or 100 μ M (Figure S2). None of the *E. coli* hyperpermeable strains were able to grow at concentrations as low as 25 μ M (5.18 μ g/mL), indicating BAY 11-7082 is an effective antibiotic even in the presence of common resistance elements.

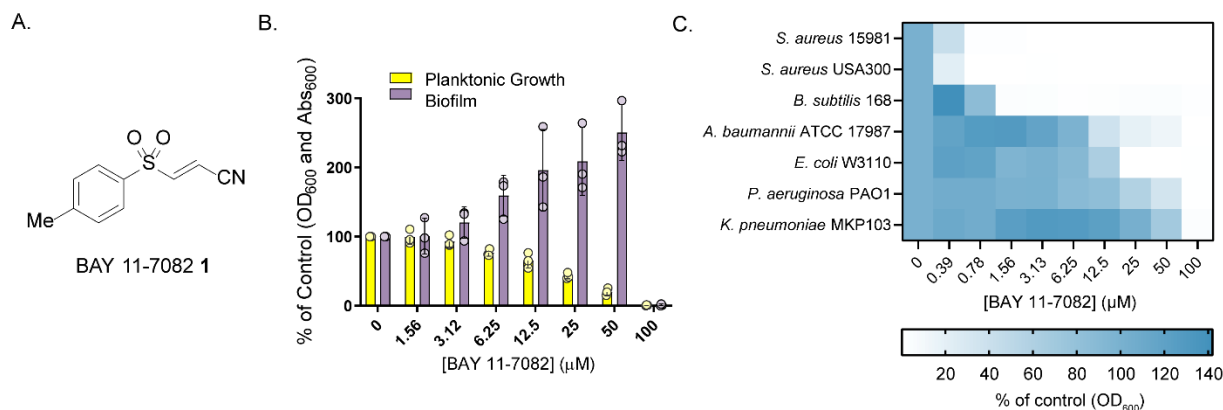


Figure 1. BAY 11-7082 1 stimulates *P. aeruginosa* biofilm formation and has modest antibacterial activity against Gram-negative species and potent antibacterial activity against Gram-positive species. (A) Structure of BAY 11-7082. (B) BAY 11-7082 stimulates biofilm formation (absorbance of crystal violet at 600 nm as a percent of the DMSO control) and decreases planktonic growth (optical density at 600 nm as a percent of the DMSO control) of *P. aeruginosa* PAO1 in 10% LB. (C) BAY 11-7082 inhibits planktonic growth (optical density at 600 nm as a percent of the DMSO control) of seven bacterial species in 10% LB. Heatmap represents an average of three independent experiments performed in triplicate.

Synthesis and antibacterial activity of analogues

To improve potency and better understand the molecule's SAR, we synthesized a series of 15 informative structural analogues (Figure 2) and evaluated them for anti-MRSA activity.

Analogues **5-18** were synthesized following General Procedure A (Supplementary Information), where a sodium sulfinate **2** was combined with 2,3-dibromopropane nitrile, carboxamide or methyl ester **3** to allow for installation of the alkene and the nitrile, or an alternate electron withdrawing group, on the right side of the molecule. Analogues were designed with modifications to the left and/or right sides, including those with alternate heterocycles or alternate substituents on the benzene ring on the left side (**5-8**, **10-16**, **18**, **19**), to assess the effect of ring size and electronic properties on the compound's affinity for its target, and those with alternate electron withdrawing groups on the right side (**7**, **9-11**, **13-18**), to determine if the nitrile

is required for antibiotic activity. Included in this group of analogues is BAY 11-7085 **6** which, like BAY 11-7082, has reported anti-inflammatory activity.¹⁵ To determine if the alkene is essential for antimicrobial activity, suggesting the mechanism requires irreversible binding to a target at that position, we synthesized **19** through hydrogenation over palladium on carbon of the potent analogue **5**.

Only **5** and **6** had improved potency against MRSA compared to BAY 11-7082. Moving from a methyl group to the fluorine **5** or tert-butyl **6** increased potency, likely by increasing specificity for the molecular target. Similarly, **8**, which lacked substituents on the benzene ring, was less potent than BAY 11-7082. With the surprising exception of **7**, analogues with substituents larger than a tert-butyl group, including the bicyclic heterocycles, had reduced potency, potentially due to steric hinderance at the molecular target. All other analogues with a non-nitrile group on the right side of the molecule were also less active, leading us to conclude the nitrile is necessary for potent antimicrobial activity. As expected, **19** lacked antimicrobial activity up to the highest concentration tested of 100 μ M.

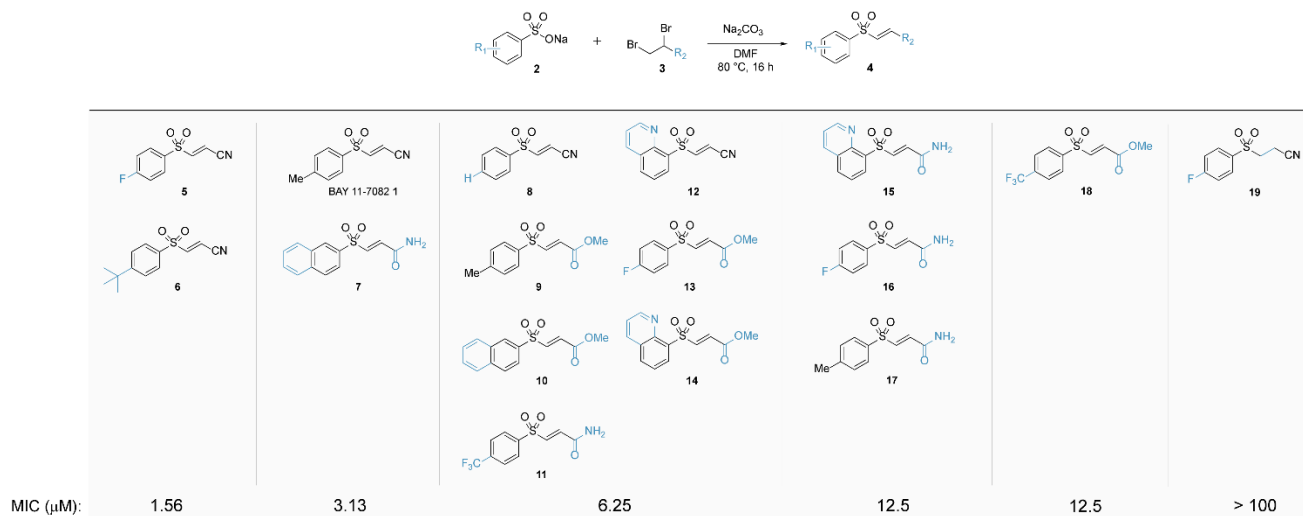


Figure 2. Synthesis (top) and antibacterial activity (bottom) of BAY 11-7082 **1** and its analogues **5-19**. Structures are arranged in order of increasing MIC values reported in μM for *S. aureus* 15981 grown in MHB.

To further explore the molecule's SAR we transitioned to a similar scaffold with an additional ring, offering new sites for diversification. We selected 3-(phenylsulfonyl)-2-pyrazinecarbonitrile (PSPC) **20** due to its structural similarities to BAY 11-7082 and its reported *in vivo* activity against MRSA in a *Caenorhabditis elegans* nematode infection model.²² This scaffold also had the advantage of lacking the αβ-unsaturated sulfone in BAY 11-7082 that could lead to toxicity. We first confirmed that PSPC stimulated *P. aeruginosa* biofilm formation and had a similar spectrum of antibacterial activity, including potent activity against MRSA (Figure S3), then synthesized the analogues **24-34** following General Procedure B (Supplementary Information), where a chlorocarbonitrile pyrazine or pyridine **21** was combined with a sulfonyl chloride **22** (Figure 3). PSPC differs from BAY 11-7082 by the addition of a pyrazine between the sulfone and the nitrile. While all analogues retain the nitrile group, some have a pyridine instead of a pyrazine (**33**, **34**), to assess the effect of alternate heterocycles on activity. Capitalizing on our success with the fluorine analogue **5**, we designed analogues with halogen substituents at the para position of the benzene (**24**, **25**, **28**, **33**, **34**), as well as **30** with a meta fluorine, three

analogues with two fluorine substituents at differing positions (**27**, **31**, **32**), and **26** with a para trifluoromethyl group. We also explored a nitrile group (**29**) as an example of a non-halogen para electron withdrawing substituent.

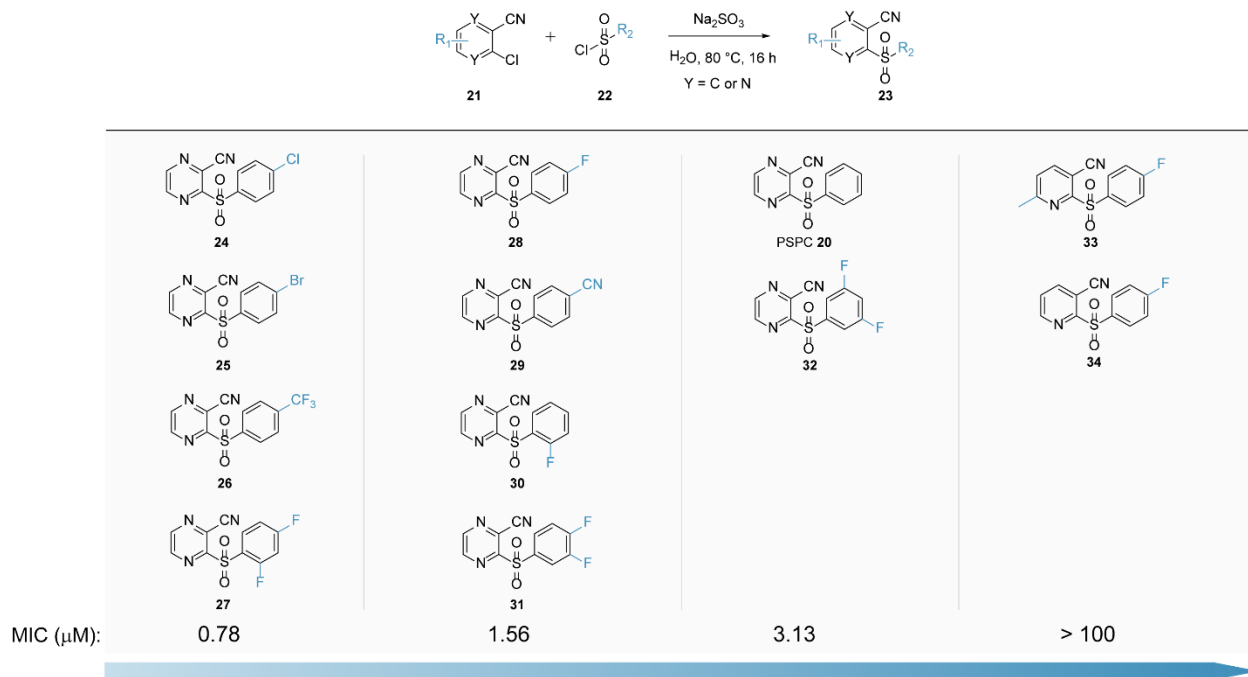


Figure 3. Synthesis (top) and antibacterial activity (bottom) of PSPC **20** and its analogues **24-34**. Structures are arranged in order of increasing MIC values reported in μM for *S. aureus* 15981 grown in MHB.

Analogues **24-31** all exhibited increased anti-MRSA activity relative to BAY 11-7082 and their parent compound PSPC, with MICs as low as 0.78 μM . Similar to our results with the first series of analogues, the addition of a halogen or other relatively small electron withdrawing substituent on the benzene ring increased potency, though the number or position of these groups had little effect. Pyridine analogues **33** and **34** lack antibacterial activity up to the highest concentration tested of 100 μM , indicating that while the pyrazine itself is not necessary for antibacterial activity – as in BAY 11-7082 and analogues **5-14** – the addition of a more basic heterocycle abrogates activity.

Evolving mutants resistant to BAY 11-7082 and PSPC

To understand BAY 11-7082 and PSPC's mechanism of action (MOA) and determine whether the two scaffolds shared a common target, we attempted to evolve resistant mutants of *S. aureus* 15981. While we initially isolated colonies grown on MHA using supra-MIC (6X and 8X MIC) concentrations of BAY 11-7082, those colonies did not grow when re-streaked on fresh MHA containing the compounds. We were similarly unable to develop spontaneous resistance in *E. coli* or *A. baumannii*. We had more success developing resistant mutants by serially passaging *S. aureus* 15981 cultures in liquid media containing ~0.5X, ~1X MIC, or ~2X MIC concentrations of BAY 11-7082 or PSPC for 14 days. After purification of resistant mutants on MHA, six colonies were selected for further evaluation, all of which displayed a 4-fold increase in MIC compared to the parent strain (Figure 4A). Mutants selected using BAY 11-7082 displayed cross-resistance to PSPC and vice versa, suggesting that these two compounds act via a conserved antibacterial mechanism (Figure 4B). To test whether resistance was retained in the absence of selective pressure, the six mutants were serially passaged in MHB for five days and the compounds' MIC was recorded each day. Over five days there was no decrease in MIC, indicating resistance is stably inherited (Figure 4C). In growth experiments, all six mutants showed shorter lag times and increased final optical density over 16 hours compared to the unpassaged parent strain ($p < 0.0001$) (Figure 4D), perhaps due to a general increase in fitness resulting from passage. To ensure these mutants did not have elevated antibiotic tolerance in general, we determined the MICs to tetracycline and piperacillin, and both were unchanged in the mutants compared to the parent strain (Figure S4). To identify the genetic changes responsible for these mutants' resistance to BAY 11-7082 and PSPC, we purified and sequenced genomic DNA from the parent strain *S. aureus* 15981 and the six mutants. Unexpectedly, the

mutants lacked shared genetic changes that could be associated with the acquisition of resistance (Table S1), forcing us to pursue other strategies to better understand the antibacterial MOA.

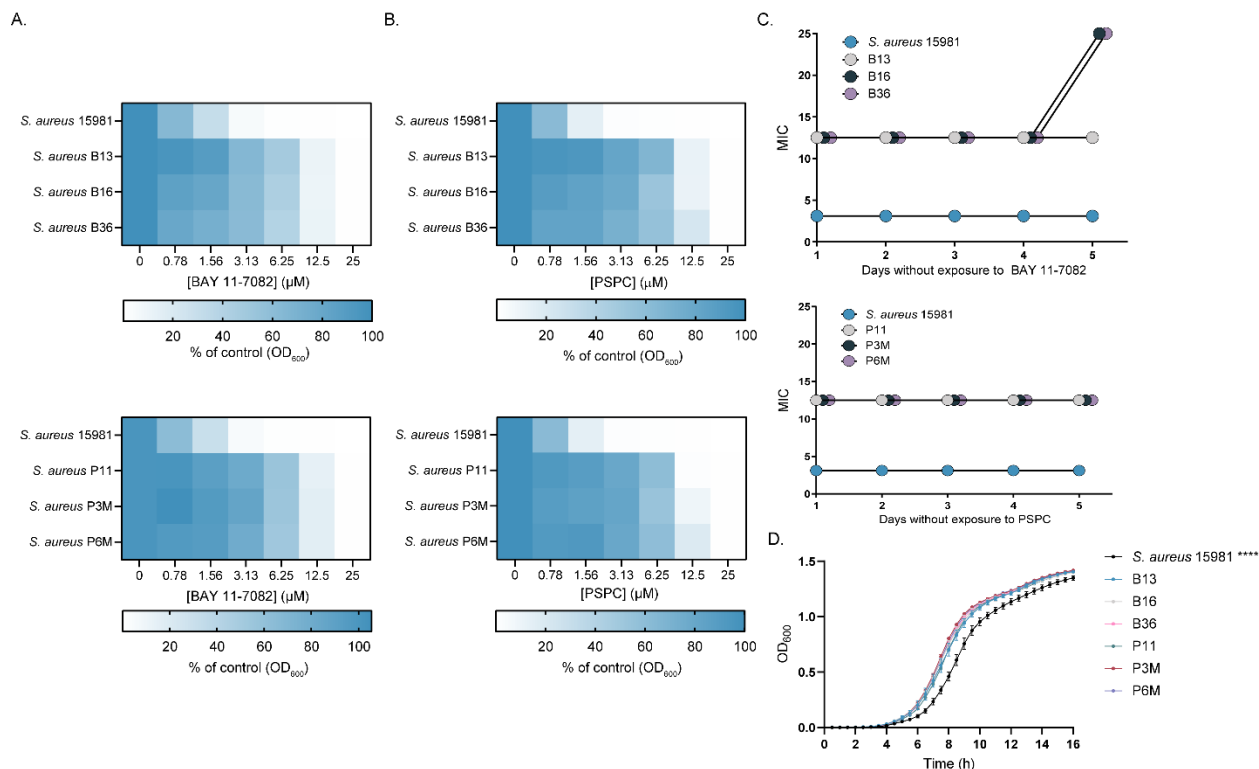


Figure 4. Mutants resistant to BAY 11-7082 and PSPC. (A) Planktonic growth (optical density at 600 nm as a percent of the DMSO control) of *S. aureus* 15981 and BAY 11-7082- (top) or PSPC-resistant (bottom) mutants grown with increasing concentrations of the compound used for selection. (B) Planktonic growth (optical density at 600 nm as a percent of the DMSO control) of *S. aureus* 15981 and BAY 11-7082- (top) or PSPC-resistant (bottom) mutants grown with increasing concentrations of the other compound. (C) MIC values for *S. aureus* 15981 or resistant mutants determined each day for five days during serial passage in the absence of compound. (D) Planktonic growth (optical density at 600 nm) of *S. aureus* 15981 or resistant mutants over 16 h. **** $p < 0.0001$.

Exploring inhibition of TAT secretion as a potential mechanism

BAY 11-7082 was previously identified as a hit in a screen for inhibitors of the *P. aeruginosa* twin arginine translocase (TAT) system, a Sec-independent protein export system responsible for transporting folded proteins across the cytoplasmic membrane.²³ While TAT is not essential,^{24,25} we were curious whether BAY 11-7082 would inhibit the *S. aureus* TAT system and if this would

provide insight into its antibacterial mechanism. The TAT system is broadly conserved in prokaryotes but its protein composition varies between species, with the *P. aeruginosa* TAT system comprising three genes (*tatA*, *tatB*, and *tatC*) while the *S. aureus* system comprises two (*tatA* and *tatC*), with *tatA* and *tatC* essential for protein translocation in both species.^{26,27} We determined the potency of BAY 11-7082 and PSPC against *tatC* transposon mutants of *P. aeruginosa* PA14, from the PA14NR Set transposon mutant library,²⁸ and *S. aureus* USA300, from the Nebraska transposon mutant library,²⁹ and saw a 2-fold increase in sensitivity to BAY 11-7082 and PSPC relative to wild type only for *P. aeruginosa* (Figure 5). This was consistent with the fact that we saw no genetic changes in TAT-related genes in the BAY 11-7082 and PSPC- resistant mutants of MRSA and allowed us to rule out involvement of the TAT system or proteins exported by the system in the compounds' MOA.

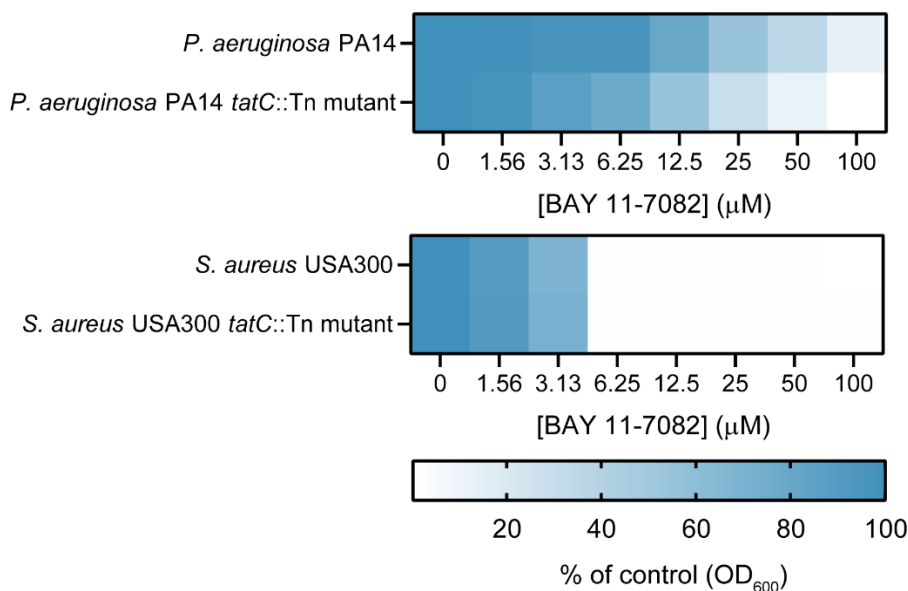


Figure 5. Planktonic growth (optical density at 600 nm as a percent of the DMSO control) of the parent strain *P. aeruginosa* PA14 and a *tatC* transposon mutant grown in 10% LB (top) or the parent strain *S. aureus* USA300 and a *tatC* transposon mutant grown in MHB (bottom) in the presence of increasing concentrations of BAY 11-7082.

Insight into BAY 11-7082's uptake and effect on the proton motive force

Given the challenges of isolating BAY 11-7082- and PSPC-resistant mutants and our inability to isolate mutants with greater than a 4-fold increase in MIC, plus the lack of consistent genetic changes in the mutants isolated, we wondered if BAY 11-7082 and PSPC had a more general MOA, such as inhibition of the proton motive force (PMF). The PMF has two components, a proton gradient (ΔpH) and an electric potential ($\Delta\psi$), which the cell coordinates to control the electrochemical gradient across the membrane.³⁰ To test this idea, we determined the MIC of BAY 11-7082 and PSPC against *S. aureus* 15981 in pH adjusted MHB (Figure 6A). Both BAY 11-7082 and PSPC displayed reduced potency in more basic conditions and increased potency in more acidic conditions, similar to tetracycline, which is taken up via the ΔpH component,³¹ suggesting that BAY 11-7082 and PSPC may also experience ΔpH -dependent uptake across the cytoplasmic membrane.

To determine if BAY 11-7082 and PSPC affected the PMF, we used 3,3'-dipropylthiadicarbocyanine iodide ($\text{DiSC}_3(5)$), a fluorescent dye sensitive to changes in the PMF (Figure 6B). The dye is taken up and transported to the cytoplasm via the $\Delta\psi$ component, where it accumulates and self-quenches fluorescence. If $\Delta\psi$ is inhibited, dye does not accumulate, resulting in increased fluorescence, while if ΔpH is inhibited, the cell compensates by increasing flux through $\Delta\psi$, resulting in decreased fluorescence. Valinomycin, nigericin, and carbonyl cyanide m-chlorophenyl hydrazine (CCCP) all dissipate the PMF and were used as positive controls. Unlike the controls ($p < 0.0001$), neither BAY 11-7082 nor PSPC significantly altered $\text{DiSC}_3(5)$ fluorescence ($p > 0.9999$), confirming that while their uptake is PMF-dependent, they themselves do not destabilize the PMF.

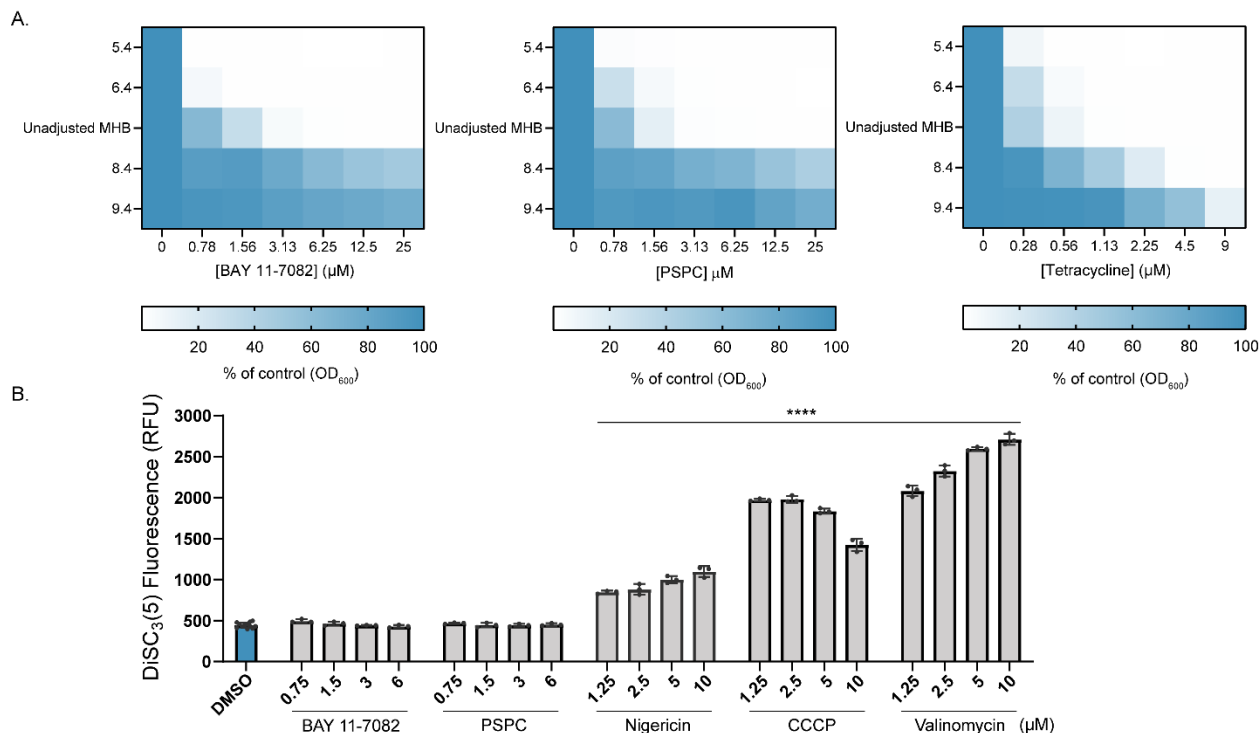
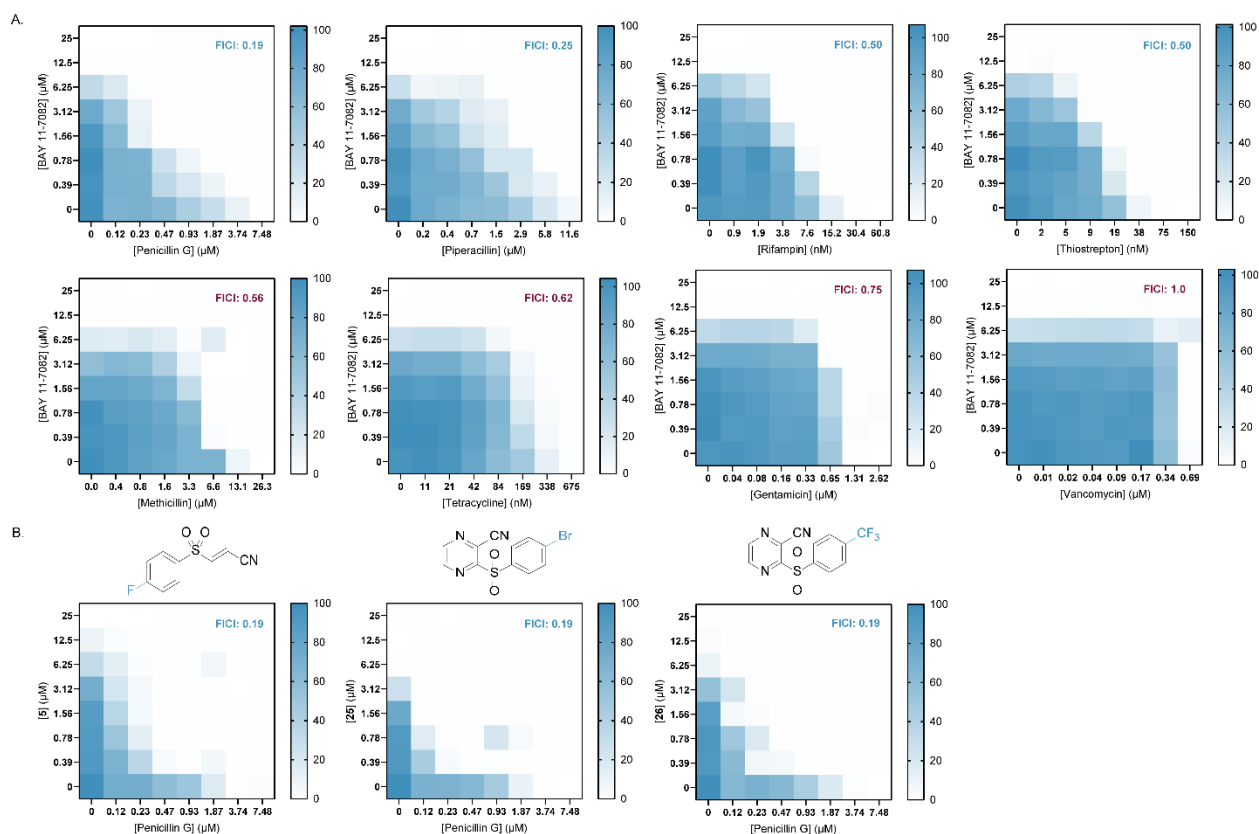


Figure 6. (A) Planktonic growth (optical density at 600 nm as a percent of the DMSO control) of *S. aureus* 15981 grown in pH adjusted MHB with increasing concentrations of BAY 11-7082 (left), PSPC (center), or tetracycline (right). Y-axis indicates pH of the media. (B) DiSC₃(5) fluorescence in relative fluorescence units of *S. aureus* USA300 in the presence of the vehicle DMSO, BAY 11-7082, PSPC, or the membrane active controls nigericin, CCCP, or valinomycin. **** $p < 0.0001$.

BAY 11-7082 synergizes with multiple classes of antibiotics

We next looked at whether BAY 11-7082 and its analogues could act as adjuvants to potentiate the activity of other antibiotics. We conducted checkerboard experiments using the clinically-relevant MRSA strain *S. aureus* USA300. It should be noted here that the MIC for BAY 11-7082 and its analogues were ~4-fold higher for *S. aureus* USA300 than the MICs for *S. aureus* 15981 reported in Figures 2 and 3. Using the fractional inhibitory concentration index (FICI), where values < 0.5 represent synergy and values > 4 represent antagonism,³² we determined that BAY 11-7082 synergized with the β -lactam antibiotics penicillin G and piperacillin, the RNA

polymerase inhibitor rifampin, and the translation inhibitor thiostrepton (Figure 7A). BAY 11-7082 did not affect the activity of antibiotics dependent on the PMF for uptake, including tetracycline (ΔpH -dependent) and gentamicin ($\Delta\psi$ -dependent) (Figure 7A), consistent with our observations that it does not alter the PMF. BAY 11-7082 did not synergize with the glycopeptide cell wall synthesis inhibitor vancomycin or the β -lactam methicillin, to which *S. aureus* USA300 is intrinsically resistant (Figure 7A). Given that we saw the strongest synergy between BAY 11-7082 and penicillin G, we tested some of our more potent analogues in combination with that β -lactam. We selected the BAY 11-7082 para-fluorine analogue **5** (MIC for *S. aureus* USA300: 12.5 μM) and the para-bromine and para-trifluoromethyl PSPC analogues **25** and **26** (MICs for *S. aureus* USA300: 6.25 μM); both potentiated penicillin G activity to the same degree as BAY 11-7082 (FICI: 0.19) (Figure 7B).



(A) or its analogues **5**, **25**, or **26** (B) with antibiotics of different classes. Synergy (FICI<0.5) is represented in blue text while indifference (FICI>0.5) is represented in red. Checkerboards represent an average of at least three independent experiments.

Anti-inflammatory properties of BAY 11-7082 and its analogues

Since the original BAY 11-7082 compound has anti-inflammatory activity, we tested whether alterations made to the scaffold would allow us to separate its anti-inflammatory and antimicrobial properties. We treated mouse bone marrow-derived macrophages with *E. coli* O111:B4 lipopolysaccharide (LPS) and nigericin and measured IL-1 β production, as a key effector cytokine produced by priming and activating the NLRP3/caspase-1 inflammasome, in the presence or absence of BAY 11-7082 and four analogues (**5**, **12**, **17**, and **19**) (Figure 8). As expected, treatment with BAY 11-7082 at 1 and 2.5 μ M significantly reduced ($p<0.0001$) IL-1 β production compared to the no-treatment control. The potent antimicrobial **5** caused a similar reduction in IL-1 β production at both 1 ($p=0.0057$) and 2.5 ($p<0.0001$) μ M, as did the weaker antimicrobials **12** ($p<0.0001$) and **17** ($p<0.0001$). As expected, there was no significant difference in IL-1 β production between treatment with **19**, which lacks antimicrobial activity due to the reduction of the alkene, at 2.5 μ M and the no treatment control ($p=0.5600$), while treatment with 1 μ M actually resulted in a significant increase in IL-1 β production ($p=0.0061$), supporting our notion that covalent binding is required for the scaffold's anti-inflammatory activity. Surprisingly, treatment with **17**, which has an MIC 4-fold higher than that of BAY 11-7082, resulted in a greater, though not significant ($p>0.9999$), reduction in IL-1 β production at 2.5 μ M compared to BAY 11-7082, indicating the terminal nitrile is not required for anti-inflammatory potency. This result suggests that while it may not be possible to develop a potent antimicrobial that does not also target the inflammasome, there may be room to develop a potent anti-inflammatory compound with a reduced impact on the microbiome.

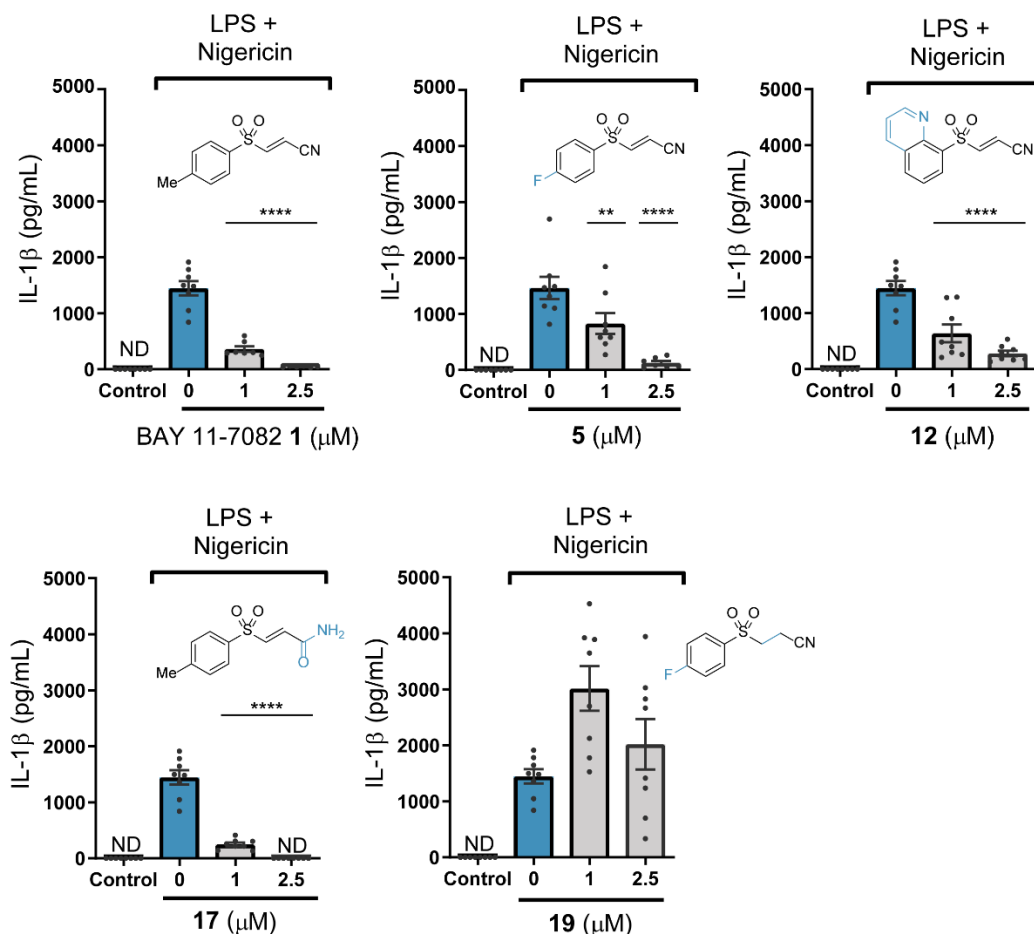


Figure 8. Production of IL-1 β by bone marrow-derived macrophages stimulated with 200 ng/mL LPS and 10 μ M nigericin in the presence or absence of BAY 11-7082, or the analogue **5**, **12**, **17**, or **19** at 1 or 2.5 μ M. Control cells did not receive stimulation with LPS and nigericin. ND (not detected) indicates IL-1 β levels for that condition were below the level of detection based on a standard curve generated for IL-1 β concentration. ** $p < 0.01$, **** $p < 0.0001$

Discussion

Biofilm stimulation occurs in response to exposure to sub-inhibitory concentrations of antibiotics, independent of their MOA,^{14,33} making it a useful tool with advantages over traditional growth assays. The biofilm assay does not rely on growth inhibition at an arbitrary screening concentration, alerting us to hits with potential MICs above the test concentration. Our previous work showed that *P. aeruginosa* biofilm production is a useful proxy for antimicrobial activity, both for narrow spectrum anti-*Pseudomonas* compounds and for broad range molecules

like the antibiotic thiostrepton.²⁰ Here we confirmed that *P. aeruginosa* biofilm stimulation by the anti-inflammatory BAY 11-7082 at 10 μ M signalled its antimicrobial activity against a variety of species, including MRSA.

BAY 11-7085 **6**, another anti-inflammatory and structural analogue of BAY 11-7082, was recently identified as an antimicrobial with activity against *S. aureus* and *Candida albicans*.³⁴ Similar to our findings, BAY 11-7085 lacked activity against *P. aeruginosa* and *K. pneumoniae* strains up to 276.7 μ M, and Escobar *et al.* were unable to isolate BAY 11-7085-resistant mutants of *S. aureus*. Using vancomycin resistant *S. aureus* VRS1 they found an MIC of 16 μ M in MHB and showed that BAY 11-7085 inhibited cell surface attachment and biofilm formation and eradicated established biofilms in brain heart infusion broth media with 0.1% glucose. Interestingly, they did not report biofilm stimulation in response to sub-MIC concentrations of BAY 11-7085.

When initially describing BAY 11-7082 and BAY 11-7085's anti-inflammatory activity, Pierce *et al.* suggested they act via preventing I κ B- α phosphorylation initiated by cytokines like tumor necrosis factor- α (TNF- α), resulting in lower NF- κ B activation and nuclear translocation, where it regulates transcription of κ B sequences with various roles in immunity, cell survival, and apoptosis. Pierce *et al.* proposed BAY 11-7082 and BAY 11-7085 could inhibit a protein tyrosine kinase upstream of I κ B- α but did not propose a specific target. Subsequent work showed that BAY 11-7082 binds and irreversibly inhibits mammalian PTPs through nucleophilic attack by a cysteine in the enzyme's active site,¹⁸ suggesting that BAY 11-7082's antibacterial target could be a PTP. In bacteria, classical PTPs play roles in virulence and host immune evasion while low

molecular weight PTPs are primarily involved in polysaccharide transport.³⁵ *S. aureus* contains two low molecular weight PTPs, PtpA and PtpB, both of unknown function.³⁶ We also considered the TAT system as a target, as BAY 11-7082 was previously identified as a *P. aeruginosa* TAT inhibitor, where it was also suggested to bind a nucleophilic cysteine.²³ However, another study reported that BAY 11-7082 failed to inhibit protein export via the *E. coli* TAT system.³⁷ Further, loss of the TAT system in these species is not lethal,^{24,25} incongruent with the antimicrobial activity of BAY 11-7082, nor was its activity different in a *S. aureus* TAT mutant (Figure 3). Finally, we saw no insertions, deletions, or single nucleotide polymorphisms in PTP or TAT-related genes in mutants with increased resistance to BAY 11-7082 or PSPC (Table S1), consistent with our conclusion that BAY 11-7082's antibacterial MOA is unrelated to either of these systems. Given our inability to identify a molecular target for BAY 11-7082, we suggest that the mechanism is likely complex and multifaceted. While this may be due in part to the potential promiscuity conferred by BAY 11-7082's $\alpha\beta$ -unsaturated sulfonyl, this moiety is absent in PSPC, suggesting it does not play a role in the compound's MOA.

The $\alpha\beta$ -unsaturated center, characteristic of highly-reactive Michael acceptors, makes BAY 11-7082 an unlikely drug candidate. Compounds containing Michael acceptors are traditionally considered problematic in drug development due to high reactivity, low stability, and concerns the compounds could irreversibly bind off-target proteins. However, views on the suitability of Michael acceptors and other covalent modifiers as drugs are changing – particularly in the anticancer space – with several recent examples of $\alpha\beta$ -unsaturated carbonyls under development.³⁸⁻⁴¹ This approach works best when the $\alpha\beta$ -unsaturated carbonyl binds a known and biologically-uncommon target, reducing the likelihood of irreversible covalent off-target

binding. Despite our efforts, we were unable to identify a specific molecular target for BAY 11-7082, suggesting the compound enacts its antibacterial effect via multiple mechanisms. We were also unable to identify an analogue of BAY 11-7082 lacking anti-inflammatory activity but retaining antibiotic potency. While dual antibiotic-anti-inflammatory compounds are an interesting concept and, indeed, many antibiotics have been shown to affect the inflammasome,⁴² this does raise concern for potential side effects. Research from the Taunton lab aimed at developing reversible cysteine residue inhibitors showed that positioning a nitrile group on olefins increases thiol reactivity reversibility, as does positioning electron withdrawing groups at the α or β position of acrylonitriles.^{43,44} It is important to note that with the exploration of PSPC and the development of analogues **24-31**, we showed that the $\alpha\beta$ -unsaturated center is not required for potent anti-MRSA activity.

Beyond its anti-inflammatory activity, BAY 11-7082 has anticancer, anti-diabetes, and neuroprotective properties.⁴⁵⁻⁴⁸ It is thus noteworthy that its potent activity against Gram-positive species could prove problematic should the compound be developed for one of these indications, as it has potential to impact the microbiome. This is not uncommon among drugs with human targets. Indeed, a recent study found 24% of all human-directed drugs tested inhibited growth of at least one bacterial species common to the microbiome.⁴⁹ We found that analogue **17**, a weak anti-*Staphylococcal*, maintains strong anti-inflammatory activity, suggesting it could be possible to separate the activities through careful design.

Due to its potential off-target effects, perhaps a better use of this antibacterial scaffold would be as a lead for adjuvants used in combination with β -lactams to treat MRSA infections. Although

BAY 11-7082 did not re-sensitize MRSA strain USA300 to methicillin, at 1.56 μM it reduced the MIC of penicillin G from 3.74 μM to 0.23 μM – a 16-fold reduction. This concentration of BAY 11-7082 is well below the 10 μM reported IC_{50} for inhibition of $\text{I}\kappa\text{B-}\alpha$ phosphorylation,¹⁵ but above the concentration that significantly reduced inflammation in our macrophage model (Figure 6) and the K_i for some mammalian PTPs,¹⁸ suggesting that even at the low concentrations afforded by combination therapy, using this scaffold may result in off-target effects. The BAY 11-7082 analogue **5** and the PSPC analogues **25** and **26** also synergized with penicillin G and can be used at even lower concentrations (0.78 μM for **7** and 0.39 μM for **25** and **26**) than BAY 11-7082 to achieve the same 0.23 μM MIC for penicillin G. Both **25** and **26** have the advantage of lacking the $\alpha\beta$ -unsaturated center found in BAY 11-7082 and **5**, making them the most promising candidates for development of antibacterial combination therapies. While we saw no evidence of cytotoxicity to macrophages for BAY 11-7082 and its analogues in our NLRP3 inflammasome assays, more conclusive cytotoxicity studies would be necessary to further pursue these compounds as leads.

Conclusion

A high-throughput screen using *P. aeruginosa* biofilm stimulation as an indicator of antibacterial activity led to identification of BAY 11-7082 as a broad-spectrum antimicrobial, with activity against multiple priority pathogens, including MRSA. This work confirms biofilm stimulation as a useful screening method for identifying compounds with broad activity. We were able to improve upon the potency of BAY 11-7082 by switching to a new chemical scaffold based on the molecule PSPC, which lacks the $\alpha\beta$ -unsaturated center that may be associated with off-target effects and toxicity. Our analogues **25** and **26** potentiate the activity of β -lactams like penicillin G

to reduce the concentration needed to inhibit the growth of MRSA. These two compounds therefore represent an interesting starting point for the development of an antibacterial adjuvant for the treatment of MRSA.

Methods

Bacterial strains, culture conditions, and chemicals

Bacterial strains used in this study include *P. aeruginosa* PAO1⁵⁰, *S. aureus* 15981,⁵¹ *B. subtilis* 168,⁵² *E. coli* K-12 W3110⁵³, *A. baumannii* ATCC 17987²⁰, and *K. pneumoniae* MKP103.⁵⁴ *P. aeruginosa* PA14 and the Δ *tatC* transposon mutant were from the PA14NR Set transposon mutant library²⁸ and *S. aureus* USA300 and the Δ *tatC* transposon mutant was from the Nebraska transposon mutant library.²⁹ Bacterial cultures were grown in lysogeny broth (LB), 10% LB (10% LB, 90% 1X phosphate buffered saline), or Mueller-Hinton broth (MHB). Solid media was solidified with 1.5% agar. Compounds **1**, **7-22**, and **26-37** were synthesized for this work. One hundred mM stock solutions were made in DMSO and stored at -20 °C. Stock solutions of tetracycline (EMD Millipore), piperacillin (Sigma, 40 mg/mL stock solution), penicillin G (Fluka Analytica), rifampin (Sigma, 1 mg/mL stock solution prepared in DMSO), thiostrepton (Sigma, 5 mM stock solution prepared in DMSO), methicillin (Cayman Chemicals), gentamicin (BioShops), and vancomycin (Sigma, stock solution prepared in DMSO) were prepared at 10 mg/mL in sterile de-ionized H₂O except where noted and stored at -20 °C.

Compound screening

The McMaster Bioactive compound collection was screened using a biofilm modulation assay, as previously described.²⁰

Inhibitory concentration assays

All bacterial strains were inoculated from -80 °C glycerol stocks into 5 mL media, and incubated with shaking, 200 rpm, 37 °C for 16 h. Cultures were sub-cultured in a 1:500 dilution, grown for 4 h, and diluted in fresh media to an OD₆₀₀ of ~ 0.1, then diluted 1:500. Minimal inhibitory concentration values were determined in 96-well plates (Nunc) using compounds serially diluted in DMSO. Each well had a final volume of 150 µL. Sterile control wells contained 148 µL of corresponding broth and 2 µL DMSO while vehicle control wells contained 148 µL dilute bacterial culture and 2 µL DMSO. Plates were sealed in a container and incubated with shaking, 200 rpm, 37 °C, 16 h. The OD₆₀₀ of plates was read using a Multiscan GO (Thermo Fisher Scientific) and used to calculate the inhibitory concentration. All MIC values presented in Figure 2 and Figure 3 were conducted with *S. aureus* 15981 grown in MHB and are based on experiments performed in duplicate. All other inhibitory concentration data was conducted in media as specified and is based on at least three independent experiments performed in triplicate. MIC values were defined as < 20% of the vehicle control, where growth is no longer visible.²⁰ Where specified, media was pH-adjusted using 6 N sodium hydroxide and 6 M hydrogen chloride.

Biofilm modulation assays

Biofilm assays were performed as previously described.²⁰ Briefly, *P. aeruginosa* PAO1 was inoculated from -80 °C glycerol stocks into 5 mL 10% LB, and incubated with shaking, 200 rpm, 37 °C for 16 h. Cultures were sub-cultured in a 1:500 dilution, grown for 4 h, and diluted in fresh media to an OD₆₀₀ of ~ 0.1, then diluted 1:500. Plates were set up as for the inhibitory concentration assays. Biofilms were formed on the polystyrene pegs of MicroWell lids (Nunc),

which were placed on assay plates prior to 16 h incubation with shaking, 200 rpm, 37 °C.

Following incubation, lids were removed and planktonic growth (OD_{600}) was measured. Lids were immersed in 1X phosphate buffered saline and washed for 10 min, then biofilms adhering to the lids were stained in 0.1% crystal violet for 15 min. Excess crystal violet was removed by immersing the lids in deionized water for 5 min, then repeating this wash step four additional times. Lids dried for 1 h then were transferred to a new 96-well plate containing 200 μ L 33.3% acetic acid per well for 5 min to solubilize the crystal violet. The absorbance (Abs_{600}) of the 96-well plates was read using a Multiscan GO (Thermo Fisher Scientific). Three independent experiments were preformed in triplicate and technical triplicates were averaged. The mean and standard error of the independent biological replicates are shown.

Liquid serial passage assays

S. aureus 15981 was taken from -80 °C stocks, inoculated into 5 mL MHB, and grown with shaking, 200 rpm, 37°C for 24 h. One hundred μ L culture was inoculated into fresh MHB supplemented with BAY 11-7082 or PSPC at 1 (B13, B16, and P11), 3 (B36, P3M), or 6 (P6M) μ M and grown with shaking 200 rpm, 37°C for 24 h. One hundred μ L culture was inoculated into fresh MHB supplemented with BAY 11-7082 or PSPC at the same concentration as the previous day. This serial liquid passage continued for 14 days, at which point cultures were purified on MHA with or without compound.

Genome assembly and identification of SNPs

Genomic DNA was purified using the Wizard Genomic DNA purification kit (Promega) then sequenced via Illumina sequencing. Quality control and trimming of sequencing reads was

accomplished using Galaxy through FASTQC for quality control, FASTQC Groomer to reformat reads, Trimmomatic to trim poor quality reads, FASTQC Interlacer to reorder reads, and FASTQC De-Interlacer. Contigs were assembled for the *S. aureus* 15981 genome using SPAdes and genomes were mapped to reference genomes of two closely related species, *S. aureus* USA300 and USA500, using BreSeq.

Growth curves

S. aureus 15981 and the six BAY 11-7082- or PSPC-resistant mutants (B13, B16, B36, P11, P3M, P6M) were taken from -80 °C stocks, inoculated into 2 mL MHB, and grown with shaking, 200 rpm, 37°C for 16 h. Overnight cultures were sub-cultured in a 1:500 dilution, grown for 4 h, and diluted in fresh media to an OD₆₀₀ of ~ 0.1, then diluted 1:500. Three replicates of 150 µL of each sample was added to a 96-well plate and incubated with moderate shaking at 37 °C (BioTek Synergy 4 Plate Reader) and the OD₆₀₀ was measured at 30 min intervals for 16 h. Technical replicates were averaged and the experiment was repeated at least three times for each strain. The mean and standard error of the independent biological replicates are shown. P-values were calculating using a one-way ANOVA and Tukey's multiple comparison test.

DiSC₃(5) assays

The DiSC₃(5) assay was preformed in accordance with modifications by Farha *et al*⁵⁵ to a method by Epanand *et al*⁵⁶, with some modifications. Briefly, *S. aureus* USA300 was taken from -80 °C stock, inoculated into 5 mL MHB, and grown with shaking, 200 rpm, 37 °C for 16 h. Cultures were sub-cultured in a 1:500 dilution and grown for 4 h. Cells were pelleted and washed three times in buffer (10 mM potassium phosphate, 5 mM MgSO₄, and 250 mM sucrose, pH

7.0), then resuspended in buffer to an OD₆₀₀ of 0.1. DiSC₃(5) was added at 1 μM and allowed to stabilize at room temperature in the dark for 20 minutes. BAY 11-7082, PSPC, valinomycin, nigericin, and CCCP were diluted in DMSO and added in triplicate to a white, clear-bottom, 96-well plate (Costar, Corning Inc), along with cells. Vehicle control wells contained 2 μL DMSO and 148 μL bacteria suspended in buffer with dye. Fluorescence was measured (BioTek Synergy 4 Plate Reader) at an excitation wavelength of 620 nm and an emission wavelength of 685 nm at the start time, then every 50 s for 10 min and every 5 min for the next 30 min. The mean and standard error of three technical replicates for each condition are plotted at the start time. P-values were calculating using a one-way ANOVA and Tukey's multiple comparison test.

Checkerboard assays

Checkerboard assays were set up identically to inhibitory concentration assays, except compounds were added to an 8x8 section of a 96-well plate with increasing concentrations of one compound across the X-axis and increasing concentrations of the other compound across the Y-axis. Plates were incubated with shaking, 200 rpm, 37 °C, 16 h. The OD₆₀₀ of plates was read using a Multiscan GO (Thermo Fisher Scientific). At least three biological replicates were averaged for each checkerboard. Synergy was determined using the following formular for fractional inhibitory concentration index (FICI), where values < 0.5 represent synergy and values > 4 represent antagonism³²:

$$\frac{\text{MIC}_{\text{Compound A in combination}}}{\text{MIC}_{\text{Compound A alone}}} + \frac{\text{MIC}_{\text{Compound B in combination}}}{\text{MIC}_{\text{Compound B alone}}}$$

NLRP3 inflammasome assays

In-house male wild type C57BL/6 J mice (Jackson Laboratory) aged four to twelve weeks were humanely sacrificed to generate bone marrow derived macrophages (BMDMs), as previously described.⁵⁷ Briefly, bone marrow was isolated by flushing the marrow cavity of the femur with sterile saline. Cells recovered from femur flushes were propagated in tissue culture flasks at 1×10^6 cells/mL in L929 differentiation media at 37 °C for four days. Additional L929 media was added and cells were transferred to 24-well plates and incubated for another 5-7 days to allow for maturation of BMDMs. L929 media was removed from BMDMs, wells were washed with PBS, and Dulbecco's Modified Eagle Medium (DMEM) (600 μ L) was added. BMDMs were treated with BAY 11-7082 or analogues at a final concentration of 1 and 2.5 μ M and *E. coli* O111:B4 LPS diluted in endotoxin-free ultra pure water at a final concentration of 200 ng/mL and incubated at 37 °C for 3 h. Nigericin diluted in DMEM was added at a final concentration of 10 μ M and cells were incubated for an additional 45 min. Each condition was tested in at least six biological replicates in BMDMs from a single mouse. Two hundred and fifty μ L of media was removed from each well and frozen until IL-1 β secretion could be measured by ELISA, (DuoSet ELISA, Mouse IL-1 β /IL-1F2, R&D Systems), as previously described.⁵⁸ Media was diluted in a 1:10 ratio in ELISA reagent dilute (1% BSA in PBS) for the LPS and nigericin condition and all test conditions. Media from the control condition, which lacked LPS, nigericin, or the analogues, was diluted in a 1:1 ratio in ELISA reagent dilute. Absorbance at 450 and 570 nm of the 96-well plate following ELISA was read and values at 570 nm were subtracted from values at 450 nm to correct for optical imperfections. IL-1 β levels corresponding to the subtracted absorbance values were determined by interpolating from a standard curve generated using IL-1 β concentrations ranging from 0 pg/mL to 1000 pg/mL. The mean and standard error for at least six independent

biological replicates is shown. P-values were calculating using a one-way ANOVA and Tukey's multiple comparison test.

Acknowledgments

We thank Gerry Wright for access to the Antibiotic Resistance Platform, Derek Chan and Kara Tsang for their assistance with BreSeq, and Meghan Fragis for determining exact masses of the compounds. This work was supported by grants from the Natural Sciences and Engineering Research Council (NSERC) RGPIN-2016-06521 and Ontario Research Fund RE07-048 to LLB and a seed grant from the David Braley Centre for Antibiotic Discovery to LLB and JM. The NMR machine was purchased with funding from a Canada Foundation for Innovation grant. VEC was supported by a Summer Studentship from the David Braley Centre for Antibiotic Discovery and a CIHR Canadian Graduate Scholarship – Master's Award.

Abbreviations Used

ARP, Antibiotic Resistance Platform; CCCP, carbonyl cyanide m-chlorophenyl hydrazine; DiSC₃(5), 3,3'-dipropylthiadicarbocyanine iodide; FICI, fractional inhibitory concentration index; LB, lysogeny broth; MHA, Mueller-Hinton agar; MHB, Mueller-Hinton broth; PMF, proton motive force; PSPC, 3-(phenylsulfonyl)-2-pyrazinecarbonitrile; PTP, protein tyrosine phosphatase; TAT, twin arginine translocase

References

- (1) Rice, L. B. Federal Funding for the Study of Antimicrobial Resistance in Nosocomial Pathogens: No ESKAPE. *J. Infect. Dis.* **2008**, *197* (8), 1079–1081. <https://doi.org/10.1086/533452>.
- (2) Boucher, H. W.; Talbot, G. H.; Bradley, J. S.; Edwards, J. E.; Gilbert, D.; Rice, L. B.; Scheld, M.; Spellberg, B.; Bartlett, J. Bad Bugs, No Drugs: No ESKAPE! An Update from the Infectious Diseases Society of America. *Clin. Infect. Dis.* **2009**, *48* (1), 1–12. <https://doi.org/10.1086/595011>.
- (3) Spellberg, B.; Powers, J. H.; Brass, E. P.; Miller, L. G.; Edwards, J. E. Trends in Antimicrobial Drug Development: Implications for the Future. *Clin. Infect. Dis.* **2004**, *38* (9), 1279–1286. <https://doi.org/10.1086/420937>.
- (4) Deak, D.; Outterson, K.; Powers, J. H.; Kesselheim, A. S. Progress in the Fight Against Multidrug-Resistant Bacteria? A Review of U.S. Food and Drug Administration–Approved Antibiotics, 2010–2015. *Ann. Intern. Med.* **2016**, *165* (5), 363–372. <https://doi.org/10.7326/M16-0291>.
- (5) Liu, C.; Bayer, A.; Cosgrove, S. E.; Daum, R. S.; Fridkin, S. K.; Gorwitz, R. J.; Kaplan, S. L.; Karchmer, A. W.; Levine, D. P.; Murray, B. E.; Rybak, M. J.; Talan, D. A.; Chambers, H. F. Clinical Practice Guidelines by the Infectious Diseases Society of America for the Treatment of Methicillin-Resistant *Staphylococcus aureus* Infections in Adults and Children. *Clin. Infect. Dis.* **2011**, *52* (3), e18–e55. <https://doi.org/10.1093/cid/ciq146>.
- (6) Nannini, E.; Murray, B. E.; Arias, C. A. Resistance or Decreased Susceptibility to Glycopeptides, Daptomycin, and Linezolid in Methicillin-Resistant *Staphylococcus aureus*. *Curr. Opin. Pharmacol.* **2010**, *10* (5), 516–521. <https://doi.org/10.1016/j.coph.2010.06.006>.
- (7) Tsiodras, S.; Gold, H. S.; Sakoulas, G.; Eliopoulos, G. M.; Wennersten, C.; Venkataraman, L.; Moellering, R. C.; Ferraro, M. J. Linezolid Resistance in a Clinical Isolate of *Staphylococcus aureus*. *The Lancet* **2001**, *358* (9277), 207–208. [https://doi.org/10.1016/S0140-6736\(01\)05410-1](https://doi.org/10.1016/S0140-6736(01)05410-1).
- (8) Boucher, H. W.; Sakoulas, G. Perspectives on Daptomycin Resistance, with Emphasis on Resistance in *Staphylococcus aureus*. *Clin. Infect. Dis.* **2007**, *45* (5), 601–608. <https://doi.org/10.1086/520655>.
- (9) Bishop, E.; Melvani, S.; Howden, B. P.; Charles, P. G. P.; Grayson, M. L. Good Clinical Outcomes but High Rates of Adverse Reactions during Linezolid Therapy for Serious Infections: A Proposed Protocol for Monitoring Therapy in Complex Patients. *Antimicrob. Agents Chemother.* **2006**, *50* (4), 1599–1602. <https://doi.org/10.1128/AAC.50.4.1599-1602.2006>.
- (10) Silver, L. L. Challenges of Antibacterial Discovery. *Clin. Microbiol. Rev.* **2011**, *24* (1), 71–109. <https://doi.org/10.1128/CMR.00030-10>.
- (11) Lewis, K. The Science of Antibiotic Discovery. *Cell* **2020**, *181* (1), 29–45. <https://doi.org/10.1016/j.cell.2020.02.056>.
- (12) Lewis, K. Platforms for Antibiotic Discovery. *Nat. Rev. Drug Discov.* **2013**, *12* (5), 371–387. <https://doi.org/10.1038/nrd3975>.
- (13) Sateriale, A.; Bessoff, K.; Sarkar, I. N.; Huston, C. D. Drug Repurposing: Mining Protozoan Proteomes for Targets of Known Bioactive Compounds. *J. Am. Med. Inform. Assoc.* **2014**, *21* (2), 238–244. <https://doi.org/10.1136/amiajnl-2013-001700>.

- (14) Ranieri, M. R.; Whitchurch, C. B.; Burrows, L. L. Mechanisms of Biofilm Stimulation by Subinhibitory Concentrations of Antimicrobials. *Curr. Opin. Microbiol.* **2018**, *45*, 164–169. <https://doi.org/10.1016/j.mib.2018.07.006>.
- (15) Pierce, J. W.; Schoenleber, R.; Jesmok, G.; Best, J.; Moore, S. A.; Collins, T.; Gerritsen, M. E. Novel Inhibitors of Cytokine-Induced I κ B α Phosphorylation and Endothelial Cell Adhesion Molecule Expression Show Anti-Inflammatory Effects in Vivo. *J. Biol. Chem.* **1997**, *272* (34), 21096–21103. <https://doi.org/10.1074/jbc.272.34.21096>.
- (16) Juliana, C.; Fernandes-Alnemri, T.; Wu, J.; Datta, P.; Solorzano, L.; Yu, J.-W.; Meng, R.; Quong, A. A.; Latz, E.; Scott, C. P.; Alnemri, E. S. Anti-Inflammatory Compounds Parthenolide and Bay 11-7082 Are Direct Inhibitors of the Inflammasome. *J. Biol. Chem.* **2010**, *285* (13), 9792–9802. <https://doi.org/10.1074/jbc.M109.082305>.
- (17) Lee, J.; Rhee, M. H.; Kim, E.; Cho, J. Y. BAY 11-7082 Is a Broad-Spectrum Inhibitor with Anti-Inflammatory Activity against Multiple Targets. *Mediators Inflamm.* **2012**. <https://doi.org/10.1155/2012/416036>.
- (18) Krishnan, N.; Bencze, G.; Cohen, P.; Tonks, N. K. The Anti-Inflammatory Compound BAY-11-7082 Is a Potent Inhibitor of Protein Tyrosine Phosphatases. *FEBS J.* **2013**, *280* (12), 2830–2841. <https://doi.org/10.1111/febs.12283>.
- (19) Wenderska, I. B.; Chong, M.; McNulty, J.; Wright, G. D.; Burrows, L. L. Palmitoyl-DL-Carnitine Is a Multitarget Inhibitor of *Pseudomonas aeruginosa* Biofilm Development. *ChemBioChem* **2011**, *12* (18), 2759–2766. <https://doi.org/10.1002/cbic.201100500>.
- (20) Ranieri, M. R. M.; Chan, D. C. K.; Yaeger, L. N.; Rudolph, M.; Karabelas-Pittman, S.; Abdo, H.; Chee, J.; Harvey, H.; Nguyen, U.; Burrows, L. L. Thiostrepton Hijacks Pyoverdine Receptors To Inhibit Growth of *Pseudomonas aeruginosa*. *Antimicrob. Agents Chemother.* **2019**, *63* (9). <https://doi.org/10.1128/AAC.00472-19>.
- (21) Cox, G.; Sieron, A.; King, A. M.; Pascale, G. D.; Pawlowski, A. C.; Koteva, K.; Wright, G. D. A Common Platform for Antibiotic Dereplication and Adjuvant Discovery. *Cell Chem. Biol.* **2017**, *24* (1), 98–109. <https://doi.org/10.1016/j.chembiol.2016.11.011>.
- (22) Rajamuthiah, R.; Jayamani, E.; Majed, H.; Conery, A. L.; Kim, W.; Kwon, B.; Fuchs, B. B.; Kelso, M. J.; Ausubel, F. M.; Mylonakis, E. Antibacterial Properties of 3-(Phenylsulfonyl)-2-Pyrazinecarbonitrile. *Bioorg. Med. Chem. Lett.* **2015**, *25* (22), 5203–5207. <https://doi.org/10.1016/j.bmcl.2015.09.066>.
- (23) Vasil, M. L.; Tomaras, A. P.; Pritchard, A. E. Identification and Evaluation of Twin-Arginine Translocase Inhibitors. *Antimicrob. Agents Chemother.* **2012**, *56* (12), 6223–6234. <https://doi.org/10.1128/AAC.01575-12>.
- (24) Biswas, L.; Biswas, R.; Nerz, C.; Ohlsen, K.; Schlag, M.; Schäfer, T.; Lamkemeyer, T.; Ziebandt, A.-K.; Hantke, K.; Rosenstein, R.; Götz, F. Role of the Twin-Arginine Translocation Pathway in *Staphylococcus*. *J. Bacteriol.* **2009**, *191* (19), 5921–5929. <https://doi.org/10.1128/JB.00642-09>.
- (25) Ochsner, U. A.; Snyder, A.; Vasil, A. I.; Vasil, M. L. Effects of the Twin-Arginine Translocase on Secretion of Virulence Factors, Stress Response, and Pathogenesis. *Proc. Natl. Acad. Sci.* **2002**, *99* (12), 8312–8317. <https://doi.org/10.1073/pnas.082238299>.
- (26) Yen, M.-R.; Tseng, Y.-H.; Nguyen, E. H.; Wu, L.-F.; Saier, M. H. Sequence and Phylogenetic Analyses of the Twin-Arginine Targeting (Tat) Protein Export System. *Arch. Microbiol.* **2002**, *177* (6), 441–450. <https://doi.org/10.1007/s00203-002-0408-4>.

- (27) Dilks, K.; Rose, R. W.; Hartmann, E.; Pohlschröder, M. Prokaryotic Utilization of the Twin-Arginine Translocation Pathway: A Genomic Survey. *J. Bacteriol.* **2003**, *185* (4), 1478–1483. <https://doi.org/10.1128/JB.185.4.1478-1483.2003>.
- (28) Liberati, N. T.; Urbach, J. M.; Miyata, S.; Lee, D. G.; Drenkard, E.; Wu, G.; Villanueva, J.; Wei, T.; Ausubel, F. M. An Ordered, Nonredundant Library of *Pseudomonas aeruginosa* Strain PA14 Transposon Insertion Mutants. *Proc. Natl. Acad. Sci.* **2006**, *103* (8), 2833–2838. <https://doi.org/10.1073/pnas.0511100103>.
- (29) Fey, P. D.; Endres, J. L.; Yajjala, V. K.; Widhelm, T. J.; Boissy, R. J.; Bose, J. L.; Bayles, K. W. A Genetic Resource for Rapid and Comprehensive Phenotype Screening of Nonessential *Staphylococcus aureus* Genes. *mBio* *4* (1), e00537-12. <https://doi.org/10.1128/mBio.00537-12>.
- (30) Kashket, E. R. The Proton Motive Force in Bacteria: A Critical Assessment of Methods. *Annu. Rev. Microbiol.* **1985**, *39* (1), 219–242. <https://doi.org/10.1146/annurev.mi.39.100185.001251>.
- (31) Yamaguchi, A.; Ohmori, H.; Kaneko-Ohdera, M.; Nomura, T.; Sawai, T. Delta pH-Dependent Accumulation of Tetracycline in *Escherichia coli*. *Antimicrob. Agents Chemother.* **1991**, *35* (1), 53–56. <https://doi.org/10.1128/AAC.35.1.53>.
- (32) Odds, F. C. Synergy, Antagonism, and What the Chequerboard Puts between Them. *J. Antimicrob. Chemother.* **2003**, *52* (1), 1–1. <https://doi.org/10.1093/jac/dkg301>.
- (33) Townsley, L.; Shank, E. A. Natural-Product Antibiotics: Cues for Modulating Bacterial Biofilm Formation. *Trends Microbiol.* **2017**, *25* (12), 1016–1026. <https://doi.org/10.1016/j.tim.2017.06.003>.
- (34) Escobar, I. E.; Possamai Rossatto, F. C.; Kim, S. M.; Kang, M. H.; Kim, W.; Mylonakis, E. Repurposing Kinase Inhibitor Bay 11-7085 to Combat *Staphylococcus aureus* and *Candida albicans* Biofilms. *Front. Pharmacol.* **2021**, *12*, 675300. <https://doi.org/10.3389/fphar.2021.675300>.
- (35) Böhmer, F.; Szedlacsek, S.; Taberner, L.; Östman, A.; Hertog, J. den. Protein Tyrosine Phosphatase Structure–Function Relationships in Regulation and Pathogenesis. *FEBS J.* **2013**, *280* (2), 413–431. <https://doi.org/10.1111/j.1742-4658.2012.08655.x>.
- (36) Soulat, D.; Vaganay, E.; Duclos, B.; Genestier, A.-L.; Etienne, J.; Cozzone, A. J. *Staphylococcus aureus* Contains Two Low-Molecular-Mass Phosphotyrosine Protein Phosphatases. *J. Bacteriol.* **2002**, *184* (18), 5194–5199. <https://doi.org/10.1128/JB.184.18.5194-5199.2002>.
- (37) Bageshwar, U. K.; VerPlank, L.; Baker, D.; Dong, W.; Hamsanathan, S.; Whitaker, N.; Sacchettini, J. C.; Musser, S. M. High Throughput Screen for *Escherichia coli* Twin Arginine Translocation (Tat) Inhibitors. *PLOS ONE* **2016**, *11* (2), e0149659. <https://doi.org/10.1371/journal.pone.0149659>.
- (38) Jackson, P. A.; Widen, J. C.; Harki, D. A.; Brummond, K. M. Covalent Modifiers: A Chemical Perspective on the Reactivity of α,β -Unsaturated Carbonyls with Thiols via Hetero-Michael Addition Reactions. *J. Med. Chem.* **2017**, *60* (3), 839–885. <https://doi.org/10.1021/acs.jmedchem.6b00788>.
- (39) Singh, J.; Petter, R. C.; Baillie, T. A.; Whitty, A. The Resurgence of Covalent Drugs. *Nat. Rev. Drug Discov.* **2011**, *10* (4), 307–317. <https://doi.org/10.1038/nrd3410>.
- (40) Bauer, R. A. Covalent Inhibitors in Drug Discovery: From Accidental Discoveries to Avoided Liabilities and Designed Therapies. *Drug Discov. Today* **2015**, *20* (9), 1061–1073. <https://doi.org/10.1016/j.drudis.2015.05.005>.

- (41) Potashman, M. H.; Duggan, M. E. Covalent Modifiers: An Orthogonal Approach to Drug Design. *J. Med. Chem.* **2009**, *52* (5), 1231–1246. <https://doi.org/10.1021/jm8008597>.
- (42) Labro, M. T. Anti-Inflammatory Activity of Macrolides: A New Therapeutic Potential? *J. Antimicrob. Chemother.* **1998**, *41* (suppl_2), 37–46. https://doi.org/10.1093/jac/41.suppl_2.37.
- (43) Krishnan, S.; Miller, R. M.; Tian, B.; Mullins, R. D.; Jacobson, M. P.; Taunton, J. Design of Reversible, Cysteine-Targeted Michael Acceptors Guided by Kinetic and Computational Analysis. *J. Am. Chem. Soc.* **2014**, *136* (36), 12624–12630. <https://doi.org/10.1021/ja505194w>.
- (44) Serafimova, I. M.; Pufall, M. A.; Krishnan, S.; Duda, K.; Cohen, M. S.; Maglathlin, R. L.; McFarland, J. M.; Miller, R. M.; Frödin, M.; Taunton, J. Reversible Targeting of Nucleophilic Cysteines with Chemically Tuned Electrophiles. *Nat. Chem. Biol.* **2012**, *8* (5), 471–476. <https://doi.org/10.1038/nchembio.925>.
- (45) White, D. E.; Burchill, S. A. BAY 11-7082 Induces Cell Death through NF- κ B-Independent Mechanisms in the Ewing's Sarcoma Family of Tumours. *Cancer Lett.* **2008**, *268* (2), 212–224. <https://doi.org/10.1016/j.canlet.2008.03.045>.
- (46) García, M. G.; Alaniz, L.; Lopes, E. C.; Blanco, G.; Hajos, S. E.; Alvarez, E. Inhibition of NF- κ B Activity by BAY 11-7082 Increases Apoptosis in Multidrug Resistant Leukemic T-Cell Lines. *Leuk. Res.* **2005**, *29* (12), 1425–1434. <https://doi.org/10.1016/j.leukres.2005.05.004>.
- (47) Kolati, S. R.; Kasala, E. R.; Bodduluru, L. N.; Mahareddy, J. R.; Uppulapu, S. K.; Gogoi, R.; Barua, C. C.; Lahkar, M. BAY 11-7082 Ameliorates Diabetic Nephropathy by Attenuating Hyperglycemia-Mediated Oxidative Stress and Renal Inflammation via NF- κ B Pathway. *Environ. Toxicol. Pharmacol.* **2015**, *39* (2), 690–699. <https://doi.org/10.1016/j.etap.2015.01.019>.
- (48) Goffi, F.; Boroni, F.; Benarese, M.; Sarnico, I.; Benetti, A.; Spano, P. F.; Pizzi, M. The Inhibitor of I κ B α Phosphorylation BAY 11-7082 Prevents NMDA Neurotoxicity in Mouse Hippocampal Slices. *Neurosci. Lett.* **2005**, *377* (3), 147–151. <https://doi.org/10.1016/j.neulet.2004.11.088>.
- (49) Maier, L.; Pruteanu, M.; Kuhn, M.; Zeller, G.; Telzerow, A.; Anderson, E. E.; Brochado, A. R.; Fernandez, K. C.; Dose, H.; Mori, H.; Patil, K. R.; Bork, P.; Typas, A. Extensive Impact of Non-Antibiotic Drugs on Human Gut Bacteria. *Nature* **2018**, *555* (7698), 623–628. <https://doi.org/10.1038/nature25979>.
- (50) Cavallari, J. F.; Lamers, R. P.; Scheurwater, E. M.; Matos, A. L.; Burrows, L. L. Changes to Its Peptidoglycan-Remodeling Enzyme Repertoire Modulate β -Lactam Resistance in *Pseudomonas aeruginosa*. *Antimicrob. Agents Chemother.* **2013**, *57* (7), 3078–3084. <https://doi.org/10.1128/AAC.00268-13>.
- (51) Nguyen, U. T.; Wenderska, I. B.; Chong, M. A.; Koteva, K.; Wright, G. D.; Burrows, L. L. Small-Molecule Modulators of *Listeria monocytogenes* Biofilm Development. *Appl. Environ. Microbiol.* **2012**, *78* (5), 1454–1465. <https://doi.org/10.1128/AEM.07227-11>.
- (52) Kunst, F.; Ogasawara, N.; Moszer, I.; Albertini, A. M.; Alloni, G.; Azevedo, V.; Bertero, M. G.; Bessières, P.; Bolotin, A.; Borchert, S.; Borriss, R.; Boursier, L.; Brans, A.; Braun, M.; Brignell, S. C.; Bron, S.; Brouillet, S.; Bruschi, C. V.; Caldwell, B.; Capuano, V.; Carter, N. M.; Choi, S.-K.; Codani, J.-J.; Connerton, I. F.; Cummings, N. J.; Daniel, R. A.; Denizot, F.; Devine, K. M.; Düsterhöft, A.; Ehrlich, S. D.; Emmerson, P. T.; Entian, K. D.; Errington, J.; Fabret, C.; Ferrari, E.; Foulger, D.; Fritz, C.; Fujita, M.; Fujita, Y.;

- Fuma, S.; Galizzi, A.; Galleron, N.; Ghim, S.-Y.; Glaser, P.; Goffeau, A.; Golightly, E. J.; Grandi, G.; Guiseppi, G.; Guy, B. J.; Haga, K.; Haiech, J.; Harwood, C. R.; Hénaut, A.; Hilbert, H.; Holsappel, S.; Hosono, S.; Hullo, M.-F.; Itaya, M.; Jones, L.; Joris, B.; Karamata, D.; Kasahara, Y.; Klaerr-Blanchard, M.; Klein, C.; Kobayashi, Y.; Koetter, P.; Koningstein, G.; Krogh, S.; Kumano, M.; Kurita, K.; Lapidus, A.; Lardinois, S.; Lauber, J.; Lazarevic, V.; Lee, S.-M.; Levine, A.; Liu, H.; Masuda, S.; Mauël, C.; Médigue, C.; Medina, N.; Mellado, R. P.; Mizuno, M.; Moestl, D.; Nakai, S.; Noback, M.; Noone, D.; O'Reilly, M.; Ogawa, K.; Ogiwara, A.; Oudega, B.; Park, S.-H.; Parro, V.; Pohl, T. M.; Portetelle, D.; Porwollik, S.; Prescott, A. M.; Presecan, E.; Pujic, P.; Purnelle, B.; Rapoport, G.; Rey, M.; Reynolds, S.; Rieger, M.; Rivolta, C.; Rocha, E.; Roche, B.; Rose, M.; Sadaie, Y.; Sato, T.; Scanlan, E.; Schleich, S.; Schroeter, R.; Scoffone, F.; Sekiguchi, J.; Sekowska, A.; Seror, S. J.; Serror, P.; Shin, B.-S.; Soldo, B.; Sorokin, A.; Tacconi, E.; Takagi, T.; Takahashi, H.; Takemaru, K.; Takeuchi, M.; Tamakoshi, A.; Tanaka, T.; Terpstra, P.; Tognoni, A.; Tosato, V.; Uchiyama, S.; Vandenbol, M.; Vannier, F.; Vassarotti, A.; Viari, A.; Wambutt, R.; Wedler, E.; Wedler, H.; Weitzenegger, T.; Winters, P.; Wipat, A.; Yamamoto, H.; Yamane, K.; Yasumoto, K.; Yata, K.; Yoshida, K.; Yoshikawa, H.-F.; Zumstein, E.; Yoshikawa, H.; Danchin, A. The Complete Genome Sequence of the Gram-Positive Bacterium *Bacillus subtilis*. *Nature* **1997**, *390* (6657), 249–256. <https://doi.org/10.1038/36786>.
- (53) Yao, Z.; Valvano, M. A. Genetic Analysis of the O-Specific Lipopolysaccharide Biosynthesis Region (Rfb) of *Escherichia coli* K-12 W3110: Identification of Genes That Confer Group 6 Specificity to Shigella Flexneri Serotypes Y and 4a. *J. Bacteriol.* **1994**, *176* (13), 4133–4143. <https://doi.org/10.1128/jb.176.13.4133-4143.1994>.
- (54) Snitkin, E. S.; Zelazny, A. M.; Thomas, P. J.; Stock, F.; Program, N. C. S.; Henderson, D. K.; Palmore, T. N.; Segre, J. A. Tracking a Hospital Outbreak of Carbapenem-Resistant *Klebsiella pneumoniae* with Whole-Genome Sequencing. *Sci. Transl. Med.* **2012**, *4* (148), 148ra116-148ra116. <https://doi.org/10.1126/scitranslmed.3004129>.
- (55) Farha, M. A.; Verschoor, C. P.; Bowdish, D.; Brown, E. D. Collapsing the Proton Motive Force to Identify Synergistic Combinations against *Staphylococcus aureus*. *Chem. Biol.* **2013**, *20* (9), 1168–1178. <https://doi.org/10.1016/j.chembiol.2013.07.006>.
- (56) Epand, R. F.; Pollard, J. E.; Wright, J. O.; Savage, P. B.; Epand, R. M. Depolarization, Bacterial Membrane Composition, and the Antimicrobial Action of Ceragenins. *Antimicrob. Agents Chemother.* **2010**, *54* (9), 3708–3713. <https://doi.org/10.1128/AAC.00380-10>.
- (57) Henriksbo, B. D.; Lau, T. C.; Cavallari, J. F.; Denou, E.; Chi, W.; Lally, J. S.; Crane, J. D.; Duggan, B. M.; Foley, K. P.; Fullerton, M. D.; Tarnopolsky, M. A.; Steinberg, G. R.; Schertzer, J. D. Fluvastatin Causes NLRP3 Inflammasome-Mediated Adipose Insulin Resistance. *Diabetes* **2014**, *63* (11), 3742–3747. <https://doi.org/10.2337/db13-1398>.
- (58) Henriksbo, B. D.; Tamrakar, A. K.; Xu, J.; Duggan, B. M.; Cavallari, J. F.; Phulka, J.; Stampfli, M. R.; Ashkar, A. A.; Schertzer, J. D. Statins Promote Interleukin-1 β -Dependent Adipocyte Insulin Resistance Through Lower Prenylation, Not Cholesterol. *Diabetes* **2019**, *68* (7), 1441–1448. <https://doi.org/10.2337/db18-0999>.

Supporting Information

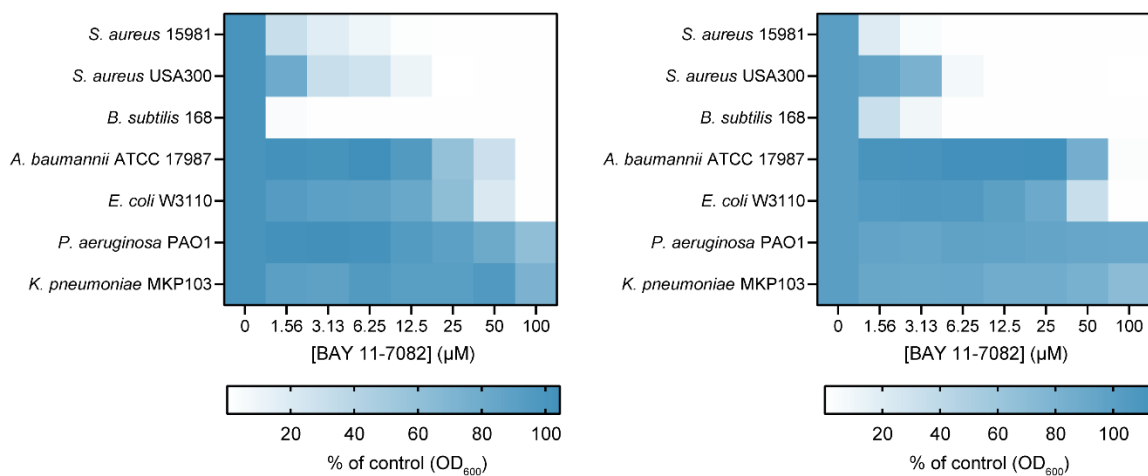


Figure S1. Planktonic growth (optical density at 600 nm as a percent of the DMSO control) of seven bacterial species grown in LB (left) or MHB (right) with increasing concentrations of BAY 11-7082. The MIC is equal to 20% or less of control growth.

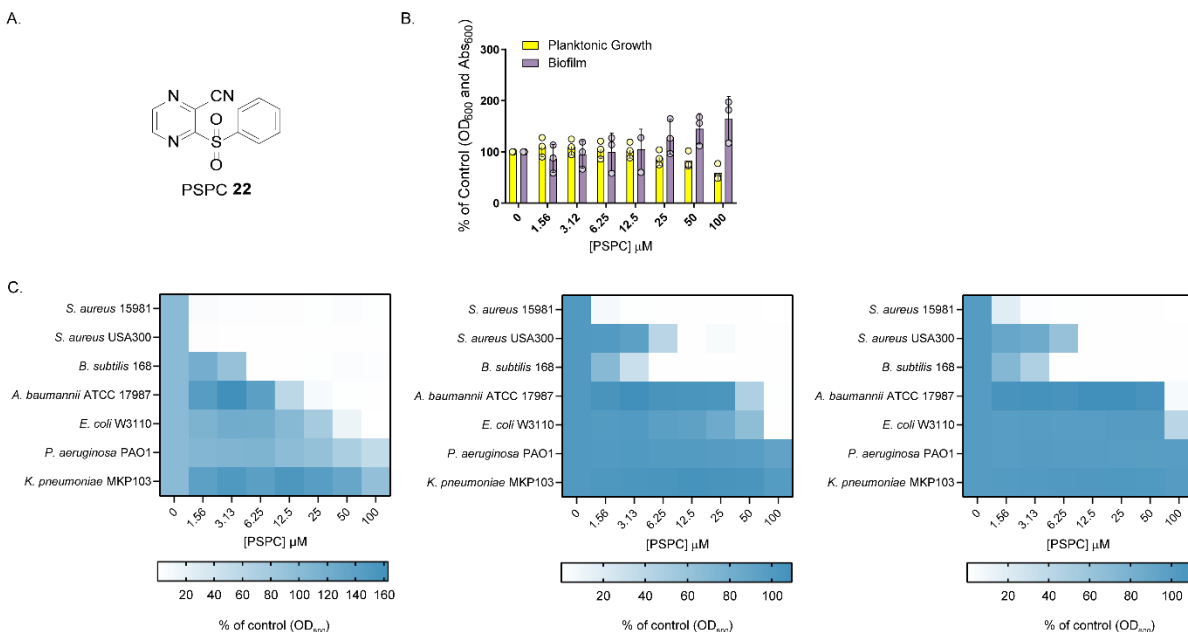


Figure S3. PSPC (**22**), like BAY 11-7082, stimulates biofilm formation and has potent anti-Staphylococcal activity. (A) Structure of PSPC. (B) PSPC stimulates biofilm formation (absorbance of crystal violet at 600 nm as a percent of the DMSO control) and decreases planktonic growth (optical density at 600 nm as a percent of the DMSO control) of *P. aeruginosa* PAO1 in 10% LB. (C) Planktonic growth (optical density at 600 nm as a percent of the DMSO control) of seven bacterial species grown in 10% LB (left), LB (center) or MHB (right) with increasing concentrations of PSPC.

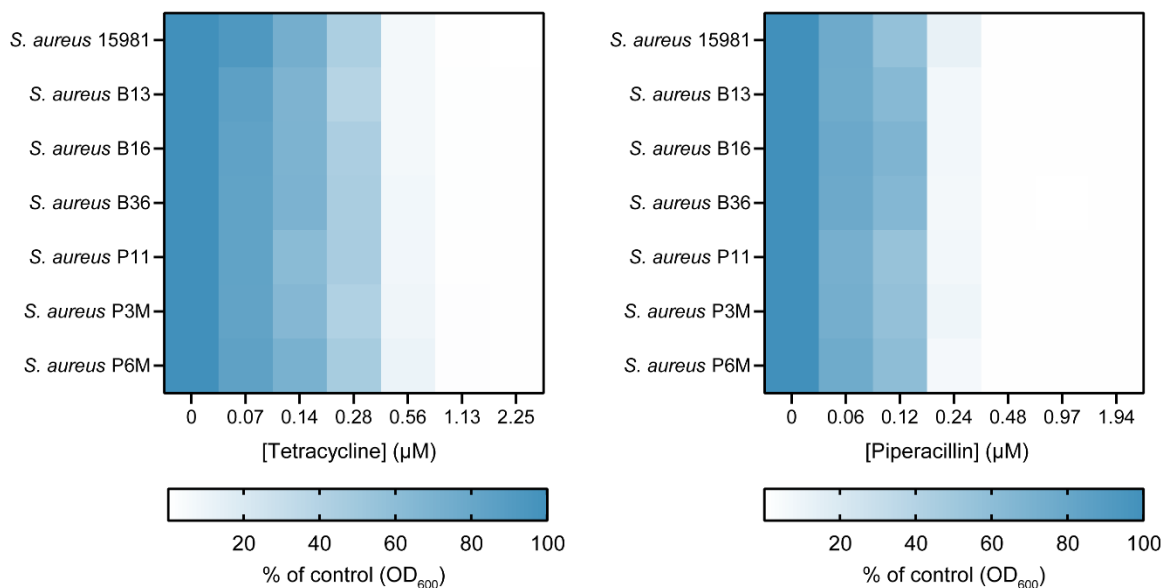
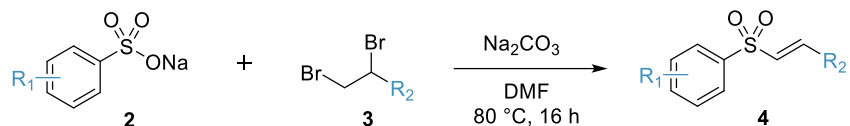


Figure S4. BAY 11-7082 and PSPC-resistant mutants and the parent strain *S. aureus* 15981 are equally susceptible to tetracycline and piperacillin. Planktonic growth (optical density at 600 nm as a percent of the DMSO control) of *S. aureus* 15981 or a mutant strain grown in MHB with increasing concentrations of tetracycline (left) or piperacillin (right).

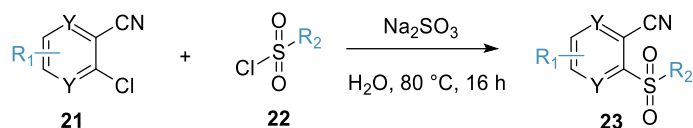
Table S1. Summary of single nucleotide polymorphisms in BAY 11-7082 and PSPC-resistant mutants that differ from the parent *S. aureus* 15981 strain. Available from the authors on request as an Excel file.

General Procedure A for the formation of acrylonitriles, acrylamides and methyl acrylates sulfones:



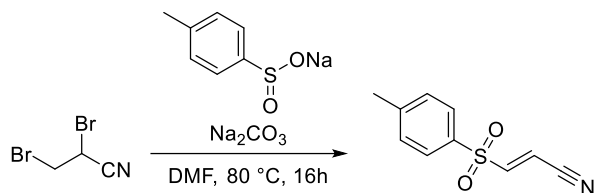
Adapted from a procedure by Gian *et al.*,² to a stirring solution of **sodium sulfinate (2)** (2 equiv.) and **Na₂CO₃** (2 equiv.) in **DMF** (0.25 M) was added **2,3-dibromopropane nitrile, carboxamide or methyl ester (3)** (1 equiv.). The resulting mixture was heated up to 80 °C and was stirred overnight. The crude mixture was cooled to room temperature, diluted in water, and extracted with EtOAc (3x). The organic layers were combined and washed with brine (1x), dried over MgSO₄, filtered and concentrated under reduced pressure. Purification was executed by normal phase flash chromatography.

General Procedure B for the formation of *o*-sulfonylcarbonitrile pyrazines and pyridines:



To a stirring solution of ***o*-chlorocarbonitrile pyrazine or pyridine (21)** (1 equiv.) and **Na₂SO₃** (1.3 equiv.) in **H₂O** (0.2 M) was added **sulfonyl chloride (22)** (1.2 equiv.). The resulting mixture was heated to 100 °C and stirred overnight. The crude mixture was cooled to room temperature and extracted with EtOAc (3x). The organic layers were combined and washed with H₂O (1x) and brine (1x), dried over MgSO₄, filtered and concentrated under reduced pressure. Purification was executed by reverse phase chromatography, compound-rich fractions were concentrated to dryness, taken into nanopure water, frozen, and lyophilized to yield the desired products.

Synthesis of (*E*)-3-tosylacrylonitrile (1):



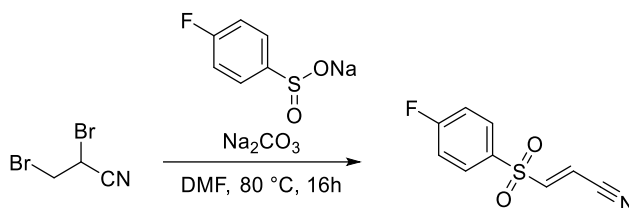
Following the general procedure **A** on 213 mg (1.00 mmol) of **2,3-dibromopropanenitrile**, purification afforded 7.0 mg (3% yield) of (*E*)-3-tosylacrylonitrile as a white solid. (Gradient from 0 to 20% EtOAc/hexanes)

¹H NMR (700 MHz, Chloroform-*d*) δ 7.78 (d, *J* = 8.1 Hz, 2H), 7.41 (d, *J* = 8.0 Hz, 2H), 7.21 (d, *J* = 15.7 Hz, 1H), 6.51 (d, *J* = 15.7 Hz, 1H), 2.48 (s, 3H).

¹³C NMR (176 MHz, Chloroform-*d*) δ 149.48, 146.68, 134.35, 130.73, 128.73, 113.54, 110.25, 21.93.

HRMS (ESI⁺): [M+Na]⁺ calculated for C₁₀H₉NO₂SNa = 230.02462 m/z; found = 230.02529 m/z.

Synthesis of (*E*)-3-((4-fluorophenyl)sulfonyl)acrylonitrile (5):



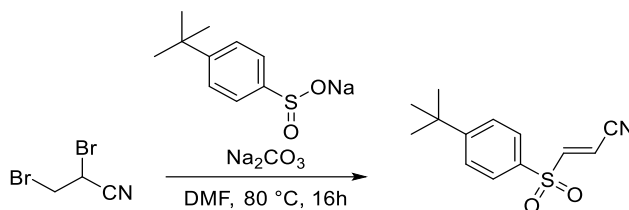
Following the general procedure **A** on 213 mg (1.00 mmol) of **2,3-dibromopropanenitrile**, purification afforded 17.8 mg (9% yield) of (*E*)-3-((4-fluorophenyl)sulfonyl)acrylonitrile as a white solid. (Gradient from 0 to 20% EtOAc/hexanes)

¹H NMR (700 MHz, Chloroform-*d*) δ 7.95 – 7.92 (m, 2H), 7.31 (t, *J* = 8.9, 8.0 Hz, 2H), 7.21 (d, *J* = 15.6 Hz, 1H), 6.56 (d, *J* = 15.6 Hz, 1H).

¹³C NMR (176 MHz, Chloroform-*d*) δ 167.40, 165.93, 148.81, 131.63, 117.53, 113.19, 110.92.

HRMS (ESI⁺): [M+Na]⁺ calculated for C₉H₆FNO₂SNa = 233.99952 m/z; found = m/z.

Synthesis of (*E*)-3-((4-(*tert*-butyl)phenyl)sulfonyl)acrylonitrile (6):



Following the general procedure **A** on 212.9 mg (1.00 mmol) of **2,3-dibromopropanenitrile**, purification afforded 75.6 mg (30% yield) of (*E*)-3-((4-(*tert*-butyl)phenyl)sulfonyl)acrylonitrile as a white solid. (Gradient from 0 to 20% EtOAc/hexanes)

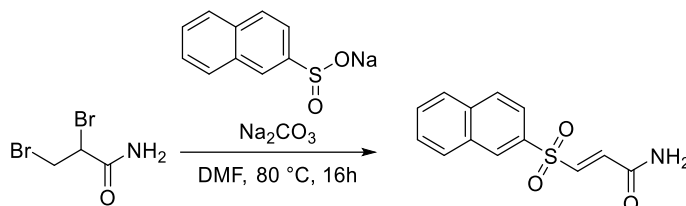
^1H NMR (700 MHz, DMSO- d_6) δ 8.22 (d, J = 15.6 Hz, 1H), 7.86 – 7.82 (m, 2H), 7.76 – 7.72 (m, 2H), 6.89 (d, J = 15.6 Hz, 1H), 1.31 (s, 9H).

^{13}C NMR (176 MHz, DMSO- d_6) δ 158.82, 149.85, 135.07, 128.51, 127.44, 115.11, 112.22, 35.65, 31.13.

HRMS (ESI $^+$): $[\text{M}+\text{H}]^+$ calculated for $\text{C}_{13}\text{H}_{16}\text{NO}_2\text{S}$ = 250.08958 m/z; found = 250.08857 m/z.

HRMS (ESI $^+$): $[\text{M}+\text{Na}]^+$ calculated for $\text{C}_{13}\text{H}_{15}\text{NO}_2\text{SNa}$ = 272.07152 m/z; found = 272.07121 m/z.

Synthesis of (*E*)-3-(naphthalen-2-ylsulfonyl)acrylamide (7):



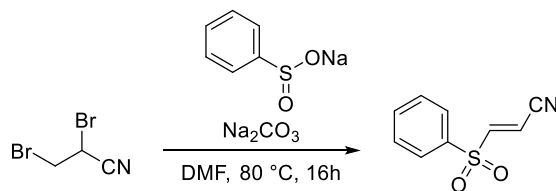
Following the general procedure **A** on 230.9 mg (1.00 mmol) of **2,3-dibromopropanecarboxamide**, purification afforded 256.9 mg (98% yield) of (*E*)-3-(naphthalen-2-ylsulfonyl)acrylamide as a white solid. (Gradient from 0 to 20% EtOAc/hexanes)

^1H NMR (700 MHz, DMSO- d_6) δ 8.64 (d, J = 1.9 Hz, 1H), 8.24 (dd, J = 8.1, 1.2 Hz, 1H), 8.21 (d, J = 8.7 Hz, 1H), 8.12 – 8.08 (m, 1H), 8.04 (s, 1H), 7.89 (dd, J = 8.7, 1.9 Hz, 1H), 7.77 (ddd, J = 8.2, 6.8, 1.3 Hz, 1H), 7.72 (ddd, J = 8.1, 6.8, 1.3 Hz, 1H), 7.69 (s, 1H), 7.52 (d, J = 15.0 Hz, 1H), 7.03 (d, J = 15.0 Hz, 1H).

^{13}C NMR (176 MHz, DMSO- d_6) δ 163.08, 139.02, 135.81, 135.36, 134.94, 131.82, 129.94, 129.71, 129.58, 129.49, 127.98, 127.93, 122.42.

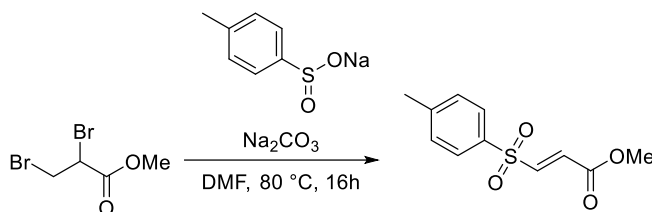
HRMS (ESI $^+$): $[\text{M}+\text{Na}]^+$ calculated for $\text{C}_{13}\text{H}_{11}\text{NO}_3\text{SNa}$ = 284.03522 m/z; found = 284.03519 m/z.

Synthesis of (*E*)-3-(phenylsulfonyl)acrylonitrile (**8**):



Following the general procedure **A** on 212.9 mg (1.00 mmol) of **2,3-dibromopropanenitrile**, purification afforded 75.6 mg of (*E*)-3-(phenylsulfonyl)acrylonitrile as a brown solid. (Gradient from 0 to 20% EtOAc/hexanes)

Synthesis of methyl (*E*)-3-tosylacrylate (**9**):



Following the general procedure **A** on 230.9 mg (1.00 mmol) of **methyl 2,3-dibromopropionate**, purification afforded 180.5 mg (80% yield) of **methyl (*E*)-3-tosylacrylate** as a white solid. (Gradient from 0 to 20% EtOAc/hexanes)

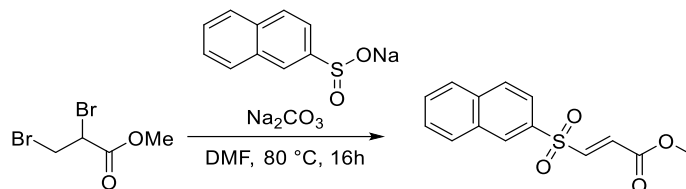
¹H NMR (700 MHz, DMSO-*d*₆) δ 7.85 – 7.82 (m, 2H), 7.78 (d, *J* = 15.2 Hz, 1H), 7.52 – 7.48 (m, 2H), 6.75 (d, *J* = 15.2 Hz, 1H), 3.73 (s, 3H), 2.42 (s, 3H).

¹³C NMR (176 MHz, DMSO-*d*₆) δ 164.16, 145.95, 143.73, 135.76, 130.79, 130.76, 128.57, 53.11, 21.63.

HRMS (ESI⁺): [M+H]⁺ calculated for C₁₁H₁₃O₄S = 241.05288 m/z; found = 241.05289 m/z.

HRMS (ESI⁺): [M+Na]⁺ calculated for C₁₁H₁₂O₄SNa = 263.03482 m/z; found = 263.03452 m/z.

Synthesis of methyl (*E*)-3-(naphthalen-2-ylsulfonyl)acrylate (10):



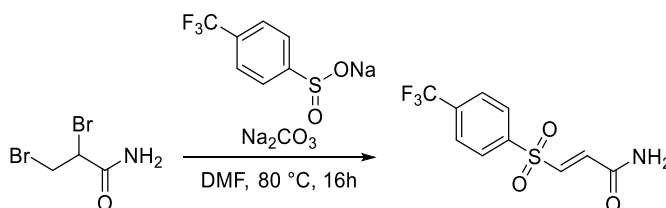
Following the general procedure **A** on 212.8 mg (1.00 mmol) of **methyl 2,3-dibromopropanoate**, purification afforded 10.0 mg (4% yield) of **methyl (*E*)-3-(naphthalen-2-ylsulfonyl)acrylate** as a white solid. (Gradient from 0 to 20% EtOAc/hexanes)

^1H NMR (700 MHz, Chloroform-*d*) δ 8.56 – 8.51 (m, 1H), 8.05 – 7.99 (m, 2H), 7.95 (d, J = 8.2 Hz, 1H), 7.84 (dd, J = 8.6, 1.9 Hz, 1H), 7.71 (ddd, J = 8.2, 6.9, 1.3 Hz, 1H), 7.67 – 7.64 (m, 1H), 7.40 (d, J = 15.1 Hz, 1H), 6.89 (d, J = 15.1 Hz, 1H), 3.80 (s, 3H).

^{13}C NMR (176 MHz, Chloroform-*d*) δ 163.93, 143.51, 135.61, 135.20, 132.30, 130.52, 130.51, 130.04, 129.80, 129.54, 128.08, 127.99, 122.57, 52.79.

HRMS (ESI⁺): [M+Na]⁺ calculated for C₁₄H₁₂O₄SNa = 299.03482 m/z; found = 299.03521 m/z.

Synthesis of (*E*)-3-((4-(trifluoromethyl)phenyl)sulfonyl)acrylamide (11):



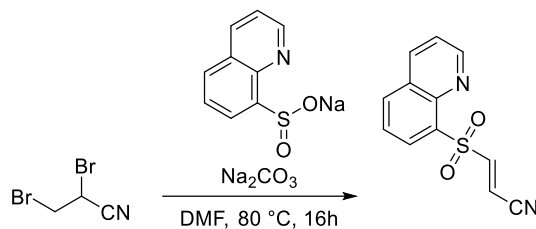
Following the general procedure **A** on 230.9 mg (1.00 mmol) of **2,3-dibromopropanecarboxamide**, purification afforded 209.5 mg (75% yield) of **(*E*)-3-((4-(trifluoromethyl)phenyl)sulfonyl)acrylamide** as a white solid. (Gradient from 0 to 40% EtOAc/hexanes)

^1H NMR (700 MHz, DMSO-*d*₆) δ 8.16 (d, J = 8.2 Hz, 2H), 8.08 (d, J = 8.3 Hz, 2H), 8.06 (s, 1H), 7.73 (s, 1H), 7.57 (d, J = 15.0 Hz, 1H), 7.07 (d, J = 15.0 Hz, 1H).

^{13}C NMR (176 MHz, DMSO-*d*₆) δ 163.33, 143.30, 138.67, 137.25, 134.23, 129.33, 127.43, 123.01.

HRMS (ESI⁺): [M+H]⁺ calculated for C₁₀H₉F₃NO₃S = 280.02498 m/z; found = 280.02643 m/z.

Synthesis of (*E*)-3-(quinolin-8-ylsulfonyl)acrylonitrile (12):



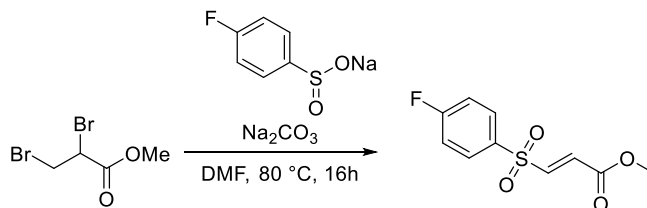
Following the general procedure **A** on 212.9 mg (1.00 mmol) of **2,3-dibromopropanenitrile**, purification afforded 75.6 mg of (*E*)-3-(quinolin-8-ylsulfonyl)acrylonitrile as a brown solid. (Gradient from 0 to 20% EtOAc/hexanes)

^1H NMR (700 MHz, Chloroform-*d*) δ 9.11 (dd, $J = 4.2, 1.7$ Hz, 1H), 8.53 (dd, $J = 7.3, 1.5$ Hz, 1H), 8.31 (dd, $J = 8.3, 1.8$ Hz, 1H), 8.25 – 8.17 (m, 2H), 7.74 (dd, $J = 8.2, 7.4$ Hz, 1H), 7.62 (dd, $J = 8.3, 4.2$ Hz, 1H), 6.70 (d, $J = 15.9$ Hz, 1H).

^{13}C NMR (176 MHz, Chloroform-*d*) δ 152.08, 150.46, 144.02, 136.96, 135.67, 135.60, 131.89, 129.14, 126.00, 122.92, 114.01, 111.55.

HRMS (ESI⁺): [M+Na]⁺ calculated for C₁₂H₈N₂O₂SNa = 267.01982 m/z; found = 267.02129 m/z.

Synthesis of methyl (*E*)-3-((4-fluorophenyl)sulfonyl)acrylate (13):



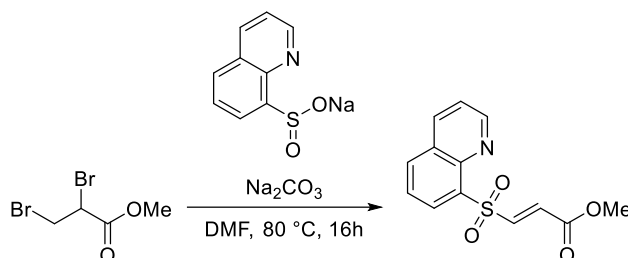
Following the general procedure **A** on 245.9 mg (1.00 mmol) of **methyl 2,3-dibromopropanate**, purification afforded 131.2 mg (34% yield) of **methyl (*E*)-3-((4-fluorophenyl)sulfonyl)acrylate** as a white solid. (Gradient from 0 to 20% EtOAc/hexanes)

^1H NMR (700 MHz, Chloroform-*d*) δ 7.94 – 7.91 (m, 2H), 7.31 (d, $J = 15.2$ Hz, 1H), 7.28 – 7.23 (m, 2H), 6.83 (d, $J = 15.1$ Hz, 1H), 3.79 (s, 3H).

^{13}C NMR (176 MHz, Chloroform-*d*) δ 167.15, 165.68, 163.94, 143.39, 131.46, 130.83, 117.21, 52.99.

HRMS (ESI⁺): [M+Na]⁺ calculated for C₁₀H₉FO₄SNa = 267.00982 m/z; found = 267.01055 m/z.

Synthesis of methyl (*E*)-3-(quinolin-8-ylsulfonyl)acrylate (14):



Following the general procedure **A** on 245.9 mg (1.00 mmol) of **2,3-dibromopropanecarboxamide**, purification afforded 139.4 mg (50% yield) of **methyl (*E*)-3-(quinolin-8-ylsulfonyl)acrylate** as a brown solid. (Gradient from 0 to 20% EtOAc/hexanes)

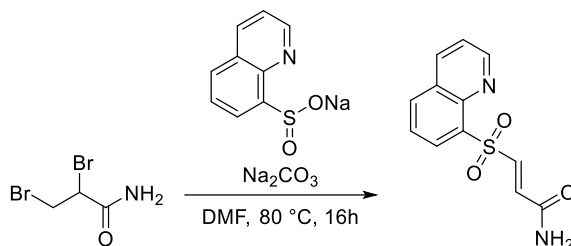
^1H NMR (700 MHz, DMSO- d_6) δ 9.14 (dd, $J = 4.2, 1.8$ Hz, 1H), 8.63 – 8.59 (m, 1H), 8.49 (dd, $J = 7.3, 1.4$ Hz, 1H), 8.45 (dd, $J = 8.3, 1.4$ Hz, 1H), 8.15 (d, $J = 15.4$ Hz, 1H), 7.87 (dd, $J = 8.1, 7.3$ Hz, 1H), 7.76 (dd, $J = 8.3, 4.2$ Hz, 1H), 6.92 (d, $J = 15.4$ Hz, 1H), 3.72 (s, 3H).

^{13}C NMR (176 MHz, DMSO- d_6) δ 164.28, 152.51, 144.21, 143.49, 137.73, 136.27, 135.87, 131.77, 131.65, 129.18, 126.60, 123.46, 53.16.

HRMS (ESI $^+$): $[\text{M}+\text{H}]^+$ calculated for $\text{C}_{13}\text{H}_{12}\text{NO}_4\text{S} = 278.04818$ m/z; found = 278.04803 m/z.

HRMS (ESI $^+$): $[\text{M}+\text{Na}]^+$ calculated for $\text{C}_{13}\text{H}_{11}\text{NO}_4\text{SNa} = 300.03012$ m/z; found = 300.03023 m/z.

Synthesis of (*E*)-3-(quinolin-8-ylsulfonyl)acrylamide (15):



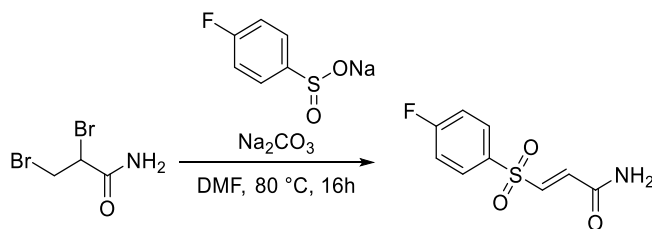
Following the general procedure **A** on 230.9 mg (1.00 mmol) of **2,3-dibromopropanecarboxamide**, purification afforded 43.3 mg (17% yield) of **(*E*)-3-(quinolin-8-ylsulfonyl)acrylamide** as a brown solid. (Gradient from 0 to 20% EtOAc/hexanes)

^1H NMR (700 MHz, DMSO- d_6) δ 9.14 (dd, $J = 4.2, 1.7$ Hz, 1H), 8.61 (dd, $J = 8.4, 1.8$ Hz, 1H), 8.45 (ddd, $J = 24.6, 7.8, 1.5$ Hz, 2H), 8.05 (s, 1H), 7.94 (d, $J = 15.2$ Hz, 1H), 7.86 (dd, $J = 8.2, 7.3$ Hz, 1H), 7.76 (dd, $J = 8.3, 4.2$ Hz, 1H), 7.67 (s, 1H), 7.12 (d, $J = 15.2$ Hz, 1H).

^{13}C NMR (176 MHz, DMSO- d_6) δ 163.69, 152.41, 143.52, 140.33, 137.68, 136.56, 136.35, 135.98, 131.32, 129.19, 126.56, 123.40.

HRMS (ESI $^+$): $[\text{M}+\text{Na}]^+$ calculated for $\text{C}_{12}\text{H}_{10}\text{N}_2\text{O}_3\text{SNa} = 285.03042$ m/z; found = 285.03116 m/z.

Synthesis of (*E*)-3-((4-fluorophenyl)sulfonyl)acrylamide (**16**):



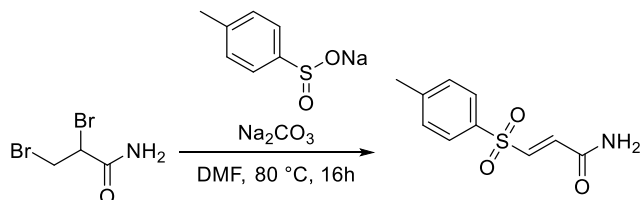
Following the general procedure **A** on 230.9 mg (1.00 mmol) of **2,3-dibromopropanecarboxamide**, purification afforded 125.0 mg (55% yield) of (*E*)-3-((4-fluorophenyl)sulfonyl)acrylamide as a white solid. (Gradient from 0 to 20% EtOAc/hexanes)

¹H NMR (700 MHz, DMSO-*d*₆) δ 8.03 (s, 1H), 8.02 – 7.99 (m, 2H), 7.69 (s, 1H), 7.56 – 7.52 (m, 2H), 7.49 (d, *J* = 15.0 Hz, 1H), 6.98 (d, *J* = 15.0 Hz, 1H).

¹³C NMR (176 MHz, DMSO-*d*₆) δ 165.82, 163.50, 139.41, 135.89, 135.70, 131.58, 117.57.

HRMS (ESI⁺): [M+H]⁺ calculated for C₉H₉FNO₃S = 230.02818 m/z; found = 230.02854 m/z.

Synthesis of (*E*)-3-tosylacrylamide (**17**):



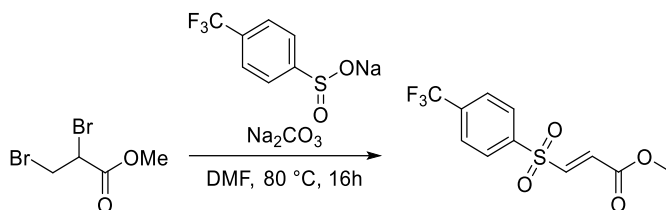
Following the general procedure **A** on 230.9 mg (1.00 mmol) of **2,3-dibromopropanecarboxamide**, purification afforded 180.5 mg (80% yield) of (*E*)-3-tosylacrylamide as a white solid. (Gradient from 0 to 40% EtOAc/hexanes)

¹H NMR (700 MHz, DMSO-*d*₆) δ 8.02 (s, 1H), 7.80 (d, *J* = 7.9 Hz, 2H), 7.67 (s, 1H), 7.48 (d, *J* = 8.0 Hz, 2H), 7.41 (d, *J* = 15.1 Hz, 1H), 6.95 (d, *J* = 14.9 Hz, 1H), 2.41 (s, 3H).

¹³C NMR (176 MHz, DMSO-*d*₆) δ 163.14, 145.09, 139.30, 135.96, 134.81, 130.26, 127.77, 21.13.

HRMS (ESI⁺): [M+Na]⁺ calculated for C₁₀H₁₁NO₃SNa = 248.03522 m/z; found = 248.03636 m/z.

Synthesis of methyl (*E*)-3-((4-(trifluoromethyl)phenyl)sulfonyl)acrylate (18):



Following the general procedure **A** on 245.9 mg (1.00 mmol) of **methyl 2,3-dibromopropanoate**, purification afforded 129.0 mg (44% yield) of **methyl (*E*)-3-((4-(trifluoromethyl)phenyl)sulfonyl)acrylate** as a white solid. (Gradient from 0 to 20% EtOAc/hexanes)

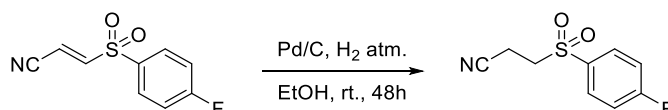
^1H NMR (700 MHz, DMSO- d_6) δ 8.21 – 8.16 (m, 2H), 8.10 – 8.06 (m, 2H), 7.93 (d, J = 15.2 Hz, 1H), 6.89 (d, J = 15.2 Hz, 1H), 3.74 (s, 3H).

^{13}C NMR (176 MHz, DMSO- d_6) δ 163.94, 142.71, 142.53, 134.47, 132.76, 129.65, 127.42, 123.63, 53.19.

HRMS (ESI $^+$): [M+H] $^+$ calculated for C $_{11}$ H $_{10}$ F $_3$ O $_4$ S = 295.02468 m/z; found = 295.02445 m/z.

HRMS (ESI $^+$): [M+Na] $^+$ calculated for C $_{11}$ H $_9$ F $_3$ O $_4$ SNa = 317.00662 m/z; found = 317.00673 m/z.

Synthesis of 3-((4-fluorophenyl)sulfonyl)propanenitrile (19):



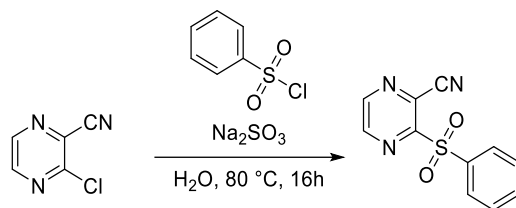
110 mg (0.52 mmol) of **(*E*)-3-((4-fluorophenyl)sulfonyl)acrylonitrile (5)** was dissolved in 5 mL ethanol and 20% w/w Pd/C was added. The reaction was stirred at room temperature under hydrogen atmosphere for 48 h and filtered through a silica pad using DCM. Purification afforded 100 mg (90% yield) of **3-((4-fluorophenyl)sulfonyl)propanenitrile** as a white solid.

^1H NMR (700 MHz, DMSO- d_6) δ 8.03 – 7.99 (m, 2H), 7.56 – 7.51 (m, 2H), 3.75 (t, J = 6.9 Hz, 2H), 2.87 (t, J = 6.9 Hz, 2H).

^{13}C NMR (176 MHz, DMSO- d_6) δ 165.89, 134.79, 131.86, 118.14, 117.33, 50.10, 11.94.

HRMS (ESI $^+$): [M+Na] $^+$ calculated for C $_9$ H $_8$ FNO $_2$ SNa = 236.01522 m/z; found = 236.01540 m/z.

Synthesis of 3-(phenylsulfonyl)pyrazine-2-carbonitrile (20):



Following the general procedure **B** on 100 mg (0.72 mmol) of **3-chloropyrazine-2-carbonitrile**, purification afforded 26.2 mg (15% yield) of **3-(phenylsulfonyl)pyrazine-2-carbonitrile** as a white solid. (Gradient from 5 to 100% MeCN/H₂O)

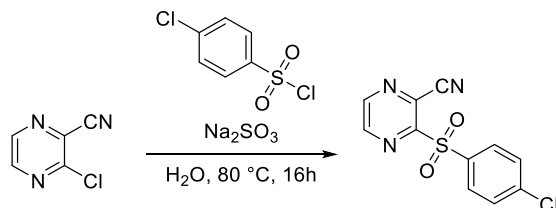
¹H NMR (700 MHz, Chloroform-*d*) δ 8.86 (d, *J* = 2.3 Hz, 1H), 8.82 (d, *J* = 2.3 Hz, 1H), 8.19 – 8.16 (m, 2H), 7.73 (ddt, *J* = 8.7, 7.4, 1.3 Hz, 1H), 7.65 – 7.61 (m, 2H).

¹³C NMR (176 MHz, Chloroform-*d*) δ 157.14, 147.06, 145.92, 137.03, 135.26, 129.69, 128.40, 113.05.

HRMS (ESI⁺): [M+H]⁺ calculated for C₁₁H₈N₃O₂S = 246.03318 m/z; found = 246.03185 m/z.

HRMS (ESI⁺): [M+Na]⁺ calculated for C₁₁H₇N₃O₂SNa = 268.01512 m/z; found = 268.01459 m/z.

Synthesis of 3-((4-chlorophenyl)sulfonyl)pyrazine-2-carbonitrile (24):



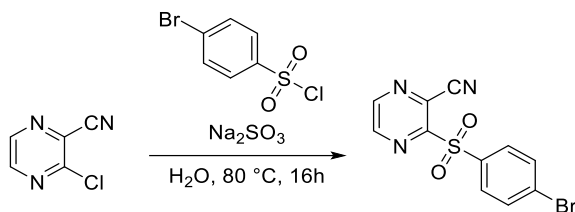
Following the general procedure **B** on 100 mg (0.72 mmol) of **3-chloropyrazine-2-carbonitrile**, purification afforded 11.6 mg (6% yield) of **3-((4-chlorophenyl)sulfonyl)pyrazine-2-carbonitrile** as a white solid. (Gradient from 5 to 100% MeCN/H₂O)

¹H NMR (700 MHz, DMSO-*d*₆) δ 9.12 – 9.09 (m, 1H), 9.04 – 9.01 (m, 1H), 8.06 (d, *J* = 8.3 Hz, 2H), 7.81 (d, *J* = 8.4 Hz, 2H).

¹³C NMR (176 MHz, DMSO-*d*₆) δ 155.10, 148.63, 147.42, 140.65, 135.34, 131.20, 130.01, 126.82, 113.80.

HRMS (ESI⁺): [M+Na]⁺ calculated for C₁₁H₆ClN₃O₂SNa = 301.97612 m/z; found = 301.97751 m/z.

Synthesis of 3-((4-bromophenyl)sulfonyl)pyrazine-2-carbonitrile (25):



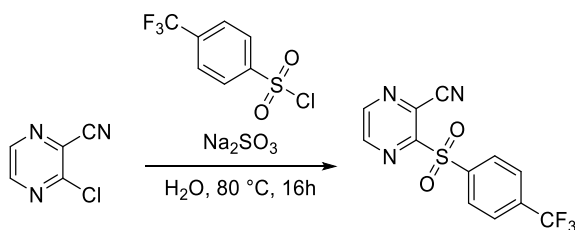
Following the general procedure **B** on 100 mg (0.72 mmol) of **3-chloropyrazine-2-carbonitrile**, purification afforded 10.0 mg (4% yield) of **3-((4-bromophenyl)sulfonyl)pyrazine-2-carbonitrile** as a white solid. (Gradient from 5 to 100% MeCN/ H_2O)

^1H NMR (700 MHz, $\text{DMSO}-d_6$) δ 9.11 (d, $J = 2.3$ Hz, 1H), 9.02 (d, $J = 2.3$ Hz, 1H), 7.99 – 7.93 (m, 4H).

^{13}C NMR (176 MHz, $\text{DMSO}-d_6$) δ 155.54, 149.10, 147.91, 136.25, 133.43, 131.64, 130.40, 127.29, 114.28.

HRMS (ESI^+): $[\text{M}+\text{Na}]^+$ calculated for $\text{C}_{11}\text{H}_6\text{BrN}_3\text{O}_2\text{SNa} = 345.92562$ m/z; found = 345.92701 m/z.

Synthesis of 3-((4-(trifluoromethyl)phenyl)sulfonyl)pyrazine-2-carbonitrile (26):



Following the general procedure **B** on 100 mg (0.72 mmol) of **3-chloropyrazine-2-carbonitrile**, purification afforded 24.0 mg (11% yield) of **3-((4-(trifluoromethyl)phenyl)sulfonyl)pyrazine-2-carbonitrile** as a white solid. (Gradient from 5 to 100% MeCN/ H_2O)

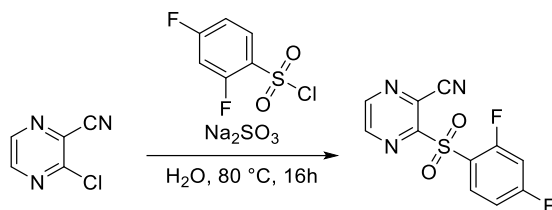
^1H NMR (700 MHz, $\text{DMSO}-d_6$) δ 9.12 (d, $J = 2.2$ Hz, 1H), 9.03 (dd, $J = 2.3, 1.0$ Hz, 1H), 8.28 (d, $J = 8.2$ Hz, 2H), 8.12 (d, $J = 8.2$ Hz, 2H).

^{13}C NMR (176 MHz, $\text{DMSO}-d_6$) δ 154.68, 148.77, 147.44, 140.56, 134.62, 134.44, 130.39, 127.14, 126.92, 113.77.

HRMS (ESI^+): $[\text{M}+\text{H}]^+$ calculated for $\text{C}_{12}\text{H}_7\text{F}_3\text{N}_3\text{O}_2\text{S} = 314.02057$ m/z; found = 314.02177 m/z.

HRMS (ESI^+): $[\text{M}+\text{Na}]^+$ calculated for $\text{C}_{12}\text{H}_6\text{F}_3\text{N}_3\text{O}_2\text{SNa} = 336.00252$ m/z; found = 336.00414 m/z.

Synthesis of 3-((2,4-difluorophenyl)sulfonyl)pyrazine-2-carbonitrile (27):



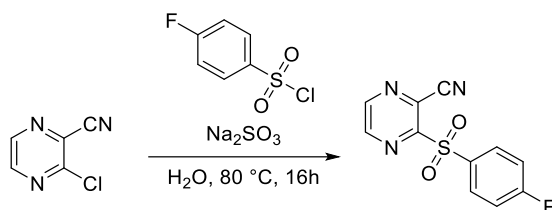
Following the general procedure **B** on 100 mg (0.72 mmol) of **3-chloropyrazine-2-carbonitrile**, purification afforded 39.8 mg (20% yield) of **3-((2,4-difluorophenyl)sulfonyl)pyrazine-2-carbonitrile** as a white solid. (Gradient from 5 to 100% MeCN/H₂O)

¹H NMR (700 MHz, DMSO-*d*₆) δ 9.18 – 9.15 (m, 1H), 9.07 – 9.04 (m, 1H), 8.19 (q, *J* = 8.1 Hz, 1H), 7.67 (td, *J* = 10.3, 1.9 Hz, 1H), 7.48 (ddd, *J* = 10.0, 5.8, 2.1 Hz, 1H).

¹³C NMR (176 MHz, DMSO-*d*₆) δ 167.86, 166.40, 161.23, 159.76, 154.55, 149.13, 147.55, 133.62, 126.74, 121.07, 113.48.

HRMS (ESI⁺): [M+Na]⁺ calculated for C₁₁H₃F₂N₃O₂SNa = 303.99632 m/z; found = 303.99700 m/z.

Synthesis of 3-((4-fluorophenyl)sulfonyl)pyrazine-2-carbonitrile (28):



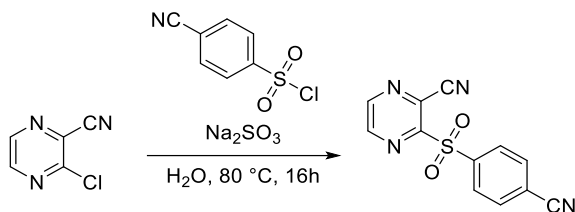
Following the general procedure **B** on 100 mg (0.72 mmol) of **3-chloropyrazine-2-carbonitrile**, purification afforded 15.7 mg (12% yield) of **3-((4-fluorophenyl)sulfonyl)pyrazine-2-carbonitrile** as a white solid. (Gradient from 5 to 100% MeCN/H₂O)

¹H NMR (700 MHz, DMSO-*d*₆) δ 9.10 (d, *J* = 2.3 Hz, 1H), 9.02 (d, *J* = 2.3 Hz, 1H), 8.16 – 8.11 (m, 2H), 7.61 – 7.55 (m, 2H).

¹³C NMR (176 MHz, DMSO-*d*₆) δ 166.02, 155.30, 147.99, 132.79, 132.71, 126.71, 117.21, 113.83.

HRMS (ESI⁺): [M+Na]⁺ calculated for C₁₁H₆FN₃O₂SNa = 286.00572 m/z; found = 286.00707 m/z.

Synthesis of 3-((4-cyanophenyl)sulfonyl)pyrazine-2-carbonitrile (29):



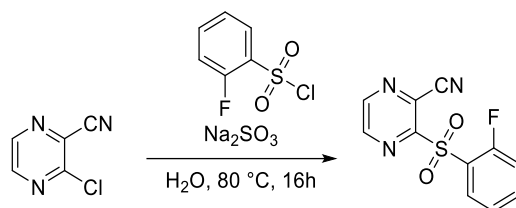
Following the general procedure **B** on 100 mg (0.72 mmol) of **3-chloropyrazine-2-carbonitrile**, purification afforded 42.8 mg (22% yield) of **3-((4-cyanophenyl)sulfonyl)pyrazine-2-carbonitrile** as a white solid. (Gradient from 5 to 100% MeCN/H₂O)

¹H NMR (700 MHz, DMSO-*d*₆) δ 9.13 (d, *J* = 2.4 Hz, 1H), 9.03 (d, *J* = 2.4 Hz, 1H), 8.22 (q, *J* = 8.4 Hz, 4H).

¹³C NMR (176 MHz, DMSO-*d*₆) δ 154.57, 148.82, 147.41, 140.62, 133.75, 129.99, 127.18, 117.50, 117.34, 113.74.

HRMS (ESI⁺): [M+Na]⁺ calculated for C₁₂H₆N₄O₂SNa = 293.01032 m/z; found = 293.00973 m/z.

Synthesis of 3-((2-fluorophenyl)sulfonyl)pyrazine-2-carbonitrile (30):



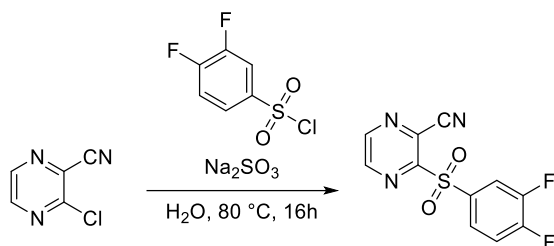
Following the general procedure **B** on 100 mg (0.72 mmol) of **3-chloropyrazine-2-carbonitrile**, purification afforded 29.2 mg (15% yield) of **3-((2-fluorophenyl)sulfonyl)pyrazine-2-carbonitrile** as a white solid. (Gradient from 5 to 100% MeCN/H₂O)

¹H NMR (700 MHz, DMSO-*d*₆) δ 9.17 (t, *J* = 1.8 Hz, 1H), 9.05 (dd, *J* = 2.3, 1.3 Hz, 1H), 8.15 – 8.10 (m, 1H), 7.95 – 7.90 (m, 1H), 7.58 (td, *J* = 7.7, 1.3 Hz, 1H), 7.53 (dd, *J* = 10.2, 8.5 Hz, 1H).

¹³C NMR (176 MHz, DMSO-*d*₆) δ 159.26, 154.72, 149.14, 147.58, 138.75, 131.06, 126.70, 125.71, 124.40, 117.69, 113.48.

HRMS (ESI⁺): [M+Na]⁺ calculated for C₁₁H₆FN₃O₂SNa = 286.00572 m/z; found = 286.00673 m/z.

Synthesis of 3-((3,4-difluorophenyl)sulfonyl)pyrazine-2-carbonitrile (31):



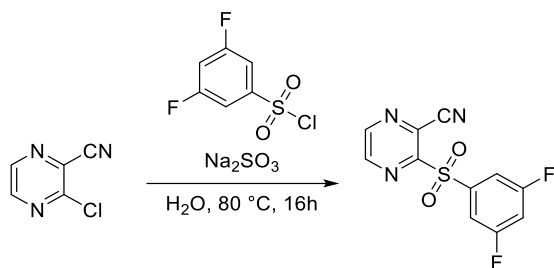
Following the general procedure **B** on 100 mg (0.72 mmol) of **3-chloropyrazine-2-carbonitrile**, purification afforded 48.4 mg (24% yield) of **3-((3,4-difluorophenyl)sulfonyl)pyrazine-2-carbonitrile** as a white solid. (Gradient from 5 to 100% MeCN/H₂O)

¹H NMR (700 MHz, DMSO-*d*₆) δ 9.12 (dd, *J* = 2.3, 1.1 Hz, 1H), 9.03 (dd, *J* = 2.3, 1.0 Hz, 1H), 8.14 (ddd, *J* = 9.6, 7.0, 2.3 Hz, 1H), 8.00 – 7.96 (m, 1H), 7.86 – 7.81 (m, 1H).

¹³C NMR (176 MHz, DMSO-*d*₆) δ 154.81, 154.63, 153.17, 150.21, 148.78, 148.03, 133.41, 127.70, 126.94, 119.30, 113.77.

HRMS (ESI⁺): [M+Na]⁺ calculated for C₁₁H₅F₂N₃O₂SNa = 303.99632 m/z; found = 303.99690 m/z.

Synthesis of 3-((3,5-difluorophenyl)sulfonyl)pyrazine-2-carbonitrile (32):



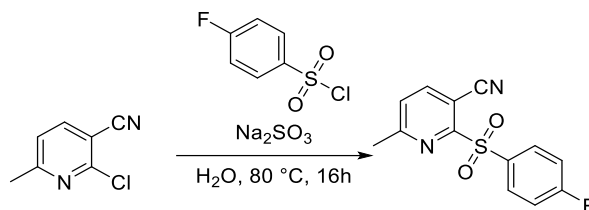
Following the general procedure **B** on 100 mg (0.72 mmol) of **3-chloropyrazine-2-carbonitrile**, purification afforded 44.8 mg (22% yield) of **3-((3,5-difluorophenyl)sulfonyl)pyrazine-2-carbonitrile** as a white solid. (Gradient from 5 to 100% MeCN/H₂O)

¹H NMR (700 MHz, DMSO-*d*₆) δ 9.14 (d, *J* = 2.3 Hz, 1H), 9.04 (d, *J* = 2.3 Hz, 1H), 7.88 – 7.83 (m, 1H), 7.82 – 7.77 (m, 2H).

¹³C NMR (176 MHz, DMSO-*d*₆) δ 162.96, 161.52, 154.38, 148.83, 147.38, 139.70, 127.18, 113.72, 111.30.

HRMS (ESI⁺): [M+Na]⁺ calculated for C₁₁H₅F₂N₃O₂SNa = 303.99632 m/z; found = 303.99757 m/z.

Synthesis of 2-((4-fluorophenyl)sulfonyl)-6-methylnicotinonitrile (33):



Following the general procedure **B** on 100 mg (0.66 mmol) of **2-chloro-6-methylnicotinonitrile**, purification afforded 55.9 mg (31% yield) of **2-((4-fluorophenyl)sulfonyl)-6-methylnicotinonitrile** as a white solid. (Gradient from 5 to 100% MeCN/H₂O)

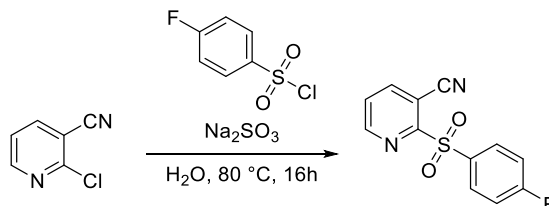
¹H NMR (700 MHz, Chloroform-*d*) δ 8.20 – 8.15 (m, 2H), 8.04 (d, *J* = 8.0 Hz, 1H), 7.43 (d, *J* = 8.0 Hz, 1H), 7.28 – 7.22 (m, 2H), 2.66 (s, 3H).

¹³C NMR (176 MHz, Chloroform-*d*) δ 166.46, 163.49, 159.09, 143.28, 133.83, 132.54, 126.27, 116.71, 114.15, 105.52, 24.89.

HRMS (ESI⁺): [M+H]⁺ calculated for C₁₃H₁₀FN₂O₂S = 277.04418 m/z; found = 277.04492 m/z.

HRMS (ESI⁺): [M+Na]⁺ calculated for C₁₃H₉FN₂O₂SNa = 299.02612 m/z; found = 299.02738 m/z.

Synthesis of 2-((4-fluorophenyl)sulfonyl)nicotinonitrile (34):



Following the general procedure **B** on 100 mg (0.73 mmol) of **2-chloronicotinonitrile**, purification afforded 53.8 mg (28% yield) of **2-((4-fluorophenyl)sulfonyl)nicotinonitrile** as a white solid. (Gradient from 5 to 100% MeCN/H₂O)

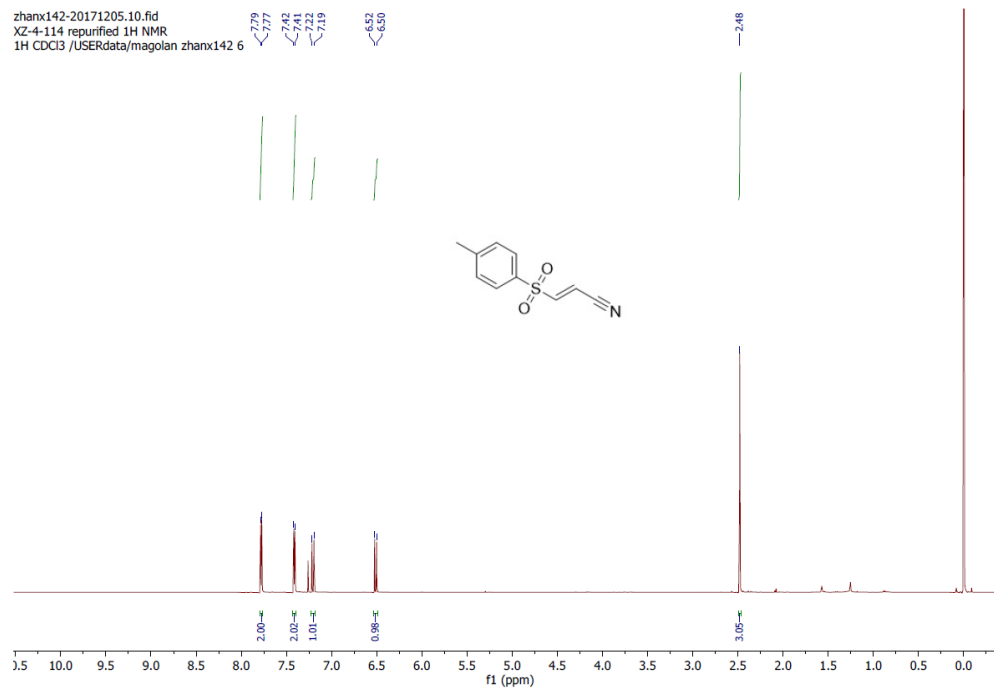
¹H NMR (700 MHz, DMSO-*d*₆) δ 8.90 (dd, *J* = 4.7, 1.6 Hz, 1H), 8.67 (dd, *J* = 7.9, 1.6 Hz, 1H), 8.13 – 8.08 (m, 2H), 7.90 (dd, *J* = 7.9, 4.8 Hz, 1H), 7.59 – 7.54 (m, 2H).

¹³C NMR (176 MHz, DMSO-*d*₆) δ 166.28, 158.76, 153.31, 145.51, 133.69, 132.91, 128.12, 117.61, 114.46, 107.35.

HRMS (ESI⁺): [M+H]⁺ calculated for C₁₂H₈FN₂O₂S = 263.02848 m/z; found = 263.02951 m/z.

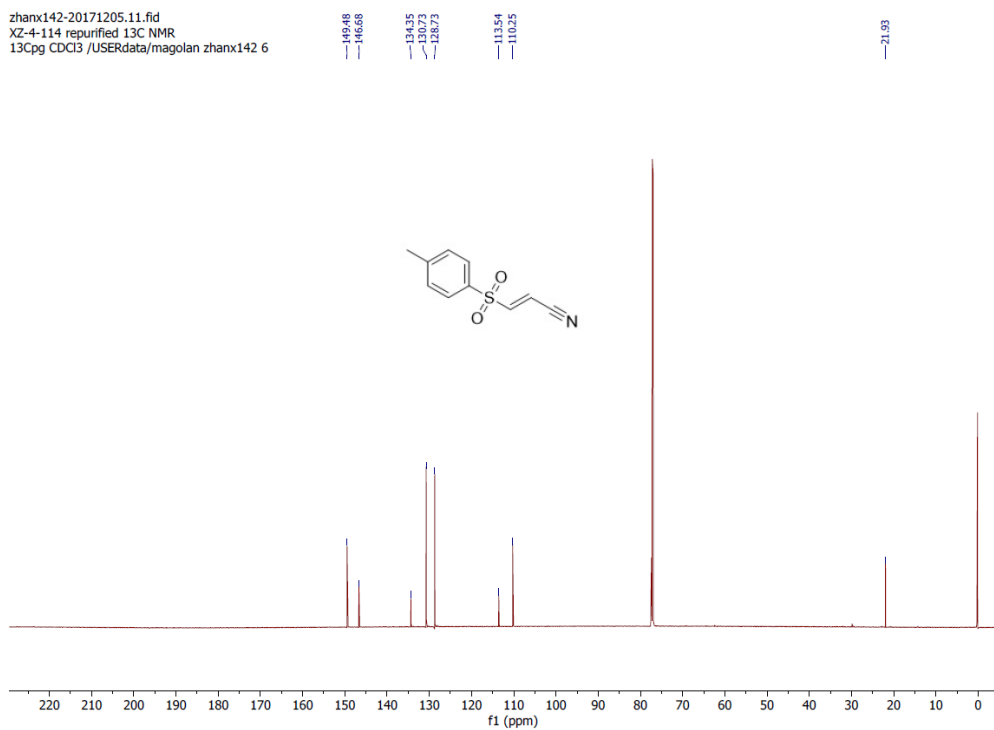
(E)-3-tosylacrylonitrile (1)

¹H NMR (700 MHz, Chloroform-*d*)



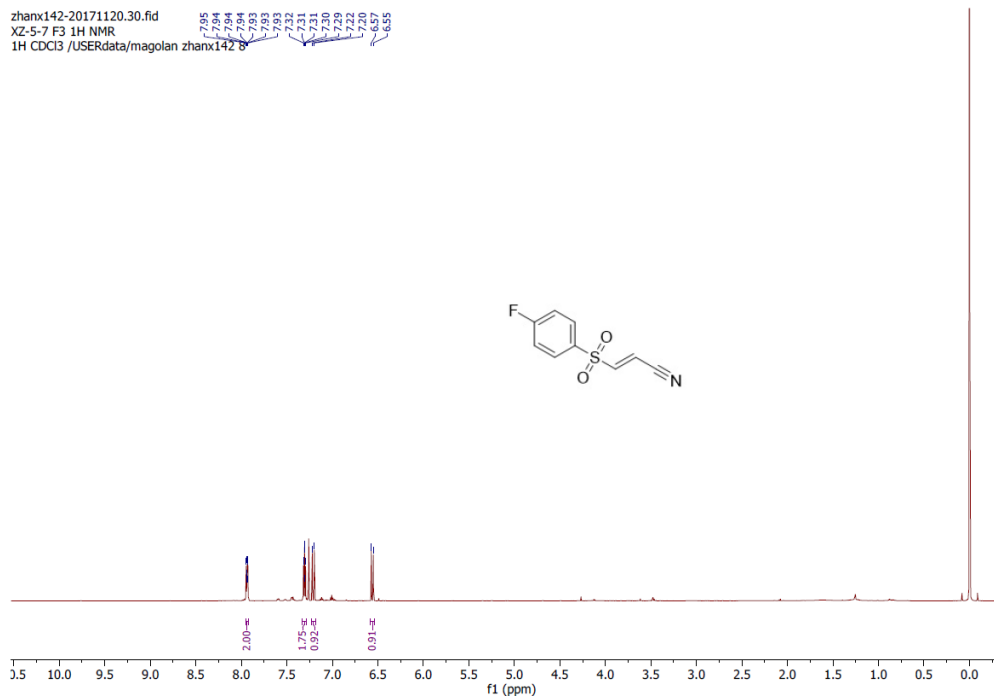
(E)-3-tosylacrylonitrile (1)

¹³C NMR (176 MHz, Chloroform-*d*)



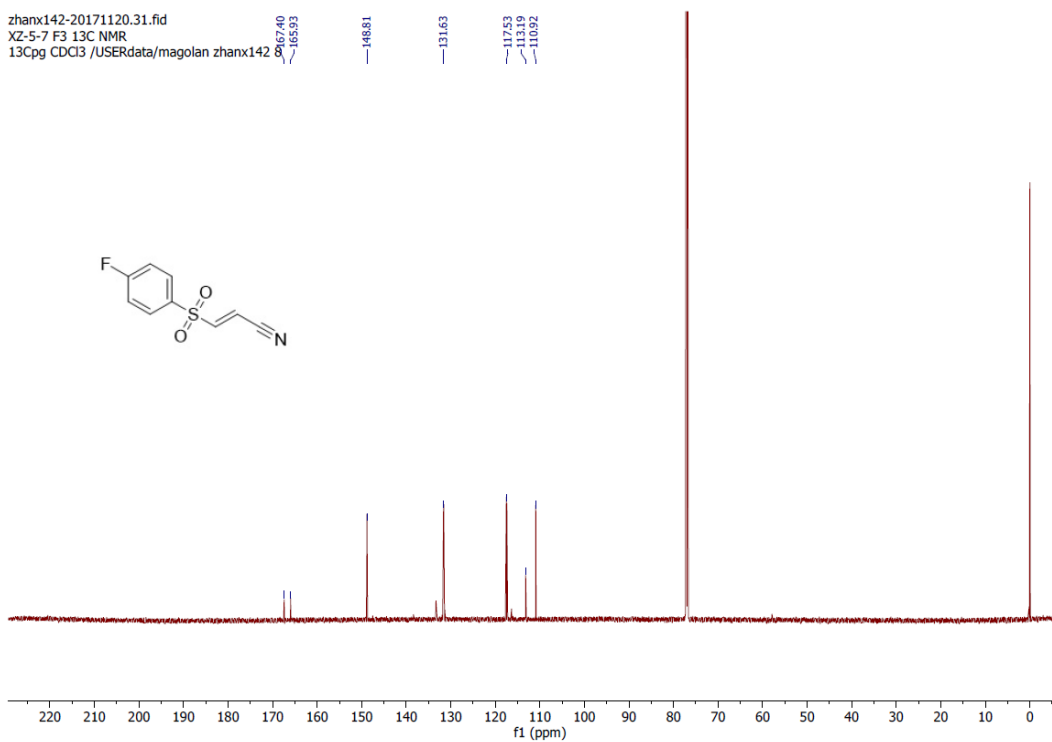
(E)-3-((4-fluorophenyl)sulfonyl)acrylonitrile (5)

¹H NMR (700 MHz, Chloroform-*d*)



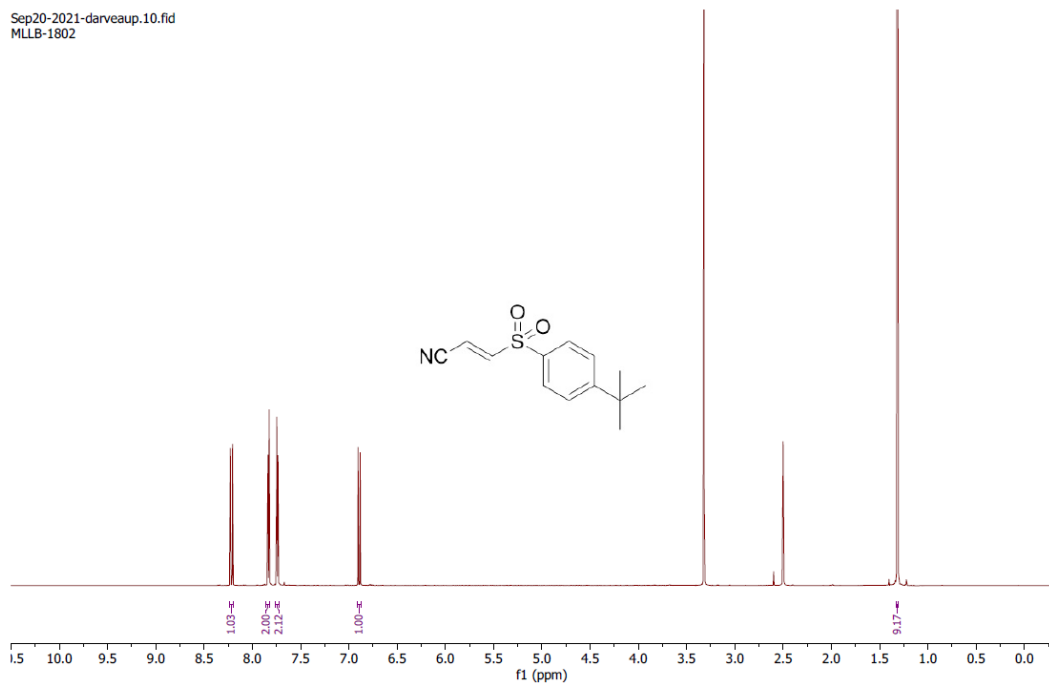
(E)-3-((4-fluorophenyl)sulfonyl)acrylonitrile (5)

¹³C NMR (176 MHz, Chloroform-*d*)



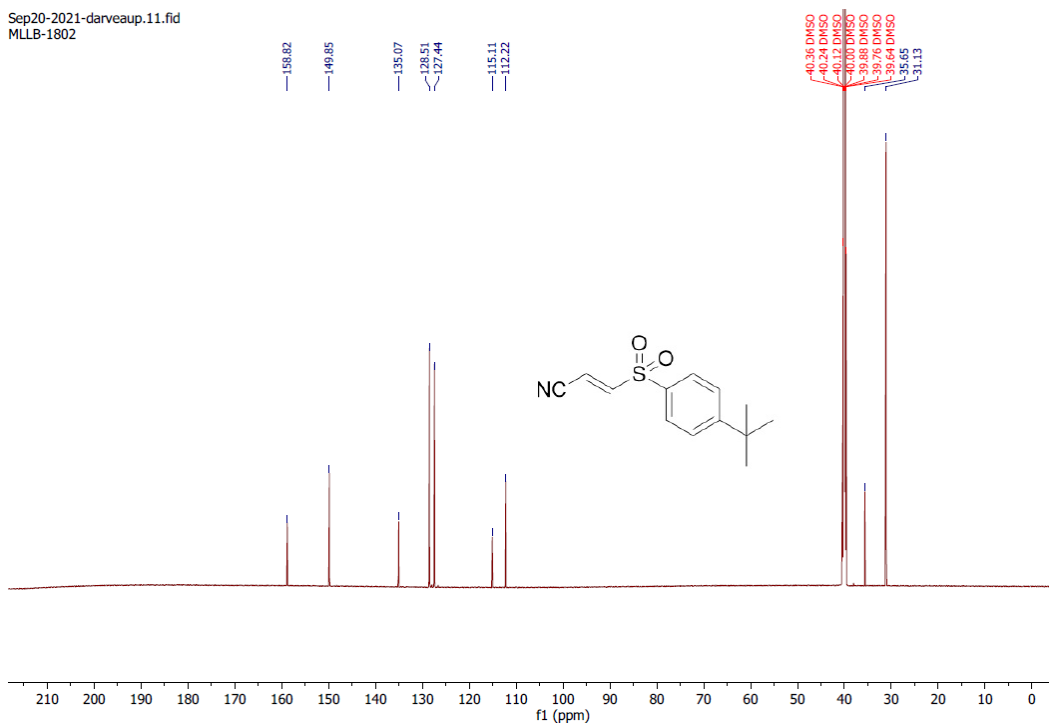
(E)-3-((4-(*tert*-butyl)phenyl)sulfonyl)acrylonitrile (6)

¹H NMR (700 MHz, DMSO-*d*₆)



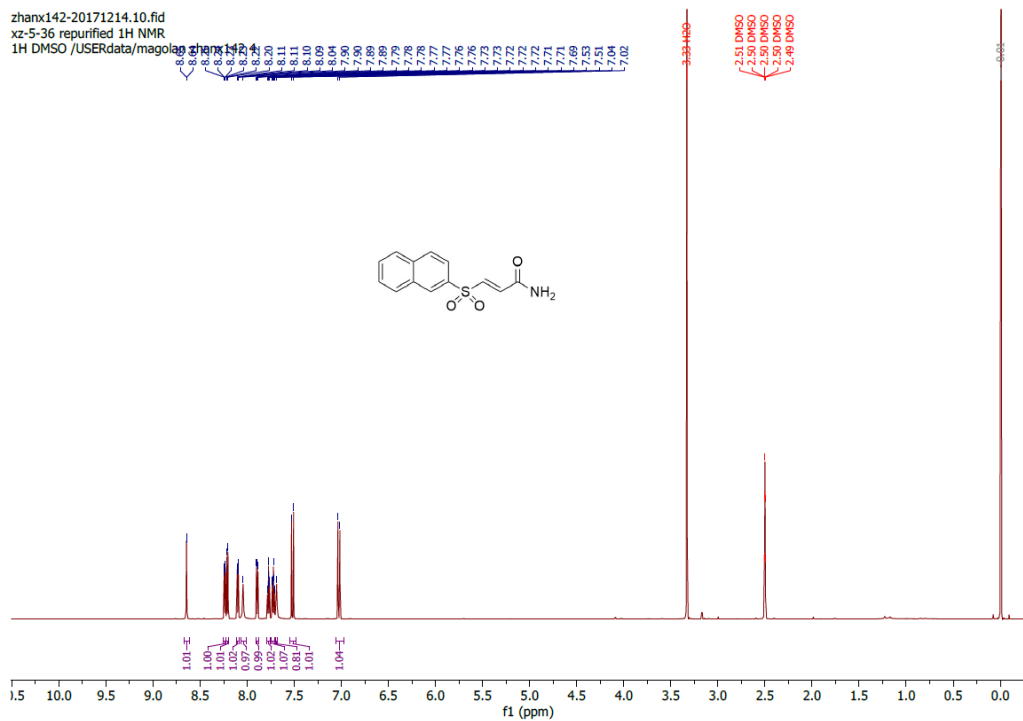
(E)-3-((4-(*tert*-butyl)phenyl)sulfonyl)acrylonitrile (6)

¹³C NMR (176 MHz, DMSO-*d*₆)



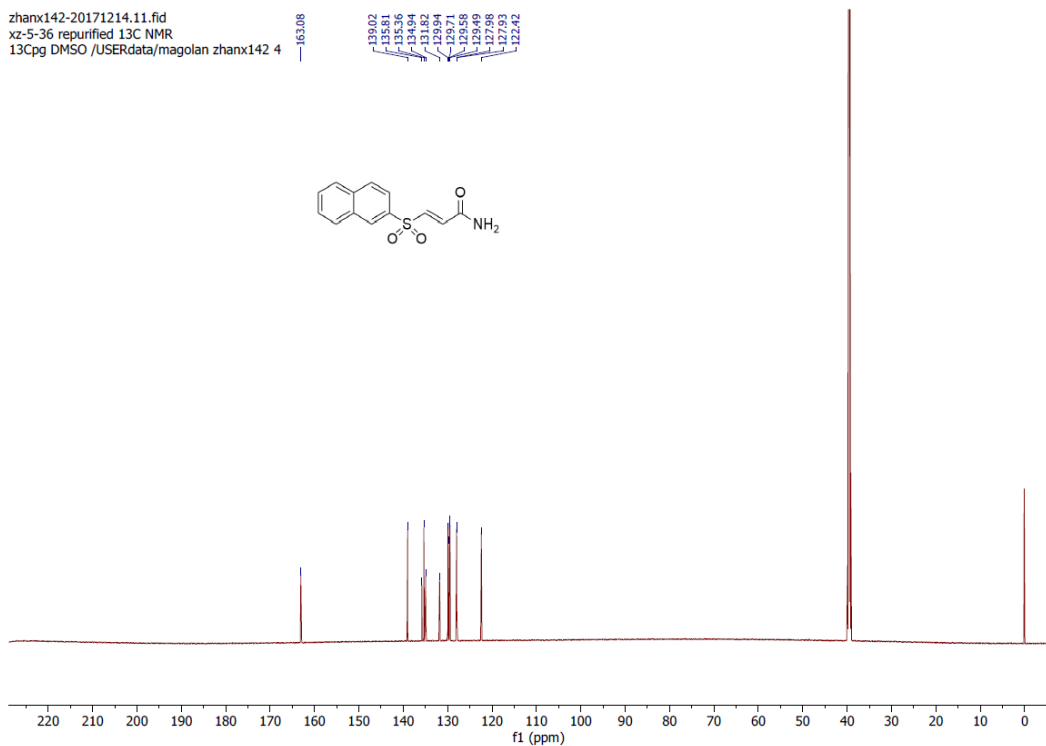
(E)-3-(naphthalen-2-ylsulfonyl)acrylamide (7)

¹H NMR (700 MHz, DMSO-*d*₆)

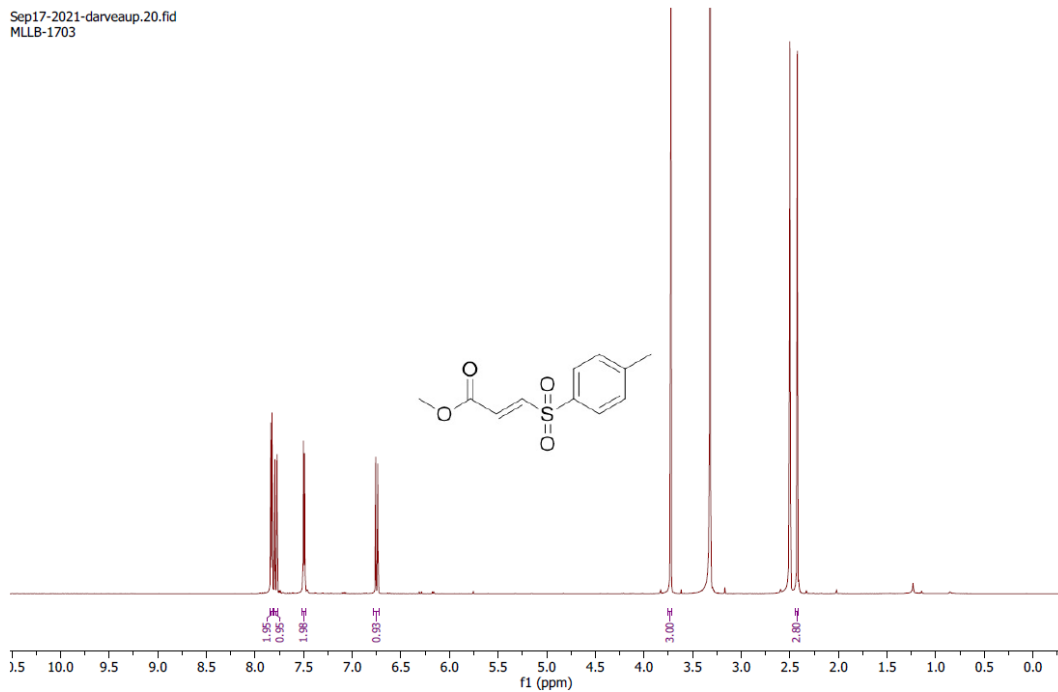


(E)-3-(naphthalen-2-ylsulfonyl)acrylamide (7)

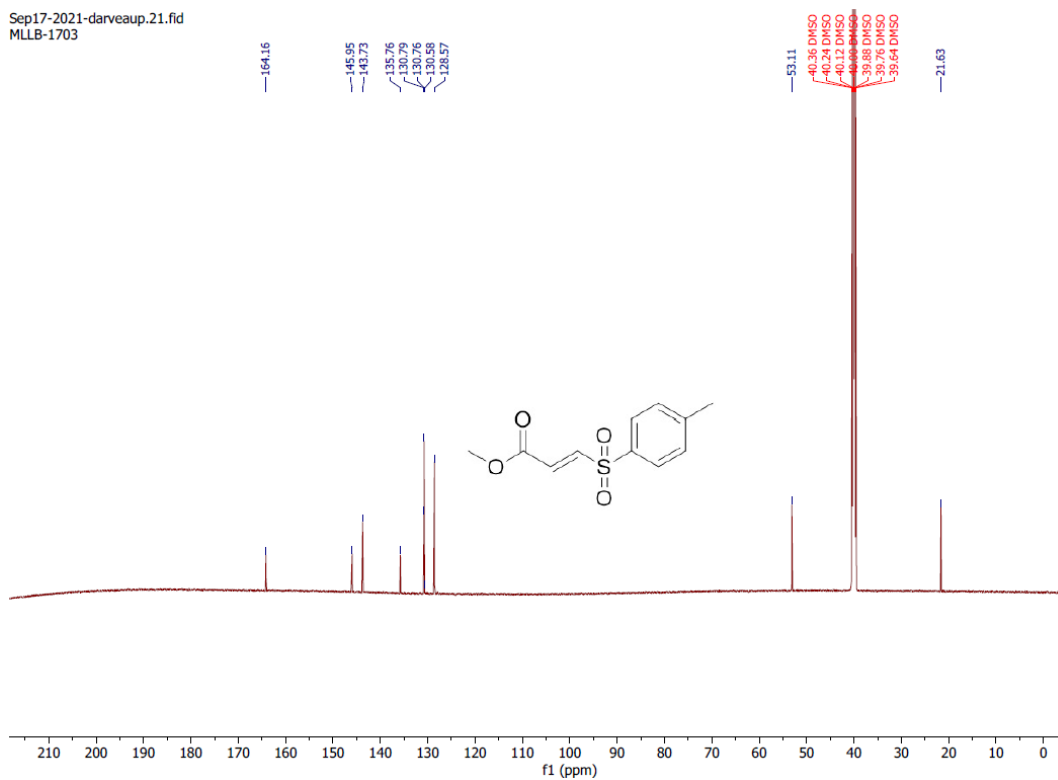
¹³C NMR (176 MHz, DMSO-*d*₆)



methyl (*E*)-3-tosylacrylate (9)
¹H NMR (700 MHz, DMSO-*d*₆)

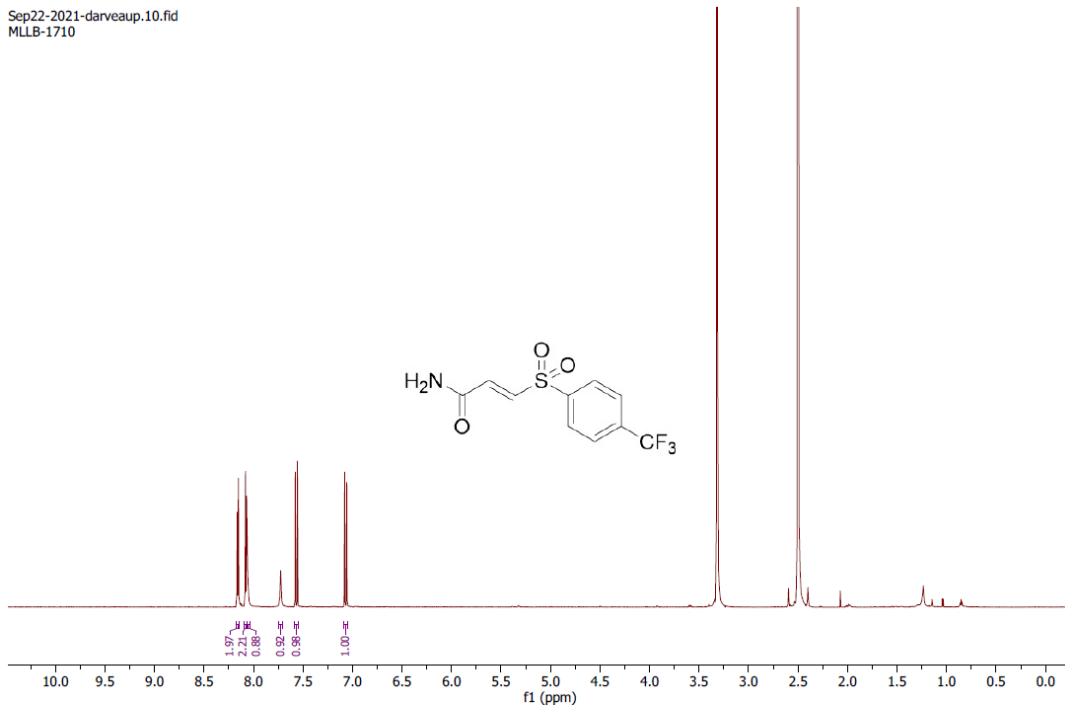


methyl (*E*)-3-tosylacrylate (9)
¹³C NMR (176 MHz, DMSO-*d*₆)



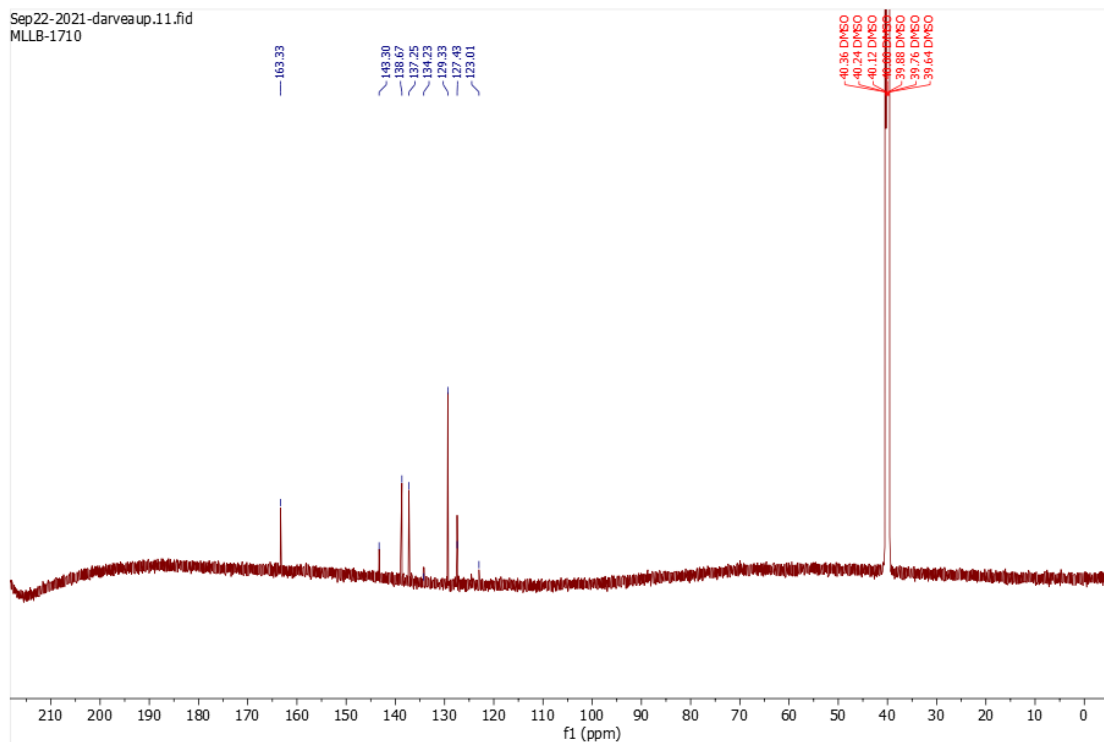
(E)-3-((4-(trifluoromethyl)phenyl)sulfonyl)acrylamide (11)

¹H NMR (700 MHz, DMSO-*d*₆)



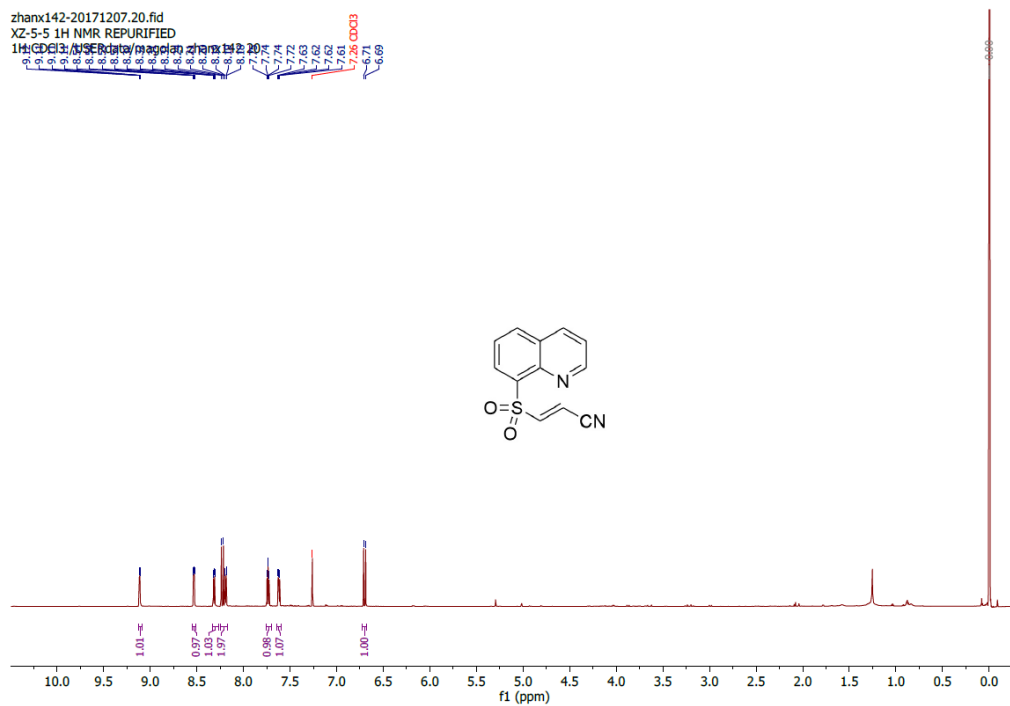
(E)-3-((4-(trifluoromethyl)phenyl)sulfonyl)acrylamide (11)

¹³C NMR (176 MHz, DMSO-*d*₆)



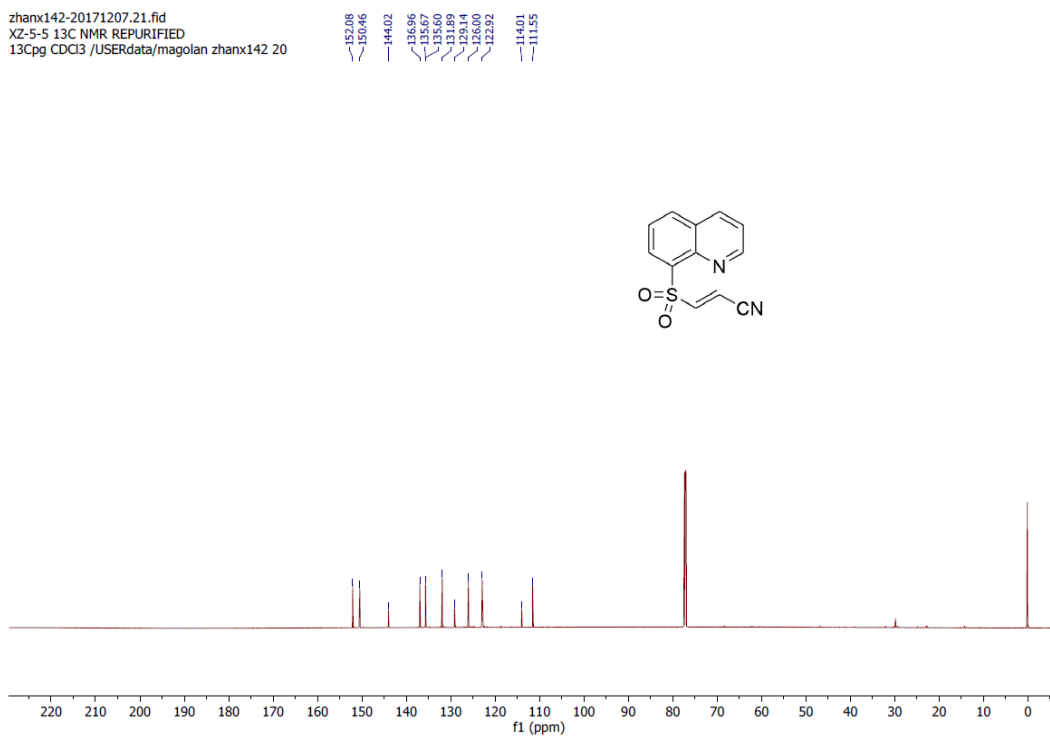
(E)-3-(quinolin-8-ylsulfonyl)acrylonitrile (12)

¹H NMR (700 MHz, Chloroform-*d*)



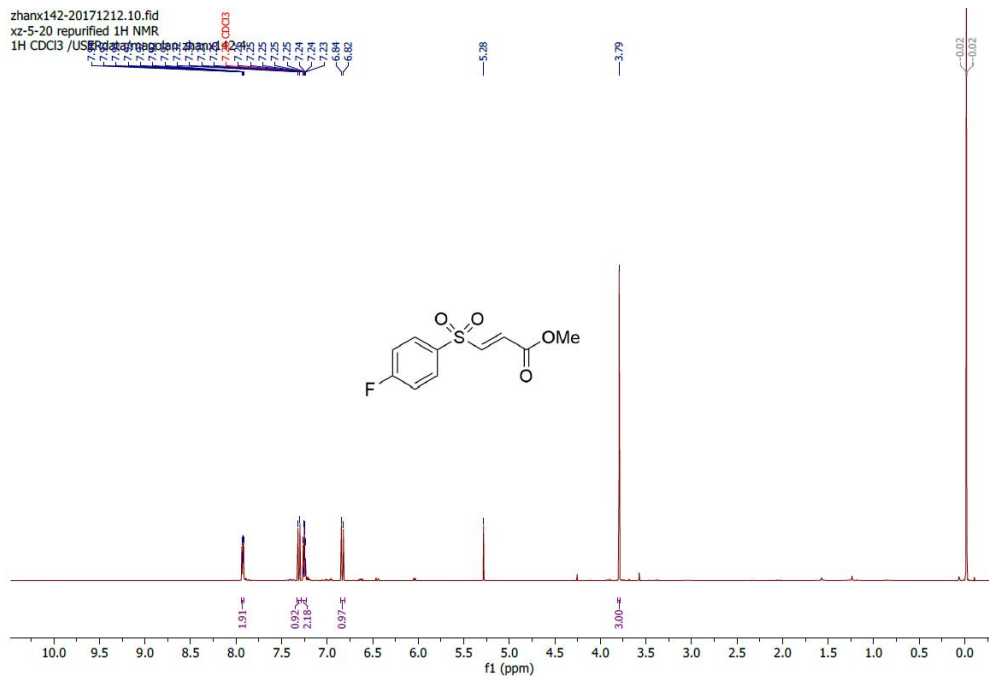
(E)-3-(quinolin-8-ylsulfonyl)acrylonitrile (12)

¹³C NMR (176 MHz, Chloroform-*d*)



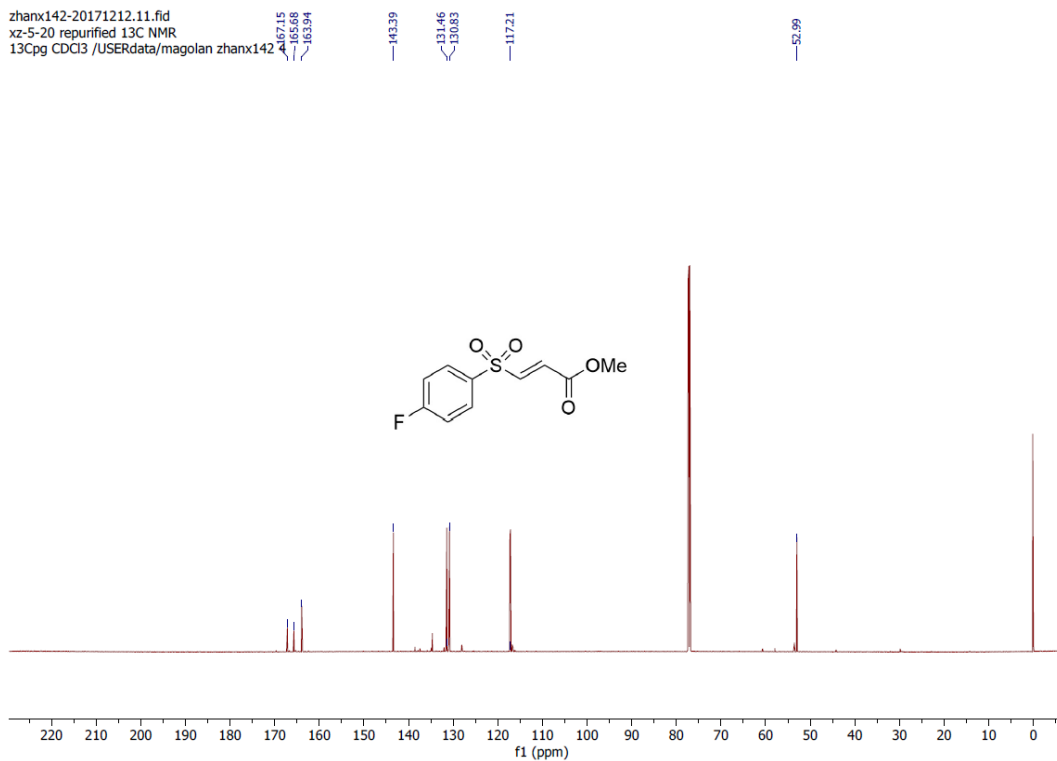
Methyl (*E*)-3-((4-fluorophenyl)sulfonyl)acrylate (13)

¹H NMR (700 MHz, Chloroform-*d*)



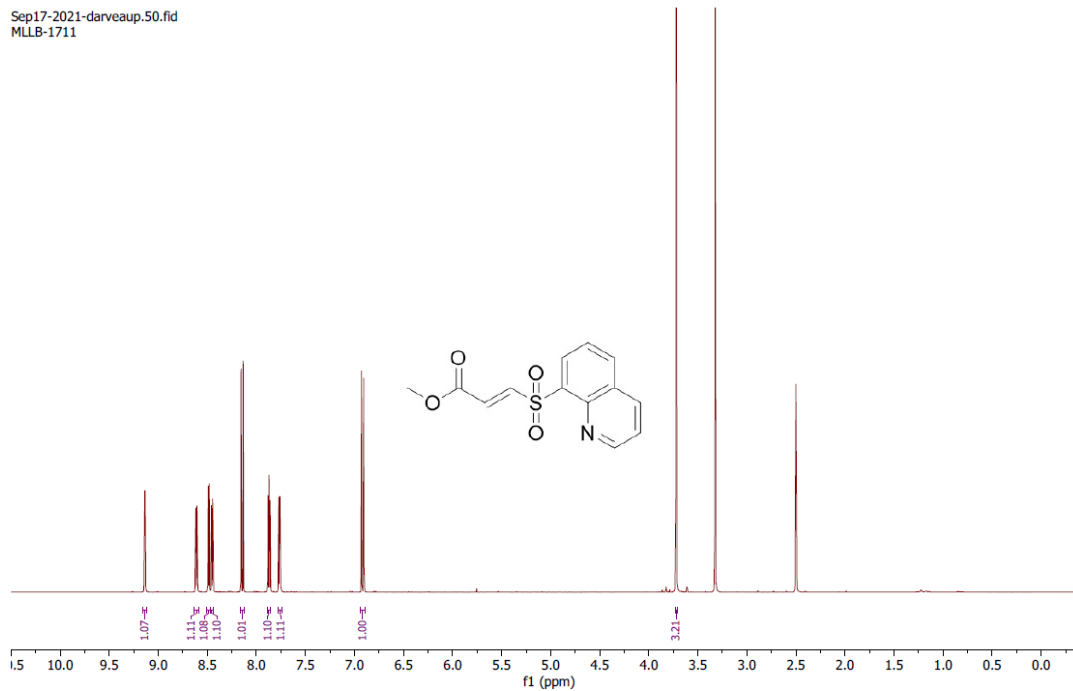
Methyl (*E*)-3-((4-fluorophenyl)sulfonyl)acrylate (13)

¹³C NMR (176 MHz, Chloroform-*d*)



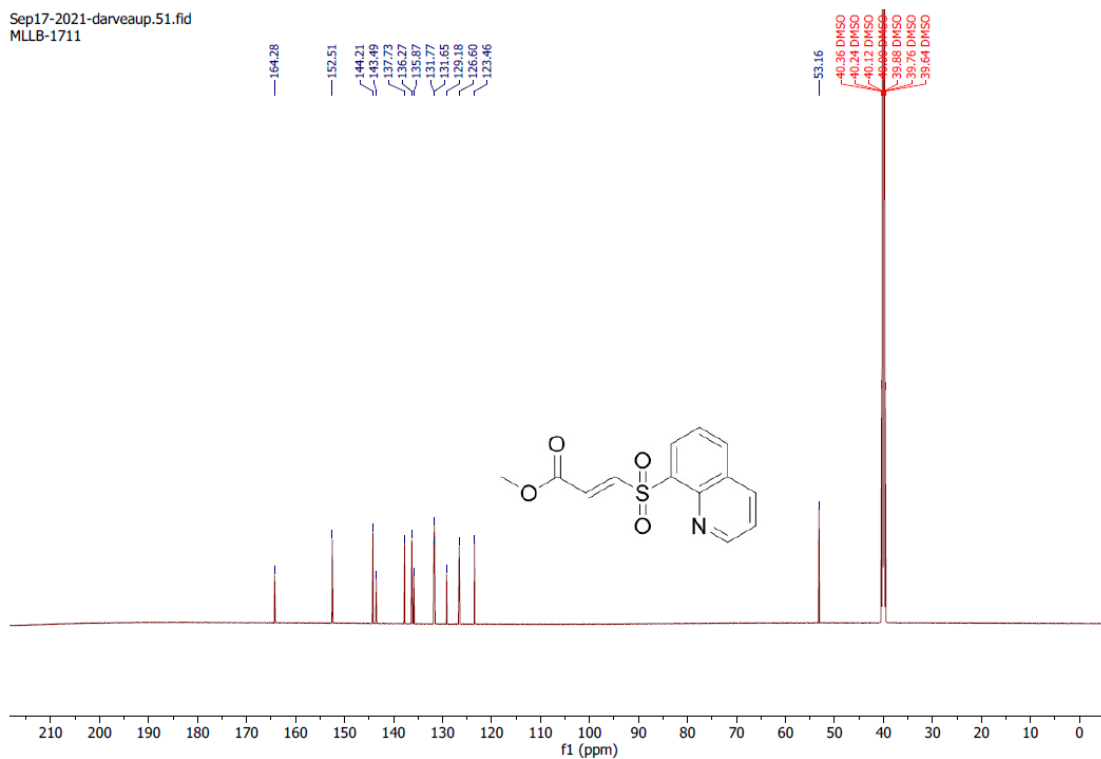
Methyl (*E*)-3-(quinolin-8-ylsulfonyl)acrylate (14)

^1H NMR (700 MHz, $\text{DMSO-}d_6$)



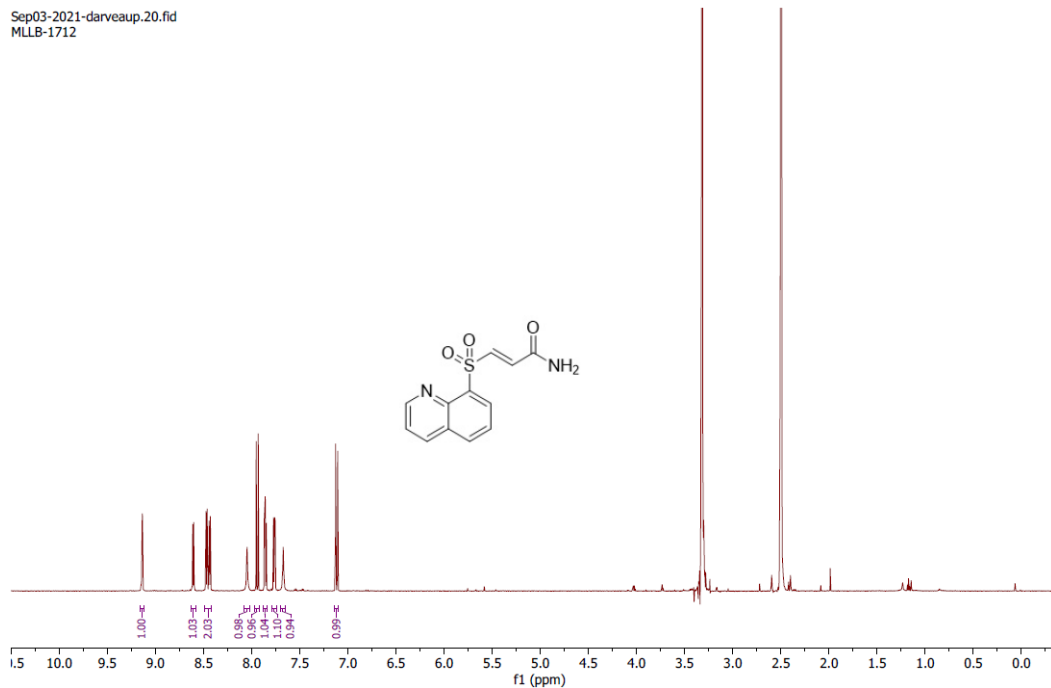
Methyl (*E*)-3-(quinolin-8-ylsulfonyl)acrylate (14)

^{13}C NMR (176 MHz, $\text{DMSO-}d_6$)



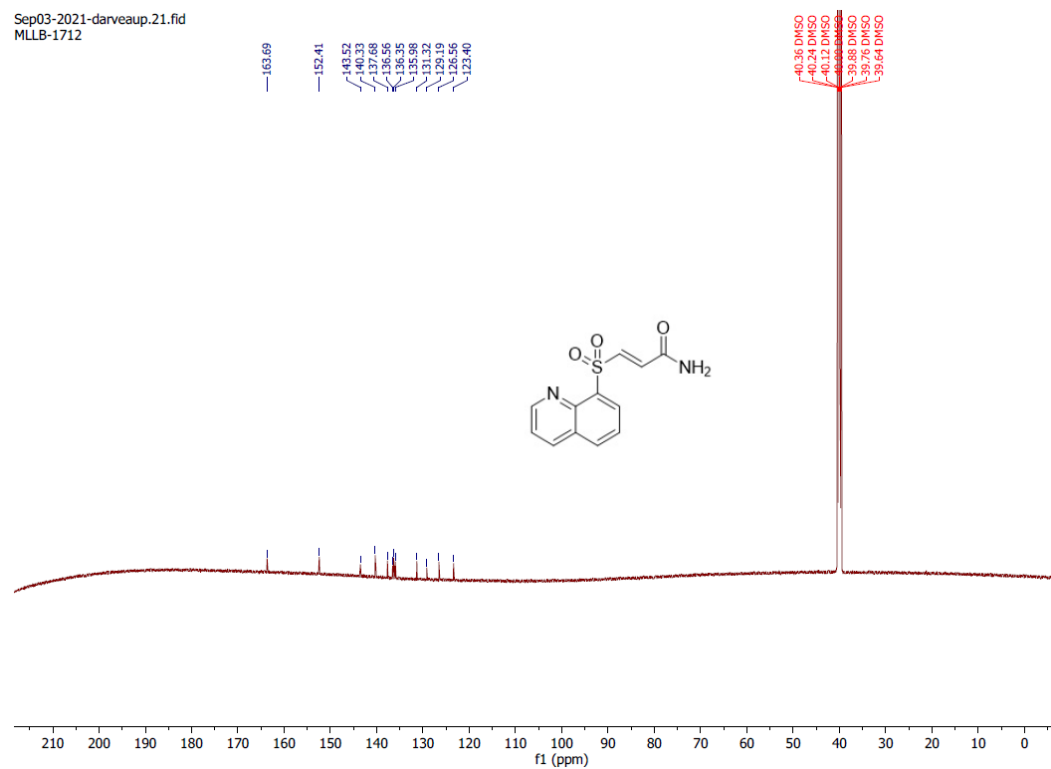
(E)-3-(quinolin-8-ylsulfonyl)acrylamide (15)

¹H NMR (700 MHz, DMSO-*d*₆)



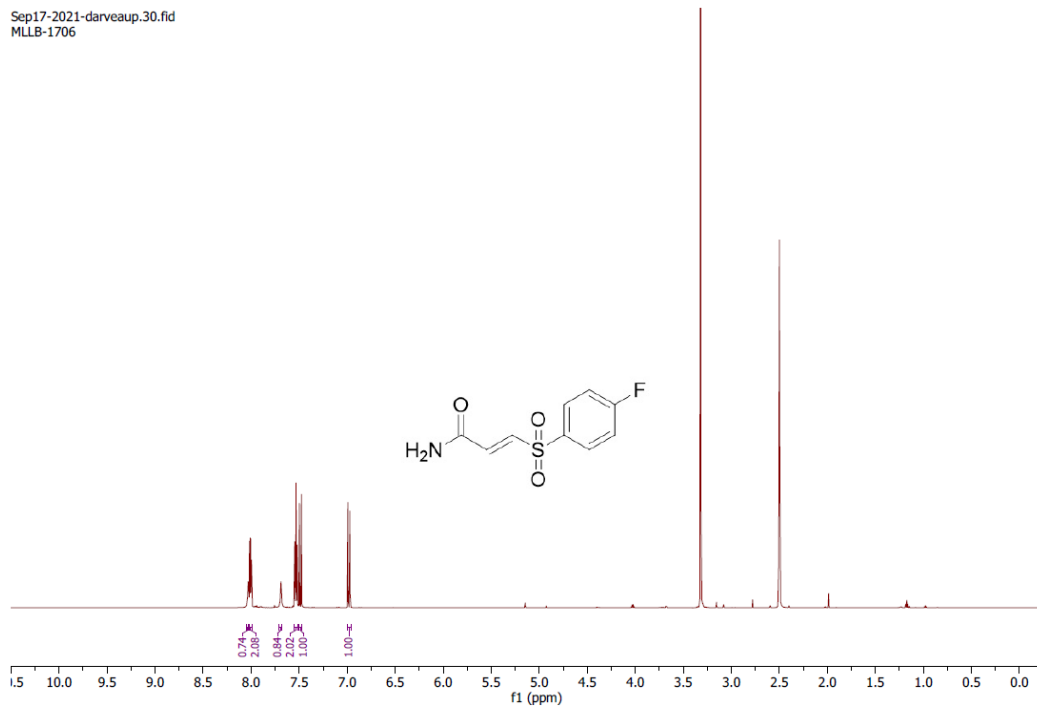
(E)-3-(quinolin-8-ylsulfonyl)acrylamide (15)

¹³C NMR (176 MHz, DMSO-*d*₆)



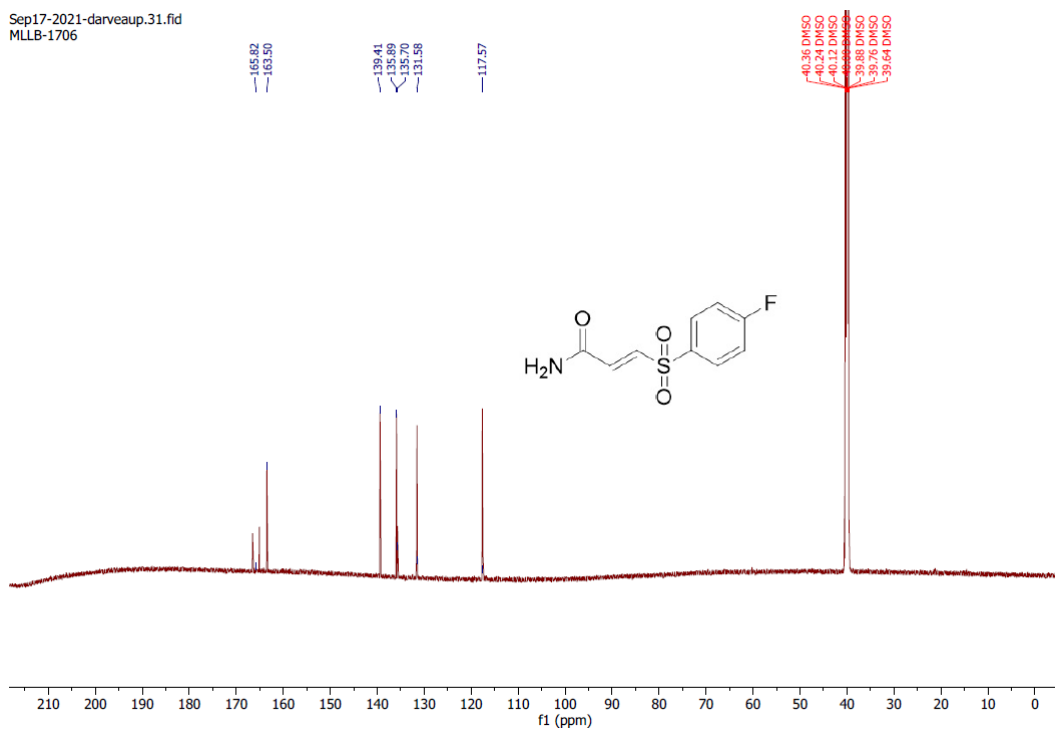
(E)-3-((4-fluorophenyl)sulfonyl)acrylamide (16)

¹H NMR (700 MHz, DMSO-*d*₆)



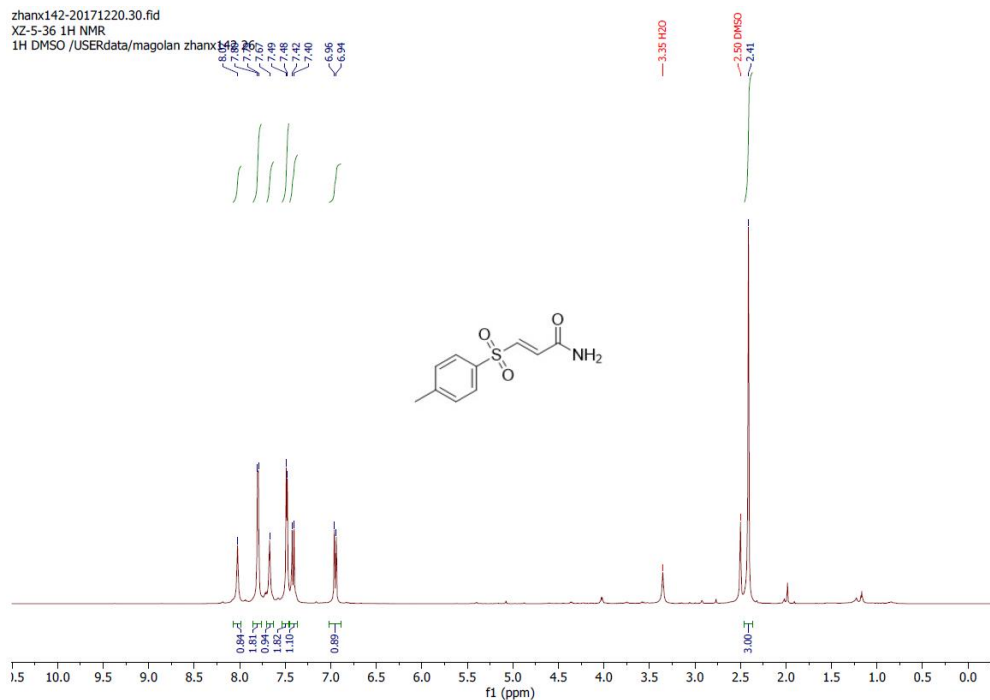
(E)-3-((4-fluorophenyl)sulfonyl)acrylamide (16)

¹³C NMR (176 MHz, DMSO-*d*₆)



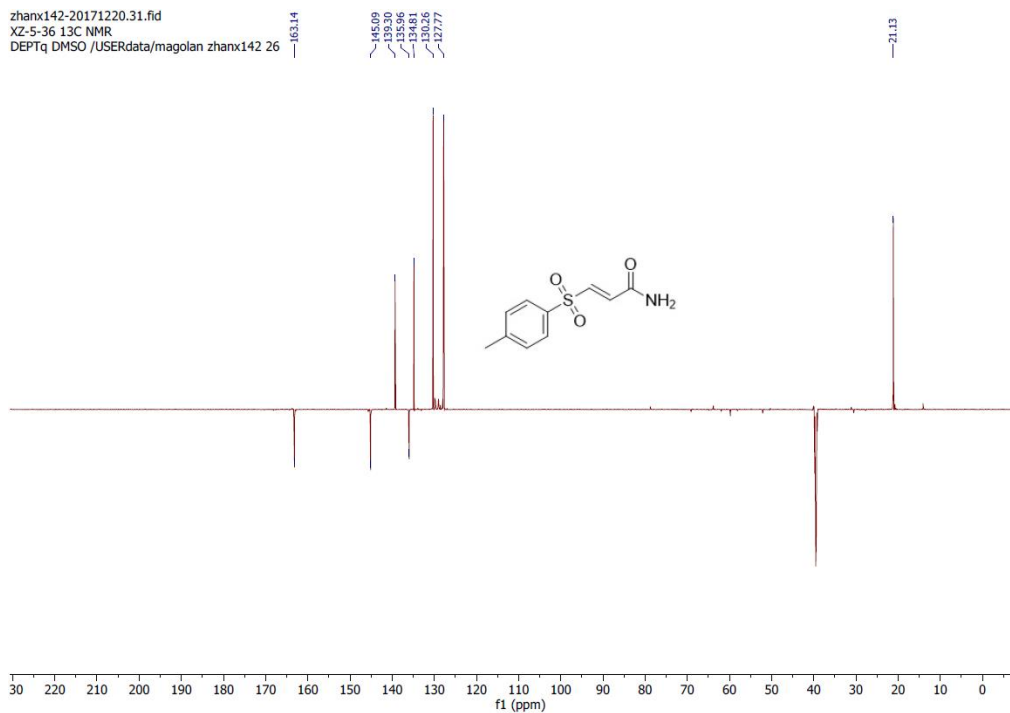
(E)-3-tosylacrylamide (17)

¹H NMR (700 MHz, DMSO-*d*₆)



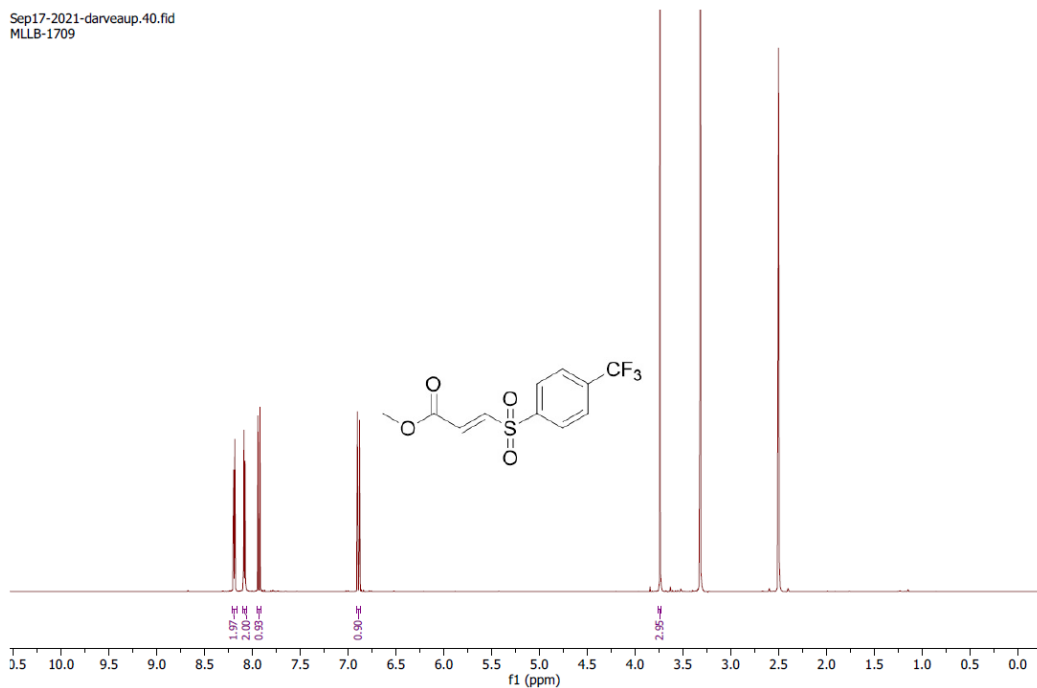
(E)-3-tosylacrylamide (17)

¹³C NMR (176 MHz, DMSO-*d*₆)



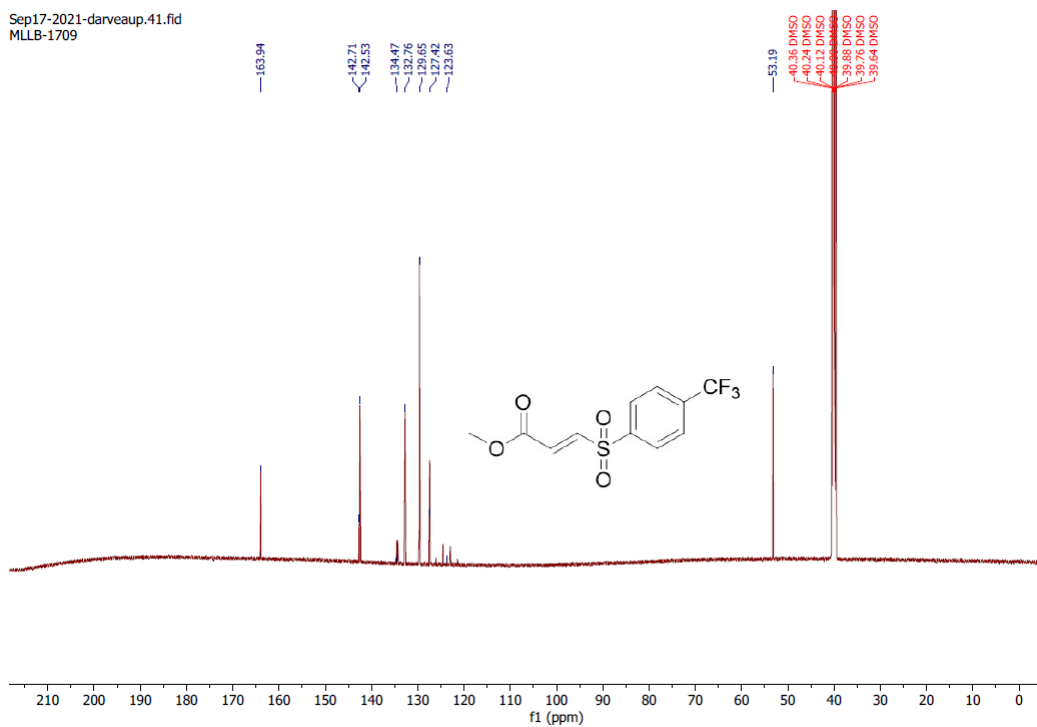
Methyl (*E*)-3-((4-(trifluoromethyl)phenyl)sulfonyl)acrylate (18)

¹H NMR (700 MHz, DMSO-*d*₆)



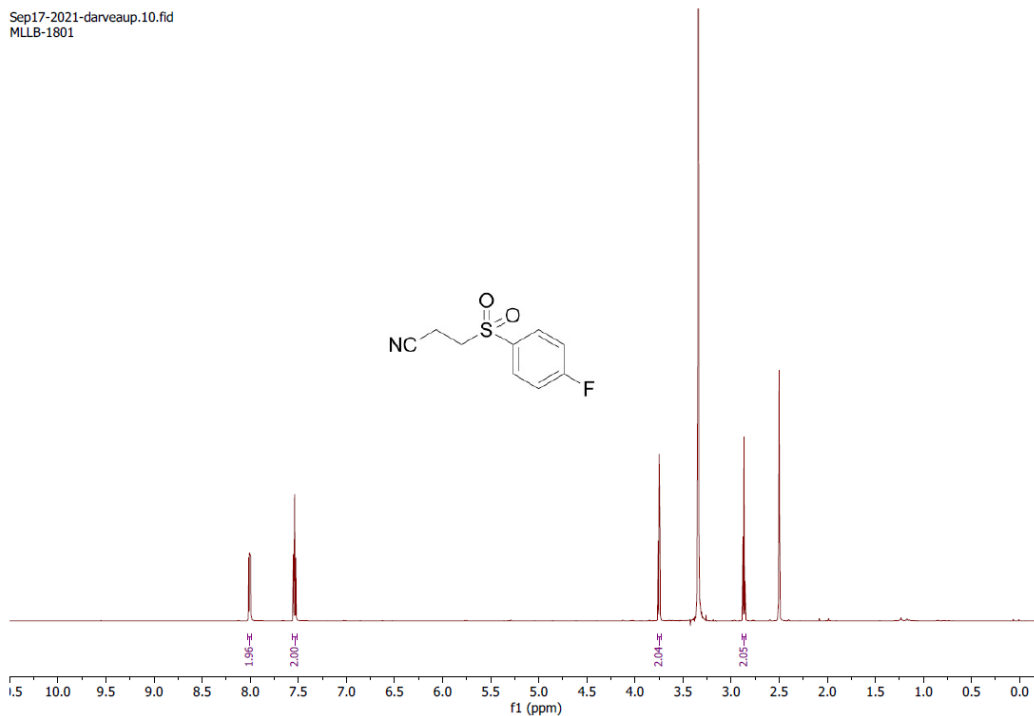
Methyl (*E*)-3-((4-(trifluoromethyl)phenyl)sulfonyl)acrylate (18)

¹³C NMR (176 MHz, DMSO-*d*₆)



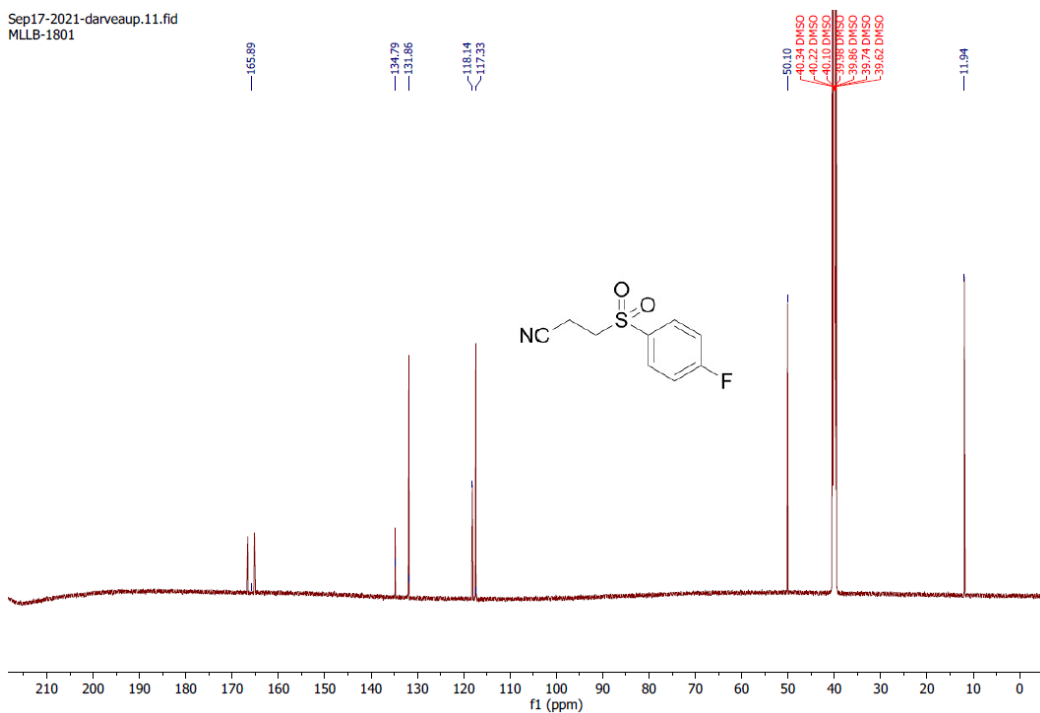
3-((4-fluorophenyl)sulfonyl)propanenitrile (19)

^1H NMR (700 MHz, $\text{DMSO}-d_6$)



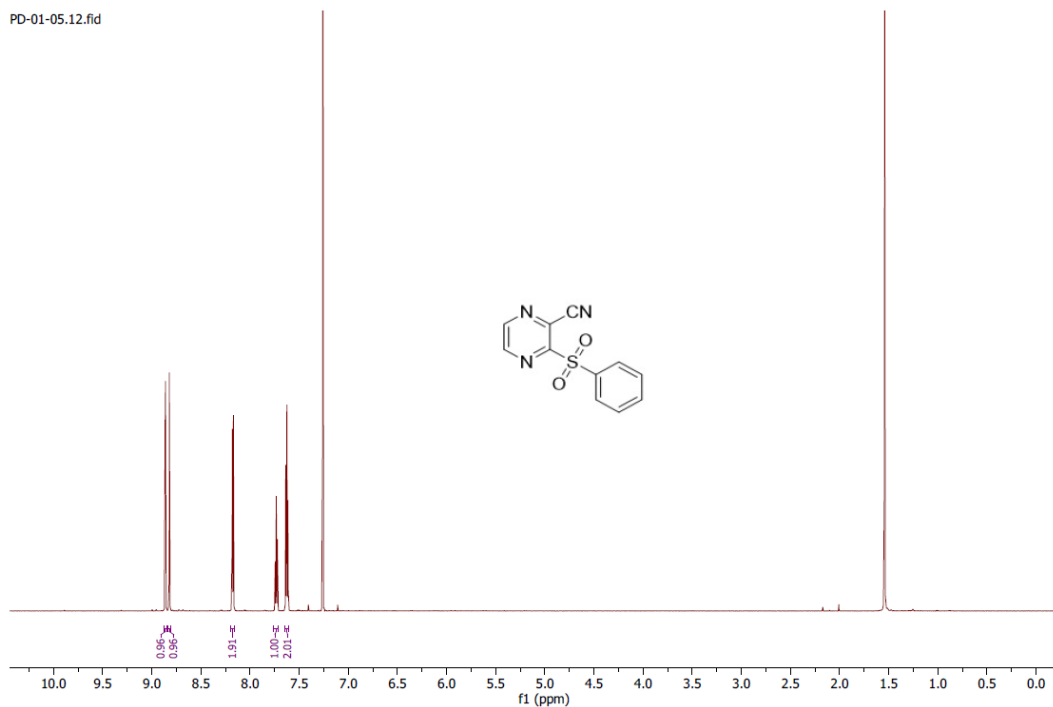
3-((4-fluorophenyl)sulfonyl)propanenitrile (19)

^{13}C NMR (176 MHz, $\text{DMSO}-d_6$)



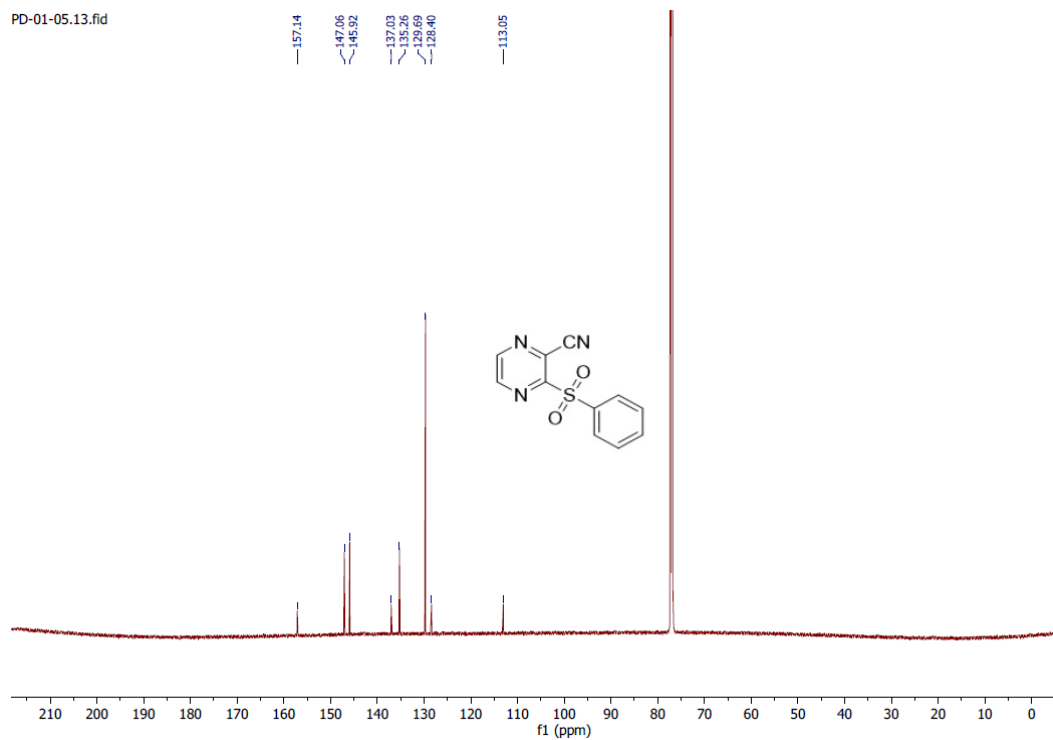
3-(phenylsulfonyl)pyrazine-2-carbonitrile (20)

^1H NMR (700 MHz, Chloroform-*d*)



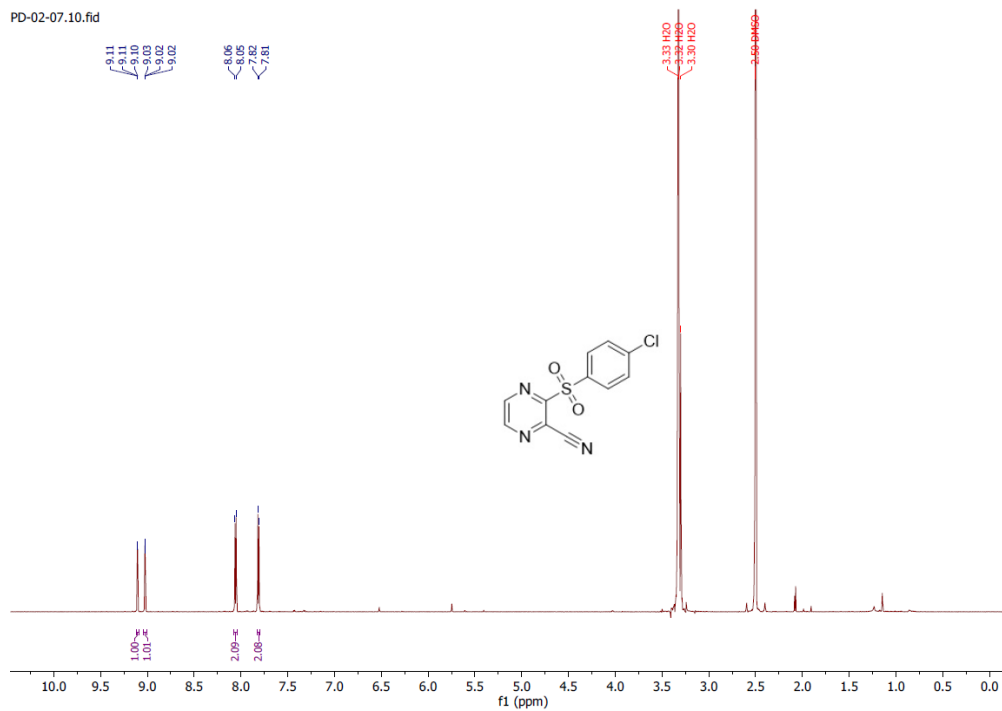
3-(phenylsulfonyl)pyrazine-2-carbonitrile (20)

^{13}C NMR (176 MHz, Chloroform-*d*)



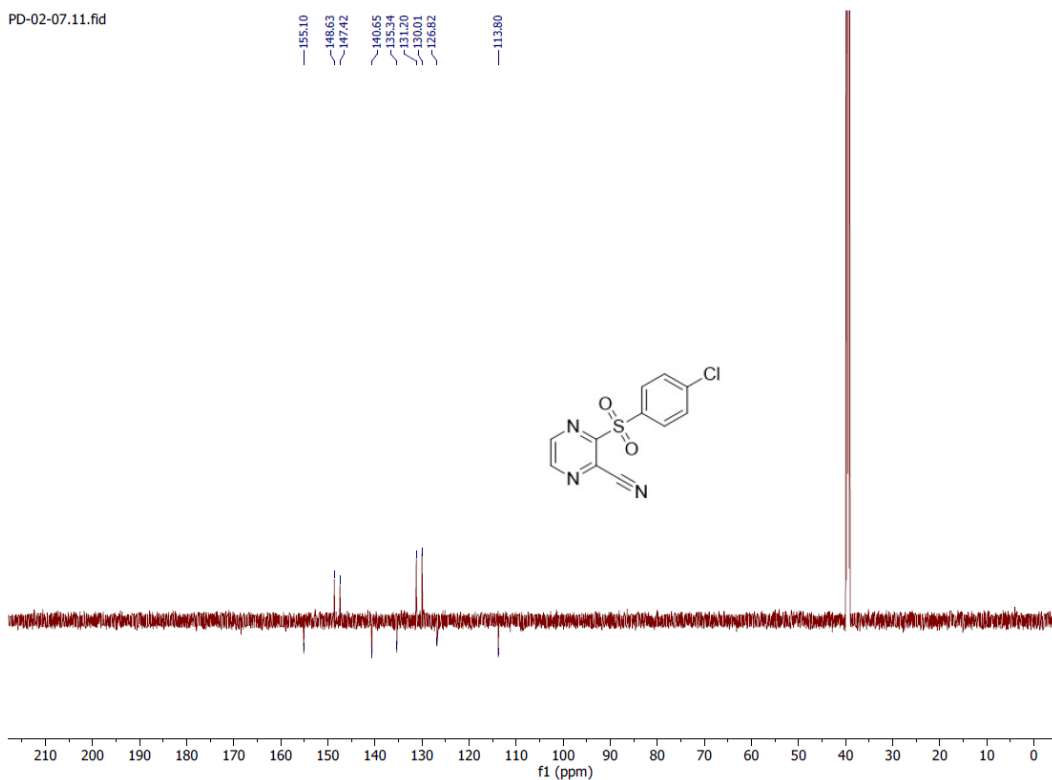
3-((4-chlorophenyl)sulfonyl)pyrazine-2-carbonitrile (24)

^1H NMR (700 MHz, $\text{DMSO-}d_6$)



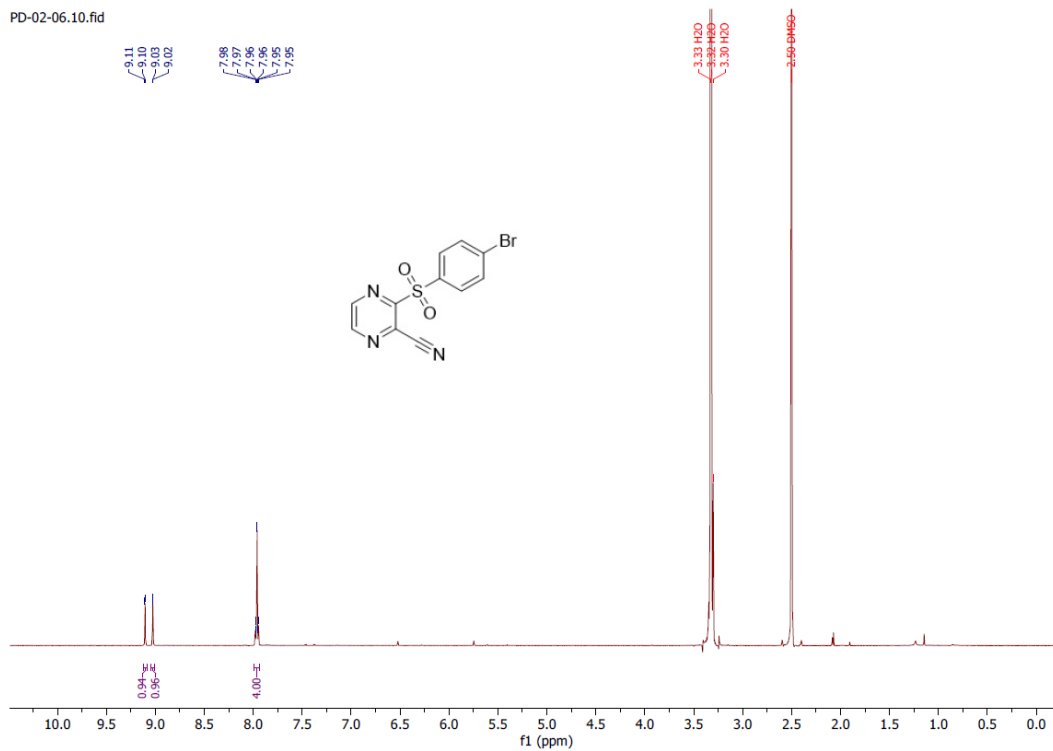
3-((4-chlorophenyl)sulfonyl)pyrazine-2-carbonitrile (24)

^{13}C NMR (176 MHz, $\text{DMSO-}d_6$)



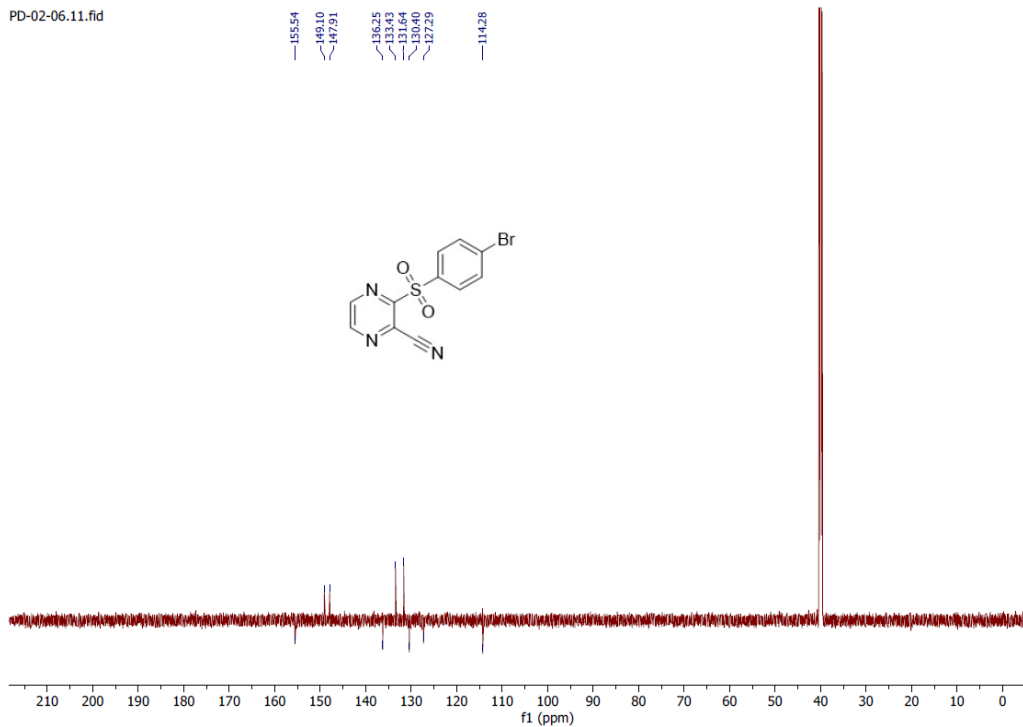
3-((4-bromophenyl)sulfonyl)pyrazine-2-carbonitrile (25)

^1H NMR (700 MHz, $\text{DMSO-}d_6$)



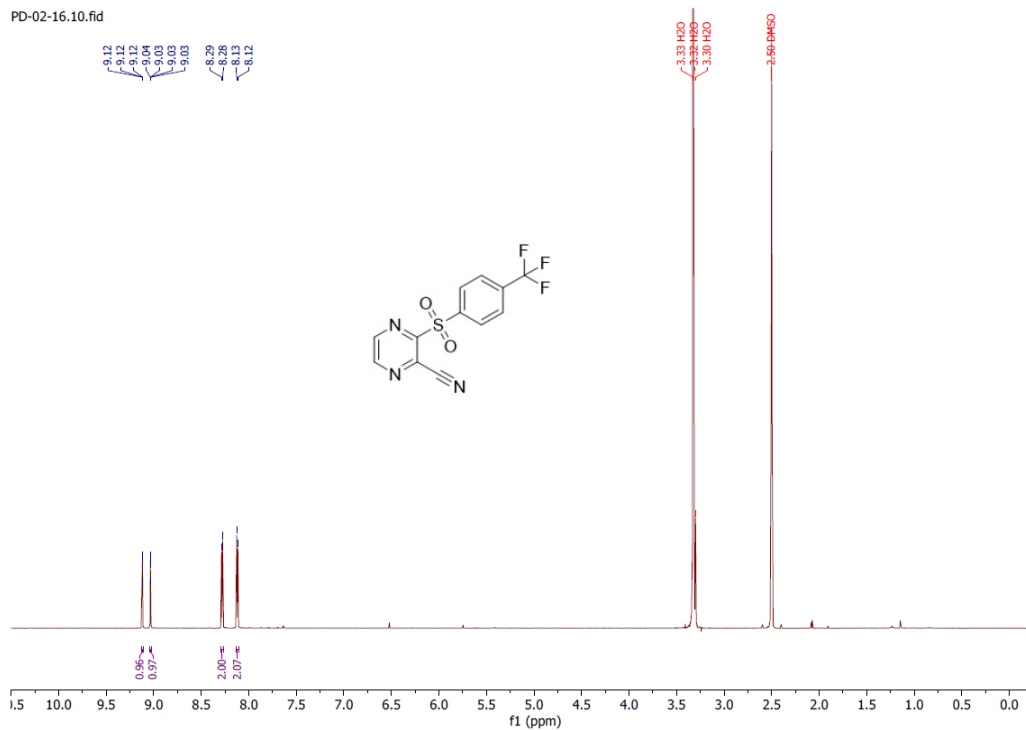
3-((4-bromophenyl)sulfonyl)pyrazine-2-carbonitrile (25)

^{13}C NMR (176 MHz, $\text{DMSO-}d_6$)



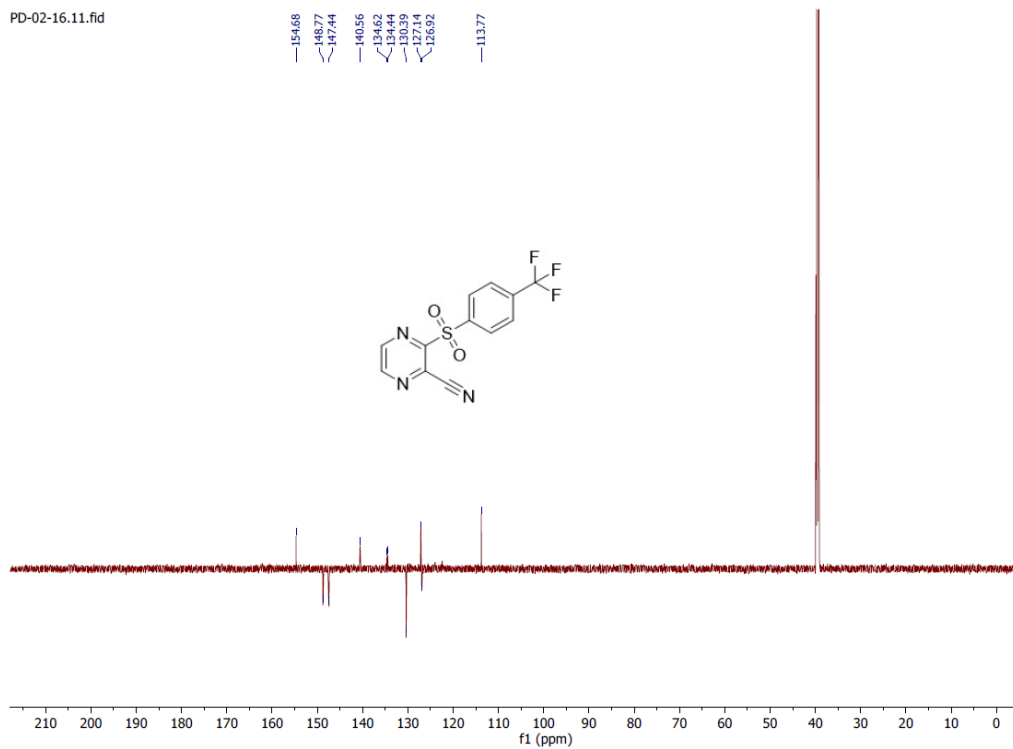
3-((4-(trifluoromethyl)phenyl)sulfonyl)pyrazine-2-carbonitrile (26)

^1H NMR (700 MHz, $\text{DMSO}-d_6$)



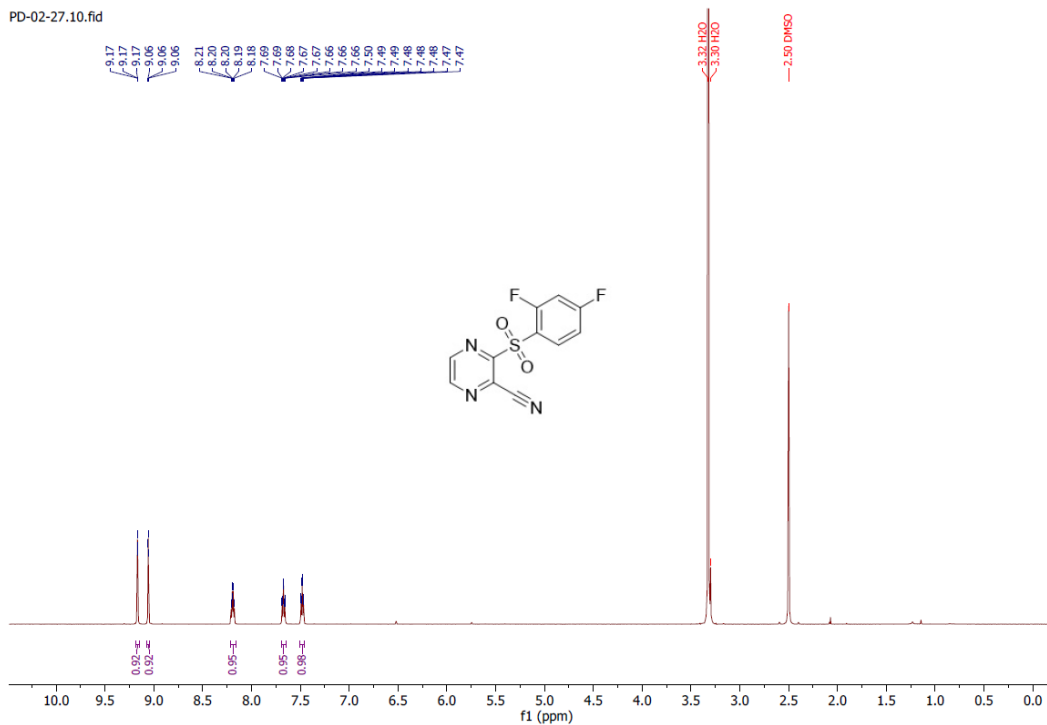
3-((4-(trifluoromethyl)phenyl)sulfonyl)pyrazine-2-carbonitrile (26)

^{13}C NMR (176 MHz, $\text{DMSO}-d_6$)



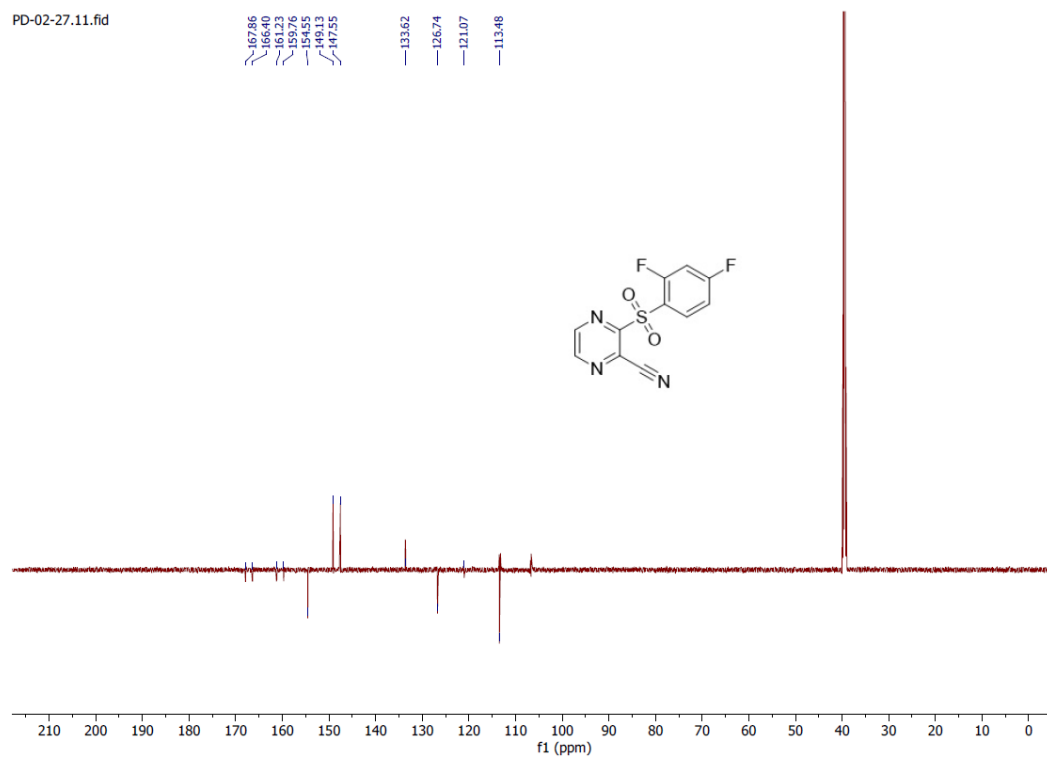
3-((2,4-difluorophenyl)sulfonyl)pyrazine-2-carbonitrile (27)

^1H NMR (700 MHz, $\text{DMSO-}d_6$)



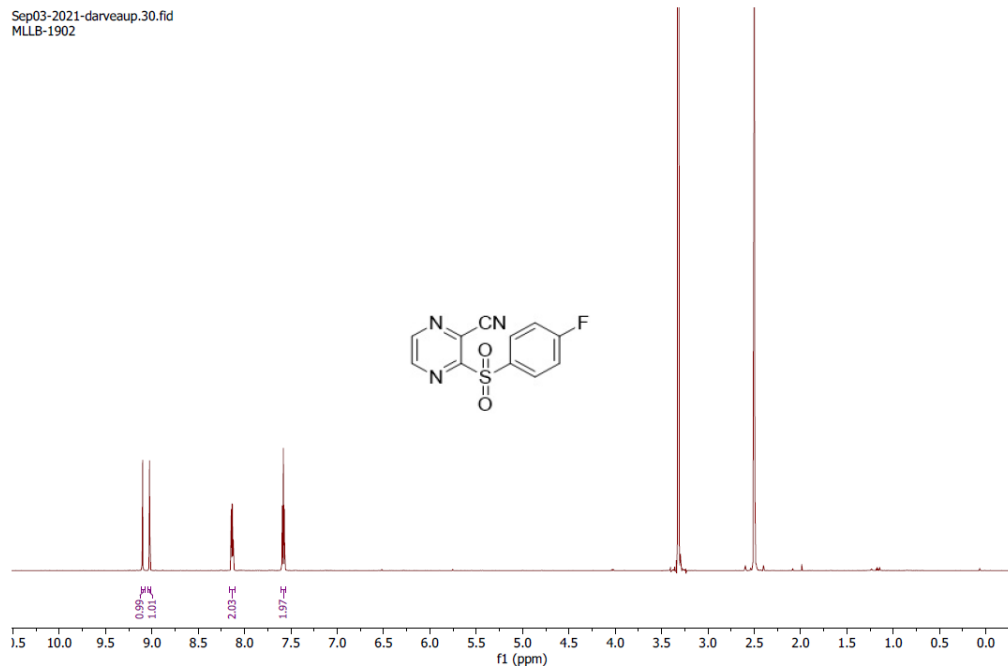
3-((2,4-difluorophenyl)sulfonyl)pyrazine-2-carbonitrile (27)

^{13}C NMR (176 MHz, $\text{DMSO-}d_6$)



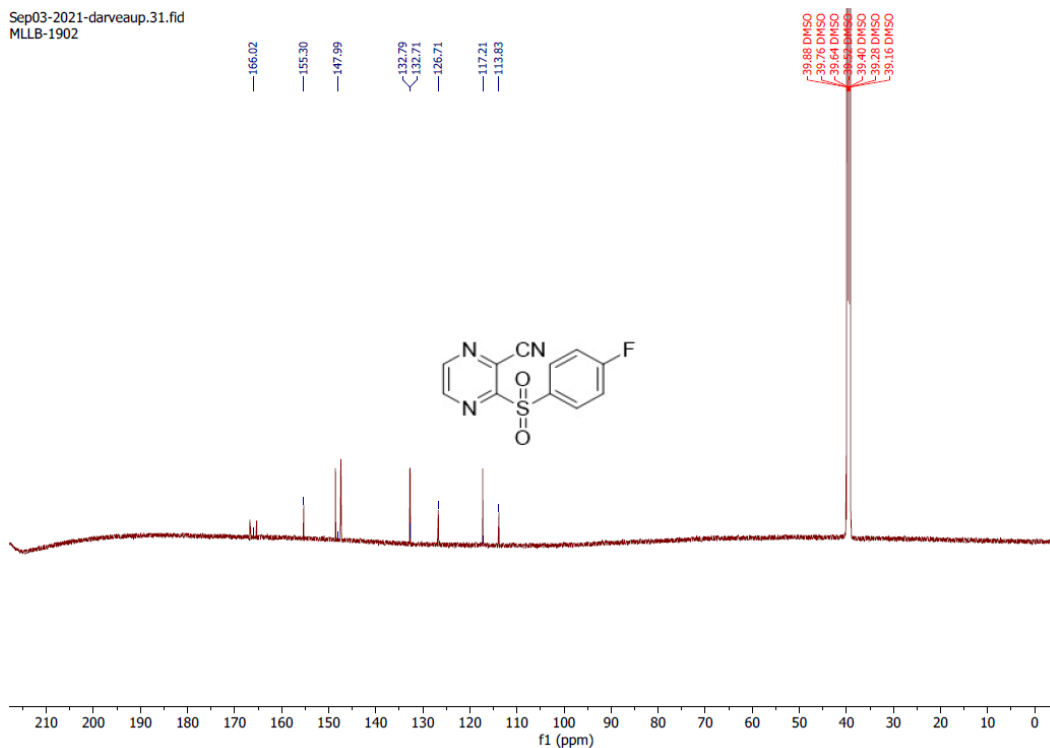
3-((4-fluorophenyl)sulfonyl)pyrazine-2-carbonitrile (28)

^1H NMR (700 MHz, $\text{DMSO-}d_6$)



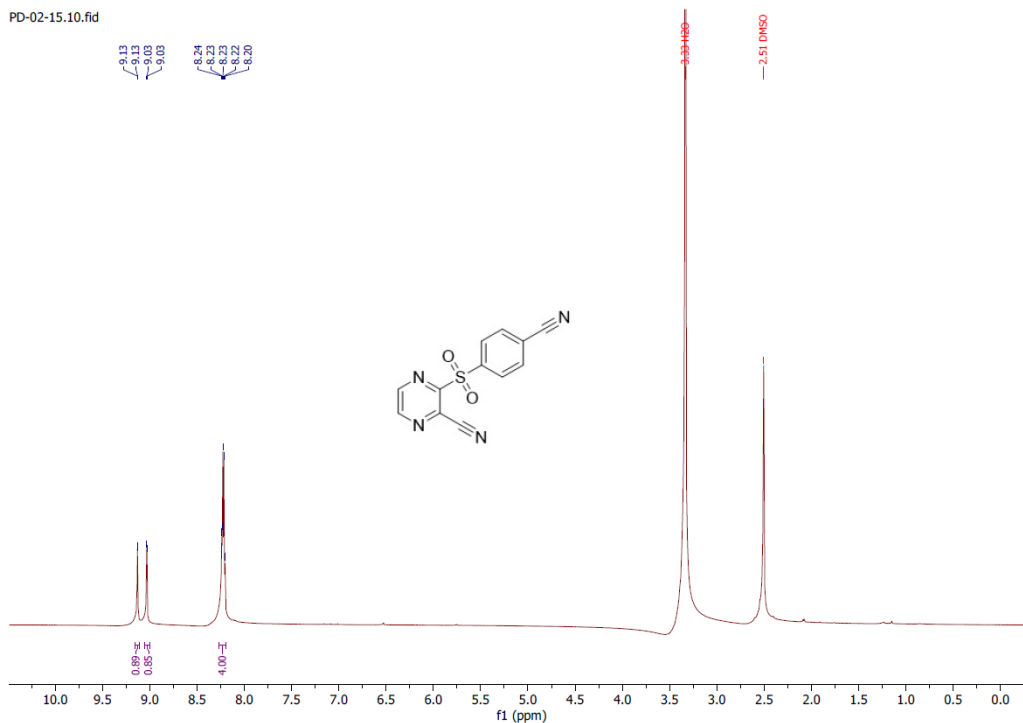
3-((4-fluorophenyl)sulfonyl)pyrazine-2-carbonitrile (28)

^{13}C NMR (176 MHz, $\text{DMSO-}d_6$)



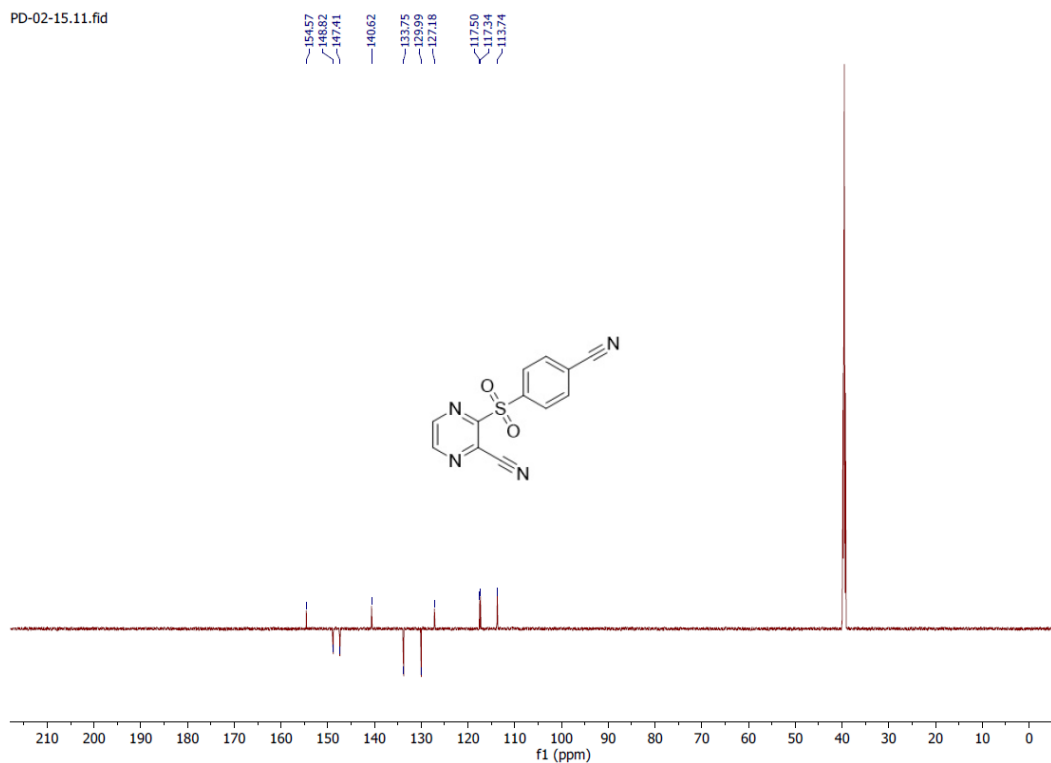
3-((4-cyanophenyl)sulfonyl)pyrazine-2-carbonitrile (29)

^1H NMR (700 MHz, $\text{DMSO-}d_6$)



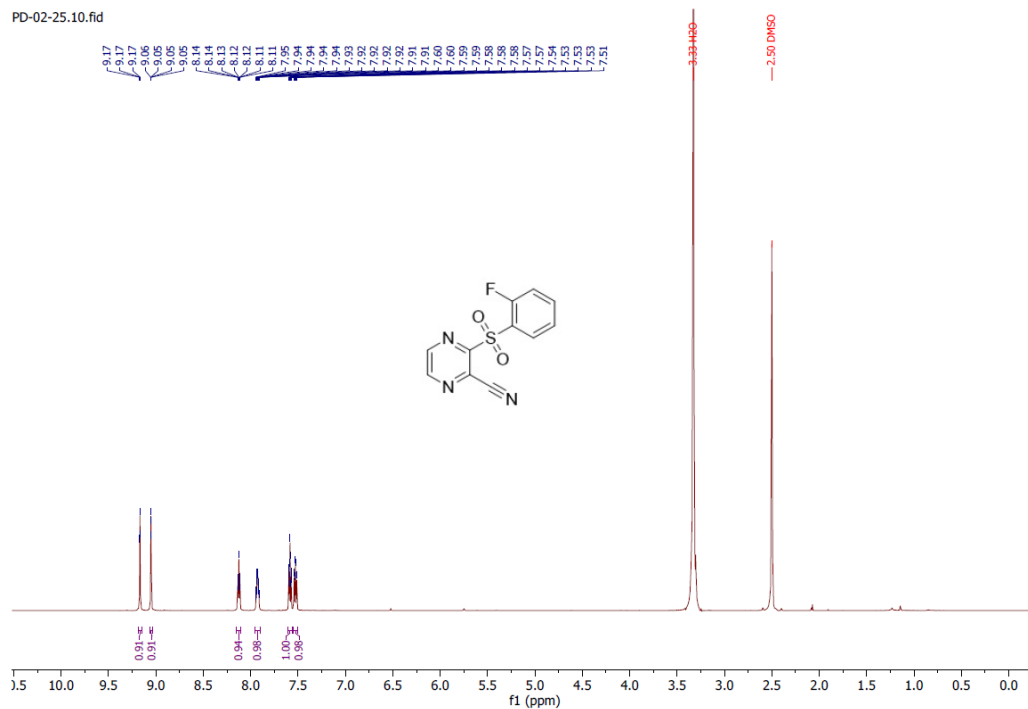
3-((4-cyanophenyl)sulfonyl)pyrazine-2-carbonitrile (29)

^{13}C NMR (176 MHz, $\text{DMSO-}d_6$)



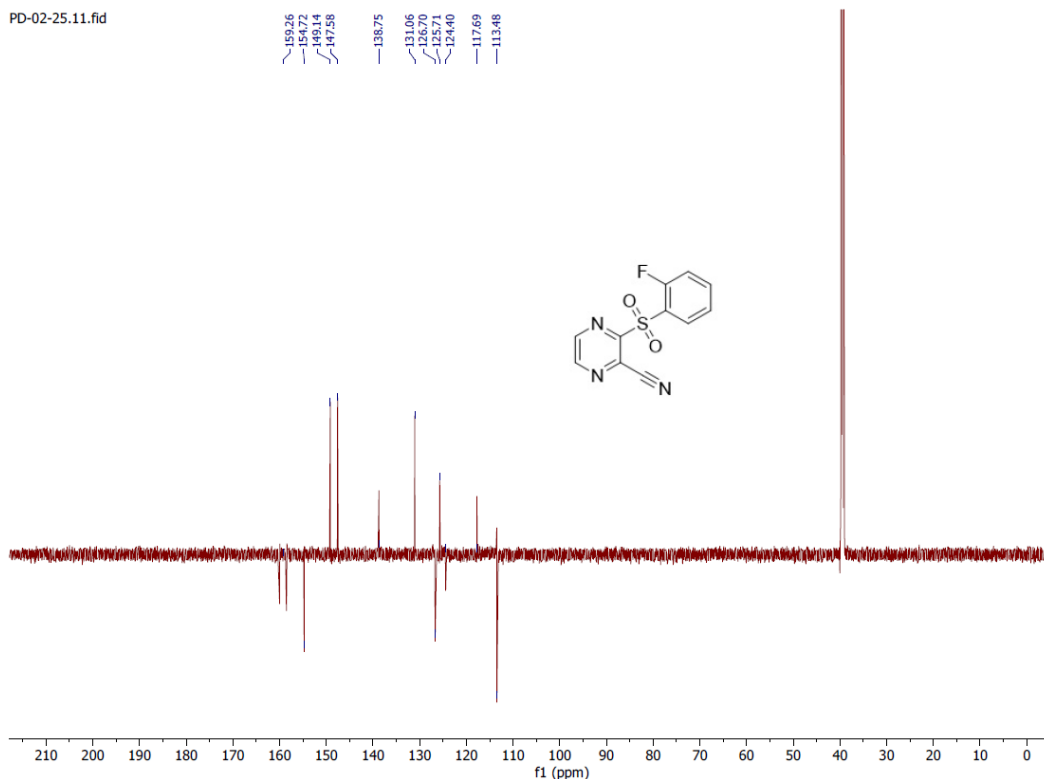
3-((2-fluorophenyl)sulfonyl)pyrazine-2-carbonitrile (30)

¹H NMR (700 MHz, DMSO-*d*₆)



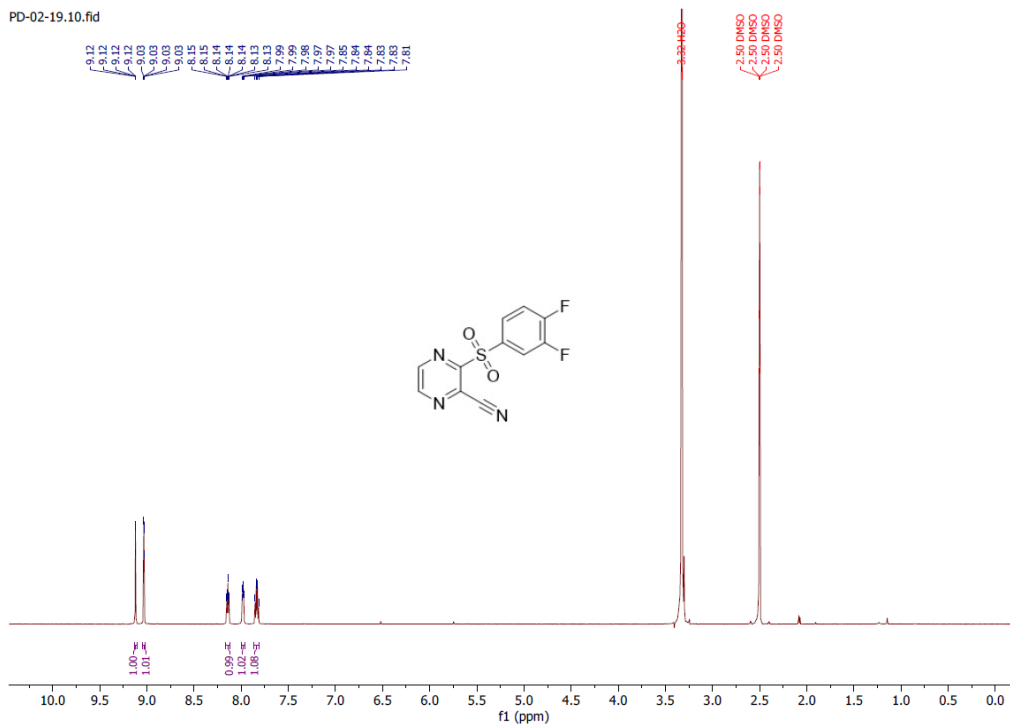
3-((2-fluorophenyl)sulfonyl)pyrazine-2-carbonitrile (30)

¹³C NMR (176 MHz, DMSO-*d*₆)



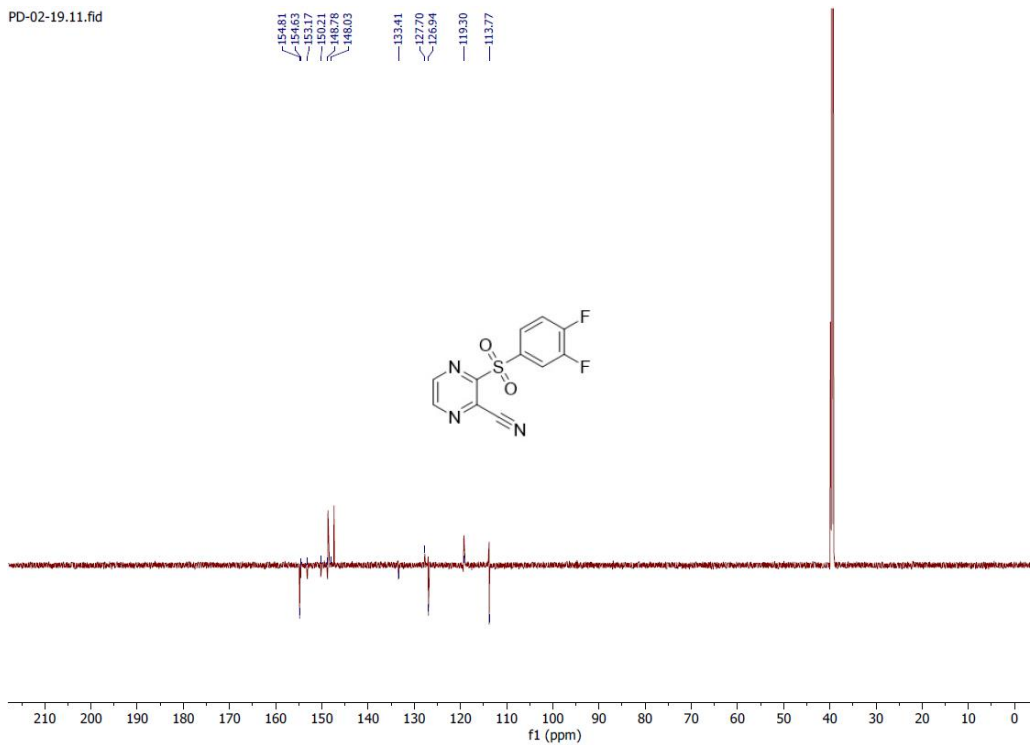
3-((3,4-difluorophenyl)sulfonyl)pyrazine-2-carbonitrile (31)

^1H NMR (700 MHz, $\text{DMSO-}d_6$)



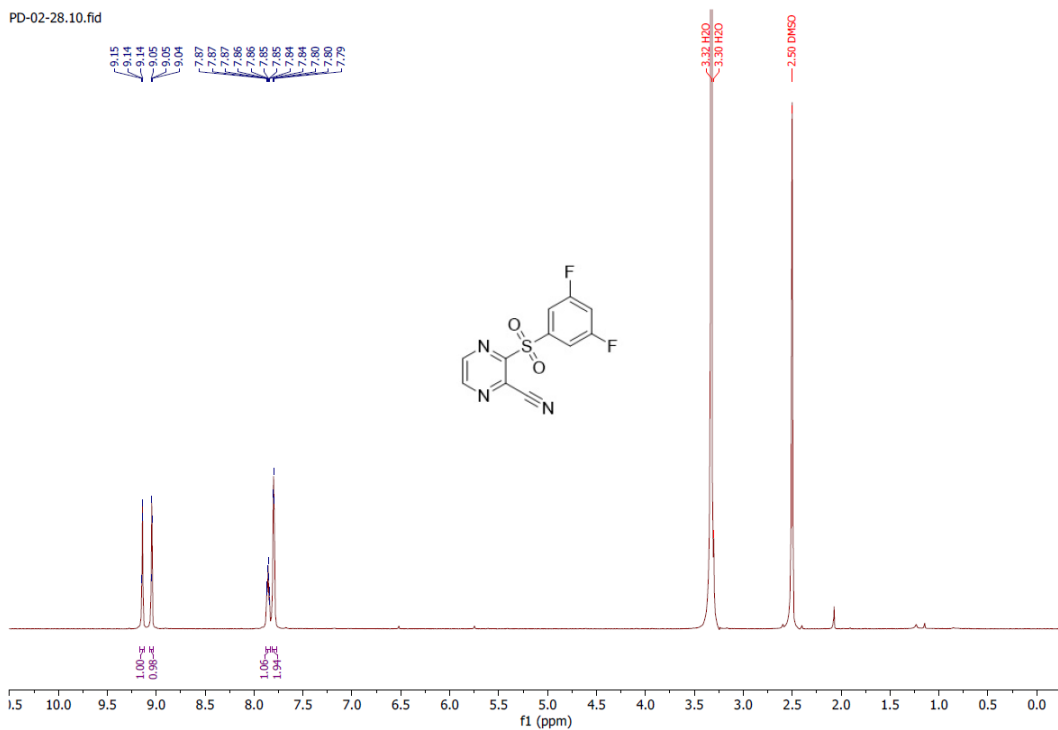
3-((3,4-difluorophenyl)sulfonyl)pyrazine-2-carbonitrile (31)

^{13}C NMR (176 MHz, $\text{DMSO-}d_6$)



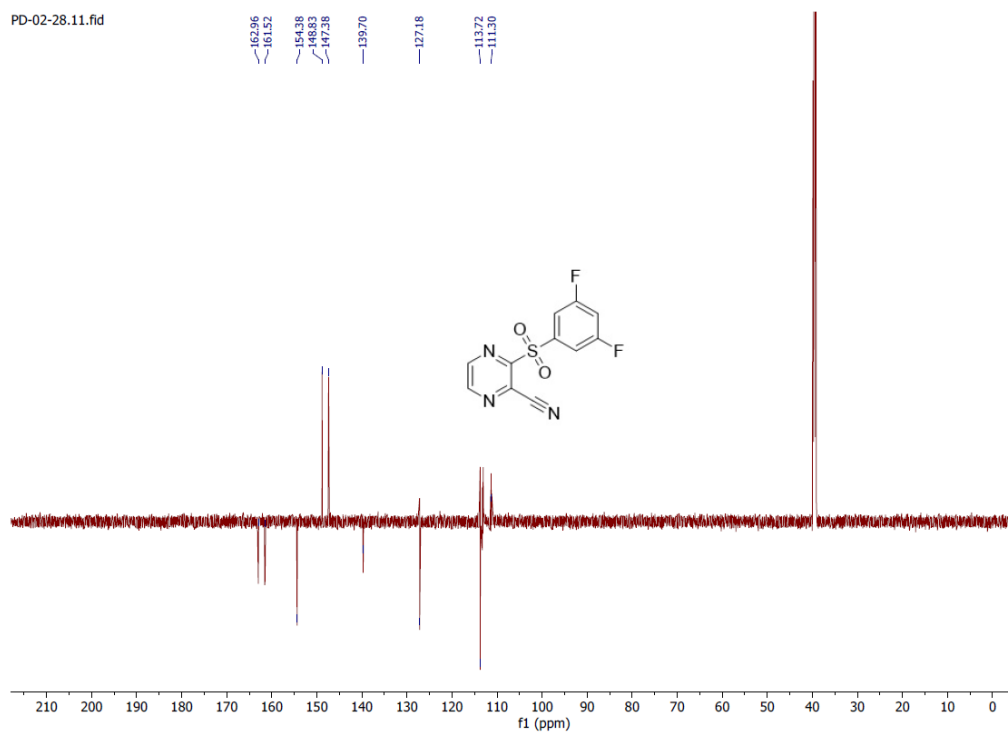
3-((3,5-difluorophenyl)sulfonyl)pyrazine-2-carbonitrile (32)

^1H NMR (700 MHz, $\text{DMSO-}d_6$)



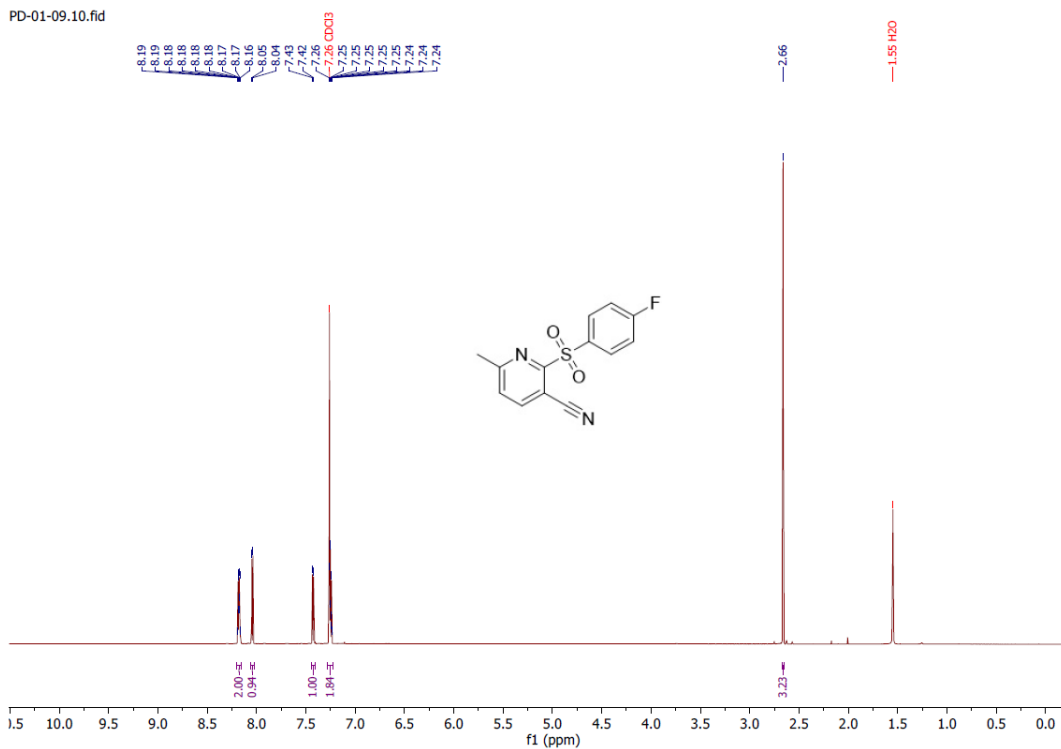
3-((3,5-difluorophenyl)sulfonyl)pyrazine-2-carbonitrile (32)

^{13}C NMR (176 MHz, $\text{DMSO-}d_6$)



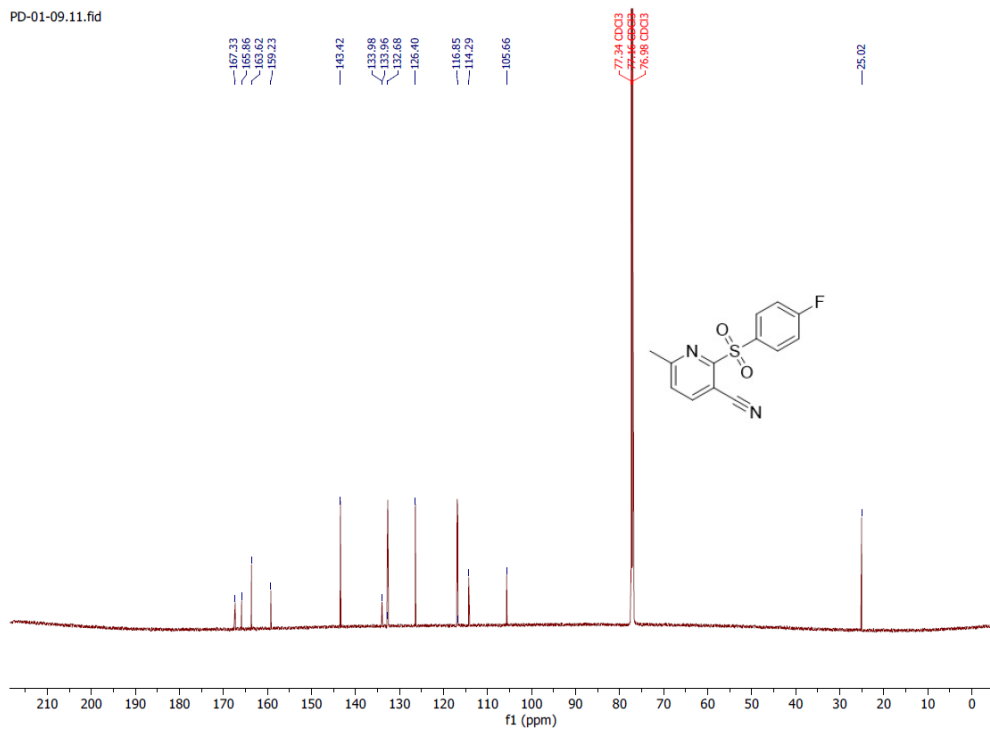
2-((4-fluorophenyl)sulfonyl)-6-methylnicotinonitrile (33)

^1H NMR (700 MHz, Chloroform-*d*)



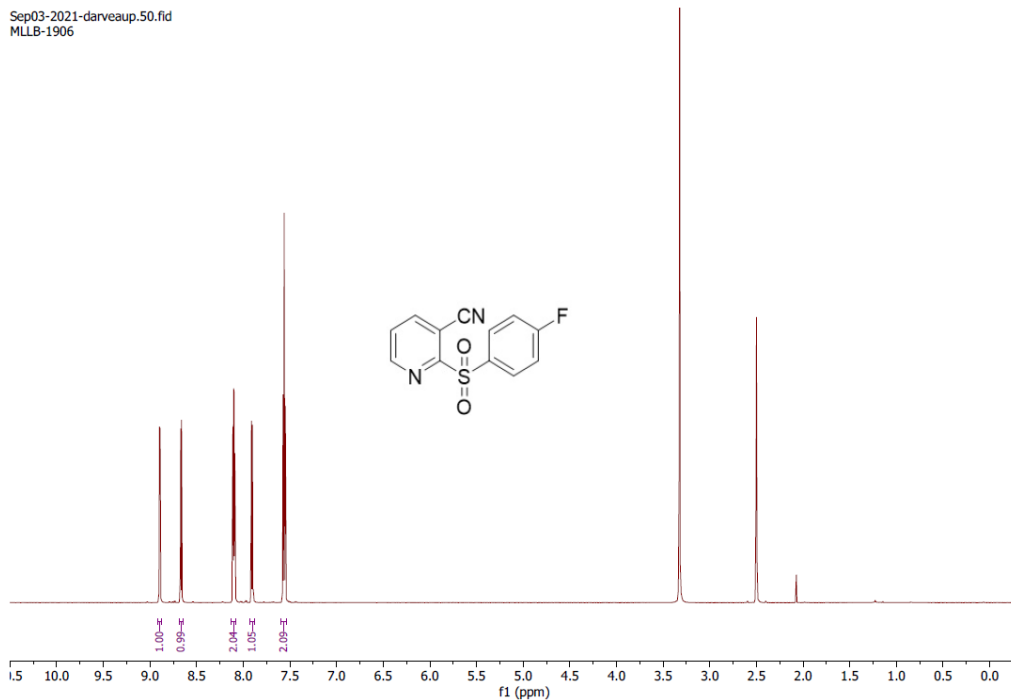
2-((4-fluorophenyl)sulfonyl)-6-methylnicotinonitrile (33)

^{13}C NMR (176 MHz, Chloroform-*d*)



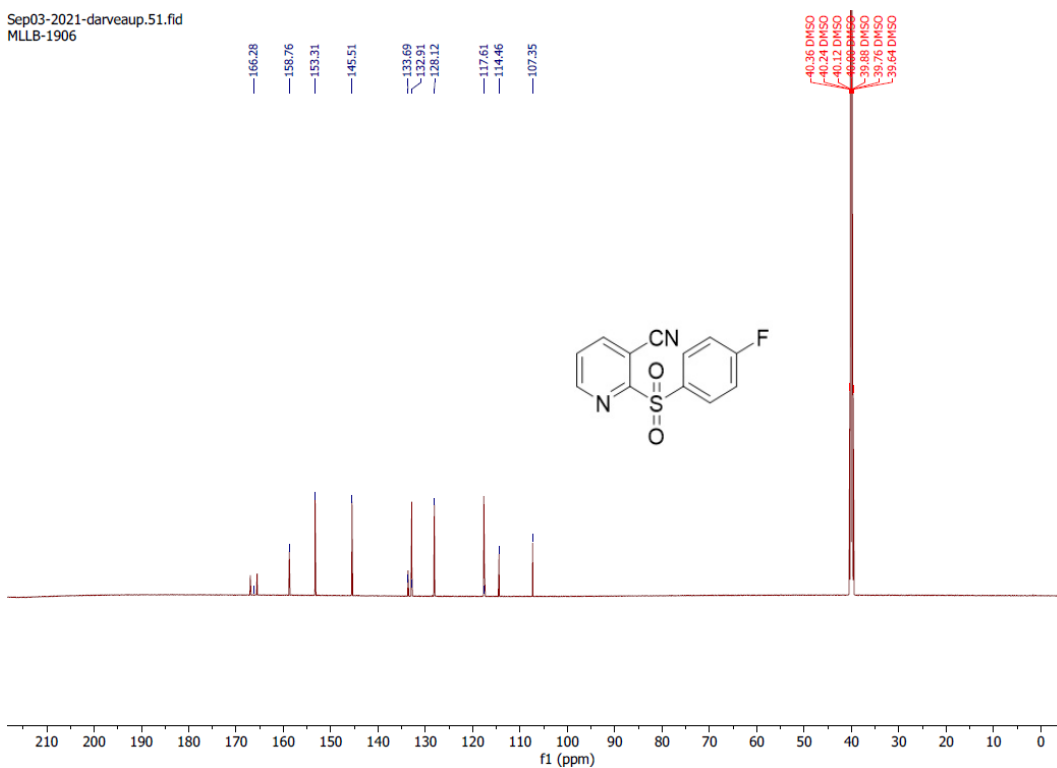
2-((4-fluorophenyl)sulfonyl)nicotinonitrile (34)

^1H NMR (700 MHz, $\text{DMSO-}d_6$)



2-((4-fluorophenyl)sulfonyl)nicotinonitrile (34)

^{13}C NMR (176 MHz, $\text{DMSO-}d_6$)



References for supporting information

- (1) Cox, G.; Sieron, A.; King, A. M.; Pascale, G. D.; Pawlowski, A. C.; Koteva, K.; Wright, G. D. A Common Platform for Antibiotic Dereplication and Adjuvant Discovery. *Cell Chem. Biol.* **2017**, *24* (1), 98–109. <https://doi.org/10.1016/j.chembiol.2016.11.011>.
- (2) Guan, Z.-H.; Zuo, W.; Zhao, L.-B.; Ren, Z.-H.; Liang, Y.-M. An Economical and Convenient Synthesis of Vinyl Sulfones. *Synthesis* **2007**, *2007* (10), 1465–1470. <https://doi.org/10.1055/s-2007-966039>.

Chapter Three: BAY 11-7082 synergizes with PBP2-targeting β -lactams to inhibit the growth of methicillin-resistant *Staphylococcus aureus*

Preface

The work presented in this chapter represents a manuscript in preparation for submission, as of July 2024.

Coles, V. E.; Burrows, L. L. BAY 11-7082 synergizes with PBP2-targeting β -lactams to inhibit the growth of methicillin-resistant *Staphylococcus aureus*. *In preparation*.

VEC and LLB designed all experiments and wrote the manuscript. VEC conducted all experiments.

Abstract

β -lactams are an important class of antibiotics that target penicillin binding proteins (PBPs) essential to bacterial cell wall synthesis. They are commonly used to treat a variety of bacterial infections, including those caused by *Staphylococcus aureus*. Some strains of *S. aureus* carry the resistance gene *mecA*, which encodes β -lactam insensitive PBP2A that allows for peptidoglycan synthesis even in the presence of a β -lactam like methicillin, limiting treatment options. We previously identified the anti-inflammatory compound BAY 11-7082 as having antibacterial activity against methicillin-resistant *S. aureus* (MRSA). We also found that it re-sensitizes MRSA to β -lactams like penicillin G, making BAY 11-7082 and its synthetic analogues promising candidates for the development of an antibiotic adjuvant. While BAY 11-7082's direct antibacterial mechanism remains undefined, here we aimed to better understand how it potentiates β -lactam activity. We tested BAY 11-7082 in combination with a variety of different β -lactams that preferentially bind each traditional PBP expressed in *S. aureus* and found that BAY 11-7082 specifically synergizes with β -lactams that preferentially bind PBP2. We hypothesized that it disrupts the crucial coordination between PBP2 and PBP2A in MRSA, possibly by targeting other factors required for proper PBP localization. We showed that while BAY 11-7082 does not directly target the biosynthesis of wall teichoic acids (WTAs), nonessential polymers anchored to the cell wall, the production of WTA is required for BAY 11-7082- β -lactam synergy. We provide evidence that its mechanism of synergy is distinct from compounds previously identified in the literature, making it a useful tool for better understanding the many factors involved in β -lactam resistance.

Introduction

β -lactams are the most widely used class of antibiotics. They target penicillin-binding proteins (PBPs), essential enzymes that polymerize subunits and crosslink strands during peptidoglycan synthesis. The broad spectrum and low toxicity of β -lactams contribute to their importance in the treatment of infections; however, their utility is decreased in the presence of β -lactamases, enzymes that bind and inactivate β -lactams. In such cases, β -lactams are co-administered with a β -lactamase inhibitor to extend their usability. This is one of the few clinically validated examples of an antibiotic adjuvant, a therapeutic that enhances the effectiveness of an existing antibiotic. While some strains of the pathogen *Staphylococcus aureus* encode β -lactamases, others can carry the *mecA* gene that encodes for PBP2A, a β -lactam-insensitive PBP capable of crosslinking glycan strands even in the presence of a β -lactam, making these organisms especially difficult to treat. Despite the global dissemination of methicillin-resistant strains of *S. aureus* (MRSA), no antibiotic adjuvants that rescue the activity of β -lactams in *mecA*-expressing strains have yet been approved.

While PBP2A is required for β -lactam resistance in *S. aureus*, it is not sufficient; there are several auxiliary factors that contribute to resistance, a promising source for potential adjuvants.^{1,2} These factors include genes involved in peptidoglycan biosynthesis (*murA-F*), assembly of the pentaglycine bridge that crosslinks glycan strands (*femA,B,X*), cell division (*ftsA,Z*), and protein secretion (*spsB*).² Inhibitors of FtsZ, an essential cell division protein that plays a role in PBP2 localization, and the type I signal peptidase SpsB, which is required for protein secretion through the Sec and TAT systems, have been identified.³⁻⁶ Other adjuvants that

inhibit auxiliary factors target the biosynthesis of wall teichoic acids (WTAs), glycopolymer chains anchored to the peptidoglycan.

While not essential for *S. aureus* viability, WTAs stabilize the cell envelope and protect peptidoglycan from degrading agents like lysozymes.⁷ Importantly, WTAs have been implicated in PBP localization, which is required for proper PBP2A function. *S. aureus* strains lacking the WTA biosynthetic machinery have abnormal PBP4 localization, resulting in decreased peptidoglycan crosslinking.^{8,9} WTA biosynthesis in *S. aureus* and certain strains of *Bacillus subtilis* is carried out by proteins encoded by the *tar* genes (Figure 1).¹⁰ The first enzyme in this pathway, TarO, reversibly catalyzes the transfer of GlcNAc phosphate to undecaprenyl phosphate. TarO inhibitors, including tunicamycin, ticlopidine, and tarocins, are nonlethal on their own but sensitize MRSA to certain β -lactams.¹¹⁻¹³ The late stage WTA biosynthesis genes *tarBDI'KS* are auxiliary factors that, when mutated, deleted, or depleted, restore the activity of β -lactams, but inhibitors of the flippase TarG, such as targocil, do not synergize with β -lactams and are lethal alone.¹⁴⁻¹⁷ This is likely due to a depletion of key precursors also needed for peptidoglycan synthesis and can be alleviated by also inhibiting the early stage biosynthesis proteins TarO or TarA.^{18,19} By leveraging this conditionally lethal phenotype, Farha *et al.* and El-Halfawy *et al.* identified the β -lactam adjuvants clomiphene and MAC-545496.^{19,20} Clomiphene, which has antibacterial activity on its own, antagonizes targocil by inhibiting undecaprenyl diphosphate synthase (UppS), limiting the availability of undecaprenyl phosphate, which is required for both WTA and peptidoglycan synthesis.¹⁹ MAC-545496 inhibits the response regulator GraR, which regulates the *dltABCD* operon responsible for installing a *D*-alanine ester on WTA.^{20,21}

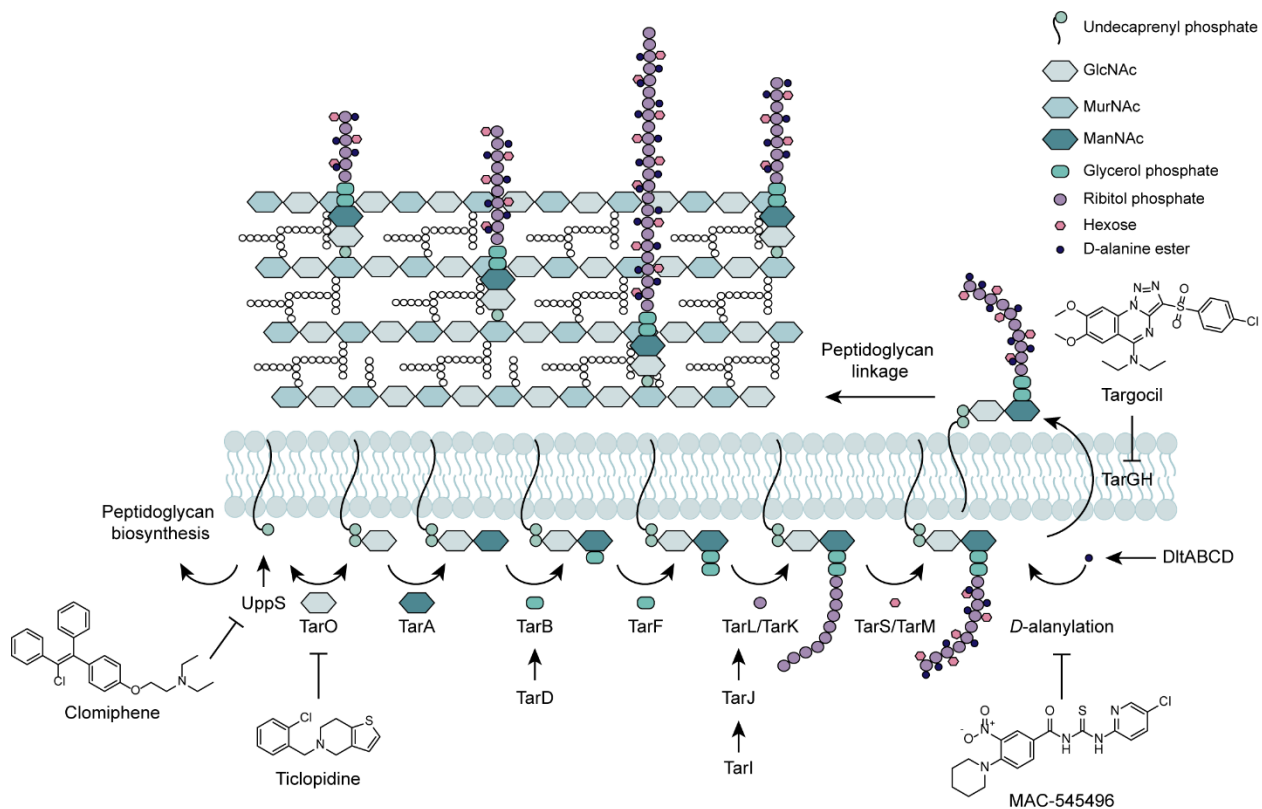


Figure 1. Wall teichoic acid biosynthetic pathway in *S. aureus*. Adapted from Swoboda *et al.* and Pasquina *et al.*^{10,22} Structures of clomiphene, ticlopidine, MAC-545496, and targocil are shown as example inhibitors of UppS, TarO, D-alanylation, and TarG, respectively.

We previously employed a novel biofilm-based screening approach to identify compounds with sub-inhibitory antibiotic activity.²³ We identified the anti-inflammatory BAY 11-7082 as having activity against a wide range of pathogens, with most potent activity against Gram-positive species including MRSA.²⁴ We were unable to identify its specific antimicrobial mechanism of action, concluding its activity may be multifaceted; however, our discovery that it re-sensitizes MRSA to β -lactams like penicillin G renewed our interest in this compound and its synthetic analogues as potential antibiotic adjuvants.

Results

BAY 11-7082 synergizes with β -lactams that primarily target the bifunctional penicillin binding protein PBP2

To define the antibiotics potentiated by BAY 11-7082, we previously conducted checkerboard assays against the MRSA strain USA300 with antibiotics from a variety of classes including aminoglycosides, tetracyclines, thiopeptides, glycopeptides, rifamycins, and β -lactams.²⁴

Interestingly, while we observed synergy (as defined by a fractional inhibitory concentration index (FICI) <0.5)²⁵ with the β -lactams penicillin G (FICI=0.19) and piperacillin (FICI=0.25), we saw no synergy (FICI=0.56) with methicillin, to which *S. aureus* USA300 is intrinsically resistant.²⁴ To better understand this discrepancy, we expanded the scope of β -lactams tested to encompass β -lactams that predominantly bind each of the four traditional PBPs in *S. aureus*, PBP1, 2, 3, and 4 (Figure 2, Figure S1). To test the impact of PBP2A, we conducted checkerboard assays and calculated FICI values for both MRSA strain USA300, which has *mecA* (Figure 2B, Figure S2), and methicillin-sensitive *S. aureus* (MSSA) strain ATCC 29213, which does not (Figure 2C, Figure S3). Interestingly, BAY 11-7082 synergized with β -lactams that primarily target PBP2 (amoxicillin, ampicillin, doripenem, imipenem, oxacillin, piperacillin, and penicillin G), but not β -lactams that primarily inhibit PBP1 and/or PBP3 (cefsulodin, ceftazidime, cloxacillin, and methicillin) (Figure 2B), and that synergy was reduced or eliminated in the MSSA strain (Figure 2C). We also explored BAY 11-7082's ability to potentiate two non- β -lactam antibiotics that target cell wall biosynthesis (Figure 2B) and found BAY 11-7082 failed to synergize with vancomycin, which prevents transglycosylation and transpeptidation by binding the terminal amino acids of lipid II, or moenomycin, a glycosyltransferase inhibitor that also synergizes with β -lactams.

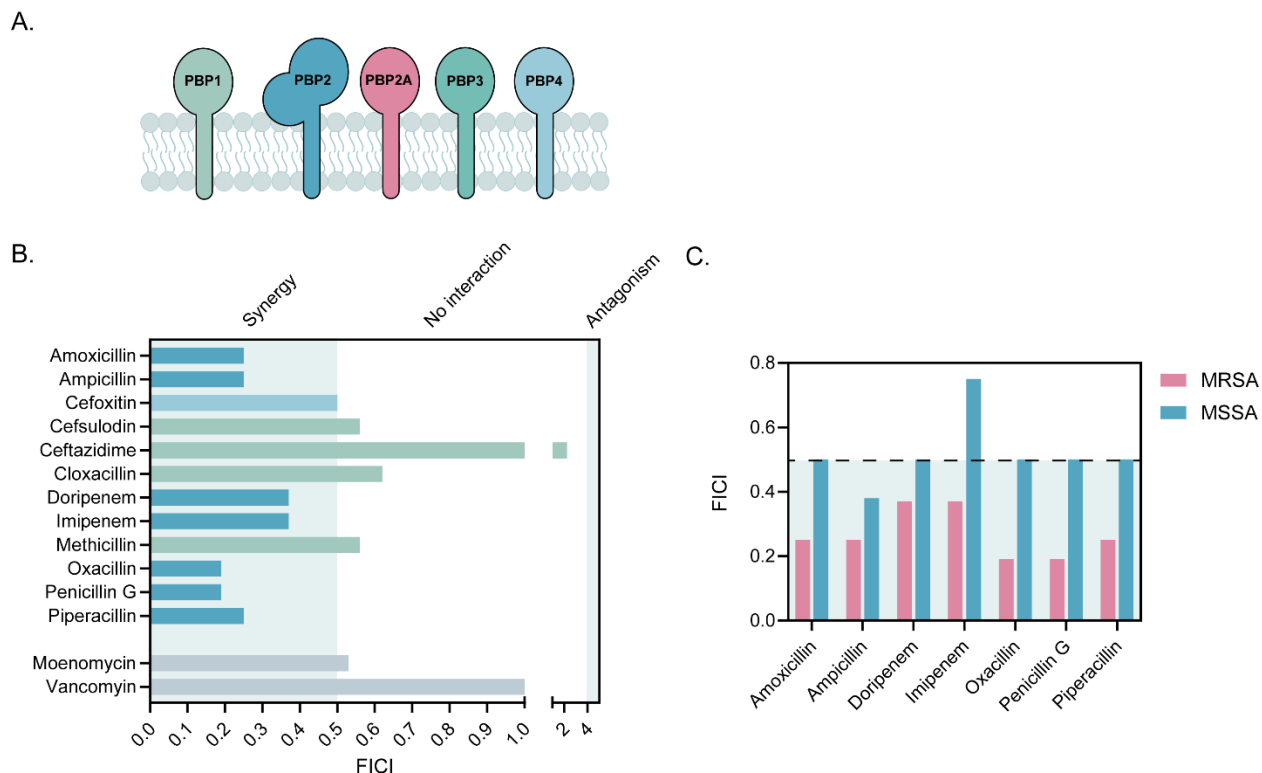


Figure 2. BAY 11-7082 synergizes with PBP2-targeting β -lactams against MRSA. (A) MRSA expresses five PBPs, PBP1, PBP2, PBP2A, PBP3, and PBP4. (B) FICI values calculated based on MRSA USA300 grown in the presence of BAY 11-7082 and another antibiotic. FICI values <0.5 represent synergy, values between 0.5-4 represent no interaction, and values >4 represent antagonism. Bars are coloured according to the primary PBP target of the β -lactam, as shown in A: β -lactams that primarily target PBP2 are shown in dark blue, β -lactams that primarily target PBP1 and/or PBP3 are shown in green, and β -lactams that primarily target PBP4 are shown in light blue. (C) FICI values based on MRSA USA300 (pink) and MSSA ATCC 29213 (blue) grown in the presence of BAY 11-7082 and a β -lactam that synergizes with BAY 11-7082 in MRSA. Data represent an average of three independent experiments performed in triplicate.

These findings were not unexpected, as PBP2 is the only bifunctional PBP in *S. aureus*, with both transpeptidase and glycosyltransferase activity and, along with PBP1, is essential. While PBP1 and PBP3 are transpeptidases that coordinate with the SEDS (shape, elongation, division, and sporulation) proteins FtsW and RodA to facilitate peptidoglycan synthesis during cell division and elongation, respectively,²⁶ PBP2, PBP4, and PBP2A function cooperatively to produce highly crosslinked peptidoglycan strands.^{27,28} The transpeptidase domain of PBP2A is

capable of crosslinking peptidoglycan in the presence of β -lactams; however, PBP2A lacks a glycosyltransferase domain, necessitating coordination with the glycosyltransferase domain of PBP2.^{27,29} We predict that BAY 11-7082 may inhibit the glycosyltransferase domain of PBP2, similar to the antibiotic moenomycin, or result in PBP2 mislocalization, interrupting this coordination and re-sensitizing MRSA to PBP2-acting β -lactams. To determine if BAY 11-7082 acts similarly to moenomycin, we used an MRSA 15981 mutant previously selected for increased resistance to BAY 11-7082 (B13), along with a mutant selected for increased resistance to the structural analogue 3-(phenylsulfonyl)-2-pyrazinecarbonitrile (PSPC) (P11).²⁴ While the minimum inhibitory concentration (MIC) of moenomycin is two-fold higher in both mutants than it is in the parent strain, neither mutant displayed cross-resistance, suggesting that BAY 11-7082 and moenomycin act via distinct mechanisms (Figure S4).

Wall teichoic acid synthesis may play a role in BAY 11-7082– β -lactam synergy

Compounds that inhibit FtsZ and WTA biosynthesis are thought to synergize with certain β -lactams against MRSA by causing PBP mislocalization, leading us to ask if BAY 11-7082 acts on one of these pathways.^{3,5,11–13} To explore BAY 11-7082's impact on WTA biosynthesis we measured activity against a $\Delta tarO$ mutant of *S. aureus* USA300, which lacks the enzyme that catalyzes the first step in this process.¹² The inhibitory concentration of BAY 11-7082 in the $\Delta tarO$ strain was similar to that of its parent strain, allowing us to conclude BAY 11-7082's antibacterial activity is not dependent on WTA biosynthesis (Figure 3A). As expected, the inhibitory concentration of penicillin G dropped by eight-fold in the $\Delta tarO$ strain (Figure 3A). Interestingly, BAY 11-7082 no longer potentiated penicillin G activity in the $\Delta tarO$ strain (FICI=0.62) (Figure 3B), suggesting that while BAY 11-7082's antibacterial activity is unrelated

to WTA biosynthesis, the polymer impacts its ability to synergize with β -lactams. To confirm that these phenotypes remained consistent for structural analogues of BAY 11-7082, we also measured the activity of the potent chlorinated PSPC-analogue MLLB-2002 (Figure 3).

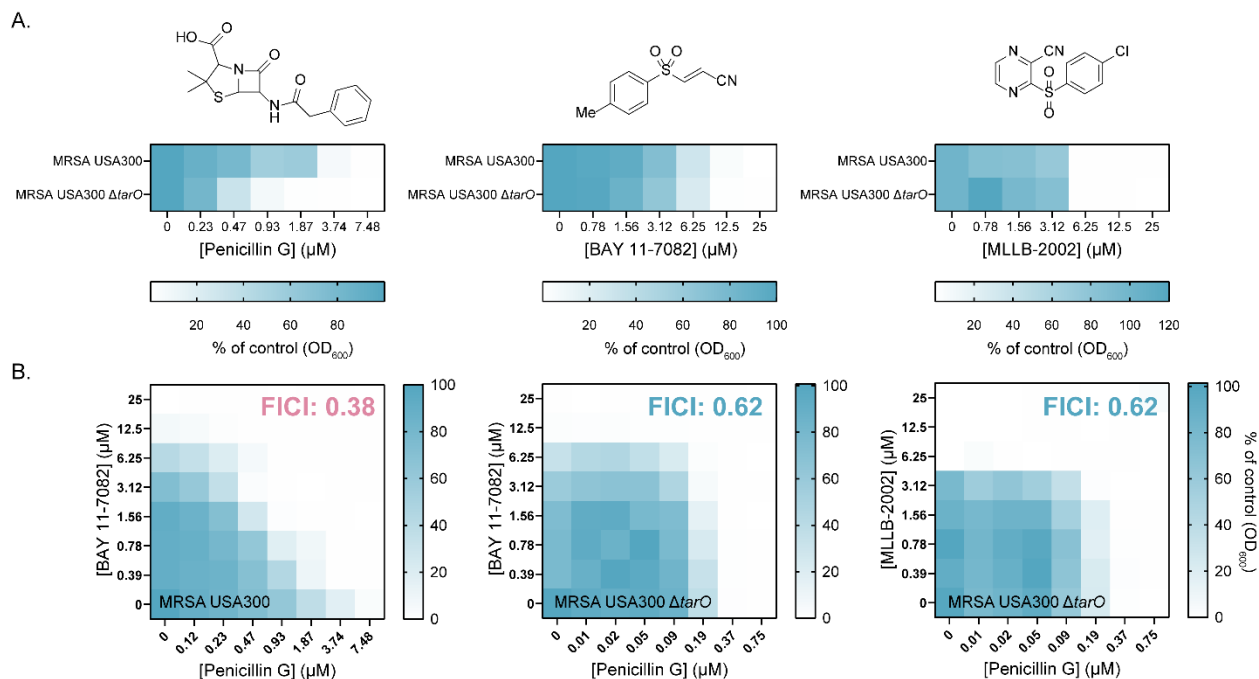


Figure 3. The absence of WTA does not impact BAY 11-7082 activity. (A) Planktonic growth (optical density at 600 nm as a percent of the vehicle control) of *S. aureus* USA300 and a $\Delta tarO$ mutant grown in the presence of increasing concentrations of penicillin G (left), BAY 11-7082 (middle), or the analogue MLLB-2002 (right) (μM). (B) Checkerboards of *S. aureus* USA300 (left) or a $\Delta tarO$ mutant (middle and right) grown with increasing concentration of penicillin G and BAY 11-7082 or MLLB-2002, where synergy ($\text{FICI} < 0.5$) is represented in pink text while indifference ($\text{FICI} \geq 0.5$) is represented in blue. Data represent an average of three independent experiments.

These phenotypes are similar to those observed with the UppS inhibitor clomiphene, which also sensitizes MRSA to β -lactams but retains its activity in strains lacking WTA.¹⁹ This raised the question of whether BAY 11-7082 inhibits an upstream enzyme common to both WTA and peptidoglycan biosynthesis. Inhibitors that deplete shared substrates of WTA and peptidoglycan synthesis antagonize the activity of the TarG inhibitor targocil by limiting resources available for WTA biosynthesis and reducing its effect on the cell.¹⁹ Unexpectedly, BAY 11-7082 did not

impact targocil activity (FICI=1.5) (Figure 4A), suggesting BAY 11-7082 does not reduce WTA biosynthesis. We also measured the activity of lysostaphin, an endopeptidase capable of cleaving the pentaglycine bridge in *S. aureus* peptidoglycan, since strains lacking WTA are more sensitive to lysostaphin than wild type (Figure 4B, D). Lysostaphin sensitivity was not altered in the presence of BAY 11-7082 (FICI=0.53) (Figure 4C). Taken together, these results suggest BAY 11-7082 does not impact WTA levels.

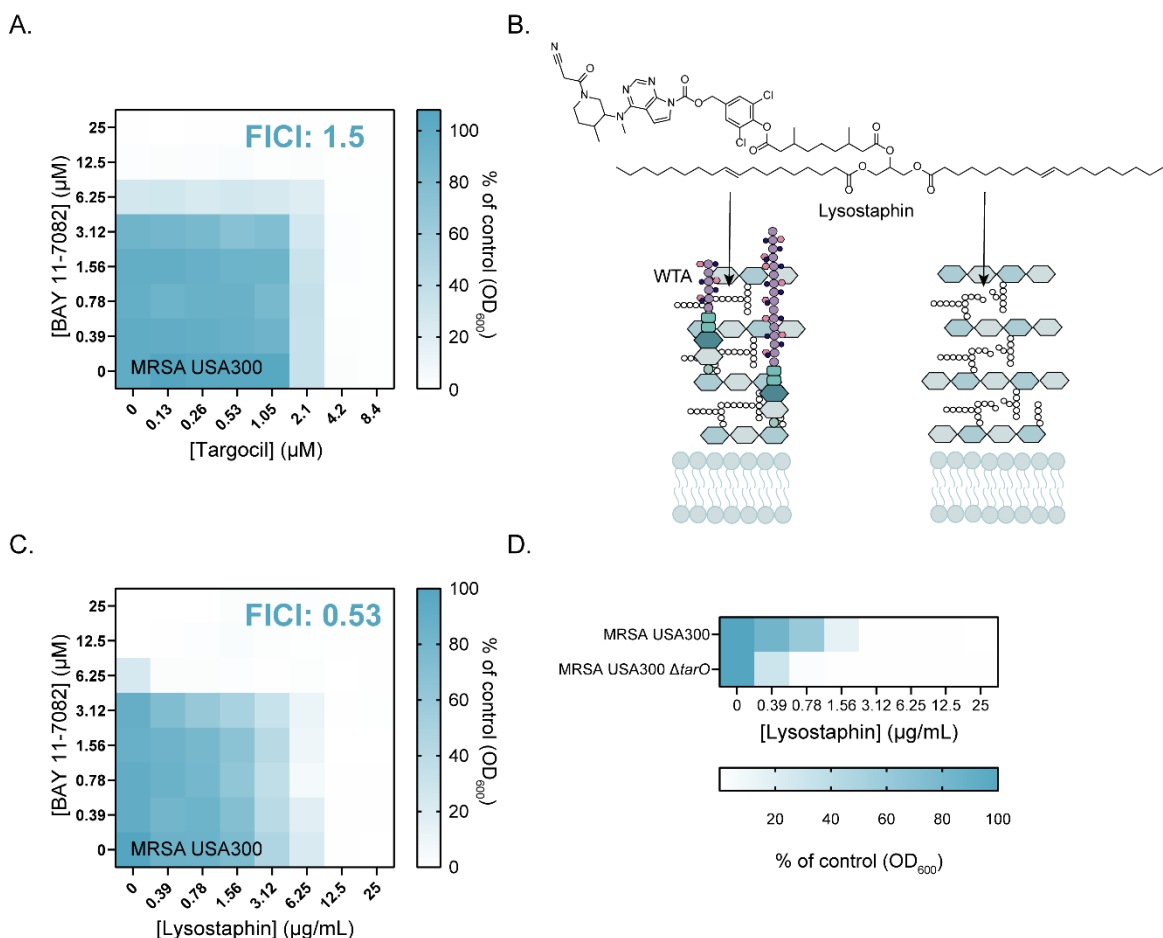


Figure 4. BAY 11-7082 does not impact WTA levels. (A) Checkerboard of *S. aureus* USA300 grown with increasing concentration of BAY 11-7082 and the TarG inhibitor targocil (µM). (B) Lysostaphin is an endopeptidase that cleaves the pentaglycine bridge in *S. aureus* peptidoglycan. Cells producing WTA are less sensitive (left) compared to those lacking WTA (right). (C) Checkerboard of *S. aureus* USA300 grown with increasing concentration of BAY 11-7082 (µM) and lysostaphin (µg/mL). (D) Planktonic growth (optical density at 600 nm as a percent of the vehicle control) of *S. aureus* USA300 and a $\Delta tarO$ mutant grown in the presence of increasing concentrations of lysostaphin (µg/mL). Data is based on three independent experiments

performed in triplicate. FICI values ≥ 0.5 represent indifference, and checkerboards are based on an average of three independent experiments.

WTA glycosylation is not required for BAY 11-7082- β -lactam synergy

While inconsistent with inhibition of TarO, lack of synergy with lysostaphin is consistent with inhibition of TarS, the glycosyltransferase responsible for installing a β -O-GlcNAc on *S. aureus* WTA.¹⁶ Mutants lacking *tarS* are viable but hypersensitive to a wide range of β -lactams.¹⁶ To explore whether WTA glycosylation impacts BAY 11-7082's ability to synergize with β -lactams, we made use of the Nebraska transposon library, a set of MRSA USA300 mutants containing single transposon insertions in non-essential genes.³⁰ A mutant with a transposon insertion in *tarS* had similar susceptibility to BAY 11-7082 as the parent strain (Figure 5A), and was still susceptible to a combination of BAY 11-7082 and penicillin G (FICI=0.37) (Figure 5B), indicating that while the presence of WTAs are required for synergy, their intact glycosylation is not.

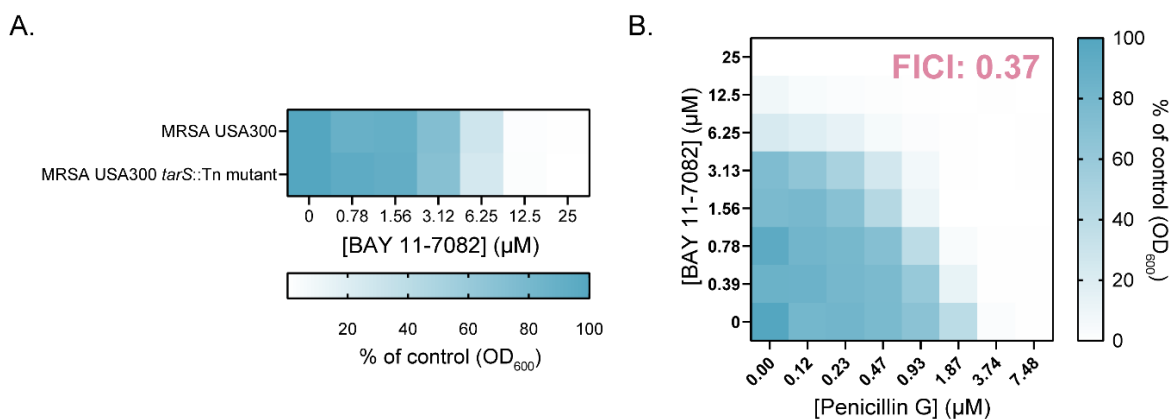


Figure 5. WTA glycosyltransferase TarS is not required for BAY 11-7082- β -lactam synergy. (A) Planktonic growth (optical density at 600 nm as a percent of the vehicle control) of *S. aureus* USA300 and a *tarS* transposon mutant grown in the presence of increasing concentrations BAY 11-7082 (μ M). (B) Checkerboard of a *tarS* transposon mutant of *S. aureus* USA300 grown with increasing concentration of penicillin G and BAY 11-7082 (μ M) where synergy (FICI<0.5) is represented in pink text. Data represent an average of three independent experiments.

BAY 11-7082 does not impact cell division

To further probe the mechanism of BAY 11-7082- β -lactam synergy and how WTAs may be involved, we explored whether BAY 11-7082 treatment impacts cell division. Septal abnormalities and division defects occur in cells treated with inhibitors of auxiliary factors like FtsZ and are also characteristic of cells lacking WTA, lipoteichoic acids (LTAs), or *D*-alanine esters.^{11,21} Cells without functional TarS, however, do not exhibit morphological or division defects.¹⁶ We conducted transmission electron microscopy (TEM) on thin-sectioned MRSA cells (Figure 6A, Figure S5A) and cells exposed to 8x or 16x MIC of BAY 11-7082 to look for division defects (Figure 6D, Figure S5D-E). We also imaged cells treated with targocil and untreated $\Delta tarO$ cells (Figure 6B-C, Figure S5B-C). As expected, $\Delta tarO$ cells exhibit a thinner outer layer and less well-defined edges, consistent with published phenotypes for cells lacking WTA, and targocil-treated cells clustered together, indicating improper separation following division.^{11,17} Cells treated with BAY 11-7082, however, more closely resembled untreated wild type cells and displayed sharp, thick outer layers, suggesting an intact peptidoglycan layer rich in WTAs, septa formation along the midcell, and separation following division. These data indicate BAY 11-7082 synergizes with β -lactams via a mechanism unlike those described previously for other WTA-targeting compounds.

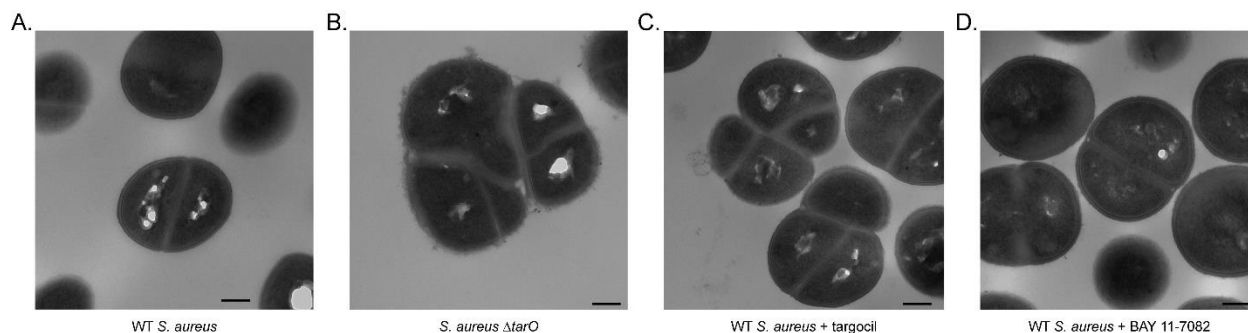


Figure 6. BAY 11-7082 treatment does not result in morphological changes or septal abnormalities. (A) Electron micrograph of wildtype (WT) untreated *S. aureus* USA300. (B) *S. aureus* USA300 $\Delta tarO$ cells exhibit morphological defects including irregular septum formation.

(C) Wildtype *S. aureus* USA300 treated with 33.6 μ M targocil fail to separate following division.
(D) Wildtype *S. aureus* USA300 treated with 50 μ M BAY 11-7082 display no noticeable morphological abnormalities. Scale bar=200 nm. Additional images are available in Figure S5.

Discussion

The anti-inflammatory compound BAY 11-7082 was first identified in our previous screen due to its broad-spectrum antibacterial activity, and further investigated here for its potential as a β -lactam adjuvant for MRSA. We first aimed to identify the subset of β -lactams potentiated by BAY 11-7082, finding that it synergizes with β -lactams that primarily target PBP2 (Figure 2B). BAY 11-7082 failed to synergize with β -lactams that primarily target PBP3, a non-essential transpeptidase involved in cell elongation, or PBP1, an essential protein with transpeptidase activity involved in cell division (Figure 2B).²⁶ Interestingly, cloxacillin, which differs from oxacillin by the addition of a single chlorine atom (Figure S1), did not synergize with BAY 11-7082 (FICI=0.62), while oxacillin did (FICI=0.19) (Figure 2B, Figure S2), likely because cloxacillin, unlike oxacillin, is highly specific for PBP1.³¹ These findings led us to propose that BAY 11-7082 interrupts a crucial coordination between the β -lactam insensitive transpeptidase domain of PBP2A and the glycosyltransferase domain of PBP2, which is required for proper cell wall synthesis in the presence of a β -lactam.²⁷ PBP4 is a nonessential PBP with transpeptidase activity that, when inactivated, sensitizes cells to β -lactams specific for PBP2.²⁸ Since PBP2 and PBP4 function cooperatively to crosslink glycan strands,²⁸ we expected BAY 11-7082 to also synergize with cefoxitin, a β -lactam with high affinity for PBP4. While combining BAY 11-7082 with cefoxitin resulted in a low FICI of 0.5 (Figure 2B, Figure S2), this interaction exceeded the cut-off (FICI<0.5) for synergy.

We found that while BAY 11-7082 did not synergize with the glycopeptide antibiotic vancomycin (Figure 2B), it did cause a slight reduction in sensitivity (Figure S2). This resembles the effect of a point mutation in the phosphorylation site of *walR*, which encodes the response regulator of WalKR, an essential two-component system that regulates autolysins involved in cleaving peptidoglycan during cell growth.³² Despite this similarity, *walR* mutants fail to potentiate PBP2-targeting β -lactams like oxacillin,³² suggesting BAY 11-7082 acts via a separate mechanism.

We predicted that BAY 11-7082 may interrupt coordination between PBP2 and PBP2A, potentially through PBP mislocalization. Since several auxiliary factors are involved in proper PBP coordination, we wondered whether BAY 11-7082 acted on any of these factors. Many auxiliary factors are directly involved in peptidoglycan biosynthesis, but some have roles in other cellular processes, including the biosynthesis of WTAs.² We showed BAY 11-7082 does not target WTA biosynthesis, since it and its synthetic analogues retain antimicrobial potency in a $\Delta tarO$ mutant (Figure 3A). We did, however, find that WTA biosynthesis is required for BAY 11-7082- β -lactam synergy (Figure 3B). It is possible that BAY 11-7082's antibacterial target is distinct from the target that potentiates β -lactams. This idea is consistent with our previous work that suggested BAY 11-7082 could have multiple cellular targets, and with its activity against Gram-negative species including *Pseudomonas aeruginosa*, *Escherichia coli*, and *Klebsiella pneumoniae*.²⁴

BAY 11-7082 may synergize with PBP2-targeting β -lactams not by interrupting coordination between PBP2 and PBP2A, but by directly inhibiting the glycosyltransferase activity of PBP2,

similar to the antibiotic moenomycin. We showed that BAY 11-7082 does not potentiate or antagonize moenomycin activity (Figure 2B, Figures S2-S3), suggesting it is possible they are acting via the same mechanism; however, we found cells with increased resistance to BAY 11-7082 or its structural analogue PSPC do not exhibit increased resistance to moenomycin (Figure S4), suggesting they do not share a conserved mechanism of action. Moenomycin resistance is rare, and few groups have identified moenomycin resistant strains. Notably, in 2013 the Walker lab identified two single point mutations in the active site of the glycosyltransferase domain of PBP2 that each confer resistance to moenomycin, which are not present in strains resistant to BAY 11-7082,^{24,33} suggesting that while BAY 11-7082 may interrupt the glycosyltransferase activity of PBP2, it would do so via an alternate mechanism.

Many compounds that synergize with β -lactams against MRSA have been identified in the literature, despite no adjuvants having made it to the clinic. For example, the β -lactam cefoxitin itself potentiates the activity of other β -lactams by inhibiting PBP4, which acts cooperatively with PBP2 and PBP2A.^{28,34} The lipopeptide daptomycin and natural flavonoid epicatechin gallate, which both target the cytoplasmic membrane, synergize with oxacillin.^{35,36} Epicatechin gallate causes PBP2 mislocalization by intercalating in the cytoplasmic membrane and reducing *D*-alanylation of WTAs; however, unlike BAY 11-7082, it induces morphological changes, interrupts proper cell separation following division, and decreases lysostaphin susceptibility.^{36,37} MAC-545496 synergizes with β -lactams including oxacillin by inhibiting the response regulator GraR, which regulates *dltABCD*, among other genes, but antagonizes the TarG inhibitor targocil, similar to the UppS inhibitor clomiphene.^{19,20} FtsZ inhibitors cause PBP2 mislocalization, but also induce division defects and cell wall invaginations.^{3,5} Due to these phenotypic differences,

we expect that BAY 11-7082 acts in a unique way from previously identified adjuvants, possibly by targeting auxiliary factors that play a role in β -lactam resistance that have not previously been targeted. LTAs, unlike WTAs, are linked to the cell membrane, synthesized via a separate pathway, and are essential.³⁸ A transposon insertion in the LTA synthase gene *ltaS* causes increased sensitivity to β -lactams, suggesting those polymers also play a role in modifying β -lactam resistance.³⁹ While inhibitors of LTA biosynthesis have not been identified, an *ltaS* transposon mutant is resistant to inhibitors of the signal peptidase SpsB, which regulates LtaS.^{39,40} Strains lacking LTA are enlarged with improper septation and separation, unlike cells treated with BAY 11-7082 (Figure 6D).²¹ While cells lacking the auxiliary factor TarS are morphologically similar to those treated with BAY 11-7082,¹⁶ synergy is maintained in a *tarS* transposon mutant, indicating it is not a target (Figure 5B). Since BAY 11-7082 likely does not target these more well-understood auxiliary factors, it may impact the function of a determinant of β -lactam resistance that is not yet fully understood, making it a useful tool in further elucidating the complex processes involved in PBP2A-mediated resistance.

Conclusions

BAY 11-7082 and its structural analogues synergize with select β -lactams against MRSA, restoring the activity of inexpensive and readily available compounds such as penicillin G. We showed that while WTA biosynthesis is required for this synergistic interaction, our data suggest that BAY 11-7082 does not target WTA biosynthesis, nor the synthesis of precursors like undecaprenyl phosphate. Unlike existing adjuvants, BAY 11-7082 treatment does not cause aberrant cell division or separation. Together, the data suggest that BAY 11-7082's mechanism of

potentiation is unique among β -lactam adjuvants reported in the literature, and thus it will be useful as a tool to better understand β -lactam resistance.

Methods

Bacterial strains, culture conditions, and chemicals

Microbial strains used include *S. aureus* USA300 (MRSA) and *S. aureus* ATCC 29213 (MSSA). *S. aureus* USA300 and the transposon mutant presented in Figure 5 were from the Nebraska transposon mutant library.³⁰ *S. aureus* USA300 $\Delta tarO$ was kindly gifted from Eric Brown's laboratory.¹² BAY 11-7082 and PSPC resistant mutants of *S. aureus* 15981 (MRSA) were generated as previously reported.²⁴ Bacterial cultures were grown in Mueller-Hinton broth (MHB). Solid media was solidified with 1.5% agar. BAY 11-7082 and its structural analogue MLLB-2002 were synthesized as previously reported and stored as 100 μ M stocks in DMSO at -20 °C.²⁴ Stock solutions of amoxicillin (Sigma, prepared in DMSO), ampicillin (BioShop, prepared in DMSO), cefoxitin (Sigma, prepared in DMSO), cefsulodin (MP Biomedicals, 2 mg/mL), ceftazidime (Sigma, 4 mg/mL), cloxacillin (Sigma, prepared in DMSO), doripenem (Sigma), imipenem (AK Scientific, prepared in DMSO), methicillin (Cayman Chemicals), oxacillin (Cayman Chemicals, prepared in DMSO), penicillin G (Fluka Analytica), piperacillin (Sigma, 40 mg/mL), moenomycin complex (Cayman Chemicals, 0.01 mg/mL, prepared in DMSO), and vancomycin (Sigma, prepared in DMSO) were prepared at 10 mg/mL in sterile de-ionized H₂O, except where noted, and stored at -20°C. Targocil was kindly gifted from the Brown Lab and prepared at 5 mg/mL in DMSO. Lysostaphin from *Staphylococcus simulans* was purchased from Sigma Aldrich and prepared at 10 mg/mL in sterile de-ionized H₂O.

Inhibitory concentration assays

All bacterial strains were inoculated from -80°C glycerol stocks into 5 mL MHB and incubated with shaking, 200 rpm, 37°C for 16 h. Cultures were sub-cultured in a 1:500 dilution, grown for 4 h, and diluted in fresh MHB to an OD₆₀₀ of ~ 0.1, then diluted 1:500. Minimal inhibitory concentration values were determined as previously described, using compounds serially diluted in DMSO or sterile water.²⁴ All MIC values are based on three independent experiments performed in triplicate.

Checkerboard assays

Checkerboard assays were set up and fractional inhibitory concentration indices (FICIs) were calculated as previously described.²⁴ Briefly, 2 µL of compounds were added to an 8x8 section of a 96-well plate with increasing concentrations of one compound across the X-axis and increasing concentrations of the other compound across the Y-axis. Plates were incubated with shaking, 200 rpm, 37°C, 16 h and OD₆₀₀ was measured and used to determine the MIC. Three biological replicates were averaged for each checkerboard.

Transmission electron microscopy

S. aureus USA300 and USA300 $\Delta tarO$ were streaked on Mueller-Hinton agar (MHA) from -80°C glycerol stocks, then incubated at 37°C for 16 h. Single colonies were inoculated into 5 mL MHB and incubated with shaking, 200 rpm, 37°C for 16 h, then diluted 1:50 in fresh MHB and incubated for an additional 1.5 h. Cultures were normalized to OD₆₀₀ ~ 0.3 and incubated with DMSO, 8X MIC targocil, or 8-16X MIC BAY 11-7082 for 3 h. Cells were pelleted, washed with 100 µL MHB, then washed with 100 µL 2% glutaraldehyde fixative in phosphate buffer before

being resuspended in 250 μ L fixative and submitted to the Canadian Centre for Electron Microscopy for processing and sectioning. Cells were imaged using a JEOL 1200EX microscope. Images were taken at 75,000 x magnification (Figure 6) or 100,000 x magnification (Figure S5).

Acknowledgments

We thank Eric D. Brown for providing targocil and the *$\Delta tarO$* strain of MRSA and Eric D. Brown, Shawn French, and Maya Farha for helpful ideas and discussions. We thank Cezar M. Khursigara and Erin M. Anderson for helpful conversations about electron microscopy. Thank you to Marcia Reid from the Canadian Centre for Electron Microscopy for sample preparation and microscopy. This work was supported by a Discovery Grant from the Natural Sciences and Engineering Research Council of Canada [RGPIN- 2021-04237]. LLB holds a Tier 1 Canada Research Chair in Microbe-Surface Interactions [CRC-2021-00103]. VEC holds an Ontario Graduate Scholarship.

References

- (1) Berger-Bächi, B.; Rohrer, S. Factors Influencing Methicillin Resistance in Staphylococci. *Arch. Microbiol.* **2002**, *178* (3), 165–171. <https://doi.org/10.1007/s00203-002-0436-0>.
- (2) Roemer, T.; Schneider, T.; Pinho, M. G. Auxiliary Factors: A Chink in the Armor of MRSA Resistance to β -Lactam Antibiotics. *Curr. Opin. Microbiol.* **2013**, *16* (5), 538–548. <https://doi.org/10.1016/j.mib.2013.06.012>.
- (3) Tan, C. M.; Therien, A. G.; Lu, J.; Lee, S. H.; Caron, A.; Gill, C. J.; Lebeau-Jacob, C.; Benton-Perdomo, L.; Monteiro, J. M.; Pereira, P. M.; Elsen, N. L.; Wu, J.; Deschamps, K.; Petcu, M.; Wong, S.; Daigneault, E.; Kramer, S.; Liang, L.; Maxwell, E.; Claveau, D.; Vaillancourt, J.; Skorey, K.; Tam, J.; Wang, H.; Meredith, T. C.; Sillaots, S.; Wang-Jarantow, L.; Ramtohol, Y.; Langlois, E.; Landry, F.; Reid, J. C.; Parthasarathy, G.; Sharma, S.; Baryshnikova, A.; Lumb, K. J.; Pinho, M. G.; Soisson, S. M.; Roemer, T. Restoring Methicillin-Resistant *Staphylococcus aureus* Susceptibility to β -Lactam

- Antibiotics. *Sci. Transl. Med.* **2012**, *4* (126).
<https://doi.org/10.1126/scitranslmed.3003592>.
- (4) Kaul, M.; Mark, L.; Parhi, A. K.; LaVoie, E. J.; Pilch, D. S. Combining the FtsZ-Targeting Prodrug TXA709 and the Cephalosporin Cefdinir Confers Synergy and Reduces the Frequency of Resistance in Methicillin-Resistant *Staphylococcus aureus*. *Antimicrob. Agents Chemother.* **2016**. <https://doi.org/10.1128/AAC.00613-16>.
 - (5) Ferrer-González, E.; Kaul, M.; Parhi, A. K.; LaVoie, E. J.; Pilch, D. S. β -Lactam Antibiotics with a High Affinity for PBP2 Act Synergistically with the FtsZ-Targeting Agent TXA707 against Methicillin-Resistant *Staphylococcus aureus*. *Antimicrob. Agents Chemother.* **2017**. <https://doi.org/10.1128/AAC.00863-17>.
 - (6) Therien, A. G.; Huber, J. L.; Wilson, K. E.; Beaulieu, P.; Caron, A.; Claveau, D.; Deschamps, K.; Donald, R. G. K.; Galgoci, A. M.; Gallant, M.; Gu, X.; Kevin, N. J.; Lafleur, J.; Leavitt, P. S.; Lebeau-Jacob, C.; Lee, S. S.; Lin, M. M.; Michels, A. A.; Ogawa, A. M.; Painter, R. E.; Parish, C. A.; Park, Y.-W.; Benton-Perdomo, L.; Petcu, M.; Phillips, J. W.; Powles, M. A.; Skorey, K. I.; Tam, J.; Tan, C. M.; Young, K.; Wong, S.; Waddell, S. T.; Miesel, L. Broadening the Spectrum of β -Lactam Antibiotics through Inhibition of Signal Peptidase Type I. *Antimicrob. Agents Chemother.* **2012**, *56* (9), 4662–4670. <https://doi.org/10.1128/aac.00726-12>.
 - (7) Weidenmaier, C.; Peschel, A. Teichoic Acids and Related Cell-Wall Glycopolymers in Gram-Positive Physiology and Host Interactions. *Nat. Rev. Microbiol.* **2008**, *6* (4), 276–287. <https://doi.org/10.1038/nrmicro1861>.
 - (8) Atilano, M. L.; Pereira, P. M.; Yates, J.; Reed, P.; Veiga, H.; Pinho, M. G.; Filipe, S. R. Teichoic Acids Are Temporal and Spatial Regulators of Peptidoglycan Cross-Linking in *Staphylococcus aureus*. *Proc. Natl. Acad. Sci.* **2010**, *107* (44), 18991–18996. <https://doi.org/10.1073/pnas.1004304107>.
 - (9) Henriques, G. F. Study of the Role of Wall Teichoic Acids in the Localization *Staphylococcus aureus* Cell Wall Synthesis Protein PBP4. masterThesis, 2013. <https://run.unl.pt/handle/10362/16316> (accessed 2024-03-01).
 - (10) Swoboda, J. G.; Campbell, J.; Meredith, T. C.; Walker, S. Wall Teichoic Acid Function, Biosynthesis, and Inhibition. *ChemBioChem* **2010**, *11* (1), 35–45. <https://doi.org/10.1002/cbic.200900557>.
 - (11) Campbell, J.; Singh, A. K.; Santa Maria, J. P.; Kim, Y.; Brown, S.; Swoboda, J. G.; Mylonakis, E.; Wilkinson, B. J.; Walker, S. Synthetic Lethal Compound Combinations Reveal a Fundamental Connection between Wall Teichoic Acid and Peptidoglycan Biosyntheses in *Staphylococcus aureus*. *ACS Chem. Biol.* **2011**, *6* (1), 106–116. <https://doi.org/10.1021/cb100269f>.
 - (12) Farha, M. A.; Leung, A.; Sewell, E. W.; D’Elia, M. A.; Allison, S. E.; Ejim, L.; Pereira, P. M.; Pinho, M. G.; Wright, G. D.; Brown, E. D. Inhibition of WTA Synthesis Blocks the Cooperative Action of PBPs and Sensitizes MRSA to β -Lactams. *ACS Chem. Biol.* **2013**, *8* (1), 226–233. <https://doi.org/10.1021/cb300413m>.
 - (13) Lee, S. H.; Wang, H.; Labroli, M.; Koseoglu, S.; Zuck, P.; Mayhood, T.; Gill, C.; Mann, P.; Sher, X.; Ha, S.; Yang, S.-W.; Mandal, M.; Yang, C.; Liang, L.; Tan, Z.; Tawa, P.; Hou, Y.; Kuvelkar, R.; DeVito, K.; Wen, X.; Xiao, J.; Batchlett, M.; Balibar, C. J.; Liu, J.; Xiao, J.; Murgolo, N.; Garlisi, C. G.; Sheth, P. R.; Flattery, A.; Su, J.; Tan, C.; Roemer, T. TarO-Specific Inhibitors of Wall Teichoic Acid Biosynthesis Restore β -Lactam Efficacy

- against Methicillin-Resistant Staphylococci. *Sci. Transl. Med.* **2016**, *8* (329), 329ra32–329ra32. <https://doi.org/10.1126/scitranslmed.aad7364>.
- (14) Wang, H.; Gill, C. J.; Lee, S. H.; Mann, P.; Zuck, P.; Meredith, T. C.; Murgolo, N.; She, X.; Kales, S.; Liang, L.; Liu, J.; Wu, J.; Santa Maria, J.; Su, J.; Pan, J.; Hailey, J.; Mcguinness, D.; Tan, C. M.; Flattery, A.; Walker, S.; Black, T.; Roemer, T. Discovery of Wall Teichoic Acid Inhibitors as Potential Anti-MRSA β -Lactam Combination Agents. *Chem. Biol.* **2013**, *20* (2), 272–284. <https://doi.org/10.1016/j.chembiol.2012.11.013>.
- (15) Lee, S. H.; Jarantow, L. W.; Wang, H.; Sillaots, S.; Cheng, H.; Meredith, T. C.; Thompson, J.; Roemer, T. Antagonism of Chemical Genetic Interaction Networks Resensitize MRSA to β -Lactam Antibiotics. *Chem. Biol.* **2011**, *18* (11), 1379–1389. <https://doi.org/10.1016/j.chembiol.2011.08.015>.
- (16) Brown, S.; Xia, G.; Luhachack, L. G.; Campbell, J.; Meredith, T. C.; Chen, C.; Winstel, V.; Gekeler, C.; Irazoqui, J. E.; Peschel, A.; Walker, S. Methicillin Resistance in *Staphylococcus aureus* Requires Glycosylated Wall Teichoic Acids. *Proc. Natl. Acad. Sci.* **2012**, *109* (46), 18909–18914. <https://doi.org/10.1073/pnas.1209126109>.
- (17) Campbell, J.; Singh, A. K.; Swoboda, J. G.; Gilmore, M. S.; Wilkinson, B. J.; Walker, S. An Antibiotic That Inhibits a Late Step in Wall Teichoic Acid Biosynthesis Induces the Cell Wall Stress Stimulon in *Staphylococcus aureus*. *Antimicrob. Agents Chemother.* **2012**, *56* (4), 1810–1820. <https://doi.org/10.1128/AAC.05938-11>.
- (18) Swoboda, J. G.; Meredith, T. C.; Campbell, J.; Brown, S.; Suzuki, T.; Bollenbach, T.; Malhowski, A. J.; Kishony, R.; Gilmore, M. S.; Walker, S. Discovery of a Small Molecule That Blocks Wall Teichoic Acid Biosynthesis in *Staphylococcus aureus*. *ACS Chem. Biol.* **2009**, *4* (10), 875–883. <https://doi.org/10.1021/cb900151k>.
- (19) Farha, M. A.; Czarny, T. L.; Myers, C. L.; Worrall, L. J.; French, S.; Conrady, D. G.; Wang, Y.; Oldfield, E.; Strynadka, N. C. J.; Brown, E. D. Antagonism Screen for Inhibitors of Bacterial Cell Wall Biogenesis Uncovers an Inhibitor of Undecaprenyl Diphosphate Synthase. *Proc. Natl. Acad. Sci.* **2015**, *112* (35), 11048–11053. <https://doi.org/10.1073/pnas.1511751112>.
- (20) El-Halfawy, O. M.; Czarny, T. L.; Flannagan, R. S.; Day, J.; Bozelli, J. C.; Kuiack, R. C.; Salim, A.; Eckert, P.; Epanand, R. M.; McGavin, M. J.; Organ, M. G.; Heinrichs, D. E.; Brown, E. D. Discovery of an Antivirulence Compound That Reverses β -Lactam Resistance in MRSA. *Nat. Chem. Biol.* **2020**, *16* (2), 143–149. <https://doi.org/10.1038/s41589-019-0401-8>.
- (21) Santa Maria, J. P.; Sadaka, A.; Moussa, S. H.; Brown, S.; Zhang, Y. J.; Rubin, E. J.; Gilmore, M. S.; Walker, S. Compound-Gene Interaction Mapping Reveals Distinct Roles for *Staphylococcus aureus* Teichoic Acids. *Proc. Natl. Acad. Sci.* **2014**, *111* (34), 12510–12515. <https://doi.org/10.1073/pnas.1404099111>.
- (22) Pasquina, L. W.; Santa Maria, J. P.; Walker, S. Teichoic Acid Biosynthesis as an Antibiotic Target. *Curr. Opin. Microbiol.* **2013**, *16* (5), 531–537. <https://doi.org/10.1016/j.mib.2013.06.014>.
- (23) Ranieri, M. R. M.; Chan, D. C. K.; Yaeger, L. N.; Rudolph, M.; Karabelas-Pittman, S.; Abdo, H.; Chee, J.; Harvey, H.; Nguyen, U.; Burrows, L. L. Thiostrepton Hijacks Pyoverdine Receptors To Inhibit Growth of *Pseudomonas aeruginosa*. *Antimicrob. Agents Chemother.* **2019**, *63* (9). <https://doi.org/10.1128/AAC.00472-19>.

- (24) Coles, V. E.; Darveau, P.; Zhang, X.; Harvey, H.; Henriksbo, B. D.; Yang, A.; Schertzer, J. D.; Magolan, J.; Burrows, L. L. Exploration of BAY 11-7082 as a Potential Antibiotic. *ACS Infect. Dis.* **2021**. <https://doi.org/10.1021/acsinfecdis.1c00522>.
- (25) Odds, F. C. Synergy, Antagonism, and What the Chequerboard Puts between Them. *J. Antimicrob. Chemother.* **2003**, *52* (1), 1–1. <https://doi.org/10.1093/jac/dkg301>.
- (26) Reichmann, N. T.; Tavares, A. C.; Saraiva, B. M.; Jouselin, A.; Reed, P.; Pereira, A. R.; Monteiro, J. M.; Sobral, R. G.; VanNieuwenhze, M. S.; Fernandes, F.; Pinho, M. G. SEDS–bPBP Pairs Direct Lateral and Septal Peptidoglycan Synthesis in *Staphylococcus aureus*. *Nat. Microbiol.* **2019**, *4* (8), 1368–1377. <https://doi.org/10.1038/s41564-019-0437-2>.
- (27) Pinho, M. G.; Lencastre, H. de; Tomasz, A. An Acquired and a Native Penicillin-Binding Protein Cooperate in Building the Cell Wall of Drug-Resistant Staphylococci. *Proc. Natl. Acad. Sci.* **2001**, *98* (19), 10886–10891. <https://doi.org/10.1073/pnas.191260798>.
- (28) Łęski, T. A.; Tomasz, A. Role of Penicillin-Binding Protein 2 (PBP2) in the Antibiotic Susceptibility and Cell Wall Cross-Linking of *Staphylococcus aureus*: Evidence for the Cooperative Functioning of PBP2, PBP4, and PBP2A. *J. Bacteriol.* **2005**. <https://doi.org/10.1128/JB.187.5.1815-1824.2005>.
- (29) Pinho, M. G.; Filipe, S. R.; de Lencastre, H.; Tomasz, A. Complementation of the Essential Peptidoglycan Transpeptidase Function of Penicillin-Binding Protein 2 (PBP2) by the Drug Resistance Protein PBP2A in *Staphylococcus aureus*. *J. Bacteriol.* **2001**, *183* (22), 6525–6531. <https://doi.org/10.1128/JB.183.22.6525-6531.2001>.
- (30) Fey, P. D.; Endres, J. L.; Yajjala, V. K.; Widhelm, T. J.; Boissy, R. J.; Bose, J. L.; Bayles, K. W. A Genetic Resource for Rapid and Comprehensive Phenotype Screening of Nonessential *Staphylococcus aureus* Genes. *mBio* *4* (1), e00537-12. <https://doi.org/10.1128/mBio.00537-12>.
- (31) Okonog, K.; Noji, Y.; Nakao, M.; Imada, A. The Possible Physiological Roles of Penicillin-Binding Proteins of Methicillin-Susceptible and Methicillin-Resistant *Staphylococcus aureus*. *J. Infect. Chemother.* **1995**, *1* (1), 50–58. <https://doi.org/10.1007/BF02347729>.
- (32) Tan, S.; Cho, K.; Nodwell, J. R. A Defect in Cell Wall Recycling Confers Antibiotic Resistance and Sensitivity in *Staphylococcus aureus*. *J. Biol. Chem.* **2022**, *298* (10). <https://doi.org/10.1016/j.jbc.2022.102473>.
- (33) Rebets, Y.; Lupoli, T.; Qiao, Y.; Schirner, K.; Villet, R.; Hooper, D.; Kahne, D.; Walker, S. Moenomycin Resistance Mutations in *Staphylococcus aureus* Reduce Peptidoglycan Chain Length and Cause Aberrant Cell Division. *ACS Chem. Biol.* **2014**, *9* (2), 459–467. <https://doi.org/10.1021/cb4006744>.
- (34) Banerjee, R.; Fernandez, M. G.; Enthaler, N.; Graml, C.; Greenwood-Quaintance, K. E.; Patel, R. Combinations of Cefoxitin plus Other β -Lactams Are Synergistic In Vitro against Community Associated Methicillin-Resistant *Staphylococcus aureus*. *Eur. J. Clin. Microbiol. Infect. Dis.* **2013**, *32* (6), 827–833. <https://doi.org/10.1007/s10096-013-1817-9>.
- (35) Rand, K. H.; Houck, H. J. Synergy of Daptomycin with Oxacillin and Other β -Lactams against Methicillin-Resistant *Staphylococcus aureus*. *Antimicrob. Agents Chemother.* **2004**, *48* (8), 2871–2875. <https://doi.org/10.1128/AAC.48.8.2871-2875.2004>.
- (36) Bernal, P.; Lemaire, S.; Pinho, M. G.; Mobashery, S.; Hinds, J.; Taylor, P. W. Insertion of Epicatechin Gallate into the Cytoplasmic Membrane of Methicillin-Resistant *Staphylococcus aureus* Disrupts Penicillin-Binding Protein (PBP) 2a-Mediated β -Lactam

- Resistance by Delocalizing PBP2. *J. Biol. Chem.* **2010**, 285 (31), 24055–24065. <https://doi.org/10.1074/jbc.M110.114793>.
- (37) Bernal, P.; Zloh, M.; Taylor, P. W. Disruption of D-Alanyl Esterification of *Staphylococcus aureus* Cell Wall Teichoic Acid by the β -Lactam Resistance Modifier (–)-Epicatechin Gallate. *J. Antimicrob. Chemother.* **2009**, 63 (6), 1156–1162. <https://doi.org/10.1093/jac/dkp094>.
- (38) Xia, G.; Kohler, T.; Peschel, A. The Wall Teichoic Acid and Lipoteichoic Acid Polymers of *Staphylococcus aureus*. *Int. J. Med. Microbiol.* **2010**, 300 (2), 148–154. <https://doi.org/10.1016/j.ijmm.2009.10.001>.
- (39) Meredith, T. C.; Wang, H.; Beaulieu, P.; Gründling, A.; Roemer, T. Harnessing the Power of Transposon Mutagenesis for Antibacterial Target Identification and Evaluation. *Mob. Genet. Elem.* **2012**, 2 (4), 171–178. <https://doi.org/10.4161/mge.21647>.
- (40) Wörmann, M. E.; Reichmann, N. T.; Malone, C. L.; Horswill, A. R.; Gründling, A. Proteolytic Cleavage Inactivates the *Staphylococcus aureus* Lipoteichoic Acid Synthase. *J. Bacteriol.* **2011**, 193 (19), 5279–5291. <https://doi.org/10.1128/jb.00369-11>.

Supporting Information

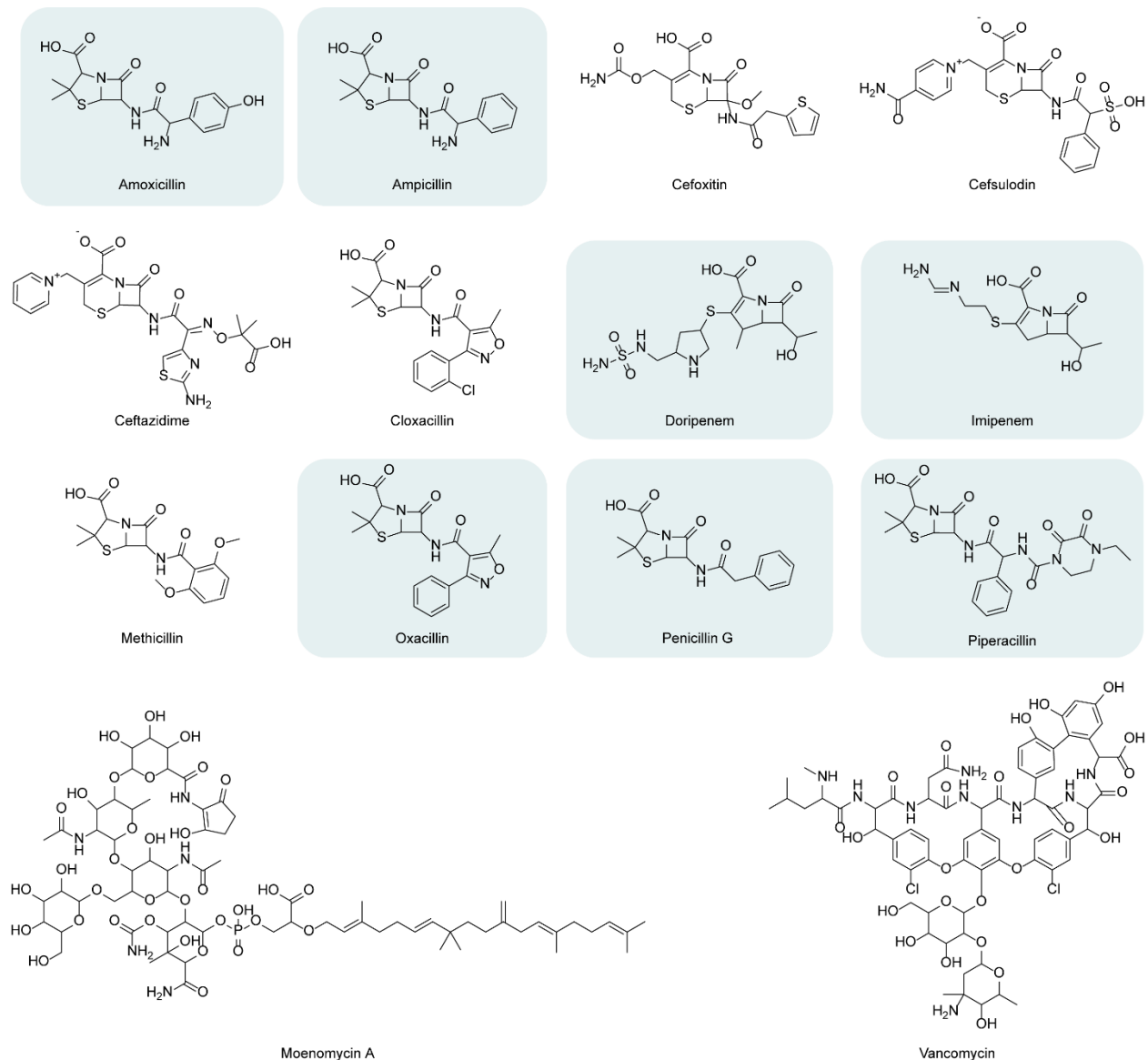


Figure S1. Structures of β -lactams and non- β -lactam peptidoglycan-targeting antibiotics tested for activity against *S. aureus* USA300 (MRSA) and ATCC 29213 (MSSA) in combination with BAY 11-7082. Compounds that synergize with BAY 11-7082 are highlighted with a box.

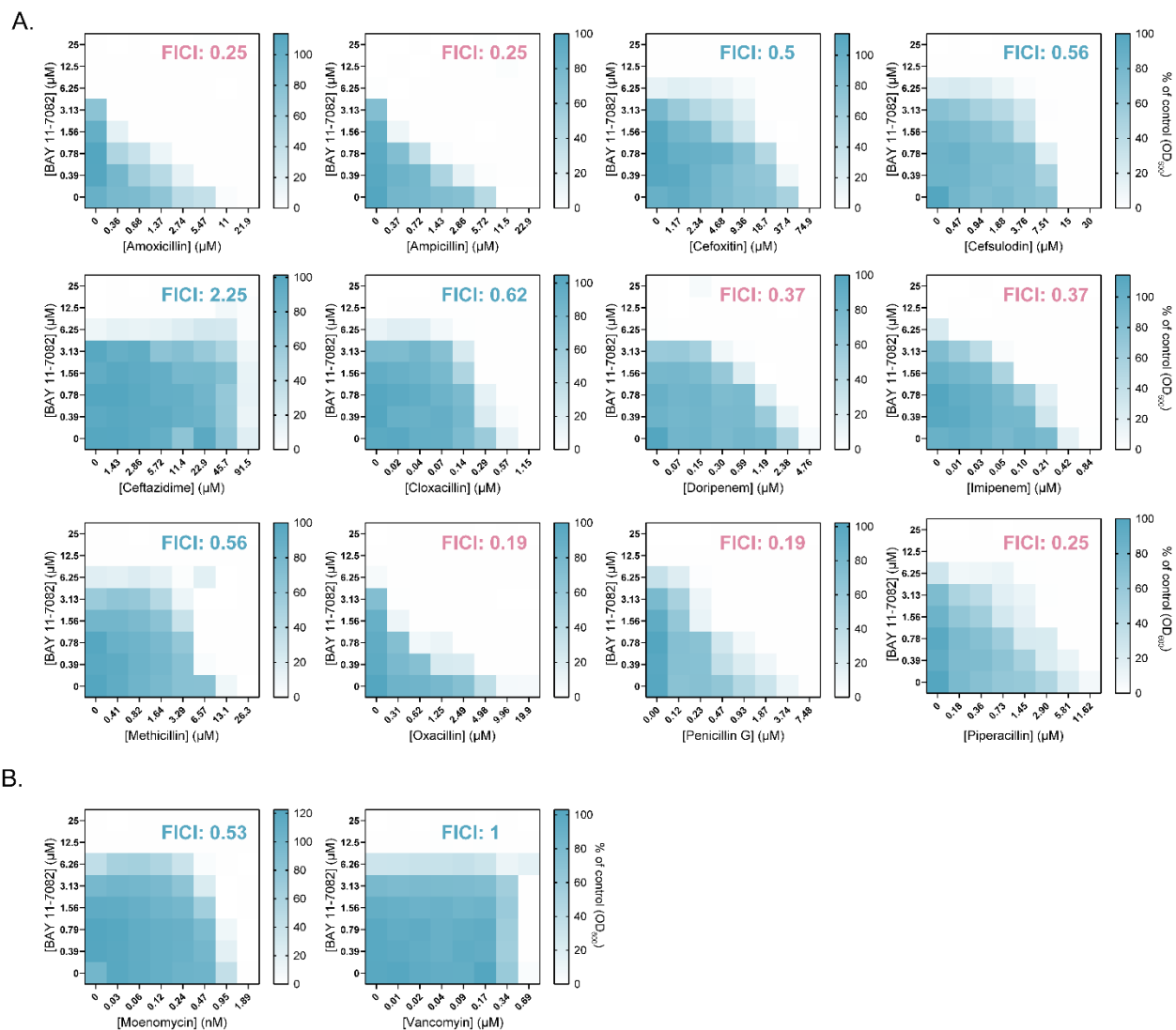


Figure S2. Checkerboards of *S. aureus* USA300 (MRSA) grown with increasing concentration of BAY 11-7082 and a β -lactam (A) or other cell-wall active antibiotic (B), where synergy ($FICI < 0.5$) is represented in pink text while indifference ($FICI \geq 0.5$) is represented in blue. Data represent an average of three independent experiments.

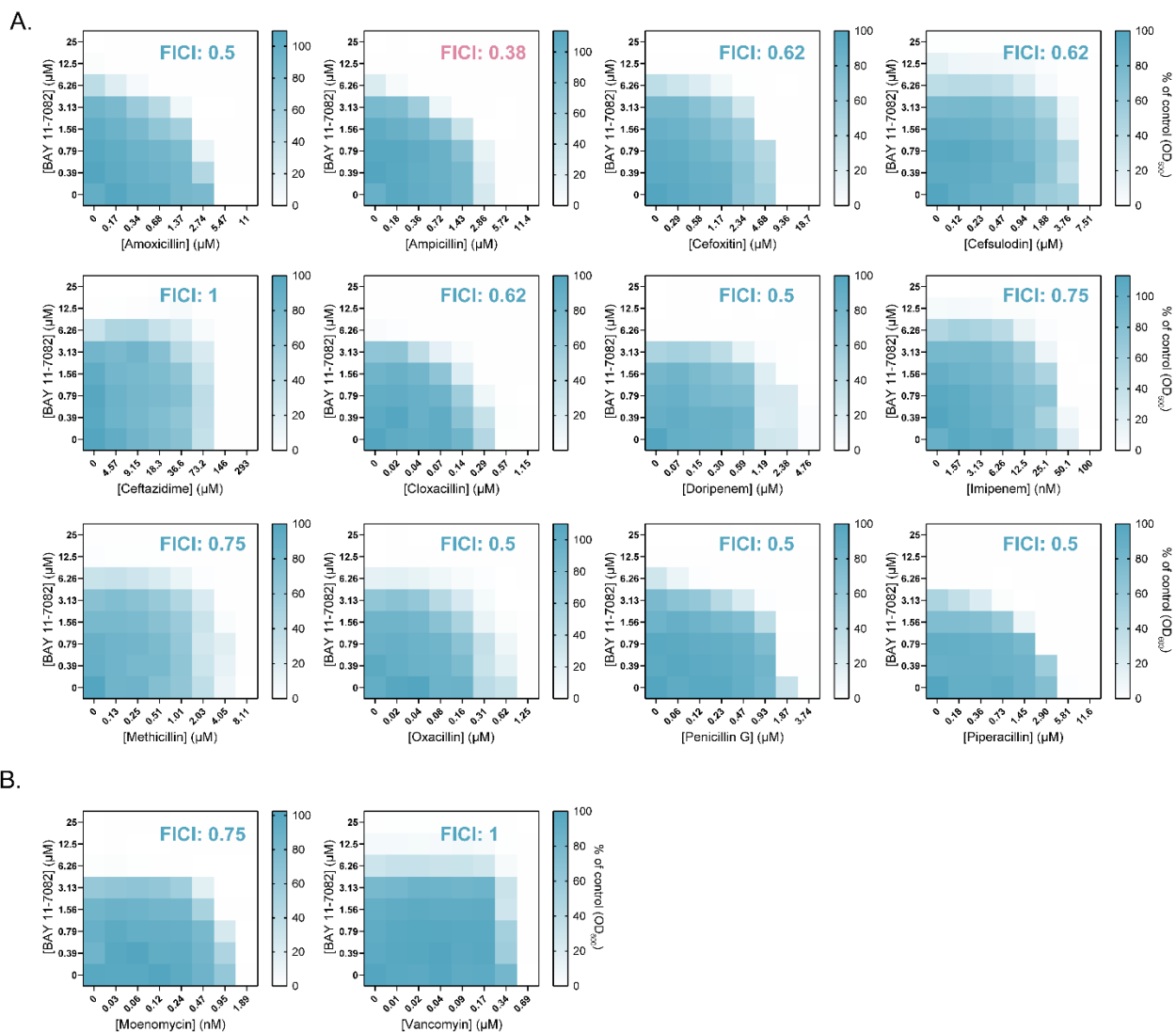


Figure S3. Checkerboards of *S. aureus* ATCC 29213 (MSSA) grown with increasing concentration of BAY 11-7082 and a β -lactam (A) or other cell-wall active antibiotic (B), where synergy (FICI < 0.5) is represented in pink text while indifference (FICI ≥ 0.5) is represented in blue. Data represent an average of three independent experiments.

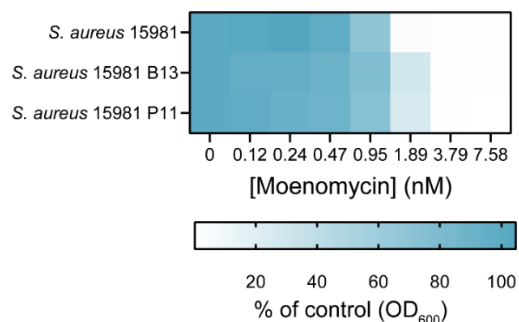


Figure S4. Planktonic growth (optical density at 600 nm as a percent of the vehicle control) of *S. aureus* 15981 (MRSA), the BAY 11-7082-resistant mutant B13, and the PSPC-resistant mutant P11. Cells grown in the presence of increasing concentrations of the antibiotic moenomycin (nM). Data represent an average of three independent experiments performed in triplicate.

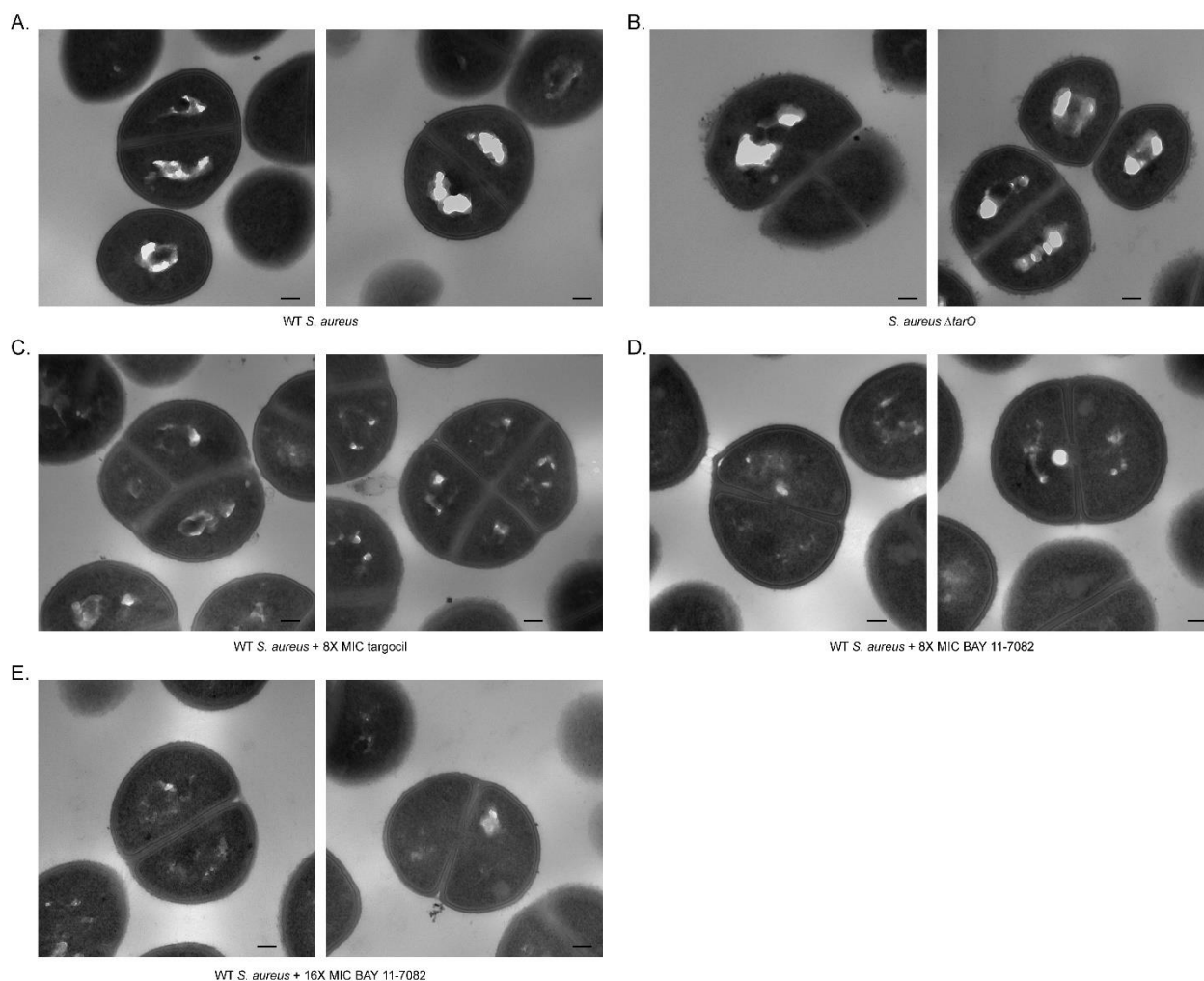


Figure S5. Additional fields of view of electron micrographs. (A) Untreated wildtype *S. aureus* USA300. (B) *S. aureus* USA300 $\Delta tarO$ cells. (C) Wildtype *S. aureus* USA300 treated with 33.6 μ M targocil. (D) Wildtype *S. aureus* USA300 treated with 50 μ M BAY 11-7082. (E) Wildtype *S. aureus* USA300 treated with 100 μ M BAY 11-7082. Scale bar=100 nm.

Chapter Four: The effects of chlorhexidine, povidone-iodine, and vancomycin on growth and biofilms of pathogens that cause prosthetic joint infections: an *in vitro* model

Preface

The work presented in this chapter has been published in:

Coles, V. E.; Puri, L.; Bhandari, M.; Wood, T. J.; Burrows, L. L. The Effects of Chlorhexidine, Povidone-Iodine, and Vancomycin on Growth and Biofilms of Pathogens That Cause Prosthetic Joint Infections: An *In Vitro* Model. *Journal of Hospital Infection*. **2024**, *151*, 99-108.
<https://doi.org/10.1016/j.jhin.2024.06.010>.

Copyright © 2024 The Authors under Creative Commons BY-NC-ND.

VEC: Conceptualization, Methodology, Investigation, Formal analysis, Writing – original draft, Visualization. **LP:** Conceptualization, Writing – review and editing. **MB:** Conceptualization, Writing – review and editing. **TJW:** Conceptualization, Writing – review and editing. **LLB:** Conceptualization, Methodology, Supervision, Writing – original draft.

Summary

Background: Chlorhexidine gluconate (CHG) and povidone-iodine (PI) are commonly used to prevent prosthetic joint infection (PJI) during total joint replacement; however, their effective concentrations and impact on biofilms are not well defined.

Aim: To determine: (1) the *in vitro* minimum inhibitory concentration of CHG and PI against model PJI-causing organisms and clinical isolates; (2) their impact on biofilm formation; (3) if there a synergistic benefit to combining the two solutions; and (4) if adding the antibiotic vancomycin impacts antiseptic activity.

Methods: We measured *in vitro* growth and biofilm formation of *Staphylococcus epidermidis*, methicillin-sensitive and methicillin-resistant *S. aureus*, *Escherichia coli*, *Pseudomonas aeruginosa*, and *Candida albicans*, as well as recent clinical isolates, in the presence of increasing concentrations of CHG and/or PI. Checkerboard assays were used to measure potential synergy of the solutions together and with vancomycin.

Findings: CHG and PI inhibited growth and biofilm formation of all model organisms tested at concentrations of 0.0004% and 0.33% or lower, respectively; highly dilute concentrations paradoxically increased biofilm formation. The solutions did not synergize with one another and acted independently of vancomycin.

Conclusion: CHG and PI are effective at lower concentrations than typically used, establishing baselines to support further clinical trials aimed at optimizing wound sterilization. There is no synergistic advantage to using both in combination. Vancomycin is effective at inhibiting the growth of *S. epidermidis* and *S. aureus*; however, it stimulates *P. aeruginosa* biofilm production, suggesting in the rare case of *P. aeruginosa* PJI, it could exacerbate infection.

Introduction

Prosthetic joint infection (PJI) remains a problematic complication of total joint replacement (TJR), a necessary surgery for managing osteoarthritis. *Staphylococcus* species including *S. epidermidis* and methicillin-sensitive (MSSA) and methicillin-resistant (MRSA) strains of *S. aureus* are the most frequent cause, present in 56% of infections [1]. Though less common, infections can also be caused by the Gram-negative pathogens *Escherichia coli* and *Pseudomonas aeruginosa* or fungi including *Candida* spp. [2–4]. When joints become infected, surgical revision is normally required, making prevention imperative [5,6]. Wound irrigation with surgical antiseptic solutions like chlorhexidine gluconate (CHG) or povidone-iodine (PI) (Figure 1A) is an important prophylactic technique. Both solutions have been widely used since the 1950s and show broad spectrum antimicrobial activity against many species of bacteria and fungi, as well as some viruses [7–9]; however, the concentrations at which they are used vary. PI is typically packaged as a 10% solution with 1% available iodine, and protocols using 0.35% PI have been effective in significantly reducing infection [10]. CHG is packaged at concentrations between 0.05-4% and diluted where necessary to a 0.05% solution. The two solutions have been previously compared to one another, with a prospective study determining chlorhexidine-alcohol was superior to PI at preventing infection [11], while other prospective and retrospective studies found no significant differences [12,13]. A 2020 systematic review concluded that both solutions resulted in improved outcomes compared to saline alone, with a pooled risk ratio of 0.62 for PI compared to saline and 0.74 for CHG compared to saline [14].

Despite their longstanding use in surgical settings, dilutions are typically based on historic practice. There are surprisingly limited *in vitro* data to define the actual minimum inhibitory

concentration (MIC) of the solutions against common microbes responsible for PJIs. Existing data suggests that the solutions may exhibit activity at concentrations much lower than currently used [15]. Further, there is no literature exploring the possible additive or synergistic effects of using the solutions in combination and little data exploring their impact on microbial biofilm formation. Many PJI-associated pathogens form biofilms, surface-associated microbial communities encased in a self-produced matrix that protects inhabitants from antibiotics [16], further complicating treatment. We previously showed that sub-minimal inhibitory antibiotic treatment can stimulate biofilm production [17–20]. Available literature suggests this may also be the case for CHG, but only a few species have been evaluated [21,22]. It is therefore important to determine whether highly dilute solutions of CHG and PI could promote the formation of antibiotic-tolerant biofilms.

Antibiotics like vancomycin are also used to prevent PJI via local administration of powder at the incision site, either alone or following surgical site irrigation [13,23–25]. Vancomycin, a glycopeptide antibiotic, inhibits bacterial cell wall synthesis and has activity against Gram-positive species, including MRSA. A 2019 systematic review and meta-analysis reported that intrawound vancomycin administration decreased the rate of PJI in knee and hip arthroplasty patients [26], while a 2020 systematic review and meta-analysis exploring the use of any local antibiotic found no significant reduction in infection and a significant increase in wound complications [27]. *In vitro* work showed that vancomycin has activity against Gram-positive PJI-associated microbes, but did not explore whether its addition impacts the effectiveness of wound irrigation solutions [15].

Infection prevention is a critical priority, as patients with PJI require repeat hospitalizations, experience decreased function, and are at increased risk of serious complications including death [28]. Given the global projections for TJR, identifying the appropriate concentrations of antiseptics compared to current practice that are required to effectively inhibit microbial growth and biofilm formation while limiting any potential side effects is imperative. Thus, the purpose of this study was to a) determine the MICs and effect on biofilm formation of the surgical antiseptics CHG and PI against model PJI-associated pathogens; b) determine if they reduce the mass of existing biofilms; c) explore any additive or synergistic effects of using the solutions in combination; and d) explore the effects on bacterial growth and biofilm formation of combining antiseptic solutions with vancomycin.

Materials and Methods

Microbial strains, culture conditions, and chemicals

Microbial strains used for this work include *S. epidermidis* P3B12, *S. aureus* USA300 (MRSA) [29] and ATCC 29213 (MSSA), *E. coli* K-12 W3110 [30], *P. aeruginosa* PAO1 [31] and PA14 [32], and *C. albicans* CA02045 [33]. Clinical isolates of *S. aureus* (SAC01-07) were obtained from Hamilton hospitals and kindly gifted by Dr. Cheryl Main (Supplementary Table I). Clinical isolates of *P. aeruginosa* (C0007, C0028, C0060, C0063, C0292, C0295) were obtained from the Wright Lab Clinical Collection [18]. Bacterial cultures were grown in lysogeny broth (LB), 10% LB (10% LB, 90% phosphate buffered saline (PBS, pH 7.4, NaCl (8 g), KCl (0.2 g), Na₂HPO₄ 7 H₂O (2.71), and KH₂PO₄ (0.24) in 1 L de-ionized H₂O)), 50% LB (50% LB, 50% PBS), tryptic soy broth (TSB), or 50% TSB (50% TSB, 90% PBS), as indicated. Povidone-iodine (Dovidine 10% solution with 1% available iodine, Laboratoire Atlas Inc.) and chlorhexidine gluconate

(Irrisept 0.05% solution) were diluted in sterile de-ionized water as indicated. A stock of vancomycin (Sigma) was prepared at 10 mg/mL in dimethyl sulfoxide (DMSO) and stored at 20°C.

Inhibitory concentration and biofilm formation assays

Microbes were cultured and inhibitory concentrations were calculated as previously described, with some modifications [20]. Briefly, antibiotics or antiseptic solutions were two-fold serially diluted to desired concentrations in DMSO or sterile de-ionized water, respectively, and 2-5 μ L of antibiotic, antiseptic solution, or DMSO/water as a control were added to each well of 96-well plates (Nunc) along with 145-148 μ L of dilute microbial culture or corresponding sterile media. *E. coli* and *P. aeruginosa* biofilms were formed on the polystyrene pegs of Immuno TSP lids (Nunc), as previously described [20], which were placed on assay plates prior to incubation, while *S. epidermidis*, *S. aureus*, and *C. albicans* biofilms were formed directly on the walls of the 96-well plate without the addition of an Immuno TSP lid. Plates with and without Immuno TSP lids were incubated for 16 h with shaking, 200 rpm, 37°C. Lids were removed from plates containing *E. coli* and *P. aeruginosa*, planktonic growth (OD_{600}) was measured, and lids were washed and stained with crystal violet as previously described [20]. *S. epidermidis*, *S. aureus*, and *C. albicans* cells were aspirated and plates were washed for 10 min with 150 μ L of PBS per well, then the solution was aspirated. Plates were stained by pipetting 150 μ L 0.1% w/v crystal violet solution into each well, staining for 1 min, then washing the plates twice with deionized water. Plates were dried for 1 h then 150 μ L 33.3% acetic acid was dispensed into each well to elute the bound dye. The absorbance (Abs_{600}) of the eluted dye was measured after 5 min using a Multiscan GO plate reader (Thermo Fisher Scientific). Three independent experiments were

performed in triplicate and technical triplicates were averaged. The mean and standard deviation of the independent biological replicates were reported. MIC was defined as growth < 20% of the vehicle control, where growth is no longer visible [18] and minimum biofilm eradication concentration was defined as biofilm < 20% of the vehicle control.

Biofilm disruption assays

S. aureus USA300 was cultured as previously described [20] and biofilms were formed in 96-well plates (Nunc) containing 150 μ L of dilute microbial culture in 50% TSB without antibiotics or antiseptics. Following incubation with shaking, 16 h, 200 rpm, 37°C, cells were aspirated and wells were washed for 10 min with 150 μ L sterile 50% TSB, then the media was aspirated.

Desired concentrations of antiseptic or sterile water were added (2-5 μ L) along with 145-148 μ L sterile 50% TSB. Plates were incubated for 16 h with shaking, 200 rpm, 37°C, then biofilm mass was measured as described for biofilm formation assays. Three independent experiments were performed in triplicate and technical triplicates were averaged. The mean and standard deviation of the independent biological replicates are reported. *P*-values were calculated using a one-way ANOVA and Dunnett's multiple comparison test (GraphPad Prism 10).

Checkerboard assays

Checkerboard assays were conducted as previously described [20], with 2-5 μ L of CHG, PI, or vancomycin added to an 8x8 section of a 96-well plate (Nunc), with increasing concentrations of one solution across the X-axis and increasing concentrations of the other solution across the Y-axis. Three biological replicates were averaged for each checkerboard. Synergy was determined

based on a fractional inhibitory concentration index (FICI), where values < 0.5 represent synergy and values > 4 represent antagonism [34].

Results

CHG and PI have broad spectrum antimicrobial and anti-biofilm activity at dilutions below those used in surgery

We measured the activity of CHG and PI against the Gram-positive species *S. epidermidis* (Figure 1B), MRSA (Figure 1C), and MSSA (Figure 1D), the Gram-negatives *E. coli* (Figure 1E) and *P. aeruginosa* (strains PAO1, Figure 1F, and PA14, Figure 1G), and a representative fungal species, *Candida albicans* (Figure 1H). CHG inhibited the growth of all organisms tested at a dilution of 0.0004% while PI inhibited growth at 0.33%. Both CHG and PI also inhibited biofilm formation of all organisms to levels comparable to the sterile control at these concentrations (Figure 1B-H). However, as reported for antibiotics [18–20], adding highly dilute solutions of CHG and PI to growth media concurrently with bacteria stimulated *P. aeruginosa* PAO1 biofilm formation (Figure 1F), with 0.0002% CHG and 0.04% PI causing biofilm levels to reach an average of 281% and 164% of the no-antiseptic control, respectively. Interestingly, despite being over 200x more potent than PI, CHG induced higher biofilm production (Figure 1F, note the Y axis scale in the left panel).

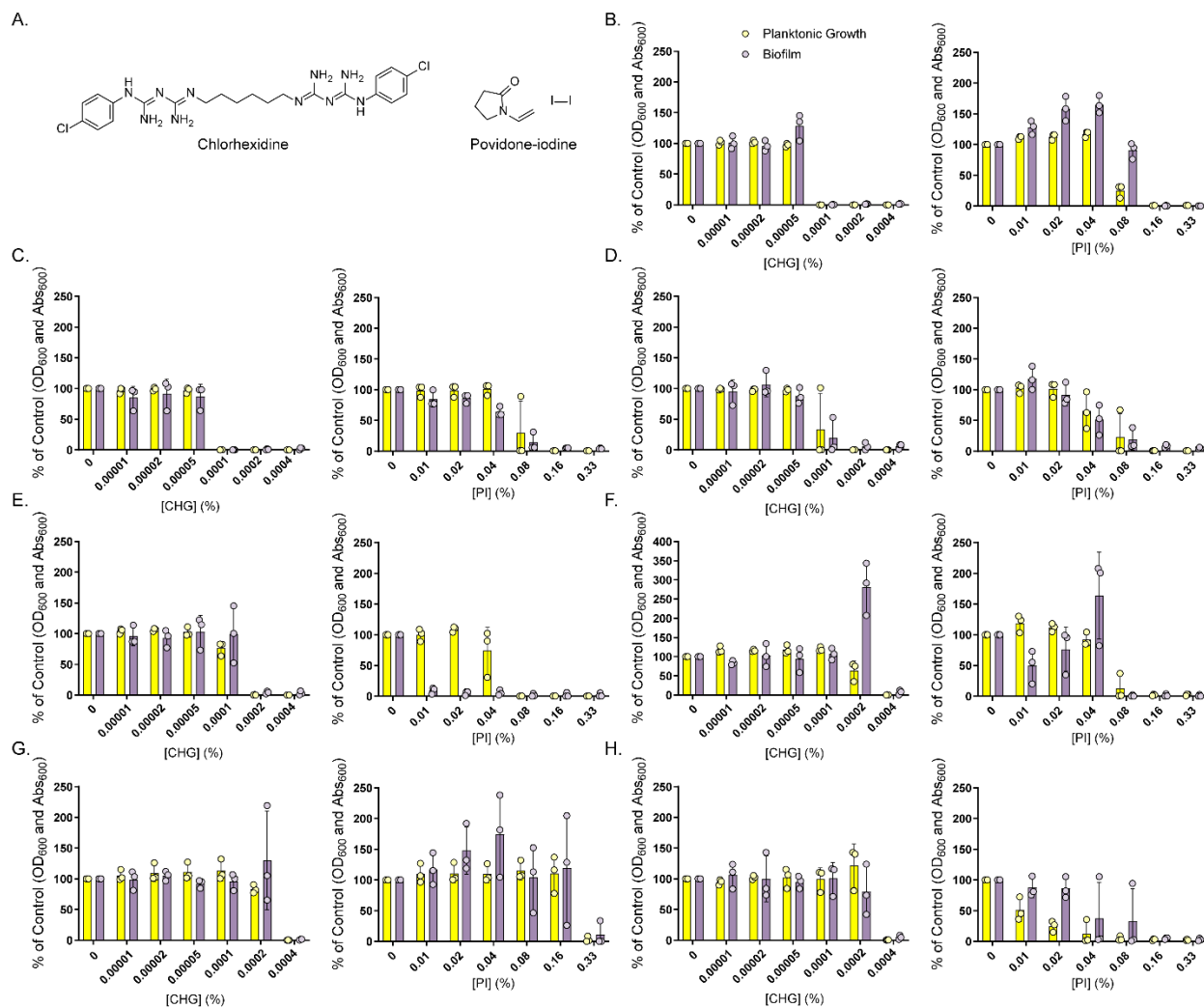


Figure 1. The antiseptic solutions CHG and PI inhibit growth and biofilm formation of model PJI-associated pathogens. (A) Structures of chlorhexidine and PI. (B-G) Planktonic growth (shown in yellow, optical density at 600 nm as a percent of the sterile water control) and biofilm formation (shown in purple, absorbance of crystal violet at 600 nm as a percent of the sterile water control) of *S. epidermidis* (B), MRSA (C), MSSA (D), *E. coli* (E), *P. aeruginosa* PAO1 (F) and PA14 (G), and *C. albicans* (H) grown in 10% LB (*P. aeruginosa* PAO1), 50% LB (*E. coli* and *P. aeruginosa* PA14), or 50% TSB (*S. epidermidis*, MRSA, MSSA, and *C. albicans*) in the presence of increasing concentrations of CHG (%) or PI (%). Individual points represent an average of three technical replicates and bars represent an average of three independent experiments. Error bars show standard deviation.

We next tested activity against seven recent *S. aureus* clinical isolates (Supplementary Table I), including one from an infected prosthetic knee (SAC06) and six recent *P. aeruginosa* clinical isolates with varying antibiotic susceptibilities [18]. CHG inhibited planktonic growth of all *S.*

aureus isolates and five of six *P. aeruginosa* isolates at a dilution of 0.0004% or lower, while 0.33% PI inhibited growth of all isolates (Figure 2). PI inhibited biofilm formation of all isolates at 0.33% or lower, while 0.0004% CHG inhibited biofilm formation of all *S. aureus* isolates and three of six *P. aeruginosa* isolates.

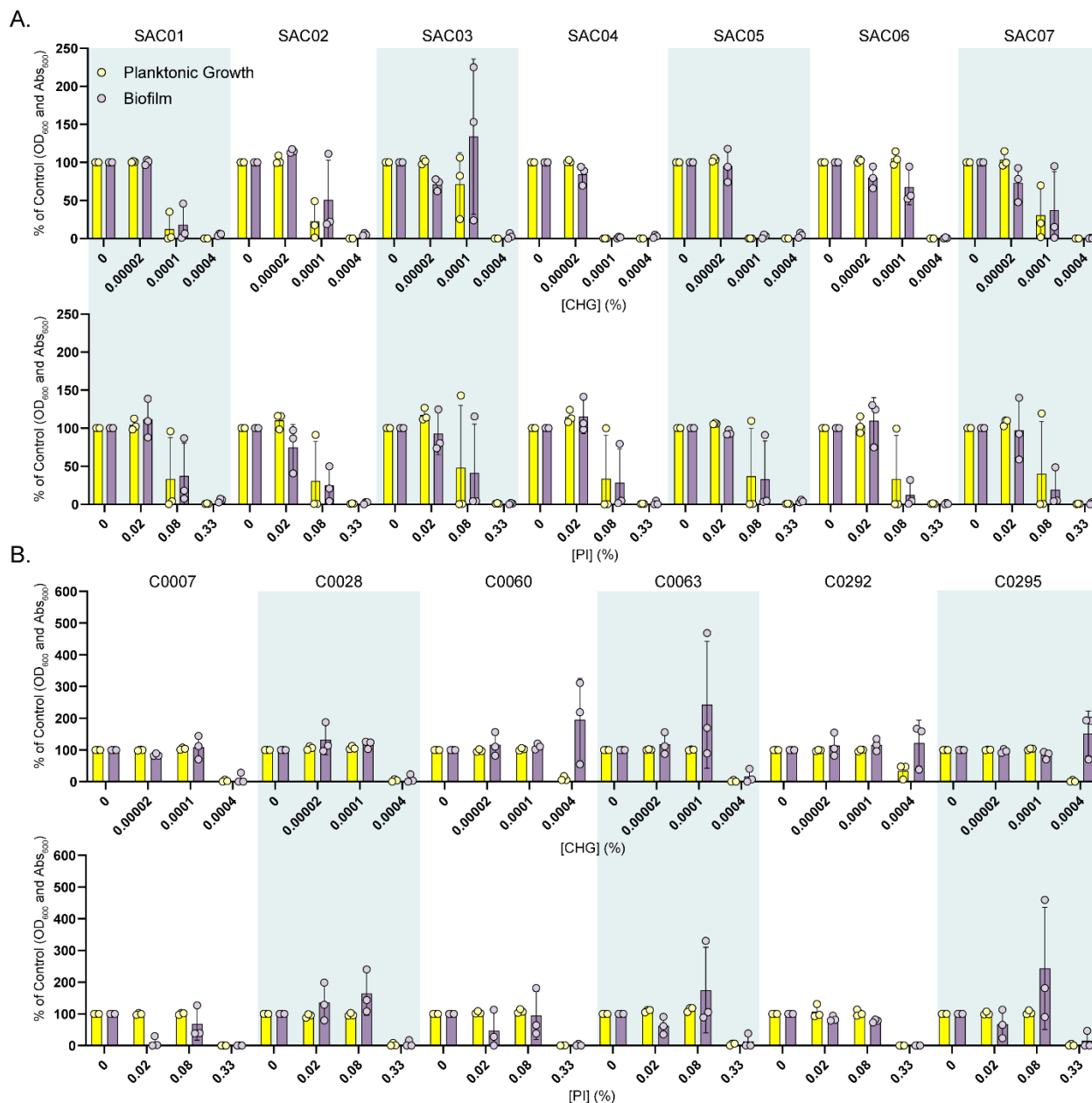


Figure 2. CHG and PI inhibit growth and biofilm formation of *S. aureus* and *P. aeruginosa* clinical isolates. Planktonic growth (shown in yellow, optical density at 600 nm as a percent of the sterile water control) and biofilm formation (shown in purple, absorbance of crystal violet at 600 nm as a percent of the sterile water control) of *S. aureus* clinical isolates SAC01-07 grown in

50% TSB (A) or *P. aeruginosa* clinical isolates C0007, C0028, C0060, C0063, C0292, and C0295 grown in 50% LB (B) with increasing concentrations of CHG (top) or PI (bottom) (%). Individual points represent an average of three technical replicates and bars represent an average of three independent experiments. Error bars show standard deviation.

CHG and PI can disperse established biofilms

We then tested whether antiseptic solutions could disperse previously established biofilms, a relevant scenario during surgical revision of infected joints. Both 0.00067% CHG ($p < 0.0001$) and 0.08% ($p = 0.0006$), 0.16% ($p = 0.0003$), or 0.33% ($p = 0.0016$) PI caused significant decreases in total biofilm (Figure 3).

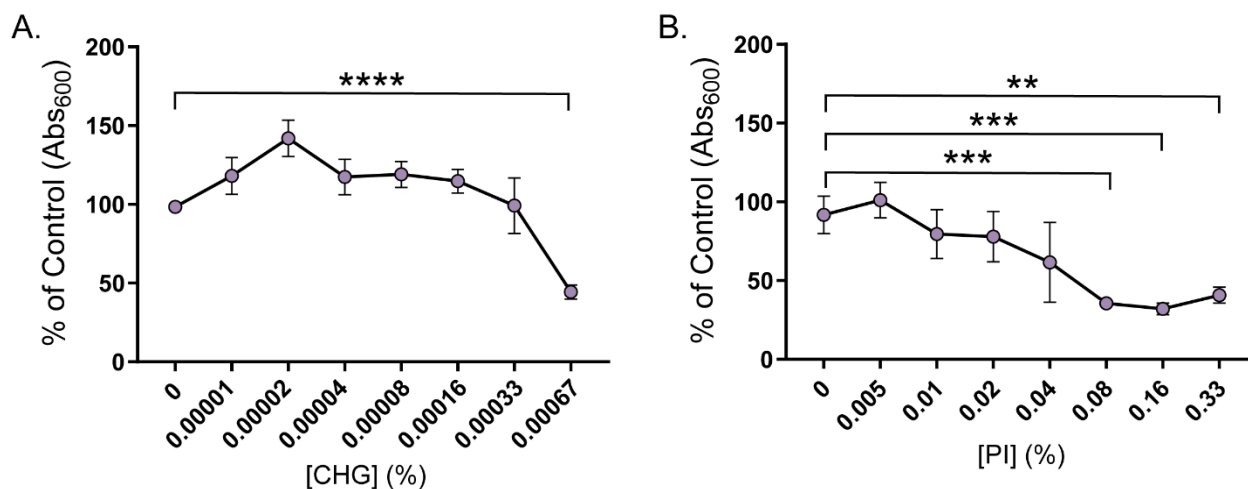


Figure 3. CHG and PI disperse established biofilms. Mass of MRSA biofilm (absorbance of crystal violet at 600 nm as a percent of the sterile water control) grown in 50% TSB for 16 h prior to incubation for 16 h with increasing concentrations of CHG (%) (A) or PI (%) (B). Points represent an average of three independent experiments conducted in triplicate. Error bars show standard deviation. ** $p < 0.01$, *** $p < 0.001$, **** $p < 0.0001$

PI and CHG lack synergistic or antagonistic activity when used in combination

To determine if PI and CHG synergize with one another, we next conducted checkerboard assays (Figure 4). As indicated by fractional inhibitory concentration index (FICI) values ≥ 0.5 , CHG and PI failed to synergize against any of the strains tested. No antagonism was observed.

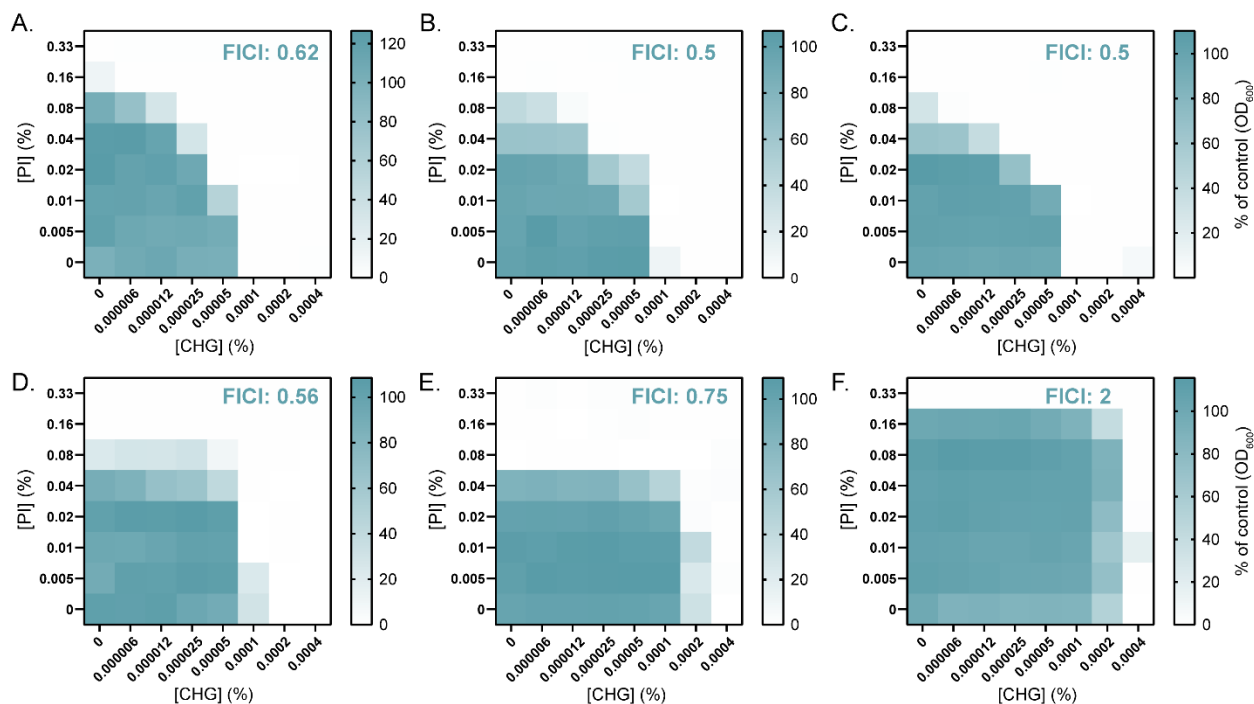


Figure 4. CHG and PI do not synergize nor antagonize one another's activity. Checkerboards of *S. epidermidis* (A), MRSA (B), MSSA (C), *E. coli* (D), and *P. aeruginosa* PAO1 (E) and PA14 (F) planktonic growth (optical density at 600 nm as a percent of the vehicle control) grown in 50% TSB (A-C), 50% LB (D and F), or 10% LB (E) with increasing concentrations of PI (%) and CHG (%). Planktonic growth (optical density at 600 nm as a percent of the control) is shown in blue while no growth is in white. A FICI ≥ 0.5 represents indifference. Checkerboards represent an average of three independent experiments.

The effects of combining wound irrigation with intrawound vancomycin administration

To mimic co-treatment with vancomycin and a surgical antiseptic, we conducted checkerboard assays using the susceptible species *S. epidermidis*, MRSA, and MSSA. CHG and PI inhibited the growth of these strains at 0.0001% and 0.17%, respectively, while the MIC of vancomycin was 1-2 $\mu\text{g}/\text{mL}$ (Figure 5A). CHG and PI neither synergized with nor antagonized vancomycin activity. We also examined the impact of vancomycin administration on Gram-negative species. Unexpectedly, vancomycin stimulated biofilm formation of *P. aeruginosa* PAO1 and PA14, but not *E. coli* (Figure 5B), likely as a result of its recently discovered antipseudomonal activity in nutrient-limited media that mimics infection conditions [35].

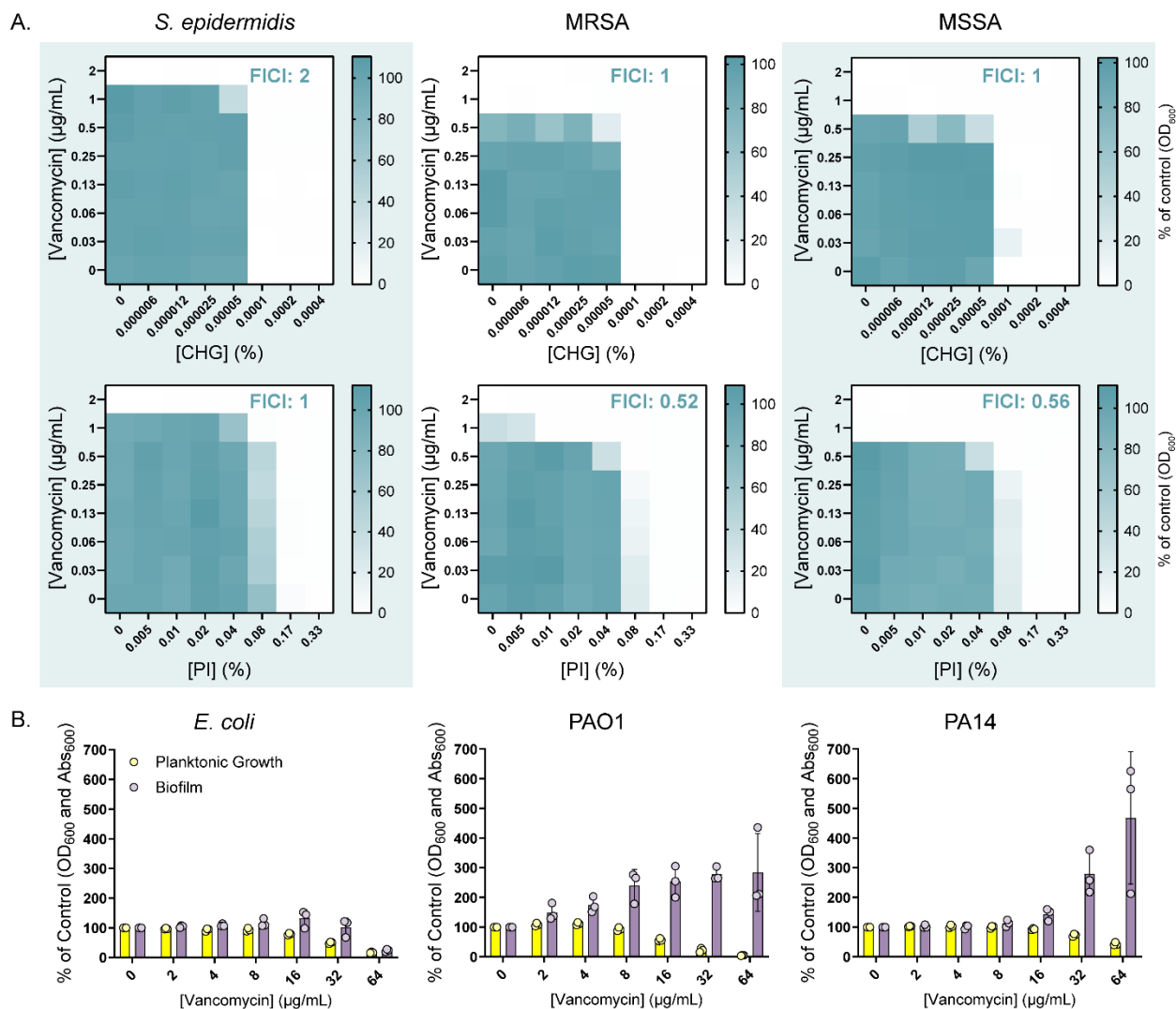


Figure 5. Vancomycin does not synergize with nor antagonize the activity of clinical antiseptics. (A) Checkerboards of *S. epidermidis* (left), MRSA (middle), and MSSA (right) planktonic growth (optical density at 600 nm as a percent of the vehicle control, shown in blue) grown in 50% TSB with increasing concentrations of vancomycin ($\mu\text{g/mL}$) and either PI (%) or CHG (%). FICI ≥ 0.5 represent indifference. Checkerboards represent an average of three independent experiments. (B) Planktonic growth (yellow) and biofilm formation (shown in purple, absorbance of crystal violet at 600 nm as a percent of the vehicle control) of *E. coli* (left) and *P. aeruginosa* PAO1 (middle) and PA14 (right) grown in 50% LB (*E. coli* and PA14) or 10% LB (PAO1) with increasing concentrations of vancomycin ($\mu\text{g/mL}$). Individual points represent an average of three technical replicates and bars represent an average of three independent experiments. Error bars show standard deviation.

Discussion

Despite the well-established use of CHG and PI for antiseptics, evidence supporting the choice of concentrations that balance effectiveness with patient safety is surprisingly limited. To gather important *in vitro* pre-clinical data on efficacy, we tested CHG and PI at increasing dilutions, alone or in combination, against a variety of clinically relevant microbes to determine their spectrum of activity and assess their impact on biofilm formation. Using the lowest effective concentration has the clear advantages of reducing costs and limiting cellular toxicity; however, concentrations used clinically must be high enough to reliably inhibit intra-wound growth without stimulating biofilm formation. CHG and PI inhibited microbial growth *in vitro* at dilutions of 0.0004% and 0.33%, respectively, with lower MICs for Gram-positive organisms (Figure 1B-H). The solutions were also active at these low concentrations against clinical isolates of *S. aureus* and *P. aeruginosa*, including *S. aureus* SAC06, a methicillin-resistant strain isolated from an infected prosthetic knee (Figure 2). These concentrations align with the limited existing literature, with differences likely due to dissimilarities in media, culture conditions, and exposure time [15,36]. Solutions of 0.05% CHG could therefore be further diluted 125-times and retain potency. PI is typically provided as a 10% solution; based on our findings, 30-times dilute solutions remain effective against all microbes tested. Despite the potential advantages of these lower concentrations, physicians should avoid using CHG or PI below their MIC, especially due to the emergence of CHG-resistant *S. aureus*, which has been linked to increased resistance to antibiotics like daptomycin [37,38]. Further exploration in an *in vivo* model is needed to determine if CHG and PI retain their clinical efficacy when used at their MIC in more complex conditions, such as with shorter contact times and in the presence of host immune factors.

We also measured microbial biofilm formation in the presence of the antiseptics, allowing us to show that low concentrations (0.0004% CHG and 0.33% PI) prevented multiple species from developing biofilms (Figure 1B-H), including all clinical isolates of *S. aureus* tested (Figure 2A) and two of five *P. aeruginosa* clinical isolates (Figure 2B). This concentration of CHG is at least five times lower than previously reported [21]. Higher concentrations of CHG would likely be needed to inhibit biofilm formation of the *P. aeruginosa* clinical isolates C0060, C0292, and C0295. CHG and PI not only prevented bacteria from forming biofilms (Figure 1, 2), but also significantly reduced the biomass of established biofilms (Figure 3), suggesting surgical irrigation may be beneficial in primary arthroplasty and both septic and aseptic revisions. In addition to possible development of resistance, sub-inhibitory concentrations of CHG and PI should be avoided since they could result in unintended increases in bacterial biofilm formation (Figure 1B-H and Figure 2). While it is present in only ~10% of PJIs [2], *P. aeruginosa*, a prolific biofilm-forming pathogen, reacts sensitively to subinhibitory concentrations of antibiotics [18,20]; we show it is also sensitive to antiseptics. Small populations of *P. aeruginosa* could form difficult-to-treat biofilms, whose antibiotic susceptibility can decrease up to 1000-fold [39]. We observed this biofilm stimulation phenotype (defined as biofilm levels >200% of the no-antiseptic control) [18] for our PAO1 laboratory strain (Figure 1F) and three of six clinical isolates (C0060, C0063, and C0295, Figure 2B), with different strains reacting differently to subinhibitory concentrations of either CHG or PI. We did not observe biofilm stimulation for other microbes tested, though subinhibitory concentrations of CHG have been reported to increase biofilms of *S. epidermidis* and some strains of MRSA [21,22].

We originally hypothesized that using the solutions in combination might make them effective at even lower concentrations; however, CHG and PI did not synergize, based on FICI values ≥ 0.5 (Figure 4), indicating that their mechanisms of action are independent. Based on a low FICI value of 0.5 in MRSA and MSSA (Figure 4B, C), we conclude there may be a small additive benefit to using the solutions in combination against *S. aureus*; however, further exploration in an *in vivo* model is needed to determine if a combination treatment would be advantageous.

Solid vancomycin, an antibiotic with activity against Gram-positive species including *S. aureus* and *S. epidermidis*, has recently been used intrawound as a preventative in TJR, usually in conjunction with antiseptics [13,23,40]. We found that its addition did not alter the activity of CHG or PI (Figure 5A). This result is consistent with clinical studies that found a vancomycin-PI protocol effective in reducing PJIs, though vancomycin use remains controversial, with some studies reporting no significant benefit [23,40,41]. There is some evidence to suggest that vancomycin, when added with PI, inhibits growth of immature biofilms [42]. Interestingly, we found that like CHG and PI, vancomycin stimulated biofilm formation of *P. aeruginosa* PAO1 and PA14, with biofilm levels reaching an average of 284 and 468% of control, respectively (Figure 5B). This was unexpected because, until recently, vancomycin was considered to have activity only against Gram-positive species [35]. These data suggest that localized vancomycin treatment, while effective against Gram-positive species, may paradoxically exacerbate rare *P. aeruginosa* infections. This is of particular concern since while vancomycin is administered at ~2 g intrawound, its distribution and local concentration varies. Average vancomycin intrawound concentrations three hours after closure ranges from 877-988 $\mu\text{g/mL}$, depending on arthroplasty site, and at 24 hours post-closure, remains extremely high at 163-280 $\mu\text{g/mL}$ [43]. While above

the values that we tested (up to 64 $\mu\text{g/mL}$), we expect these concentrations are high enough to inhibit *P. aeruginosa* growth without stimulating biofilm production; however, average post-surgery serum concentrations reach 5.2-6.6 $\mu\text{g/mL}$ [43], falling within the concentration range that stimulated *P. aeruginosa* biofilm formation (Figure 5B). These values also exceed the MIC for *Staphylococcus* species (1-2 $\mu\text{g/mL}$, Figure 5A), indicating that despite its local administration, intrawound vancomycin has the potential to impact the microbiome. Other risk factors for intrawound vancomycin administration include the possibilities of increased surgical complications and increased vancomycin resistance. A retrospective study found that vancomycin powder paired with PI significantly decreased the occurrence of coagulase-negative staphylococcal infections, but failed to note the vancomycin-susceptibility of isolates, nor did the authors measure the impact on species at distal sites [44]. A retrospective review found that vancomycin powder reduced PJI but led to an increase in wound complications [45]. Taken together, these data suggest that, while effective at inhibiting growth of *Staphylococcus* species, the potential implications of intrawound vancomycin administration should be more thoroughly investigated to support its continued use.

There are some limitations to the findings of this study. To establish important *in vitro* data, we tested the activity of the antiseptics and antibiotic on single-species cultures grown in dilute laboratory media in 96-well polystyrene plates over 16 h. Other studies have investigated the activity of antiseptics over shorter, more clinically relevant contact times, finding that 1% PI inhibits growth of organisms including MRSA immediately upon exposure, while 0.05% CHG does not kill MRSA with contact times up to 3 minutes, but did not assess biofilm formation [15]. Testing antiseptic activity in the presence of human serum would be an important future

direction to determine the impact of host immune factors on the MICs. To simplify our findings, we chose to measure activity of the antiseptics only against individual species of bacteria. While monospecies infections are representative of most PJIs, up to 15% are caused by multiple species [1]. It should also be noted that we tested only two commercially available formulations of CHG (Irrisept 0.05% solution) and PI (Dovidine 10% solution with 1% available iodine, Laboratoire Atlas Inc.). Additional testing would be required to ensure these data are applicable to other commercial formulations. Despite these limitations, our findings allowed us to understand the impact of dilute CHG, PI, and vancomycin on growth and biofilm formation of PJI-associated pathogens, contributing to the *in vitro* body of work that can help inform clinical use.

Conclusions

To support clinical practices, we aimed to characterize the activity of common wound antiseptics CHG and PI against PJI-associated pathogens and model microorganisms, finding they are effective *in vitro* at concentrations 125- and 30-times lower than typical use concentrations, respectively, even against recent clinical isolates. Since MICs vary depending on microbial growth conditions, these values are not necessarily representative of effective in-wound concentrations, but nonetheless provide valuable baseline information to support future clinical studies aimed at optimizing lavage conditions. Despite the obvious benefits of administering lower concentrations of antiseptics, we found that concentrations below the MIC can have the unwanted effect of increasing biofilm formation, making careful identification of an effective concentration range imperative. We also showed that CHG and PI can disperse established biofilms, indicating their benefit during revision of infected joints. We provide new evidence showing no synergistic benefit to using the solutions in combination, either with one another or

Ph.D. Thesis – V. E. Coles; McMaster University – Biochemistry and Biomedical Sciences

with vancomycin. Vancomycin alone is effective at inhibiting the growth of *Staphylococcus* species at low concentrations (1-2 µg/mL), but trials are needed to better understand how intrawound administration impacts bacterial biofilm formation, wound complications, and antimicrobial resistance rates.

Acknowledgments

We thank Gerry Wright for access to the Wright Lab Clinical Collection and Cheryl Main for providing *S. aureus* clinical isolates.

Conflict of interest statement

The authors declare no conflict of interest.

Funding sources

This work was supported by a Discovery Grant from the Natural Sciences and Engineering Research Council of Canada [RGPIN- 2021-04237]. LLB holds a Tier 1 Canada Research Chair in Microbe-Surface Interactions [CRC-2021-00103]. VEC holds an Ontario Graduate Scholarship.

References

- [1] Flurin L, Greenwood-Quaintance KE, Patel R. Microbiology of polymicrobial prosthetic joint infection. *Diagn Microbiol Infect Dis*. 2019;94:255–259.
- [2] Peel TN, Cheng AC, Buising KL, et al. Microbiological Aetiology, Epidemiology, and Clinical Profile of Prosthetic Joint Infections: Are Current Antibiotic Prophylaxis Guidelines Effective? *Antimicrob Agents Chemother*. 2012;56:2386–2391.
- [3] Tornero E, Senneville E, Euba G, et al. Characteristics of prosthetic joint infections due to *Enterococcus* sp. and predictors of failure: a multi-national study. *Clin Microbiol Infect*. 2014;20:1219–1224.
- [4] Lee YR, Kim HJ, Lee EJ, et al. Prosthetic Joint Infections Caused by Candida Species: A Systematic Review and a Case Series. *Mycopathologia*. 2019;184:23–33.
- [5] Tande AJ, Gomez-Urena EO, Barbari EF, et al. Management of Prosthetic Joint Infection. *Infect Dis Clin North Am*. 2017;31:237–252.
- [6] Gehrke T, Alijanipour P, Parvizi J. The management of an infected total knee arthroplasty. *Bone Jt J*. 2015;97-B:20–29.
- [7] Hiom SJ, Furr JR, Russell AD, et al. Effects of chlorhexidine diacetate on *Candida albicans*, *C. glabrata* and *Saccharomyces cerevisiae*. *J Appl Bacteriol*. 1992;72:335–340.
- [8] Hennessey TD. Some antibacterial properties of chlorhexidine. *J Periodontal Res*. 1973;8:61–67.
- [9] Zamora JL. Chemical and microbiologic characteristics and toxicity of povidone-iodine solutions. *Am J Surg*. 1986;151:400–406.
- [10] Brown NM, Cipriano CA, Moric M, et al. Dilute Betadine Lavage Before Closure for the Prevention of Acute Postoperative Deep Periprosthetic Joint Infection. *J Arthroplasty*. 2012;27:27–30.
- [11] Darouiche RO, Wall MJ, Itani KMF, et al. Chlorhexidine–Alcohol versus Povidone–Iodine for Surgical-Site Antisepsis. *N Engl J Med*. 2010;362:18–26.
- [12] Frisch NB, Kadri OM, Tenbrunsel T, et al. Intraoperative chlorhexidine irrigation to prevent infection in total hip and knee arthroplasty. *Arthroplasty Today*. 2017;3:294–297.
- [13] Driesman A, Shen M, Feng JE, et al. Perioperative Chlorhexidine Gluconate Wash During Joint Arthroplasty Has Equivalent Periprosthetic Joint Infection Rates in Comparison to Betadine Wash. *J Arthroplasty*. 2020;35:845–848.
- [14] Wood T, Ekhtiari S, Mundi R, et al. The Effect of Irrigation Fluid on Periprosthetic Joint Infection in Total Hip and Knee Arthroplasty: A Systematic Review and Meta-Analysis. *Cureus* [Internet]. 2020 [cited 2023 Feb 22];12. Available from: <https://www.cureus.com/articles/29232-the-effect-of-irrigation-fluid-on-periprosthetic-joint-infection-in-total-hip-and-knee-arthroplasty-a-systematic-review-and-meta-analysis>.
- [15] Cichos KH, Andrews RM, Wolschendorf F, et al. Efficacy of Intraoperative Antiseptic Techniques in the Prevention of Periprosthetic Joint Infection: Superiority of Betadine. *J Arthroplasty*. 2019;34:S312–S318.
- [16] Lewis K. Riddle of Biofilm Resistance. *Antimicrob Agents Chemother*. 2001;45:999–1007.
- [17] Nguyen UT, Harvey H, Hogan AJ, et al. Role of PBPD1 in Stimulation of *Listeria monocytogenes* Biofilm Formation by Subminimal Inhibitory β -Lactam Concentrations. *Antimicrob Agents Chemother* [Internet]. 2014 [cited 2022 Jan 25]; Available from: <https://journals.asm.org/doi/abs/10.1128/AAC.03671-14>.

- [18] Ranieri MRM, Chan DCK, Yaeger LN, et al. Thiostrepton Hijacks Pyoverdine Receptors To Inhibit Growth of *Pseudomonas aeruginosa*. *Antimicrob Agents Chemother* [Internet]. 2019 [cited 2020 Jan 26];63. Available from: <https://aac-asm-org.libaccess.lib.mcmaster.ca/content/63/9/e00472-19>.
- [19] Ranieri MR, Whitchurch CB, Burrows LL. Mechanisms of biofilm stimulation by subinhibitory concentrations of antimicrobials. *Curr Opin Microbiol*. 2018;45:164–169.
- [20] Coles VE, Darveau P, Zhang X, et al. Exploration of BAY 11-7082 as a Potential Antibiotic. *ACS Infect Dis* [Internet]. 2021 [cited 2021 Dec 16]; Available from: <https://doi.org/10.1021/acsinfecdis.1c00522>.
- [21] Houari A, Di Martino P. Effect of chlorhexidine and benzalkonium chloride on bacterial biofilm formation. *Lett Appl Microbiol*. 2007;45:652–656.
- [22] Park K-H, Jung M, Kim DY, et al. Effects of subinhibitory concentrations of chlorhexidine and mupirocin on biofilm formation in clinical meticillin-resistant *Staphylococcus aureus*. *J Hosp Infect*. 2020;106:295–302.
- [23] Iorio R, Yu S, Anoushiravani AA, et al. Vancomycin Powder and Dilute Povidone-Iodine Lavage for Infection Prophylaxis in High-Risk Total Joint Arthroplasty. *J Arthroplasty*. 2020;35:1933–1936.
- [24] Peng Z, Lin X, Kuang X, et al. The application of topical vancomycin powder for the prevention of surgical site infections in primary total hip and knee arthroplasty: A meta-analysis. *Orthop Traumatol Surg Res*. 2021;107:102741.
- [25] Matziolis G, Brodt S, Böhle S, et al. Intraarticular vancomycin powder is effective in preventing infections following total hip and knee arthroplasty. *Sci Rep*. 2020;10:13053.
- [26] Heckmann ND, Mayfield CK, Culvern CN, et al. Systematic Review and Meta-Analysis of Intrawound Vancomycin in Total Hip and Total Knee Arthroplasty: A Call for a Prospective Randomized Trial. *J Arthroplasty*. 2019;34:1815–1822.
- [27] Saidahmed A, Sarraj M, Ekhtiari S, et al. Local antibiotics in primary hip and knee arthroplasty: a systematic review and meta-analysis. *Eur J Orthop Surg Traumatol*. 2021;31:669–681.
- [28] Zhan C, Kaczmarek R, Loyo-Berrios N, et al. Incidence and Short-Term Outcomes of Primary and Revision Hip Replacement in the United States. *JBJS*. 2007;89:526.
- [29] Fey PD, Endres JL, Yajjala VK, et al. A Genetic Resource for Rapid and Comprehensive Phenotype Screening of Nonessential *Staphylococcus aureus* Genes. *mBio*. 4:e00537-12.
- [30] Yao Z, Valvano MA. Genetic analysis of the O-specific lipopolysaccharide biosynthesis region (rfb) of *Escherichia coli* K-12 W3110: identification of genes that confer group 6 specificity to *Shigella flexneri* serotypes Y and 4a. *J Bacteriol*. 1994;176:4133–4143.
- [31] Cavallari JF, Lamers RP, Scheurwater EM, et al. Changes to Its Peptidoglycan-Remodeling Enzyme Repertoire Modulate β -Lactam Resistance in *Pseudomonas aeruginosa*. *Antimicrob Agents Chemother*. 2013;57:3078–3084.
- [32] Liberati NT, Urbach JM, Miyata S, et al. An ordered, nonredundant library of *Pseudomonas aeruginosa* strain PA14 transposon insertion mutants. *Proc Natl Acad Sci*. 2006;103:2833–2838.
- [33] Burrows LL, Stark M, Chan C, et al. Activity of novel non-amphipathic cationic antimicrobial peptides against *Candida* species. *J Antimicrob Chemother*. 2006;57:899–907.
- [34] Odds FC. Synergy, antagonism, and what the checkerboard puts between them. *J Antimicrob Chemother*. 2003;52:1–1.

- [35] Chan DCK, Dykema K, Fatima M, et al. Nutrient Limitation Sensitizes *Pseudomonas aeruginosa* to Vancomycin. *ACS Infect Dis*. 2023;9:1408–1423.
- [36] Christopher ZK, Tran CP, Vernon BL, et al. What Is the Duration of Irrigation? An In Vitro Study of the Minimum Exposure Time to Eradicate Bacteria with Irrigation Solutions. *J Arthroplasty*. 2022;37:385-389.e2.
- [37] Madden GR, Sifri CD. Antimicrobial Resistance to Agents Used for *Staphylococcus aureus* Decolonization: Is There a Reason for Concern? *Curr Infect Dis Rep*. 2018;20:26.
- [38] Bhardwaj P, Hans A, Ruikar K, et al. Reduced Chlorhexidine and Daptomycin Susceptibility in Vancomycin-Resistant *Enterococcus faecium* after Serial Chlorhexidine Exposure. *Antimicrob Agents Chemother*. 2017;62:10.1128/aac.01235-17.
- [39] Ceri H, Olson ME, Stremick C, et al. The Calgary Biofilm Device: New Technology for Rapid Determination of Antibiotic Susceptibilities of Bacterial Biofilms. *J Clin Microbiol*. 1999;37:1771–1776.
- [40] Riesgo AM, Park BK, Herrero CP, et al. Vancomycin Povidone-Iodine Protocol Improves Survivorship of Periprosthetic Joint Infection Treated with Irrigation and Debridement. *J Arthroplasty*. 2018;33:847–850.
- [41] Yavuz IA, Oken OF, Yildirim AO, et al. No effect of vancomycin powder to prevent infection in primary total knee arthroplasty: a retrospective review of 976 cases. *Knee Surg Sports Traumatol Arthrosc*. 2020;28:1795.
- [42] Taha M, Arulanandam R, Chen A, et al. Combining povidone-iodine with vancomycin can be beneficial in reducing early biofilm formation of methicillin-resistant *Staphylococcus aureus* and methicillin-sensitive *S. aureus* on titanium surface. *J Biomed Mater Res B Appl Biomater*. 2023;111:1133–1141.
- [43] Johnson JD, Nessler JM, Horazdovsky RD, et al. Serum and Wound Vancomycin Levels After Intrawound Administration in Primary Total Joint Arthroplasty. *J Arthroplasty*. 2017;32:924–928.
- [44] Buchalter DB, Teo GM, Kirby DJ, et al. Does the Organism Profile of Periprosthetic Joint Infections Change with a Topical Vancomycin Powder and Dilute Povidone-Iodine Lavage Protocol? *J Arthroplasty*. 2021;36:S314–S319.
- [45] Dial BL, Lampley AJ, Green CL, et al. Intrawound Vancomycin Powder in Primary Total Hip Arthroplasty Increases Rate of Sterile Wound Complications. *Hip Pelvis*. 2018;30:37–44.

Supplementary Information

Supplementary Table I. Strain name and antibiotic susceptibility of *S. aureus* clinical strains isolated from patient samples as indicated.

Isolate	Site	Antibiotic susceptibility	Patient information
SAC01	Blood	MRSA, fluoroquinolone-resistant Susceptible: clindamycin, rifampin, tetracycline, sulfamethoxazole/trimethoprim	66F with bacteremia, treated with vancomycin
SAC02	Blood	MSSA, pansusceptible (including fluoroquinolones) Clindamycin-resistant	73M with bacteremia
SAC03	Blood	MSSA, pansusceptible (including to clindamycin)	80M with urosepsis
SAC04	Blood	MSSA, pansusceptible (including clindamycin)	79M with paraspinal abscess
SAC05	Wound	MRSA, fluoroquinolone-resistant Susceptible: clindamycin, rifampin tetracycline, sulfamethoxazole	2-year-old with skin lesion
SAC06	Wound	MRSA, clindamycin-resistant, fluoreoquinolone-resistant Susceptible: tetracycline, sulfamethoxazole/trimethoprim	73F with infected prosthetic knee
SAC07	Ear	MRSA, pansusceptible including fluoroquinolones	9-year-old with otitis media, perforated tympanic membrane

Chapter Five: Discussion and Future Directions

Overview of Findings

Despite steady increases in antimicrobial resistant infections, few new antibiotics have been discovered in recent decades. The work presented in this thesis aimed to address this problem in three ways: (1) identify novel antibiotics with activity against priority pathogens; (2) explore antibiotic adjuvants to resensitize resistant strains to existing antibiotics; and (3) assess the effectiveness of current antiseptic methods with the goal of preventing infections. Chapter One highlights the many reasons why developing new treatment methods is imperative, as well as factors that make antibiotic drug discovery and development challenging. In Chapter Two, we introduce a biofilm-based screening method to identify compounds with antibiotic activity that may be missed in a traditional screen. Using this method, we identified the anti-inflammatory BAY 11-7082. Through chemical derivatization, we synthesized a family of compounds based around this scaffold that have novel activity against priority pathogens. In Chapter Three we link its mechanism of action to peptidoglycan biosynthesis and show this family potentiates the activity of certain β -lactams against MRSA. In Chapter Four we examine standard surgical antiseptics, finding they are effective at inhibiting microbial growth and biofilm formation at concentrations below those used in surgery; however, subinhibitory concentrations stimulate biofilm formation. Together, these findings highlight the importance of considering the role of biofilms, both in antibiotic discovery and in infection treatment and prevention. They also highlight that there are novel antibiotic targets yet to be uncovered and pave the way for better understanding the factors that influence β -lactam resistance even in well-studied pathogens.

The importance and limitations of infection prevention

There are many challenges to antibiotic discovery, as discussed in Chapter One. These challenges are exemplified by the fact that no new classes of antibiotics have come to market in the last twenty years, and only two new classes have been developed this century. In response, several non-antibiotic methods to treat or prevent infections have been proposed. Vaccination, for example, provides a promising approach for common circulating bacterial infections.¹ While not all individuals in a population may be vaccinated, vaccination reduces the spread of resistant bacterial strains and decreases reliance on antibiotics, as seen with the pneumococcal vaccine for *Streptococcus pneumoniae*.² It is, however, difficult to predict which bacterial strains will circulate through a population and, as with antibiotic development, there are many safety and regulatory hurdles that make vaccine development difficult. Prevention in settings where infection is most likely to occur, such as in surgery, is also important, as explored in Chapter Four. While measures like antiseptic lavage reduce frequency, infection is still possible. Bacteria are ever present in our environment, and it is impossible to predict all infections, meaning that while important, prevention alone is not sufficient. Despite the many challenges, new treatment options for antibiotic resistant infections will always be needed.

The importance of measuring biofilm formation

Chapter Two highlights the utility of biofilm-based screening methods. We used *P. aeruginosa* as a model biofilm-forming organism and measured biofilm stimulation in response to small molecules, a well-documented phenomenon in which subinhibitory concentrations of antimicrobials promote an outsized increase in biofilm formation, likely as a stress response.³ We were able to identify compounds that had weak (tens of micrograms per ml) anti-Pseudomonal

activity and reasoned we could improve this activity using medicinal chemistry. This chapter acts as a proof of concept that biofilm-based screening identifies novel scaffolds with antimicrobial activity, and that this activity is not limited to only *P. aeruginosa*. While other groups have measured biofilm as a way to identify compounds that decrease biofilm formation or disperse established biofilms, screening for biofilm stimulation remains uncommon despite its many benefits.⁴⁻⁶ Our lab's experience screening for biofilm stimulators has been limited to collections of small molecules;^{7,8} however, this approach could prove particularly valuable in screening microbial extracts for natural products. Crude microbial extracts are often used in screening, but novel natural products of interest make up a small portion of these extracts, masking their effects. For this reason, libraries of fractionated extracts have higher hit rates than crude extracts.⁹ Hit rates could be further increased using biofilm-based screening, since it is more permissive, to identify antibiotics present even at low concentrations. Despite its advantages, biofilm-based screening remains relatively laborious compared to growth-only screening, and the method outlined in Chapter Two can only be conducted in 96-well plates, limiting throughput. Other methods for identifying biofilm stimulation, such as measuring dyes that bind matrix components, may prove more useful for screening large quantities of extracts.¹⁰

Biofilms are a major contributor to infections, particularly at surgical sites on implanted prosthetics, as highlighted in Chapter Four. Measuring the impact of antibacterials on biofilm formation in these settings is crucial; however, literature is limited. In this chapter we provide valuable *in vitro* data to support the use of antiseptics to prevent bacterial growth and biofilm formation at surgical sites. We also report that subinhibitory concentrations of both antiseptics and the antibiotic vancomycin stimulate biofilm formation, particularly in *P. aeruginosa*, though

similar findings have been reported for other species.^{11,12} Surgical antiseptics are often diluted inaccurately in the operating room and while solid antibiotics are applied intrawound at specific concentrations, these concentrations are based on precedence rather than evidence, and we lack a complete understanding of the concentrations reached at different body sites. Understanding the impact on biofilm development is therefore imperative. Perhaps a better approach would be the use of targeted antibiofilm therapies to prevent bacterial biofilm formation and disperse established biofilms, with a goal of decreasing reliance on antibiotics like vancomycin to which resistance is rising.

***S. aureus* biofilm inhibitors for infection treatment and prevention**

The biofilm-based screening protocol referenced in Chapter Two provides an unconventional way to identify compounds with antimicrobial activity; however, this screening set-up could simultaneously be used to identify compounds that inhibit biofilm formation. Antibiofilm agents represent a type of virulence inhibitor, which work by disarming bacteria to reduce pathogenicity *in vivo* instead of inhibiting planktonic growth directly, potentially making the development of resistance less likely.^{13–15} Virulence inhibitors rely on standard antibiotics or host immune factors to subsequently clear infections. Compounds that are active against *S. aureus* biofilms would be especially valuable, given their frequency and morbidity in catheter- and prosthetic joint-associated infections.^{16,17} Small-molecule compound libraries and natural product extracts could be screened for antibiofilm activity (Figure 1) in media that allows for quantification of the largest change between baseline and reduced biofilm formation. Simultaneous measurement of bacterial growth would be used to filter out compounds with antimicrobial activity as opposed to targeted antibiofilm activity. Compounds could also be tested for activity against *S. epidermidis* –

those that are effective against both of the most common Gram-positive PJI-associated organisms would provide the best protection – as well as recent clinical isolates from prosthetic joints. Provided they lack toxicity against human cell lines and do not interfere with the activity of validated surgical antiseptics like CHG and PI, these biofilm inhibitors would be an important addition to surgeries associated with biofilm-based infections like TJRs. This screening pipeline suffers from the same drawbacks as screening for biofilm stimulators, in that it is relatively laborious and low throughput. Artificial intelligence may prove useful in scaling up screens of synthetic small molecules, since machine learning algorithms could be trained on smaller datasets collected from a lower throughput screen and used to predict a larger set of compounds that inhibit biofilm formation.

In addition to preventing PJIs, antibiofilm therapies could also have a role in surgical revision of infected joints. While biofilms are intrinsically more antibiotic resistant than planktonic cells, compounds that prevent biofilm formation, induce biofilm dispersion, and/or compromise matrix integrity can act as adjuvants by enhancing antibiotic activity.¹⁸ It is therefore important to also measure the compounds' ability to decrease the mass of mature biofilms and determine if they synergize with traditional antibiotics used to treat PJIs like β -lactams, vancomycin, daptomycin, and linezolid to decrease planktonic and biofilm growth (Figure 1). Some microbial biofilms mask pathogen-associated molecular patterns (PAMPs), making it difficult for host immune factors to recognize and penetrate them.¹⁹ Agents that disperse biofilms consequently increase the amount of planktonic cells and aggregates, triggering an immune response. It is important to assess the impacts of dispersal *in vivo*, since, while necessary to clear infections, inadvertent overactivation of the innate immune system could have life-threatening consequences.

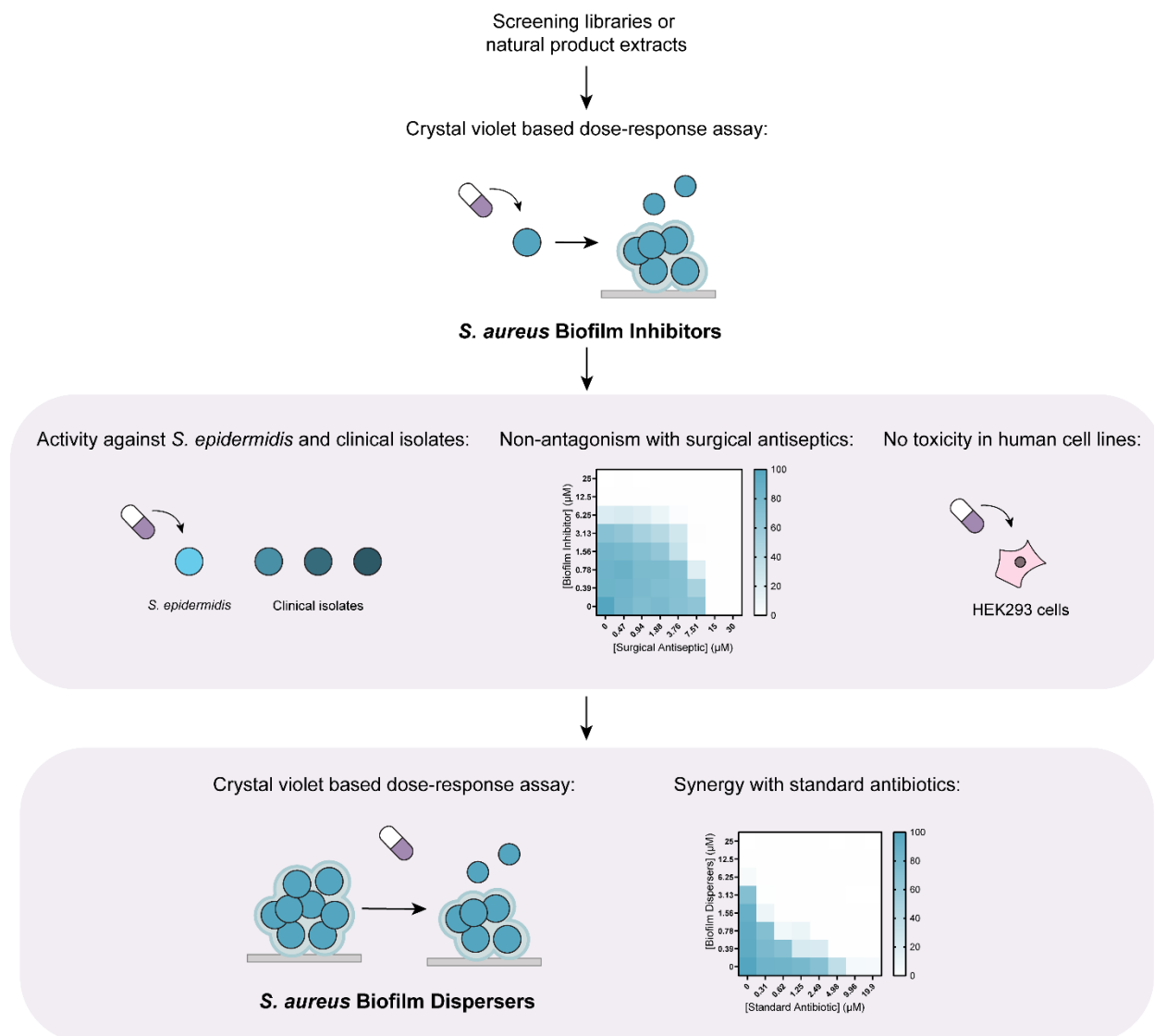


Figure 1. Workflow diagram of a proposed screen to identify antibiofilm compounds to be used in joint replacement to prevent or treat prosthetic joint infections. Screening libraries of small molecules or natural product extracts could be tested for their ability to prevent *S. aureus* biofilm formation. Those that inhibit biofilm formation below 20% of the vehicle control could be tested for antibiofilm activity against *S. epidermidis* and clinical isolates from infected prosthetic joints, checkerboard assays could be used to ensure they do not antagonize the activity of common clinical antiseptics chlorhexidine gluconate and povidone-iodine, and HEK293 cells could be used to ensure they are non-toxic to human cell lines (top purple box). Compounds that meet these criteria could also be examined as biofilm disruptors (bottom purple box) by testing to determine if they decrease the biomass of mature *S. aureus* biofilms and synergize with traditional antibiotic therapies to decrease planktonic and biofilm growth.

Biofilm inhibitors with activity against *P. aeruginosa* may also have activity against *S. aureus* biofilms. In the initial screen that identified BAY 11-7082, eight *P. aeruginosa* biofilm inhibitors were also identified (Figure 2).⁷ Additionally, *P. aeruginosa* biofilm screens performed by other research groups led to the identification of commercially-available biofilm inhibitors, four of which our lab has successfully validated (Figure 2).⁴ There are a variety of cellular processes on which compounds that disrupt biofilm formation or disperse established biofilms may act. Biofilm inhibitors may target EPS synthesis, intracellular c-di-GMP levels, and the activity of quorum sensing pathways. While most of these pathways are conserved between *S. aureus* and *P. aeruginosa* others, like motility, are not. Some *P. aeruginosa* biofilm inhibitors highlighted in Figure 2 contain moieties characteristic of iron chelators, including hydroxyquinolines and catechols (highlighted in blue). There is evidence that chelators sequester iron in the local environment, causing an increase in *P. aeruginosa* twitching motility and a corresponding decrease in biofilm formation.²⁰ While environmental iron levels impact biofilm formation of Staphylococcal species, this process is not mediated by increased twitching motility.^{21–23} Instead, decreased production of adhesins may play a causative role.²¹ Testing iron chelators like those identified in Figure 2 against *S. aureus* biofilms could validate this strategy of biofilm inhibition and further inform on its mechanism.

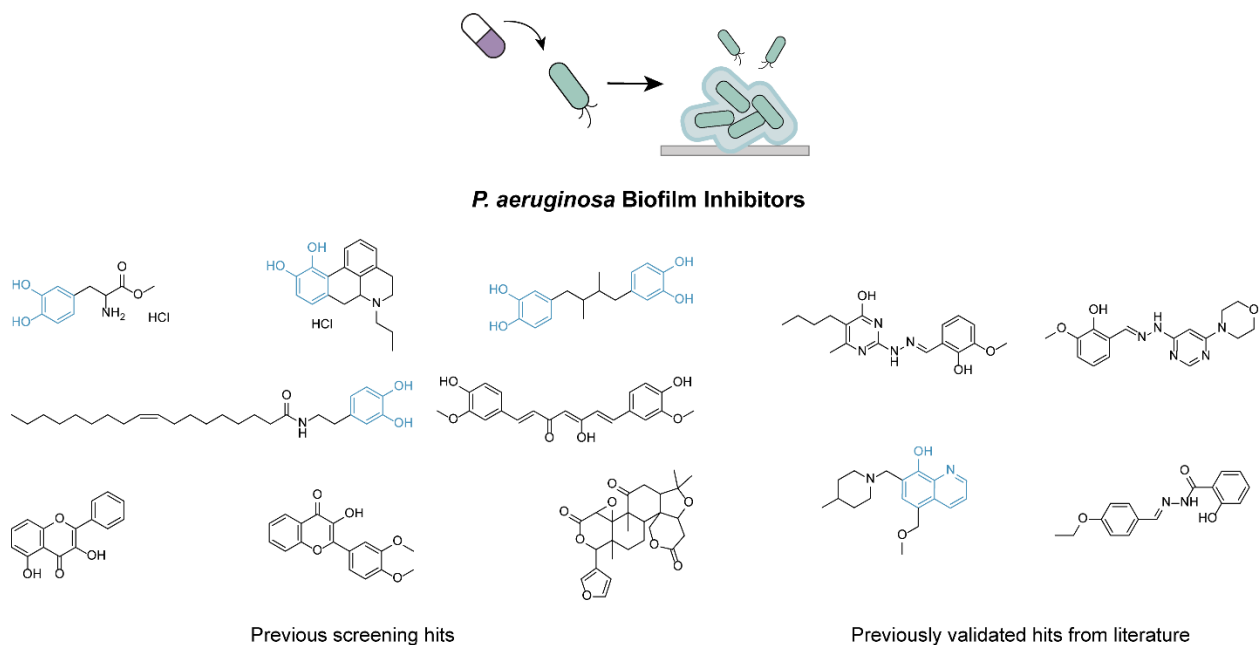


Figure 2. Structures that inhibit *P. aeruginosa* biofilm formation from our pilot biofilm screen (left) or those reported in literature and validated in our lab (right). Catechol groups and 8-hydroxyquinolones, two iron-binding motifs, are highlighted in blue.

Identification of a novel antibiotic scaffold

Despite the importance of approaches to reduce infection rates, novel antibiotics are still needed to treat MRSA. The oxazolidinone linezolid and the lipopeptide daptomycin, introduced into the clinic in 2000 and 2003, respectively, represent the most recently discovered classes of antibiotics, and their development was in response to rising rates of β -lactam resistance. In addition to these two newer antibiotics, vancomycin remains a standard-of-care treatment option for MRSA; however, resistance has arisen to all three.^{24–26} Of the 43 new compounds in the global antibiotic pipeline as of 2020, fewer than half have activity against *S. aureus*.²⁷ Of those that do, novel classes include compounds that target membrane integrity, cell division, DNA replication, protein synthesis, and fatty acid biosynthesis.²⁷ While there is still a continued push for the development of novel anti-MRSA therapies, some funders and developers have turned

their attention to Gram-negative infections including *P. aeruginosa*, *A. baumannii*, and *K. pneumoniae*, for which there are often fewer treatment options.^{27,28}

While BAY 11-7082's structural analogues BAY 11-7085 and PSPC were previously reported by other research groups to have antibiotic activity,^{29,30} our work presented in Chapter Two showed this activity is conserved among 25 structural analogues designed specifically for our study. Of these analogues, 16 were entirely novel at the time of publication. This group of compounds belong to a new antibiotic scaffold with activity against MRSA. Chapters Two and Three link the compounds' possible mechanism of action to peptidoglycan biosynthesis, showing that several compounds in this family resensitize MRSA to β -lactams. While peptidoglycan biosynthesis is a well-established target, no MRSA-targeting antibiotics in the current development pipeline act on it.²⁷ While BAY 11-7082's mechanism(s) of action remain unknown, we show that resistance occurs infrequently and cells expressing common resistance elements retain susceptibility.

Antibiotic adjuvants as an alternative strategy to antibiotic discovery

In Chapter Three we attempted to identify the mechanism through which BAY 11-7082 and its analogues potentiate certain β -lactams, exploring the utility of this scaffold as an antibiotic adjuvant. Antibiotic adjuvants provide an alternative to the discovery of new antibiotics, since they can increase the potency, broaden the spectrum, and overcome resistance to existing antibiotics that have already been proven safe and effective.¹⁸ Adjuvants advance into the clinic in combination with a specific antibiotic to minimize drug interactions and optimize dosing. Identifying a suitable pair can be difficult, and trials must be done to ensure the compounds retain suitable pharmacokinetic and pharmacodynamic properties when used together. While new

combination treatments still must go through clinical trials, development is often less complex than bringing an entirely new antibiotic to market, making this approach more economically favourable. An adjuvant approach also circumvents the need to continually develop increasingly expensive new antibiotics and, when employed in tandem with traditional antibiotic discovery programs, maximizes the treatment options available for resistant infections. Adjuvants can have a variety of different mechanisms of action. For example, antibiofilm compounds generally increase a population's susceptibility to traditional antibiotics, while β -lactamase inhibitors specifically bind β -lactamases, restoring the activity of β -lactams.

Unlike some adjuvants, including β -lactamase inhibitors, BAY 11-7082 and its analogues are antibacterial on their own. This is similar to the sulfonamide sulfamethoxazole and the folate inhibitor trimethoprim, two antibiotics that synergize with one another by inhibiting the biosynthesis of dihydrofolate and tetrahydrofolate, respectively, two steps required in the folic acid synthesis pathway.³¹ Using antibiotics in combination is a common strategy to expand the spectrum of activity and mitigate resistance, but by acting on the same pathway in concert, these compounds also potentiate one another.³² Interestingly, BAY 11-7082's ability to potentiate β -lactams is greatest in β -lactam resistant strains, suggesting that while it has its own antibacterial mechanism(s) of action, it also overcomes resistance. These mechanisms may be separate or shared. In Chapters Two and Three we showed that potent analogues are also strong β -lactam potentiators; however, we have not yet conducted a full structure-activity relationship study exploring synergy. It is possible the strongest potentiators are not the most potent antibacterials, suggesting these outcomes may be a result of binding separate cellular targets. Further chemical modifications may therefore result in discovery of stronger β -lactam potentiators.

In Chapter Three, we proposed that BAY 11-7082 and its analogues potentiate PBP2-targeting β -lactams by interrupting coordination between PBP2 and the β -lactam insensitive PBP2A. Some compounds reported to have this effect act on *fem* (factors essential for methicillin-resistance) or *aux* (auxiliary) factors.³³ Some of these factors, which are involved in *mecA*-mediated β -lactam resistance, were identified through chemical interactions between β -lactams and other peptidoglycan-targeting compounds. Fosfomycin, D-cycloserine, and moenomycin all potentiate β -lactam activity in addition to being antibacterial alone.^{34,35} Other factors were identified through experiments in which transposon mutant libraries of MRSA were screened for increased susceptibility to β -lactams.^{36,37} Other small molecule potentiators continue to be discovered, highlighting new factors involved in resistance; however, in Chapter Three we identify phenotypic differences between cells treated with BAY 11-7082 versus existing β -lactam potentiators, suggesting it may act via a novel mechanism. We previously tested strains from the Nebraska transposon mutant library³⁸ with transposon insertions in auxiliary factors of interest for susceptibility against a BAY 11-7082- β -lactam combination, but have yet to identify strains with altered susceptibility. A more comprehensive screen of strains with transposon insertions in all nonessential genes may reveal additional auxiliary factors that, when interrupted, alter susceptibility to the combination, allowing us to clarify possible mechanisms of synergy. Given that BAY 11-7082 also has antibiotic activity, it may act on an essential auxiliary factor, which would not be represented in a transposon library. Instead, CRISPR interference could be used to generate a knockdown library of essential genes to identify potential targets.

Significance and Concluding Remarks

The hunt for new antibiotics is not over, nor will it likely ever be, but there is value in better understanding what types of chemical matter modulate bacterial growth and biofilm formation. In this work, we identify a new chemical scaffold that inhibits bacterial growth and provide evidence that it works through a novel, yet undefined mechanism. These results act as a proof of concept that new antimicrobials, which work in ways we still do not fully understand, remain to be discovered. We also call attention to the many factors that play a role in *mecA*-mediated β -lactam resistance in MRSA, highlighting that there may be additional contributing factors that are not yet well understood. Using solid scientific data to build on historical precedence, we show the value of correctly diluted antiseptics in infection prevention, and propose a path forward for identification of targeted antibiofilm therapies to treat and prevent infections. Preventing infections, finding new antibiotics, and restoring the activity of existing antibiotics are separate strategies, but all have an important role to play in the continued fight against AMR.

References

- (1) Micoli, F.; Bagnoli, F.; Rappuoli, R.; Serruto, D. The Role of Vaccines in Combatting Antimicrobial Resistance. *Nat. Rev. Microbiol.* **2021**, *19* (5), 287–302. <https://doi.org/10.1038/s41579-020-00506-3>.
- (2) Sihvonen, R.; Siira, L.; Toropainen, M.; Kuusela, P.; Pätäri-Sampo, A. *Streptococcus pneumoniae* Antimicrobial Resistance Decreased in the Helsinki Metropolitan Area after Routine 10-Valent Pneumococcal Conjugate Vaccination of Infants in Finland. *Eur. J. Clin. Microbiol. Infect. Dis.* **2017**, *36* (11), 2109–2116. <https://doi.org/10.1007/s10096-017-3033-5>.
- (3) Ranieri, M. R.; Whitchurch, C. B.; Burrows, L. L. Mechanisms of Biofilm Stimulation by Subinhibitory Concentrations of Antimicrobials. *Curr. Opin. Microbiol.* **2018**, *45*, 164–169. <https://doi.org/10.1016/j.mib.2018.07.006>.
- (4) Junker, L. M.; Clardy, J. High-Throughput Screens for Small-Molecule Inhibitors of *Pseudomonas aeruginosa* Biofilm Development. *Antimicrob. Agents Chemother.* **2007**, *51* (10), 3582–3590. <https://doi.org/10.1128/AAC.00506-07>.
- (5) Siles, S. A.; Srinivasan, A.; Pierce, C. G.; Lopez-Ribot, J. L.; Ramasubramanian, A. K. High-Throughput Screening of a Collection of Known Pharmacologically Active Small

- Compounds for Identification of *Candida albicans* Biofilm Inhibitors. *Antimicrob. Agents Chemother.* **2013**, *57* (8), 3681–3687. <https://doi.org/10.1128/aac.00680-13>.
- (6) Haney, E. F.; Trimble, M. J.; Hancock, R. E. W. Microtiter Plate Assays to Assess Antibiofilm Activity against Bacteria. *Nat. Protoc.* **2021**, *16* (5), 2615–2632. <https://doi.org/10.1038/s41596-021-00515-3>.
- (7) Ranieri, M. R. M.; Chan, D. C. K.; Yaeger, L. N.; Rudolph, M.; Karabelas-Pittman, S.; Abdo, H.; Chee, J.; Harvey, H.; Nguyen, U.; Burrows, L. L. Thiostrepton Hijacks Pyoverdine Receptors to Inhibit Growth of *Pseudomonas aeruginosa*. *Antimicrob. Agents Chemother.* **2019**, *63* (9). <https://doi.org/10.1128/AAC.00472-19>.
- (8) Nguyen, U. T.; Wenderska, I. B.; Chong, M. A.; Koteva, K.; Wright, G. D.; Burrows, L. L. Small-Molecule Modulators of *Listeria monocytogenes* Biofilm Development. *Appl. Environ. Microbiol.* **2012**, *78* (5), 1454–1465. <https://doi.org/10.1128/AEM.07227-11>.
- (9) Cook, M. A.; Pallant, D.; Ejim, L.; Sutherland, A. D.; Wang, X.; Johnson, J. W.; McCusker, S.; Chen, X.; George, M.; Chou, S.; Koteva, K.; Wang, W.; Hobson, C.; Hackenberger, D.; Wagglechner, N.; Ejim, O.; Campbell, T.; Medina, R.; MacNeil, L. T.; Wright, G. D. Lessons from Assembling a Microbial Natural Product and Pre-Fractionated Extract Library in an Academic Laboratory. *J. Ind. Microbiol. Biotechnol.* **2023**, *50* (1), kuad042. <https://doi.org/10.1093/jimb/kuad042>.
- (10) Yaeger, L. N.; French, S.; Brown, E. D.; Côté, J. P.; Burrows, L. L. Central Metabolism Is a Key Player in *E. Coli* Biofilm Stimulation by Sub-MIC Antibiotics. *PLOS Genet.* **2023**, *19* (11), e1011013. <https://doi.org/10.1371/journal.pgen.1011013>.
- (11) Houari, A.; Di Martino, P. Effect of Chlorhexidine and Benzalkonium Chloride on Bacterial Biofilm Formation. *Lett. Appl. Microbiol.* **2007**, *45* (6), 652–656. <https://doi.org/10.1111/j.1472-765X.2007.02249.x>.
- (12) Park, K.-H.; Jung, M.; Kim, D. Y.; Lee, Y.-M.; Lee, M. S.; Ryu, B.-H.; Hong, S. I.; Hong, K.-W.; Bae, I.-G.; Cho, O.-H. Effects of Subinhibitory Concentrations of Chlorhexidine and Mupirocin on Biofilm Formation in Clinical Meticillin-Resistant *Staphylococcus aureus*. *J. Hosp. Infect.* **2020**, *106* (2), 295–302. <https://doi.org/10.1016/j.jhin.2020.07.010>.
- (13) Allen, R. C.; Papat, R.; Diggle, S. P.; Brown, S. P. Targeting Virulence: Can We Make Evolution-Proof Drugs? *Nat. Rev. Microbiol.* **2014**, *12* (4), 300–308. <https://doi.org/10.1038/nrmicro3232>.
- (14) Dickey, S. W.; Cheung, G. Y. C.; Otto, M. Different Drugs for Bad Bugs: Antivirulence Strategies in the Age of Antibiotic Resistance. *Nat. Rev. Drug Discov.* **2017**, *16* (7), 457–471. <https://doi.org/10.1038/nrd.2017.23>.
- (15) Maura, D.; Ballok, A. E.; Rahme, L. G. Considerations and Caveats in Anti-Virulence Drug Development. *Curr. Opin. Microbiol.* **2016**, *33*, 41–46. <https://doi.org/10.1016/j.mib.2016.06.001>.
- (16) Høiby, N.; Bjarnsholt, T.; Moser, C.; Bassi, G. L.; Coenye, T.; Donelli, G.; Hall-Stoodley, L.; Holá, V.; Imbert, C.; Kirketerp-Møller, K.; Lebeaux, D.; Oliver, A.; Ullmann, A. J.; Williams, C. ESCMID Guideline for the Diagnosis and Treatment of Biofilm Infections 2014. *Clin. Microbiol. Infect.* **2015**, *21*, S1–S25. <https://doi.org/10.1016/j.cmi.2014.10.024>.
- (17) Flurin, L.; Greenwood-Quaintance, K. E.; Patel, R. Microbiology of Polymicrobial Prosthetic Joint Infection. *Diagn. Microbiol. Infect. Dis.* **2019**, *94* (3), 255–259. <https://doi.org/10.1016/j.diagmicrobio.2019.01.006>.

- (18) Wright, G. D. Antibiotic Adjuvants: Rescuing Antibiotics from Resistance. *Trends Microbiol.* **2016**, *24* (11), 862–871. <https://doi.org/10.1016/j.tim.2016.06.009>.
- (19) Wang, S.; Zhao, Y.; Breslawec, A. P.; Liang, T.; Deng, Z.; Kuperman, L. L.; Yu, Q. Strategy to Combat Biofilms: A Focus on Biofilm Dispersal Enzymes. *Npj Biofilms Microbiomes* **2023**, *9* (1), 1–14. <https://doi.org/10.1038/s41522-023-00427-y>.
- (20) Singh, P. K.; Parsek, M. R.; Greenberg, E. P.; Welsh, M. J. A Component of Innate Immunity Prevents Bacterial Biofilm Development. *Nature* **2002**, *417* (6888), 552–555. <https://doi.org/10.1038/417552a>.
- (21) Lin, M.-H.; Shu, J.-C.; Huang, H.-Y.; Cheng, Y.-C. Involvement of Iron in Biofilm Formation by *Staphylococcus aureus*. *PLOS ONE* **2012**, *7* (3), e34388. <https://doi.org/10.1371/journal.pone.0034388>.
- (22) Coraça-Huber, D. C.; Dichtl, S.; Steixner, S.; Nogler, M.; Weiss, G. Iron Chelation Destabilizes Bacterial Biofilms and Potentiates the Antimicrobial Activity of Antibiotics against Coagulase-Negative Staphylococci. *Pathog. Dis.* **2018**, *76* (5), fty052. <https://doi.org/10.1093/femspd/fty052>.
- (23) Oliveira, F.; França, Â.; Cerca, N. *Staphylococcus epidermidis* Is Largely Dependent on Iron Availability to Form Biofilms. *Int. J. Med. Microbiol.* **2017**, *307* (8), 552–563. <https://doi.org/10.1016/j.ijmm.2017.08.009>.
- (24) Nannini, E.; Murray, B. E.; Arias, C. A. Resistance or Decreased Susceptibility to Glycopeptides, Daptomycin, and Linezolid in Methicillin-Resistant *Staphylococcus aureus*. *Curr. Opin. Pharmacol.* **2010**, *10* (5), 516–521. <https://doi.org/10.1016/j.coph.2010.06.006>.
- (25) Tsiodras, S.; Gold, H. S.; Sakoulas, G.; Eliopoulos, G. M.; Wennersten, C.; Venkataraman, L.; Moellering, R. C.; Ferraro, M. J. Linezolid Resistance in a Clinical Isolate of *Staphylococcus aureus*. *The Lancet* **2001**, *358* (9277), 207–208. [https://doi.org/10.1016/S0140-6736\(01\)05410-1](https://doi.org/10.1016/S0140-6736(01)05410-1).
- (26) Boucher, H. W.; Sakoulas, G. Perspectives on Daptomycin Resistance, with Emphasis on Resistance in *Staphylococcus aureus*. *Clin. Infect. Dis.* **2007**, *45* (5), 601–608. <https://doi.org/10.1086/520655>.
- (27) *Antibiotics Currently in Global Clinical Development*. <http://pew.org/1YkUFkT> (accessed 2024-06-26).
- (28) *CARB-X launches new funding round to fill major R&D gaps in global pipeline*. Carb-X. <https://carb-x.org/carb-x-news/2024-funding-round/> (accessed 2024-07-01).
- (29) Escobar, I. E.; Possamai Rossatto, F. C.; Kim, S. M.; Kang, M. H.; Kim, W.; Mylonakis, E. Repurposing Kinase Inhibitor Bay 11-7085 to Combat *Staphylococcus aureus* and *Candida albicans* Biofilms. *Front. Pharmacol.* **2021**, *12*, 675300. <https://doi.org/10.3389/fphar.2021.675300>.
- (30) Rajamuthiah, R.; Jayamani, E.; Majed, H.; Conery, A. L.; Kim, W.; Kwon, B.; Fuchs, B. B.; Kelso, M. J.; Ausubel, F. M.; Mylonakis, E. Antibacterial Properties of 3-(Phenylsulfonyl)-2-Pyrazinecarbonitrile. *Bioorg. Med. Chem. Lett.* **2015**, *25* (22), 5203–5207. <https://doi.org/10.1016/j.bmcl.2015.09.066>.
- (31) Brumfitt, W.; Hamilton-Miller, J. M. T.; Kosmidis, J. Trimethoprim-Sulfamethoxazole: The Present Position. *J. Infect. Dis.* **1973**, *128* (Supplement_3), S778–S791. https://doi.org/10.1093/infdis/128.Supplement_3.S778.
- (32) Eliopoulos, G. M.; Eliopoulos, C. T. Antibiotic Combinations: Should They Be Tested? *Clin. Microbiol. Rev.* **1988**, *1* (2), 139–156. <https://doi.org/10.1128/cmr.1.2.139>.

- (33) Roemer, T.; Schneider, T.; Pinho, M. G. Auxiliary Factors: A Chink in the Armor of MRSA Resistance to β -Lactam Antibiotics. *Curr. Opin. Microbiol.* **2013**, *16* (5), 538–548. <https://doi.org/10.1016/j.mib.2013.06.012>.
- (34) Sieradzki, K.; Tomasz, A. Suppression of Beta-Lactam Antibiotic Resistance in a Methicillin-Resistant *Staphylococcus aureus* through Synergic Action of Early Cell Wall Inhibitors and Some Other Antibiotics. *J. Antimicrob. Chemother.* **1997**, *39* (suppl_1), 47–51. https://doi.org/10.1093/jac/39.suppl_1.47.
- (35) Pinho, M. G.; Lencastre, H. de; Tomasz, A. An Acquired and a Native Penicillin-Binding Protein Cooperate in Building the Cell Wall of Drug-Resistant Staphylococci. *Proc. Natl. Acad. Sci.* **2001**, *98* (19), 10886–10891. <https://doi.org/10.1073/pnas.191260798>.
- (36) de Lencastre, H.; Tomasz, A. Reassessment of the Number of Auxiliary Genes Essential for Expression of High-Level Methicillin Resistance in *Staphylococcus aureus*. *Antimicrob. Agents Chemother.* **1994**, *38* (11), 2590–2598. <https://doi.org/10.1128/aac.38.11.2590>.
- (37) De Lencastre, H.; Wu, S. W.; Pinho, M. G.; Ludovice, A. M.; Filipe, S.; Gardete, S.; Sobral, R.; Gill, S.; Chung, M.; Tomasz, A. Antibiotic Resistance as a Stress Response: Complete Sequencing of a Large Number of Chromosomal Loci in *Staphylococcus aureus* Strain COL That Impact on the Expression of Resistance to Methicillin. *Microb. Drug Resist.* **1999**, *5* (3), 163–175. <https://doi.org/10.1089/mdr.1999.5.163>.
- (38) Fey, P. D.; Endres, J. L.; Yajjala, V. K.; Widhelm, T. J.; Boissy, R. J.; Bose, J. L.; Bayles, K. W. A Genetic Resource for Rapid and Comprehensive Phenotype Screening of Nonessential *Staphylococcus aureus* Genes. *mBio* *4* (1), e00537-12. <https://doi.org/10.1128/mBio.00537-12>.